FUNDAMENTALS OF
AIRCRAFT STRUCTURES

PRENTICE-HALL AERONAUTICAL ENGINEERING SERIES
K. D. WOOD, *Editor*

FUNDAMENTALS

OF

AIRCRAFT STRUCTURES

BY

MILLARD V. BARTON, PH.D.

Professor of Aeronautical Engineering
Research Engineer, Defense Research Laboratory
The University of Texas

TO GAY

Preface

As airplanes and related flying objects such as pilotless aircraft develop and are refined, additional improvements in their design require more knowledge and an increasing awareness of the results of research efforts, as well as an understanding of the fundamental principles upon which analysis is based. Modifications in design are possible only through a broad understanding of all the related design functions and analysis, coupled with an appreciation for research, development, and production. Less reliance can be placed on a strictly empirical approach.

For the reason stated, the emphasis in this book has been placed on increasing the knowledge of the fundamental principles upon which the analysis of the structure is made, along with an understanding of the physical concepts involved, rather than on rules and techniques, which change from time to time. However, many illustrative examples and problems are included so that the application of the principles to modern aircraft can be appreciated.

In presenting these fundamentals, it seems logical to divide the subject into four major parts: (1) the origin and nature of some of the loads on the aircraft; (2) the distribution of the loads through the individual members of the structure; (3) the effect of the loads on the buckling of the structural components; (4) the stress distributions and effects on the material. The text begins, therefore, with the broad subject of applied loads, becomes more detailed in following the overall actions of the loads through the structure, and finally narrows down to a study of the stress conditions from point to point of the structural material.

The author takes this opportunity to express his appreciation to all those who have assisted in preparing the manuscript. In particular, thanks are due to Dr. N. J. Hoff of the Polytechnic Institute of Brooklyn for his helpful suggestions; Mr. W. Wayne Huff Jr., Mr. Joseph Dalley, and Mr. Kendrick Radey for preparing the illustrations; Mr. Irving Liggett for checking details; and Miss Floy Storey for typing the manuscript.

<div align="right">MILLARD V. BARTON</div>

University of Texas
Austin, Texas

Contents

•••

PART I
Aircraft Loads and Design Specifications

PART II
Structural Analysis

PART III
Structural Stability

PART IV
Stress Analysis

Part 1
AIRCRAFT LOADS AND DESIGN SPECIFICATIONS

CHAPTER 1

Design Requirements

1.1 Introduction. It has been less than half a century since the first successful flight of a powered, controllable, man-carrying machine was made by the Wright brothers. That flight lasted for twelve seconds and was good for a distance of about 120 feet, or from the goal line to the 40 yard line of a football field, or about half the span of the wing of the largest present aircraft. Today, flights of thousands of miles lasting several hours are commonplace. Thousands of pounds of cargo and passengers are carried successfully to their destination. Aircraft fly at speeds in excess of 600 miles per hour at altitudes ranging up to 7 and 8 miles. In fact, many things that were considered miracles yesterday are considered so commonplace today that we are likely to underestimate the complexity of the airplane and overlook some of its limitations.

1.2 General specifications. One should always keep in mind the fact that the completed airplane is a result of compromise. It might be desirable, for example, to design and build the largest, highest-flying, fastest, lowest-landing-speed, and most maneuverable airplane in the world, but not all these characteristics could be obtained in one airplane. In order to have one advantageous feature, several disadvantageous ones must be accepted. High top speed usually means a high landing speed; load-carrying ability means loss of maneuverability; pilot armor protection means sacrificing rate of climb; and so on.

The design of an airplane begins with the selection of the general features desired and obtainable. The following is a list of a few features to be considered.

  (1) Loads
     (a) crew
     (b) passengers
     (c) cargo
     (d) fuel and equipment
  (2) Performance
     (a) speed
     (b) range
     (c) rate of climb
     (d) maneuverability
     (e) controllability
  (3) Structure
     (a) type—monoplane, biplane, helicopter, and so on

(b) number and size of engines

(c) cabin arrangement

(d) passenger comfort

(e) safety

(f) weight

(g) cost

1.3 Design of the structure. After the general specifications of the proposed airplane are established, a three-view drawing showing the
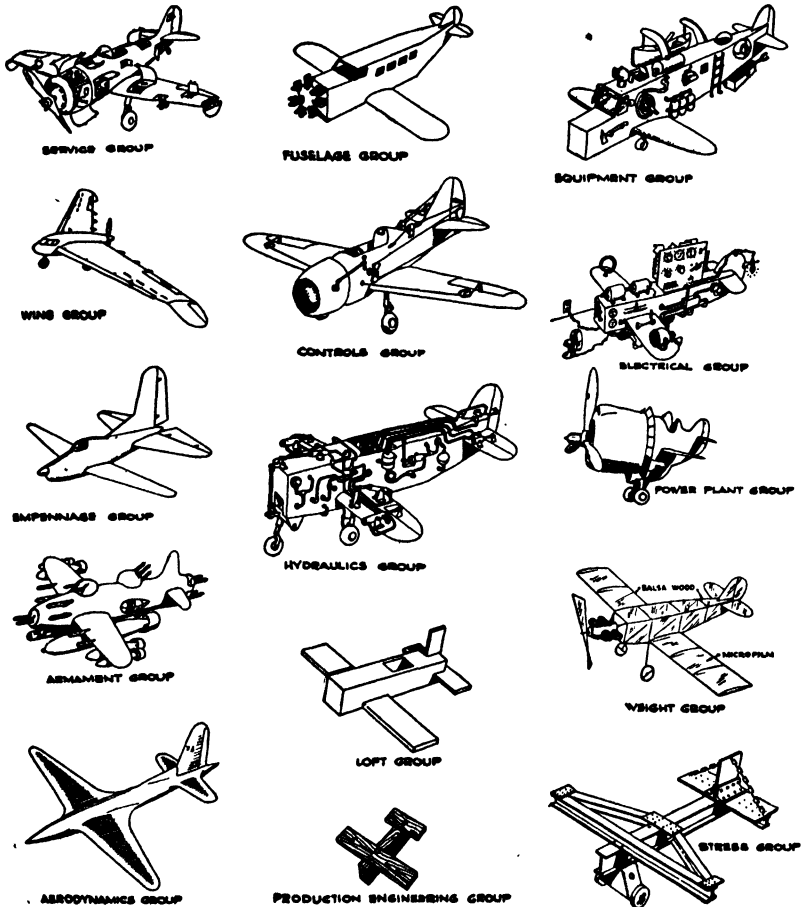
Fig. 1.1. Dream Airplanes. (Courtesy Lockheed Aircraft Corp.)

shape and approximate location of major parts, such as motor, wings, empennage, and so forth, is made.   The aerodynamicist, using the wind-tunnel as his tool, studies the performance of the proposed airplane and recommends modifications for better aerodynamic efficiency.   The design of the structure then begins.

It is the structural designer's duty to provide a structure contained as completely as possible within the outside shape specified by the aerodynamicist, capable of carrying the loads, and as light in weight as possible. The structure must be strong enough, but it must not be excessively strong because of the excess weight involved with consequent loss of pay load that the airplane can carry. These conditions require a precise structural analysis, testing, research, and close correlation between design and production. The design processes are usually broken down into separate groups. It is possible to have a fuselage group responsible for the design of the fuselage, an empennage group responsible for the design of the tail surfaces, and so on. Obviously the functions of the separate groups must be correlated closely in order to have an airplane that fits together and performs as predicted. Sometimes the separate groups become so involved in their own functions they underemphasize the importance of the other groups. Here again, as in the case of determining the general specifications, compromise between the various group functions must be made in order to produce an airplane that probably does not have all the ideal features of any group, but that is a good practical airplane with many desirable features.

The ideals of each design group are humorously shown in Figure 1.1. The difference between the weight group, responsible for keeping the weight to a minimum, and the stress group, responsible for designing a structure with sufficient strength, should be noted particularly. Weight and strength are two of the designer's major problems.

CHAPTER 2

Aircraft Loads

■■

2.1 Introduction. Before the structural design of the airplane can be completed, the loads acting on the various units of the structure must be known. The loads acting on the airframe are divided into two main groups:

(1) flight loads
(2) ground loads.

There are many kinds of *flight loads*, including the lift on the wings, drag, and inertia loads imposed during the maneuvering of the airplane. The loads may, and usually do, vary from time to time, which depends on the flight attitude of the airplane and weather conditions. These loads exist while the airplane is air-borne.

Ground loads are the loads imposed on the airplane during landing, take-off, or storing, such as tying the airplane down. These loads occur while the airplane is in contact with the ground.

The Civil Aeronautics Authority and the Army and Navy Aviation Bureaus specify load conditions for various types of aircraft. The Civil Aeronautics bulletins on airplane airworthiness classify aircraft into several categories depending on the intended operation, and the load conditions for each category are specified. Some of these classifications taken from Civil Air Regulations 03 and 04 are:

Normal (*N*). Airplanes intended for non-acrobatic, non-scheduled passenger, and non-scheduled cargo operation.
Utility (*U*). Airplanes intended for normal operation and limited acrobatic maneuvers. These airplanes are not suited for use in snap or inverted maneuvers.
Acrobatic (*A*). Airplanes with no specific restrictions as to type of maneuver permitted unless the necessity therefor is disclosed by the required flight tests.
Transport (*T*). Multi-engined airplanes limited to non-acrobatic operation and intended for, but not limited to, scheduled passenger, cargo, or combined passenger and cargo carrying operation.

Complete information on load requirements, load distribution, and location are given for the different types of aircraft in the government bulletins, but, since some of these specifications are empirical and many are constantly being modified and revised, only the fundamentals of the subject, together with some specific applications, will be discussed in this chapter. The student is referred to the references at the end of the chapter for more complete details.

2.2 Flight loads. Many possible combinations of loads exist; these possibilities depend on the flight attitude and on other factors, such as

6

velocity, weight, and size of the airplane. The airplane, when flying in level unaccelerated flight, will have entirely different forces acting on it than when a snap roll or dive pull-out is performed. The designer must determine the conditions or combination of conditions producing the most severe actions of the forces on the structure. To understand the problem a few simple flight situations will be considered.

Straight level flight at constant velocity. The forces acting on an airplane in straight, level, unaccelerated flight are shown in Figure 2.1. In this figure, W is the total weight of the airplane and all it contains acting at its center of gravity (c.g.), L is the lift of the wings, T is the propeller thrust causing the airplane to be pulled forward, D_p (parasite
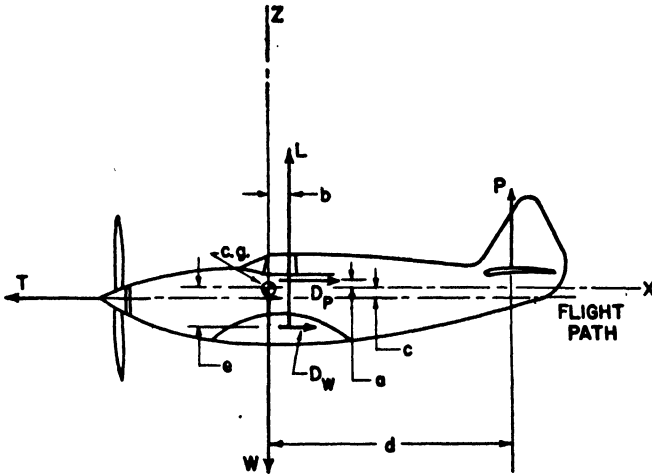
Fig. 2.1. Straight Level Flight.
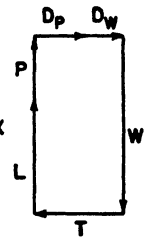
Fig. 2.2. Force Polygon.

drag) is the drag or resistance to motion through the air caused by all parts except the wing, D_w is the wing drag caused by moving the wing through the air, and P is the stabilizer load required to balance the airplane.

If a set of coordinate axes is taken perpendicular and parallel to the flight path, then, since all the forces must be in equilibrium, the following conditions must hold:

$$\Sigma F_x = 0; \ \Sigma F_z = 0; \ \Sigma M = 0 \qquad (2.1)$$

This equilibrium is shown by the force polygon, Figure 2.2.

Performing the operations indicated in Equation 2.1, we find that

$$\Sigma F_x = 0 = D_p + D_w - T \text{ (aft forces are positive, or the thrust}$$
$$\text{equals the total drag of the airplane)} \qquad (2.2)$$
$$\Sigma F_z = 0 = L + P - W \text{ (upward forces are positive)}$$

P is usually small, so that for this condition the lift is approximately equal to the weight, $L = W$.

Taking moments about the center of gravity, we find that (nosing-up moments are positive)

$$\Sigma M_{cg} = 0 = Tc - Lb + D_p a - D_w e - Pd$$

When we solve this for P,

$$P = \frac{Tc - Lb + D_p a - D_w e}{d} \qquad (2.3)$$

Accordingly, if the nosing-up moment due to the sum of the moments of thrust (Tc) and parasite drag ($D_p a$) is greater than the moment due to the
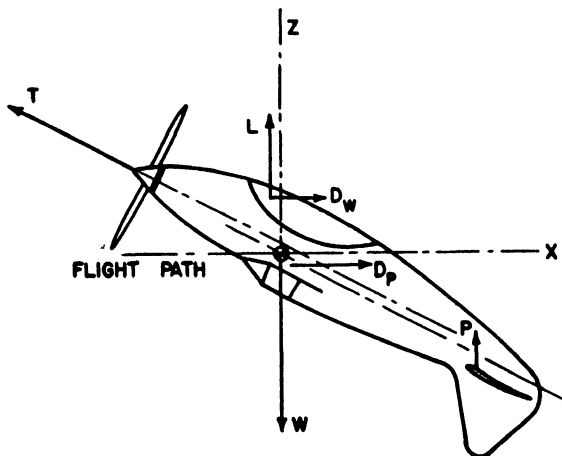
Fig. 2.3. Inverted Flight.   Fig. 2.4. Force
                                              Polygon.
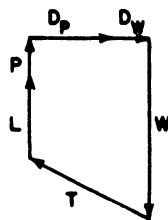
sum of the moments of wing drag ($D_w e$) and lift (Lb), then the stabilizer force (P) will be positive and in the direction assumed for this flight' condition. A change in conditions might easily make the stabilizer force act in the opposite direction, or downward.

The condition of flight during which the lift is approximately equal to the weight is called the *basic load condition*.

Inverted flight (unaccelerated). During inverted flight many of the loads are reversed and therefore may produce a critical condition. Figure 2.3 shows the forces acting in inverted flight.

Again, the conditions of equilibrium must apply so that $\Sigma F_x = 0$, $\Sigma F_z = 0$, $\Sigma M = 0$. This condition is graphically represented in Figure 2.4.

Inertia forces. In addition to the loads on the airplane in unaccelerated flight, there may be inertia loads imposed by the acceleration of the airplane during maneuvers or because of gusts. An example of inertia loads caused by maneuvers is that of the dive pull-out.

In pulling out of a dive, the airplane is forced to follow a curved path. The curvilinear path causes an acceleration perpendicular to the flight path and acting toward the center of curvature. The mass of the airplane
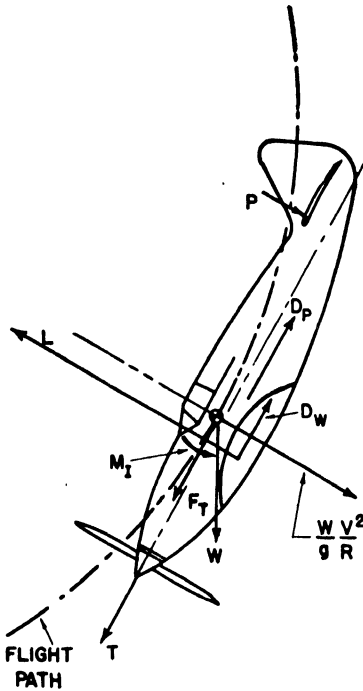
Fig. 2.5. Dive Pull-out.
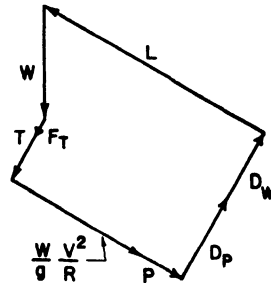
Fig. 2.6. Force Polygon.

times this acceleration gives a force which is acting to throw the airplane outward from the center of curvature. The value of this force is

$$F_n = \frac{W}{g}\frac{V^2}{R} \tag{2.4}$$

where
F_n = force normal to flight path (lb)
W = weight of airplane (lb)
g = acceleration of gravity (32.2 ft/sec^2)
V = velocity (ft/sec)
R = radius of turn (ft).

Other inertia forces that may be applied in this maneuver are the inertia force F_t acting tangential to the flight path caused by the deceleration (slowing down) and an inertia couple M_I caused by the rotation of the airplane about its center of gravity as its attitude is changed in the maneuver. The values of the force and moment are:

$$F_t = \frac{W}{g} A_t \qquad (2.5)$$
$$M_I = I\alpha$$

where F_t = force tangential to flight path (lb)

A_t = tangential acceleration (ft/sec²)

M_I = inertia moment (lb ft)

I = mass moment of inertia of airplane about the c.g. (slugs ft²)

α = angular acceleration (radians/sec²).

Consider an airplane in a dive pull-out, Figure 2.5. It is evident that the lift on the wing may be several times the weight for force equilibrium as shown in the force polygon, Figure 2.6.

Other maneuvers, such as snap rolls, loops, and so on, will impose different accelerations. A snap roll, for example, will induce a different lift on the two ends of the wings and an inertia couple about the longitudinal axis of the airplane.

2.3 Load factor. The lift on the wings during maneuvers may have a value several times the weight of the airplane. It is convenient to express this wing load in terms of the wing load for the basic flight condition. In level flight the wing load is approximately equal to the weight, $L = W$. If the ratio, n, of the lift to the weight is known for any maneuver, then the lift can be specified as the weight times the factor n. The factor n is called the *load factor*. For an example of the meaning of the load factor, consider the airplane at the bottom of a dive pull-out when the centrifugal force is seven times the weight. The total lift on the wings is therefore $7W + W = 8W$, and the load factor for this condition is 8.

Since the load factor is the ratio of force to weight, it can be considered also as the ratio of the acceleration of a weight to the acceleration of gravity, g. For this reason the load factor is sometimes called the *number of g's*. The use of load factors is not restricted only to wing loads but may be used to express the load on any part in relation to its normal load.

Load factor or acceleration factor, n. The ratio of the force acting on a mass to the weight of the mass. When the force in question represents the net external load acting in a given direction, n represents the acceleration in that direction in terms of the gravitational constant.

2.4 Maneuver load factors. The load factor imposed by a maneuver is often determined experimentally. An accelerometer (acceleration measuring device) is put in an airplane and a record made of the accelerations in a given direction during the flight of the airplane. The results are plotted as load factor versus velocity of the airplane.

A typical load factor velocity diagram is shown in Figure 2.7. The load factor in this diagram is for a direction perpendicular to the flight path.

The portion of the curve *ab* represents the load condition of the airplane in straight level flight. As the pilot puts the airplane into the dive, the load conditions are as indicated by portion *bc* of the curve. In the dive there is no load perpendicular to the flight path although the speed of the airplane is increased as shown by *cd*. When a speed of 325 mph is reached, the pilot starts to pull the airplane out of the dive. The radius of pull-out is gradually decreased so that the centrifugal force, and therefore the load factor, is increased until in this case a load factor of 8 is attained. This pull-out is indicated by *de*. When the pilot attains an acceleration of 8g, he again gradually increases his radius of pull-out; and, since the velocity is decreasing, the load factor decreases
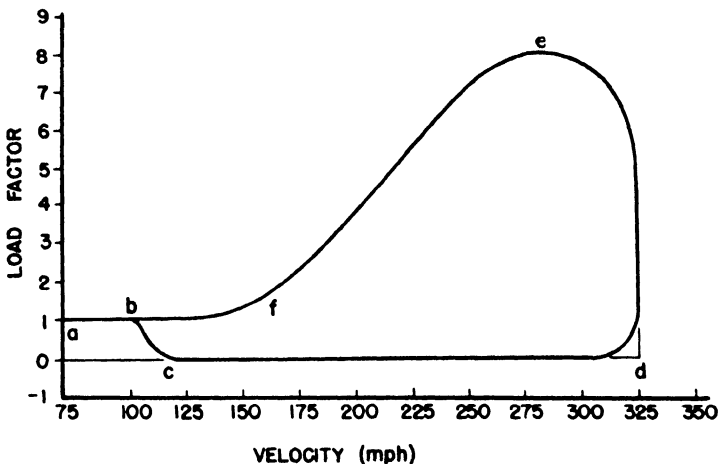
Fig. 2.7.   Maneuver Load Factor Diagram.

as shown by *ef*. At the point indicated by *f* on the curve the airplane is again flying straight and level so that the load factor is 1.

It is apparent that the loads on the airplane can become large. These same loads, however, are exerted on the pilot and passengers; and to some extent the physical limitation of the people will limit the load the airplane must withstand. If a pilot weighs 200 pounds, then during level flight the pressure exerted on the seat of his pants is 200 pounds. During an 8g pull-out all loads are increased 8 times, thus increasing the seat pressure to 1600 pounds. This increase in force acts on all parts of the pilot: forces his head down between his shoulders, makes his spine bend, and forces the blood out of his head, which causes blackout. The amount of force a pilot can stand before he blacks out depends on its duration. For example, it may be possible for the pilot to take a force of three times his weight for a relatively long period, whereas a force of eight times his weight will cause almost instant blackout. Greater forces are liable to cause permanent injury.

2.5 Limit load. It is necessary when designing an airplane to decide on the maximum loads that will be exerted. These maximum loads will vary with the type of airplane, flying conditions, and physical limitations of people. Small high-speed pursuit airplanes that are highly maneuverable will be subjected to greater inertia loads than large cargo-carrying airplanes. The greatest expected load factor during normal operations of the large airplane would, therefore, be less than for the pursuit airplane. The *limit load* is the highest load expected during the normal
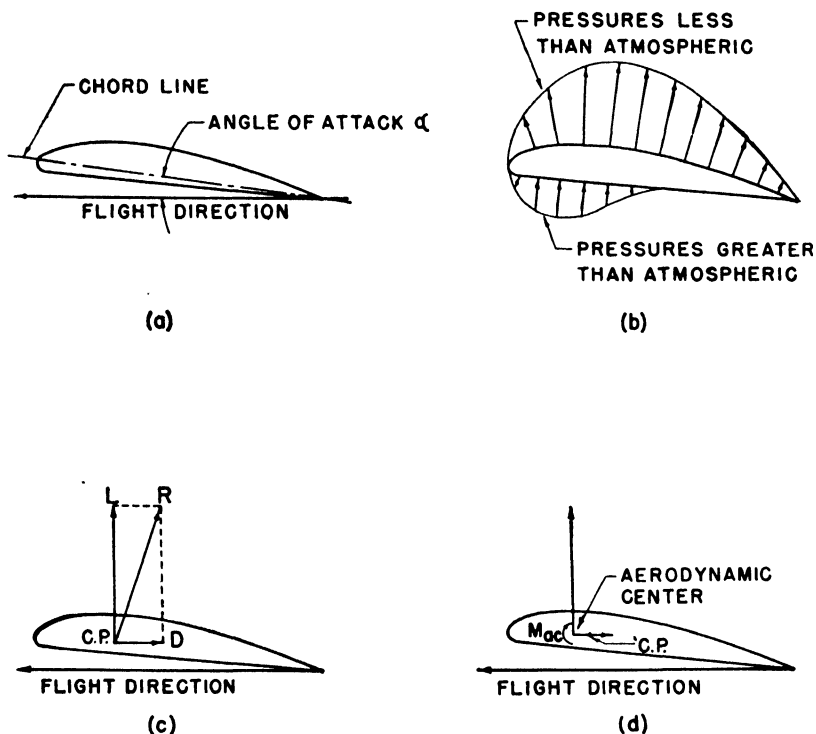
Fig. 2.8.   Airfoil Forces.

operations of the airplane. The definition of limit load given in CAR 04 is *"Limit Load: the maximum load expected in service."* The limit load should not cause yielding of the structure.

2.6 Ultimate load and factor of safety. The limit load should not cause yielding of the structure; a higher load than the limit load is required to rupture the structure. The maximum load which a part of the structure must be capable of supporting without causing failure is called the *ultimate load*, and the ratio between the ultimate load and the limit load is called the *factor of safety*. This factor is sometimes taken as 1.5.

2.7 Aerodynamic forces on airfoil. The lift on the wings is due to the shape of the wing cross section (airfoil), the velocities of the air passing over its surfaces, and other factors. The velocities of the air over the top of the airfoil are increased, causing a decrease in pressure. The pressures on the bottom of the wing are greater than atmospheric because of the decrease in velocity on this surface. This lessening of pressure on the top and increasing of pressure on the bottom results in a force with an upward component. The distribution of pressure for a low angle of attack (LAA) is shown in Figure 2.8(b). The pressure distribution will vary with angle of attack. This pressure variation along the airfoil section is known as the *chordwise load distribution*. The net effect of the pressures acting over an area of the wing can be resolved into a single force acting at the center of pressure, (c.p.) of the section. It is then customary to resolve this force into two components; one perpendicular to the flight direction, called the *lift*, and one parallel to the flight direction, called the *drag*, Figure 2.8(c).

Aerodynamic tests on airfoil sections indicate that the lift and drag forces are proportional to the area of wing, square of the velocity, and the density of the air for a given angle of attack and airfoil section. Also, if the drag force is neglected, a point exists about which the moment of the lift force is a constant for varying angles of attack. This point about which moments are taken is called the *aerodynamic center*, and the forces of lift and drag are usually considered acting at this point, Figure 2.8(d). The equations expressing the relationships for lift, drag, and moment about the aerodynamic center are:

$$L = C_L \frac{\rho}{2} V^2 S \qquad\qquad (2.6)$$

$$D = C_D \frac{\rho}{2} V^2 S$$

$$M = C_M \frac{\rho}{2} V^2 S c$$

where
L = lift (lb)
D = drag (lb)
M = moment (lb ft)
ρ = density of air (slug/ft³) 0.002378 at sea level
S = area of wing (sq ft) .
V = airplane speed (ft/sec)
c = chord of wing (ft)
C_L = coefficient of lift
C_D = coefficient of drag
C_M = coefficient of moment.

The coefficients in the above equations are dimensionless and are determined by the shape of the airfoil section and the angle of attack. The

values of coefficients for a typical airfoil are shown in Figure 2.9. It should be noticed that in this example the coefficient of moment about the aerodynamic center is negative, which indicates a diving moment.

From previous analysis it has been shown that for straight level flight the lift approximately equals the weight of the airplane, $L = W$. Equating the lift to the weight in Equation 2.6 and solving for the velocity, we obtain

$$V = \sqrt{\frac{W}{C_L \frac{\rho}{2} S}}$$

For a given angle of attack, C_L is known; and, if the weight of the airplane, density of the air, and wing area are held constant, the airspeed V is
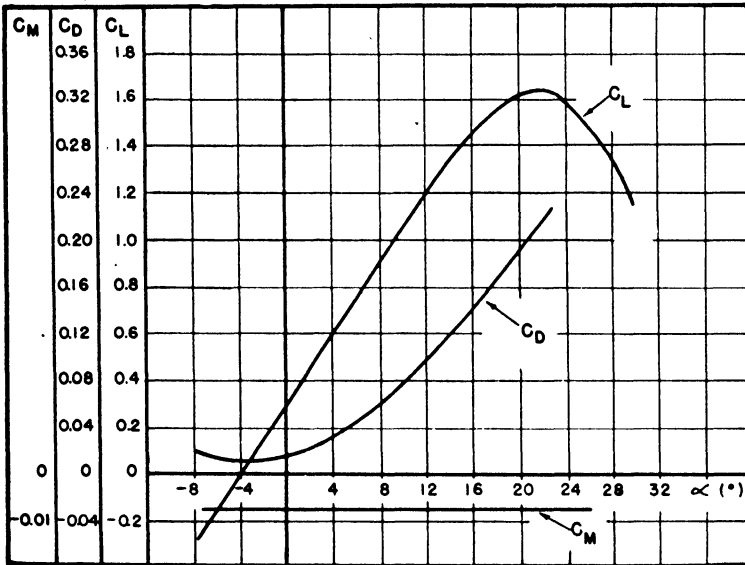
Fig. 2.9. Airfoil Coefficients.

determined. The lowest speed the airplane can fly, the stall speed (V_s), will therefore occur when the angle of attack is such as to make the coefficient of lift a maximum.

$$V_s = \sqrt{\frac{W}{C_{L_{(max)}} \frac{\rho}{2} S}} \tag{2.7}$$

This stall speed becomes important in determining the load factor in pull-ups.

2.8 Gust loads. If an airplane is in level flight and a vertical gust is exerted normal to the flight direction, the effective angle of attack of the wing is increased without a corresponding change in the forward velocity

of the airplane. The change in angle of attack is illustrated in Figure 2.10. An upward gust adds a vertical component of velocity to the horizontal velocity of the airplane so that the relative wind direction is upward and back. Since the coefficient of lift varies almost directly with the angle of attack, a sudden increase in the angle of attack results in a sudden increase in the lift on the wing. The airplane therefore accelerates upward, and a load factor greater than unity is experienced. The change in angle of attack due to gust will depend on the relative magnitudes of the horizontal velocity of the airplane and the vertical gust velocity. Experience has shown that the maximum gust velocity to be
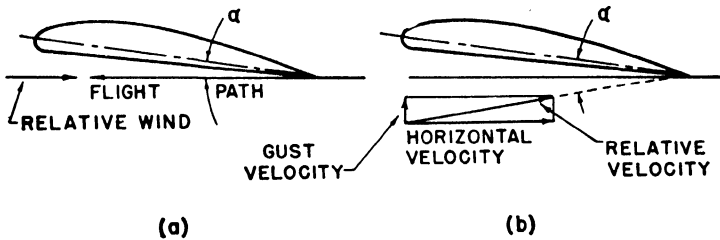
Fig. 2.10. Effect of Gusts.

expected is about 30 fps. Using this gust velocity, we find that the load factor increases approximately directly with the airspeed. It is for this reason that pilots are cautioned to slow down during gusty weather.

The value of the additional load factor due to gust given by CAR 03 is

$$\Delta n = \frac{KUVa}{575 \frac{W}{S}} \tag{2.8}$$

where

$$K = \frac{1}{2}\left(\frac{W}{S}\right)^{\frac{1}{4}} \text{ for } \frac{W}{S} < 16 \text{ lb/ft}^2$$

$$K = 1.33 - \frac{2.67}{\left(\frac{W}{S}\right)^{\frac{1}{4}}} \text{ for } \frac{W}{S} > 16 \text{ lb/ft}^2$$

U = gust velocity (ft/sec)

V = airplane speed (mph)

a = slope of the lift curve, (C_L per radian)

$\frac{W}{S}$ = wing loading (lb/ft^2).

The design shall be made for positive (up) and negative (down) gusts of 30 fps at the design cruising speed V_c and for positive and negative 15 fps gusts at design diving speed V_d. The design cruising speed and design diving speed are designated in CAR 04 and CAR 03 for each

category of airplane.   In general, these speeds are specified in terms of the wing loading.

Since the load factor without gusts for an airplane in level flight is unity, the total load factor with gusts is

$$n = 1 \pm \Delta n \tag{2.9}$$

The negative sign is used for downward gusts.

The gust load factors are assumed to vary linearly between V_c and V_d.

EXAMPLE 2.1.   Determine the gust load factors for a transport airplane weighing 50,000 pounds and having a wing area of 1460 square feet if the design cruising speed is 250 mph and the design dive speed is $1.25V_c$ or 313 mph.   The slope of the lift curve is 4.8.

Solution. $\dfrac{W}{S} = \dfrac{50,000}{1460} = 34.2 \text{ lb/ft}^2$

From Equation 2.8, since $\dfrac{W}{S} > 16 \text{ lb/ft}^2$,

$$K = 1.33 - \frac{2.67}{\left(\dfrac{W}{S}\right)^{\frac{1}{4}}} = 1.33 - \frac{2.67}{(34.2)^{\frac{1}{4}}} = 1.14$$

For V_c, $\Delta n = \dfrac{KUV_c a}{575\,\dfrac{W}{S}} = \dfrac{1.14 \times 30 \times 250 \times 4.8}{575 \times 34.2} = 2.09$

For V_d, $\Delta n = \dfrac{KUV_d a}{575\,\dfrac{W}{S}} = \dfrac{1.14 \times 15 \times 313 \times 4.8}{575 \times 34.2} = 1.31$

Then the gust load factors are

$$n = 1 \pm \Delta n = 1 \pm 2.09 = 3.09 \text{ and } -1.09 \text{ for } V_c$$
$$= 1 \pm \Delta n = 1 \pm 1.31 = 2.31 \text{ and } -0.31 \text{ for } V_d$$

2.9 Loads due to sudden pull-ups.   Another flying condition to be considered is that of sudden pull-up.   If the airplane is flying in an unaccelerated level flight at a given velocity, and the pilot suddenly pulls back on the stick, thereby increasing the angle of attack of the wing, the lift is suddenly increased without a corresponding decrease in airspeed.   Assuming that the pilot pulls up to an angle of attack corresponding to the maximum coefficient of lift, the lift in the wings would be

$$L = C_{L_{(max)}} \frac{\rho}{2} V^2 S$$

The lift before the pull-up equals the weight, and this can be expressed in terms of the stall velocity and the maximum lift coefficient

$$W = C_L \frac{\rho}{2} V^2 S = C_{L_{(max)}} \frac{\rho}{2} V_s^2 S$$

The load factor is therefore

$$n = \frac{L}{W} = \frac{V^2}{V_s^2} \qquad (2.10)$$

2.10 V-n diagram. Among other conditions, the airplane must be designed to withstand the loads imposed by maneuvers, gusts, and pull-ups. These factors must be considered in combination in order to determine the critical load conditions of the airplane. A convenient device for indicating the various load conditions on the airplane is the velocity load factor diagram, otherwise known as the *V-n diagram*. A typical *V-n* diagram is shown in Figure 2.11.
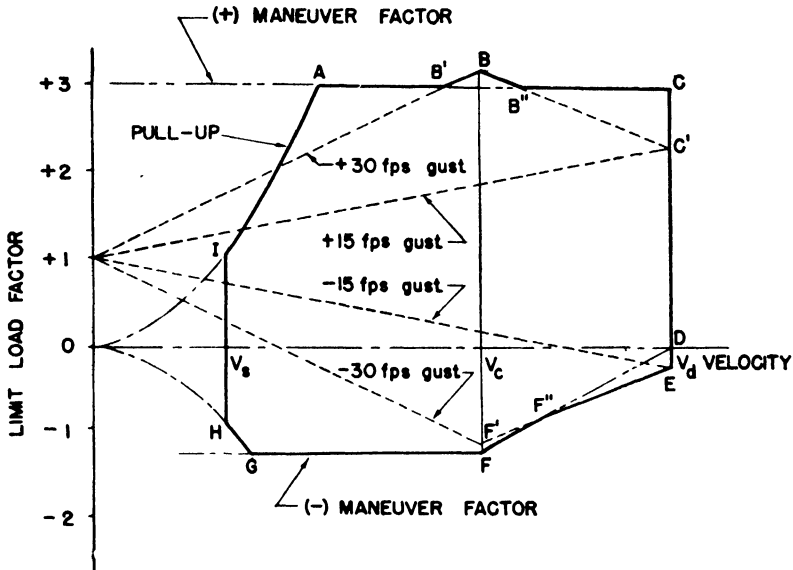
Fig. 2.11. V-n Diagram.

It has been shown that the load factor for pull-ups varies with the square of the velocity. The variation of load factor with velocity can therefore be represented by a parabola as shown by the curves *OIA* and *OHG* of Figure 2.11. Since the airplane cannot fly at a velocity lower than the stall velocity, it is apparent that only the portion of the parabola corresponding to velocities greater than the stall velocity can apply.

It is usual to limit the maneuver load factor of an airplane according to its intended use. Thus, for a transport airplane, which is not designed to do acrobatics, the maneuver load factor is less than for a pursuit airplane. In this example the positive maneuver load factor has been assumed to be 3 and the negative (inverted flight or for loads in the opposite direction to the usual sense) has been assumed to be −1.2. The positive maneuver load factor is specified as constant up to the design

dive speed, and thus line AC represents this condition. The negative maneuver load factors are usually specified a little differently from the positive ones. It is assumed that the negative maneuver load factor is constant up to the design cruising speed but is zero at the design dive speed, and varies linearly between the design cruising speed and the design dive speed. Thus, the line GFD represents this condition.

The gust loads vary linearly with the velocity. Further, the airplane is to be designed for gust loads corresponding to gusts of 30 fps up to the cruising speed and for gusts of 15 fps at the design dive speed with a linear variation of the loads from the design cruising speed to the design dive speed. Thus, the line from the load factor $+1$ to point B represents the variation of load factor with velocity for a $+30$ fps gust, and point C' represents the gust load factor at the design dive speed. The line between B and C' represents the gust load factor between V_c and V_d. The corresponding line for the negative gust is $+1F'E$.

The airplane must be designed to withstand all load factors included on or within the envelope of the curves for pull-ups, gusts, and maneuvers. This envelope is shown by the solid line $IAB'BB''CEF''FGHI$ of the figure. The question may arise of why the line for a $+30$ fps gust at a velocity near the stall velocity is not included in the envelope since the load factor for this condition is greater than for the pull-up condition. The answer is that the pull-up condition corresponds to a high angle of attack for which the coefficient of lift is a maximum and that therefore the gust which effectively increases the angle of attack cannot increase the lift greater than is already indicated by the pull-up. It should be noted also that in this example the load factor for a positive 30 fps gust is greater than the positive maneuver factor in the vicinity of the design cruising velocity. Therefore, at the design cruising speed the design would be based on the gust condition.

It should be noted also that, since point A is on the pull-up line, it corresponds to a high angle of attack condition (HAA). Point C, representing conditions at a high speed V_d, corresponds to a low angle of attack (LAA). Similarly, points G and E are for negative high angles of attack and negative low angles of attack respectively.

2.11 Airplane coefficients and balance. It is convenient to refer the forces acting on the airplane to a set of coordinate axes that are fixed with respect to the airplane and therefore move with it. These axes may be selected in any suitable direction and with any origin. We will assume that the origin is at the center of gravity of the airplane, with the X axis along the fuselage, the Y axis along the wing and perpendicular to the X axis, and the Z axis perpendicular to the other two axes, as shown in Figure 2.12. The forces shown in Figures 2.1, 2.3, 2.5, or similar forces for any other flight conditions, are now resolved into forces along the X, Y, and Z-axes, giving a force in the Z direction at the center

of gravity of P_{Az}, and so forth. The subscript A refers to airplane and the subscript w to the wing.

The forces that include the reversed effective forces are in equilibrium
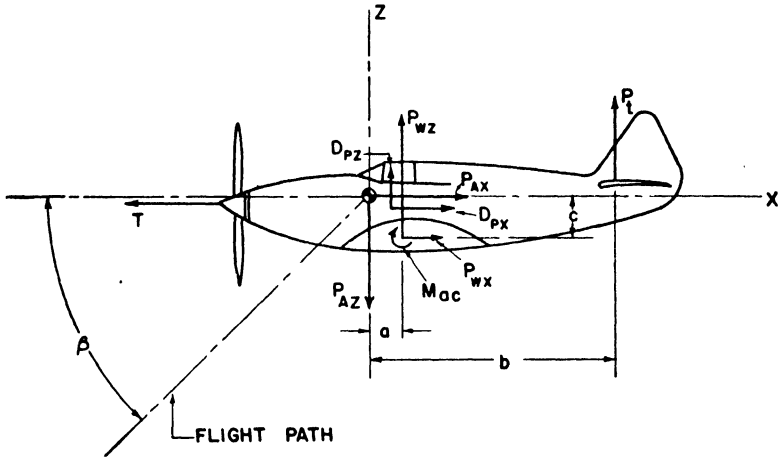
Fig. 2.12. Airplane Balance.

so that the value of a force can be determined in terms of the other forces by applying the conditions of equilibrium. Since the lines of action of the thrust force and the parasite drag usually pass close to the center of gravity for most conventional airplanes, the moments of these forces
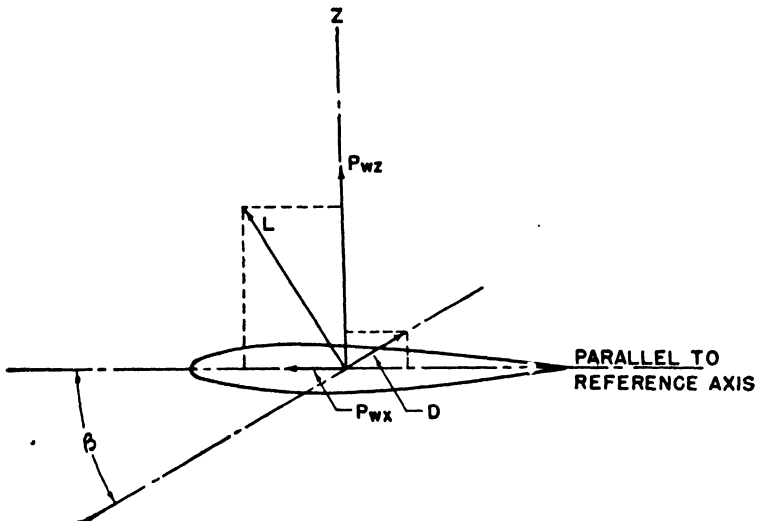
Fig. 2.13. Forces on Airfoil.

about the center of gravity are neglected. Although these moments are neglected in the following analysis, it is apparent how they could be considered.

All the forces can be expressed in terms of dimensionless coefficients similar to those used for lift and drag of an airfoil. Consider for example a wing with a lift and drag force as shown in Figure 2.13. Then the force in the Z direction is given by

$$P_{wz} = L \cos \beta + D \sin \beta$$

but

$$L = C_L \frac{\rho}{2} V^2 S$$

$$D = C_D \frac{\rho}{2} V^2 S$$

therefore,

$$P_{wz} = (C_L \cos \beta + C_D \sin \beta) \frac{\rho}{2} V^2 S$$

Since P_{wz} is proportionate to $\frac{\rho}{2} V^2 S$, let

$$P_{wz} = C_{wz} \frac{\rho}{2} V^2 S$$

where

$$C_{wz} = C_L \cos \beta + C_D \sin \beta \tag{2.11}$$

Similarly, all the other forces can be written

$$P_{Az} = C_{Az} \frac{\rho}{2} V^2 S$$

$$P_t = C_t \frac{\rho}{2} V^2 S$$

$$P_{AX} = C_{AX} \frac{\rho}{2} V^2 S \text{ and so on} \tag{2.12}$$

If the coefficients can be obtained for an airplane by wind tunnel tests or other means, the forces acting on the airplane can be determined for any flight condition. The coefficients for an airplane are shown in Figure 2.14. Of course, the coefficients are functions of the angle β so that for any flight condition the angle must be known before the forces can be determined. The value of β, and therefore the values of the constants, are determined from the design condition, which is determined from the V-n diagram. Suppose, for example, that it is necessary to compute the forces represented by point B on the V-n diagram, Figure 2.11. The load factor, which is the load factor for the whole airplane in the Z direction, for this case is slightly greater than 3 and the speed of the airplane is V_c. Then by definition

$$P_{Az} = nW = C_{Az} \frac{\rho}{2} V^2 S$$

so that

$$C_{Az} = \frac{nW}{\frac{\rho}{2} V^2 S} \tag{2.13}$$

If we have C_{Az}, we can obtain the value of β and all the other coeffi-

cients from Figure 2.14. The forces are calculated then from Equation 2.12.

EXAMPLE 2.2. Determine the forces on an airplane weighing 50,000 pounds and having a wing area of 1460 square feet if it is flying at sea

β	C_t	C_{mac}	C_{WX}	$\dfrac{C_{AZ}}{C_{WZ}}$									
				1.2									
				1.0									
20°	0.04	0.10	0.20	0.8									
15°	0.03			0.6									
10°	0.02	0.05	0.10	0.4									
5°	0.01			0.2									
0°	0	0	0	0									
-5°	-0.01			-0.2									
-10°	-0.02	-0.05	-0.10	-0.4									
-15°	-0.03			-0.6									
-20°	-0.04	-0.10	-0.20	-0.8									
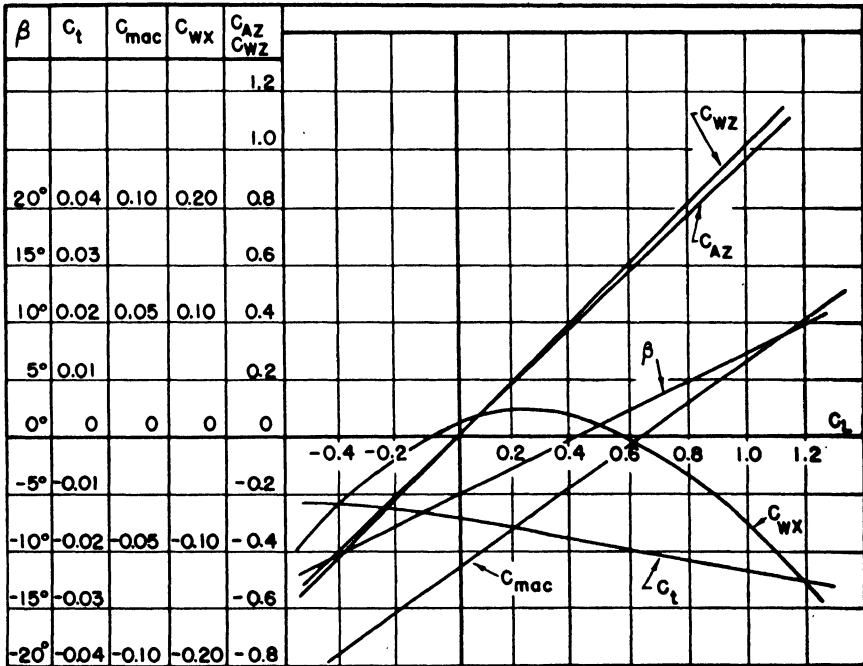
Fig. 2.14. Airplane and Wing Coefficients for Forward Position of C.G.

level with a cruising speed of 250 mph at a load factor of 3.2. The relation of the coefficients are given by Figure 2.14.

Solution.

$$V = 250 \text{ mph} = 367 \text{ ft/sec}$$

$$\frac{\rho}{2} V^2 S = \frac{1}{2} \times 0.002378 \times 367^2 \times 1460 = 233.8 \times 10^3$$

From Equation 2.13, $\quad C_{Az} = \dfrac{nW}{\dfrac{\rho}{2} V^2 S} = \dfrac{3.2 \times 50,000}{233.8 \times 10^3} = 0.684$

From Figure 2.14, corresponding to a C_{Az} of 0.684,

$$\beta = 3°$$
$$C_L = 0.70$$
$$C_{wz} = 0.70$$
$$C_t = -0.022$$
$$C_{wx} = 0.02$$

Then $P_{Az} = nW = 3.2 \times 50{,}000 = 160{,}000$ lb

$$P_{wz} = C_{wz} \frac{\rho}{2} V^2 S = 0.70 \times 233.8 \times 10^3 = 164{,}000 \text{ lb}$$

$$P_t = C_t \frac{\rho}{2} V^2 S = -0.022 \times 233.8 \times 10^3 = -5140 \text{ lb (down)}$$

$$P_{wX} = C_{wX} \frac{\rho}{2} V^2 S = 0.02 \times 233.8 \times 10^3 = 4680 \text{ lb}$$

If the coefficients for the airplane drag were known, the drag forces could be obtained in a similar manner.

It should be noticed that the sum of the forces in the Z direction nearly balance:

$$\Sigma F_z = -160{,}000 - 5140 + 164{,}000 = -1140 \text{ lb}$$

The unbalanced forces would be balanced by the Z component of the drag which has not been considered in the above calculations.

2.12 Airload distribution. In order to design the airplane structure, not only the magnitude of the loads must be known but their distribution as well.

The distribution of lift and drag along the span of a wing depends on many factors. For an untwisted wing with elliptical planform, the lift distribution is a semiellipse. The lift distribution for wings of other planform is more complicated and can be determined by the methods set forth in ANC-1, "Spanwise Airload Distribution." These methods will not be developed here, but some idea of the results will be indicated. .

Consider a wing divided into sections 1 foot apart along the span. The area of each section is therefore equal to the 1 foot times the chord of the wing at that section. The lift, drag, and moment for the 1-foot section will then be

$$l = C_l \frac{\rho}{2} V^2 c$$

$$d = C_d \frac{\rho}{2} V^2 c$$

$$m = C_m \frac{\rho}{2} V^2 c^2 \qquad (2.14)$$

where $l = $ lift per unit length of span (lb/ft)
   $d = $ drag per unit length of span (lb/ft)
   $m = $ moment about aerodynamic center per unit length of span (lb ft/ft)
   $C_l = $ local lift coefficient
   $C_d = $ local drag coefficient
   $C_m = $ local moment coefficient
   $c = $ chord of wing at section (ft).

The local wing coefficients are functions of the angle of attack and the

geometry of the wing, and can be determined by use of the ANC-1. The values of the coefficients together with the associated coefficients in the X and Z directions for a high angle of attack condition are shown in
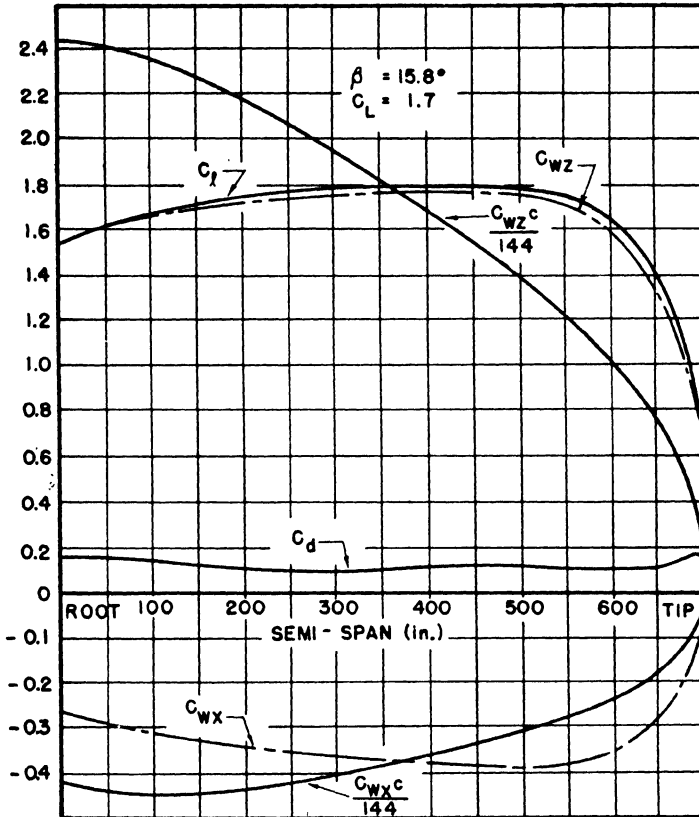
Fig. 2.15. Wing Coefficients for H.A.A.

Figure 2.15. The force per unit length in the Z direction is directly proportional to the values given by the curve $C_{wz}c$.

2.13 Airload distribution on empennage and control surfaces. The load distribution for various control surfaces is specified in the bulletins CAR 04 and CAR 03. Some of these distributions are shown in Figure 2.16. The horizontal tail-balancing load is for the case of maintaining the airplane in equilibrium with zero pitch acceleration. The maneuvering load distribution is for a sudden deflection of the control surface. The w in the figure is load per unit length of chord.

2.14 Ground loads. A rational determination of ground loads, especially those developed during landing, is complicated because of the

multiplicity of factors that enter the problem. An airplane on first contacting the ground is likely to do so with some impact similar to a weight being dropped. This impact deforms the elastic structure of the airplane, which in turn sets up vibrations very difficult to analyze. At the same time the airplane is partially air-borne since it has a forward velocity. Because of the complexity of the problem, the loads acting on the landing gear are somewhat arbitrarily chosen although they are based on experience.
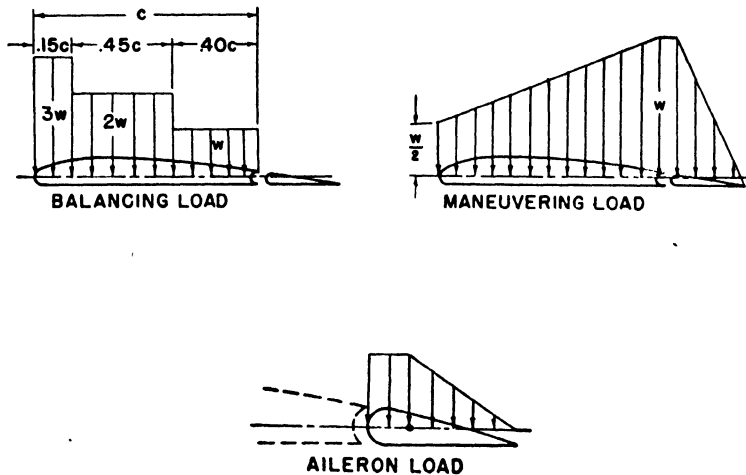
Fig. 2.16.   Control Surface Loads.

As in the case of airloads, it is usual to express the ground loads in terms of load factors that can be determined from the conditions of the design and from the airplane airworthiness specifications. For example, if it is specified that the design shall be made for a vertical descent of 10 fps and a shock absorber travel of 1 foot, the acceleration and therefore the load factor can be determined. If we assume that for the 1-foot travel the acceleration is constant, then we find that

$$A = \frac{V^2}{2s} = \frac{10^2}{2} = 50 \text{ ft/sec}^2$$

The load factor corresponding to this inertia loading is

$$n_I = \frac{A}{g} = \frac{50}{32.2} = 1.55$$

If the airplane were motionless on the ground, the wheels would have to support the weight of the airplane and this would correspond to a load factor of unity. Assuming in the landing condition that one half of the

weight is air-borne, then the load factor at the wheels is the inertia load factor plus the load factor of the non-air-borne weight or finally

$$n = 1.55 + 0.50 = 2.05$$

The total vertical force to be supported by the wheels is nW. The distribution of this force, as well as other forces due to the friction, or inertia forces caused by sliding the tires, spinning the wheels, or braking, depends on the landing condition. A few of these landing conditions and force distributions will now be investigated. The conditions apply to nontransport categories.
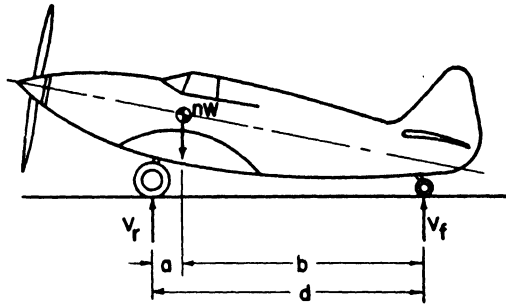
Fig. 2.17. Tail Down Landing.

Tail down landing. In this condition it will be assumed that the wheels have been brought up to speed before the maximum vertical load is applied so that the ground reactions are vertical. The airplane having a tail wheel is then in the attitude shown in Figure 2.17. Since the forces are in equilibrium, the forces on the front wheels can be determined easily.

$$\Sigma M_{tail} = 0 = V_r d - nWb$$
$$V_r = nW \frac{b}{d}$$

The load on the tail wheel is

$$V_t = nW \frac{a}{d}$$

For the airplane with a nose wheel, all the reaction must be taken by the main gear or

$$V_r = nW$$

Level landing. For a level landing condition it is assumed that drag components of force are required to accelerate the wheels up to landing speed. These drag loads are usually expressed in terms of the vertical reaction much the same as a friction force is expressed in terms of a

normal force between two sliding blocks. The situation and notation for the nose wheel type and the tail wheel type of airplane are shown in Figure 2.18. The factor K is defined as

$$K = 0.25 \text{ for } W < 3000 \text{ lb} \tag{2.14}$$
$$K = 0.33 \text{ for } W > 6000 \text{ lb}$$
$$K = 0.25 + \frac{0.035W}{3000} \text{ for } 3000 < W < 6000 \text{ lb}$$

A summary of some of these data is given in the following table taken from CAR 03-0.

Condition		Tail Wheel Type		Nose Wheel Type		
		Level Landing	Tail Down	Level Landing	Level Landing with Nose Wheel Clear	Tail Down
Vertical component at c.g.		nW	nW	nW	nW	nW
Fore and aft component at c.g.		KnW	0	KnW	KnW	0
Main wheel loads (both wheels)	V_r	nW	$nW\frac{b}{d}$	$nW\frac{b'}{d'}$	nW	nW
	D_r	KnW	0	$KnW\frac{b'}{d'}$	KnW	0
Tail (nose) wheel loads	V_f	0	$nW\frac{a}{d}$	$nW\frac{a'}{d'}$	0	0
	D_f	0	0	$KnW\frac{a'}{d'}$	0	0

n = limit load factor

It should be emphasized again that only a few of the landing conditions have been discussed. Therefore, the student is referred to the government bulletins for further details.

2.15 Weight distribution. In determining the airloads and ground loads, it has been convenient to consider the weight of the airplane concentrated at the center of gravity. This is a valid method for determining external loads, but for structural analysis the distribution of the weight should be known. The weight distribution for continuous structures, such as wings and fuselage, should be determined together with the location and amount of concentrated weight, such as fuel tanks, radio, baggage, armament, and so forth.
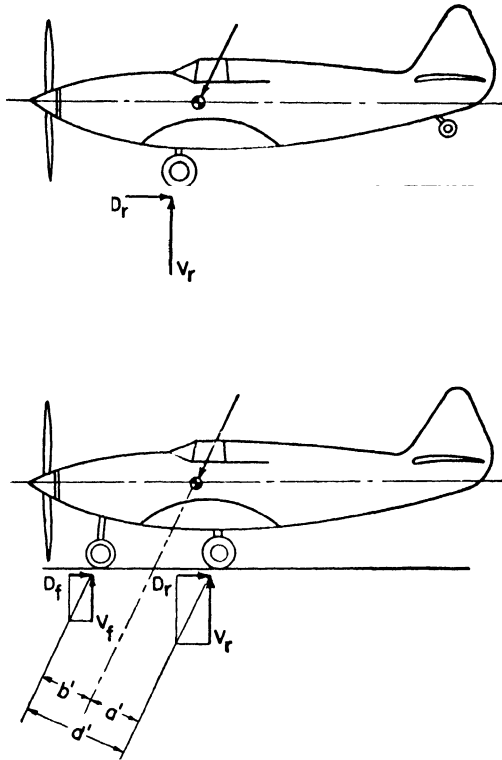
Fig. 2.18. Level Landing.

Problems

2.1. If the following data apply to the airplane shown in Figure 2.1

$$\text{gross weight} = 1450 \text{ lb}$$
$$\text{span of wing} = 35 \text{ ft}$$
$$\text{mean wing chord} = 62 \text{ in}$$
$$\text{limit load factor} = 4$$
$$\text{factor of safety} = 1.5$$
$$\text{total drag, } D_w + D_p \text{ passes through the c.g.}$$
$$b = 10 \text{ in}$$
$$c = 5 \text{ in}$$
$$d = 13 \text{ ft}$$

determine

(a) ultimate wing load
(b) limit load on horizontal stabilizer when the propeller thrust is 420 lb
(c) chordwise limit load distribution on horizontal stabilizer if the chord is 24 in.

2.2. If an airplane weighing 6000 pounds has a limit maneuver load factor of 5, determine the smallest radius of turn it can make when traveling at a speed of 400 mph.

2.3. Determine the load factor due to a sudden pull-up for an airplane weighing 2000 pounds and having a wing area of 90 square feet for which $C_{L(max)} = 1.8$, if the airplane is flying 100 mph at sea level atmospheric conditions.

2.4. Determine the gust load factors for an airplane with a wing loading of 33 pounds per square foot if the design cruising speed is 300 mph, the design dive speed is 450 mph, and the slope of the lift curve is 4.5.

2.5. Determine values and draw the V-n diagram for an airplane having the following specifications:

$$V_c = 325 \text{ mph}$$
$$V_d = 1.2V_c$$
$$V_s = 0.33V_c \text{ (flaps up)}$$
Limit maneuver factors, $+6$, -2,
wing loading $= 35 \text{ lb/ft}^2$
slope of lift curve $= 4.1$

2.6. An airplane with a wing area of 2000 square feet and a gross weight of 60,000 pounds is to be designed for a limit load factor of 3.5 at a speed of 300 mph.
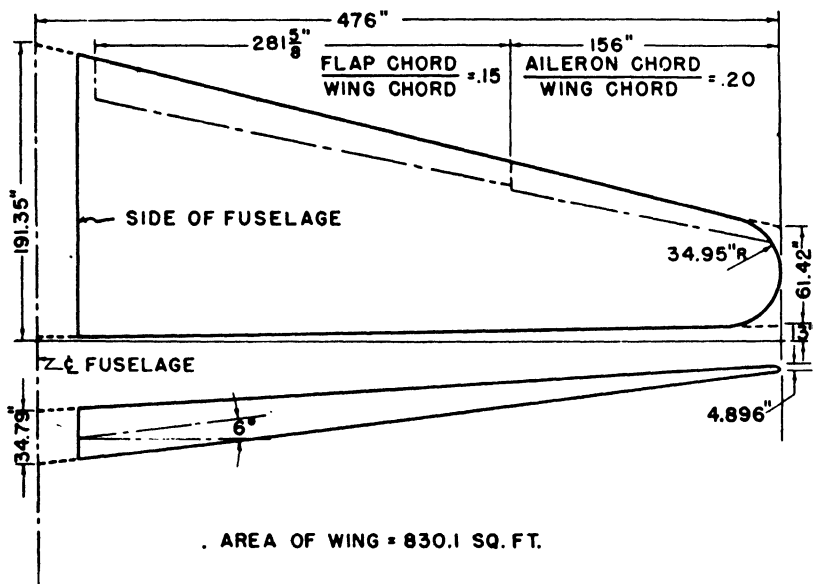
Fig. 2.19. Wing Layout.

If the tail coefficient C_t is -0.045 times the airplane coefficient C_{Az}, what is the tail load for sea level conditions?

2.7. An airplane similar to that shown in Figure 2.12 has a gross weight of 2100 pounds, a wing span of 40 feet, and a wing area of 204 square feet. For a low angle of attack ($\beta = 2°$) the limit load factor is 3.2 and the design speed is 190 mph. If $C_D = 0.08C_L$, $C_M = -0.01C_L$ and $a = 10$ inches, $b = 218$ inches, and $c = 14$ inches, determine

(a) coefficient of lift, assuming all load carried by wing (neglect tail)
(b) C_Z and C_X
(c) P_{wZ} and P_{wX}

(d) tail load for balancing, assuming thrust and parasite drag pass through the c.g.

(e) distribution of balancing load on horizontal stabilizer when the chord of the stabilizer is 20 inches.

2.8. A twin engine passenger airplane weighing 21,000 pounds has a wing as shown in Figure 2.19. The specifications for high angle of attack indicate that the limit load factor should not exceed 4.5 for a design speed of 194 mph.

If the following table gives the aerodynamic coefficients for the wing at HAA, determine the lift, drag, and moment distribution.

Draw curves of all load distributions.

NACA Series 230 Airfoil
(From ANC-1(1))

Percent of semi-span	0	20	40	60	80	90	95	97.5	100
Distance from $\mathfrak{t}$	0	95.2	190.4	285.6	380.8	428.4	452.2	464.1	476
Chord c	191.35	165.36	139.38	113.39	87.41	74.41	67.92	64.67	61.42
Aerodynamic center Fraction c	.2275	.2288	.2302	.2323	.2347	.2357	.2360	.2360	.2359

Aerodynamic Coefficients for $\alpha = 14°$, $C_L = 1.184$

Lift C_l	1.057	1.162	1.221	1.266	1.250	1.157	1.000	0.799	0
Drag C_d	.0949	.0789	.0685	.0601	.0645	.0831	.1041	.1170	—
Moment C_m	−.0062	−.0065	−.0070	−.0078	−.0086	−.0094	−.0099	−.0101	−.0105

2.9. Determine the reaction at the wheels for an airplane weighing 10,000 pounds and having a tail wheel as shown in Figure 2.17 if $a = 2$ feet and $d = 40$ feet and the limit load factor is 2.2.

2.10. For an airplane with nose wheel and the same conditions as those in Problem 2.9, except that the horizontal distance from the nose wheel to line of main wheels is 10 feet and the distance from the nose wheel to the center of gravity is 8 feet $10\frac{1}{2}$ inches, determine the wheel reactions. The distance from the center of gravity to the ground is 5 feet.

References

ANC-1(1), "Spanwise Airload Distribution." Army-Navy-Commerce Committee on Aircraft Requirements. April 1938.

ANC-1(2), "Chordwise Air-load Distribution." Army-Navy-Commerce Committee·on Aircraft Design Criteria. October 1942.

ANC-2, "Ground Loads Handbook." Army-Navy-Commerce Committee on Aircraft Design Criteria. October 1941.

Civil Aeronautics Manual 04, "Airplane Airworthiness." Revised July 1, 1944.

Civil Air Regulations Amendment 03-0, "Airplane. Airworthiness, Normal, Utility, Acrobatics, and Restricted Purpose Categories." November 13, 1945.

Civil Air Regulations Amendment 04-0, "Airplane Airworthiness, Transport Categories." November 9, 1945.

Part II
STRUCTURAL ANALYSIS

CHAPTER 3

Behavior of Loaded Material

....

3.1 Introduction. The various airloads and ground loads to which the aircraft is subjected must be transmitted through the airframe. The action of these loads on the structure can be divided into five major types: (a) tension, (b) compression, (c) shear, (d) bending, and (e) torsion. An example of a tensile action is the pull of the propeller which is transmitted along the propeller shaft. A torque or twisting action is also transmitted along the propeller shaft because of the propeller drag absorbing the powerplant torque. A compressive load is transmitted along the landing gear strut during landing. The airload on a wing causing it to become curved spanwise is an example of a bending action. The action on a rivet connecting two plates being pulled in opposite directions is an example of shear.

Structural design consists largely in properly proportioning the structural members to carry the loads. It is therefore necessary to know the amount of load the structural material can safely withstand. The basis for the material strength depends on the physical properties obtained from tests made on the materials from which the structural members are fabricated.

3.2 Physical properties of materials. At the present time the most common materials used for aircraft construction are the various aluminum alloys, steels, and magnesium alloys. Brass, copper, rubber, wood, and plastics are also extensively used, and it is probable that other new materials will be used in the future. All these materials have characteristics which must be determined before they can be used satisfactorily. Some of these characteristics, called physical properties, will now be considered.

If a specimen, such as an aluminum rod, is held vertically by one end with a weight fastened to the other end, the rod will stretch or *elongate*. This deformation may be so small that precision instruments called *strain gages* are required to measure it. If, on removal of the weight, the rod regains its former length and shape, it is said to be perfectly *elastic*. If successively heavier and heavier weights are applied, eventually the rod will not regain its initial length when the weights are removed. The elongation of the rod remaining after the removal of the load is called *permanent set*. During loading the material has passed the elastic limit and become *partially plastic* or *inelastic*. If the load is continually increased, the rod will break or rupture.

Stress and strain are convenient measures of some of the physical

properties of materials and are useful in comparing properties of several materials.

3.3 Stress and strain. Stress is a measure of the intensity of force acting at a point within the material. *Stress* is the *force per unit of area.*

Consider a uniform circular rod with an axial tensile load P applied to each end, Figure 3.1. The stress conditions on various sections within the cylinder will be different. If we assume that the load is distributed uniformly on a transverse cross section, we will see that the stress on section A-A, which is on a plane perpendicular to the axis of the cylinder, is given by

$$f = \frac{P}{A} \qquad (3.1)$$

where f = tensile stress (psi)
P = tensile load (lb)
A = cross-sectional area of rod (sq in).

This stress is called a *tensile stress.* If the stress on an oblique plane such as B-B is considered, it is evident that, since the area of this section is greater than before, the stress will be less. It is customary to consider stresses on an oblique surface divided into two components, as indicated on C-C. The stress perpendicular to the surface is called the *normal stress* and the stress parallel to the surface is called the *shear stress.* The stress conditions on section A-A consist of a normal stress P/A with no shear stress.

Under the action of the load P the cylinder will elongate in the axial direction an amount δ. The amount of elongation per unit length is called the *axial strain* and is given by

$$\epsilon = \frac{\delta}{L} \qquad (3.2)$$

Fig. 3.1. Stress Conditions in Tensile Specimen.

where
ϵ = axial strain (in/in)
δ = elongation of member (in)
L = original length of member (in).

The relationship between stress and strain provides data useful for design. This relationship for a material may be established by recording simultaneously the values of stress and strain obtained from tensile tests of a specimen. The diagram representing the variation of stress and strain is called a *stress-strain diagram* and has the general form indicated in Figure 3.2. It should be emphasized that the stress used in the stress-strain curve is the load divided by the *original* cross-section area

of the specimen, and the strain is the average strain taken over a certain length called the *gage length*, which is usually two inches.   Since the area of the cross section reduces during loading, the stress calculated on the basis of the original area is not the true stress.   Similarly, the strain is not the true local strain because the strain over the gage length is not uniform.   True-stress true-strain data are now being used in the solution
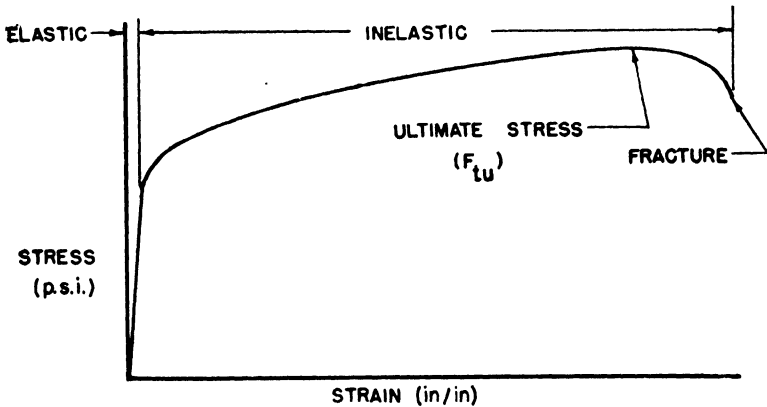
Fig. 3.2(a).   Stress-Strain Diagram for Aluminum Alloy.
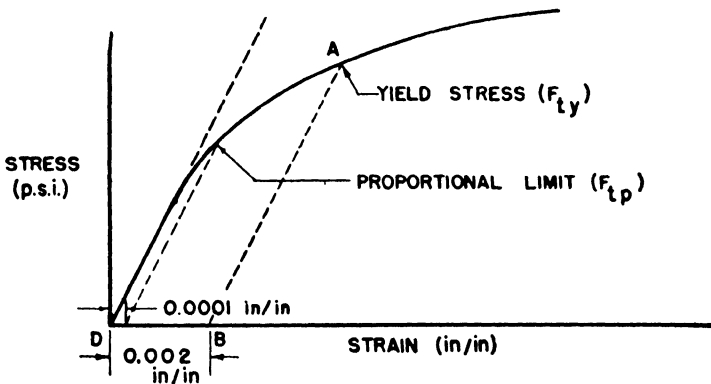
Fig. 3.2(b).   Details of Initial Range of Stress-Strain Diagram.

of some forming problems; however, the conventional stress-strain relation is used for structural design.

3.4 Proportional limit (elastic limit).   Stress-strain diagrams, such as those shown in Figure 3.2, indicate that there is a range for which the stress is directly proportional to the strain.   This is known as the *elastic range* as indicated in Figure 3.2(a), and beyond this range of stress the material is *inelastic* or *plastic*.   The value of the stress corresponding to the end of the range where the stress is no longer directly proportional to the strain is called the *proportional limit* and is denoted by the symbol F_{tp}

for the tension case. As long as the proportional limit is not exceeded the material will return to its original shape and size and will not have permanent set when the stress is reduced to zero.

The proportional limit is sometimes difficult to determine since it is the point at which the stress-strain curve departs from a straight line. The proportional limit is sometimes specified as the stress corresponding to a permanent set of 0.0001 inches per inch. The method of determining the permanent set is explained in the next article.

3.5 Yield stress. If a material is loaded so that the stress-strain curve will be as shown up to point *A* of Figure 3.2(b) and then the load reduced to zero, it will be found that the material unloads along line *AB* so that the residual strain or permanent set remaining at zero stress is *OB*. It has been arbitrarily decided that the yield stress corresponds to a permanent set of 0.002 inches per inch. The yield stress is determined by the intersection between the stress-strain curve and a straight line parallel to the slope of stress-strain curve in the elastic range and passing through a permanent set corresponding to 0.002 inches per inch.

The strain scale is greatly magnified in Figure 3.2(b) and therefore gives an erroneous impression of the relation between the yield stress and proportional limit. Actually the yield stress is only very slightly in the inelastic range.

3.6 Ultimate stress. The maximum value of the stress obtained is called the *ultimate stress*. It may seem peculiar that the ultimate stress does not correspond to the fracture point in the stress-strain curve until it is remembered that the stress is based on the original cross-section area of the test specimen. As the specimen is loaded it is found that the load increases whereas the cross-section area decreases. Eventually a point is reached where the area continues to decrease without increase in load as the stretching of the material is continued in the test machine. When this occurs the ultimate stress has been reached.

3.7 Poisson's ratio. Experiment shows that as the tensile specimen is elongated by the load the size of the cross section decreases. The ratio of the lateral strain to the axial strain is found to be constant for a material in the elastic range and is known as *Poisson's ratio*, μ. The value of Poisson's ratio for steel is about 0.3. Therefore, for an axial strain of 0.001 inches per inch, there will be a contraction in the radial direction of the cross section of $0.001 \times 0.3 = 0.0003$ inches per inch.

3.8 Modulus of elasticity. Since the stress is proportional to the strain in the elastic range, then, if the constant of proportionality is E,

$$f = E\epsilon$$

or $\qquad E = \dfrac{f}{\epsilon}$ $\hfill$ (3.3)

where $\quad E$ = modulus of elasticity (Young's modulus) (psi).

This constant of proportionality is called the *modulus of elasticity*, and it is a measure of the stiffness of the material. It should be noticed that the modulus has the same dimensions as stress, namely, pounds per square inch. Geometrically, the modulus of elasticity is the slope of the stress-strain curve.

The higher the modulus of elasticity, the greater the resistance of the material to deformation. The elongation of a tension member can now be obtained by use of Equations 3.1, 3.2 and 3.3. Thus,

$$E = \frac{f}{\epsilon} = \frac{P}{A} \bigg/ \frac{\delta}{L}$$

Then
$$\delta = \frac{PL}{AE} \qquad\qquad (3.4)$$

If it were possible to elongate the tension member a distance equal to its
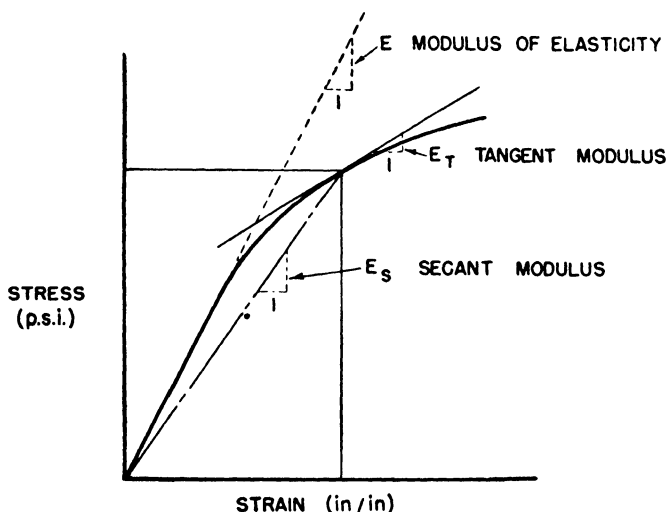
Fig. 3.3. Moduli.

own original length, the stress required would be equal to the modulus of elasticity, or

$$\frac{P}{A} = f = \frac{E\delta}{L} = E$$

Of course, materials would fracture long before such a stress could be applied. If it is remembered that steel has a modulus of elasticity of about 30 million pounds per square inch, some idea of the stiffness of the material can be realized.

The modulus of elasticity as previously defined applies only to the material in the elastic range, so that the stress is below the proportional limit. It is convenient, however, to define a somewhat similar quantity in the inelastic range called the *tangent modulus*.

The tangent modulus, E_T, is equal to the slope of the stress-strain curve at any point, Figure 3.3,

or
$$E_T = \frac{df}{d\epsilon} \tag{3.5}$$

It is evident that the tangent modulus is not a constant in the inelastic range but is a function of the stress. The tangent modulus reduces to the ordinary modulus of elasticity in the elastic range.

Curves showing the variation of tangent modulus with stress are given in the ANC-5.

3.9 Elastic energy. For the simple tensile specimen, we have seen that, as the load P is gradually increased, the elongation increases directly with the load as long as the material is elastic. Since the load starts at zero and ends at some value P at the time the elongation is δ, the work done by the force is the product of the *average* force times the distance through which it moves. Since this energy can be recovered in the unloading process, it must be stored in the specimen in the form of potential energy. This energy is known as *elastic energy* and is given by

$$U = \frac{P\delta}{2} \tag{3.6}$$

where U = elastic energy (lb in).

By use of Equation 3.4 the elastic energy can be obtained in terms of the load, the geometric properties of the rod, and the elastic properties of the material.

$$U = \frac{P^2 L}{2AE} \tag{3.7}$$

The elastic energy per unit volume that can be stored in the rod without permanent set is called the *modulus of resilience* and is given by

$$U = \frac{F_p^2}{2E} \tag{3.8}$$

where F_p = proportional limit (psi).

3.10 Endurance limit. The properties of materials previously discussed have been obtained from tests in which the load is gradually applied and unrepeated. It is well known that, if the load is fluctuating so that the stresses vary with time, failure of the material can occur at a stress lower than the ultimate stress obtained from static test. The stress which a member can just withstand for an infinite number of load cycles is called the *endurance limit*. This failure is known as *fatigue failure* and must be considered in the design of a structure subjected to vibration or impact conditions.

3.11 Structural failure and allowable stresses. The *allowable stress* for a member is the stress that must not be exceeded if failure of the

member is to be prevented. Structural failure does not always imply rupture of a member; failure may be any condition which impairs the satisfactory functioning of a member. Thus, if an excessive amount of permanent set is to be avoided, the stress in the member should not exceed the yield stress, in which case the allowable stress is the yield stress. The stress in a member, subjected to a vibratory load condition, should not exceed the endurance limit, in which case the allowable stress is the endurance limit. The selection of the allowable stress depends on the conditions of the design and the judgment of the designer, or it is specified by the licensing authority.

The allowable stresses for a simple tension member may be the yield stress, proportional limit, or ultimate stress, depending on the conditions of the design. The allowable stresses are denoted by a capital F, such as F_{ty}, and so on. Since allowable stresses are necessary for members other than those in simple tension, other tests such as compression, shear, and bearing must be made.

3.12 Margin of safety. It is necessary to have some means of comparing the value of the load or stress a structural member can carry safely without failure with the load or stress actually imposed on the member. This relation is usually expressed by the margin of safety defined as follows:

$$MS = \frac{\text{allowable load}}{\text{actual load}} - 1$$

$$MS = \frac{\text{allowable stress}}{\text{actual stress}} - 1 \tag{3.9}$$

EXAMPLE 3.1. Determine the margin of safety on yielding of a $\frac{1}{2}$-inch O.D. normalized 4130 rod carrying a limit tensile load of 13,000 pounds.

Solution. The actual tensile stress in the rod is

$$f_t = \frac{P}{A} = \frac{13,000}{\frac{\pi}{4} \times \left(\frac{1}{2}\right)^2} = 66,300 \text{ psi}$$

The allowable yield stress from page 4-12 of ANC-5 is

$$F_{ty} = 70,000 \text{ psi}$$

Therefore,

$$MS = \frac{F_{ty}}{f_t} - 1 = \frac{70,000}{66,300} - 1 = .06 \text{ or } 6\%.$$

This means the member is able to withstand 6% more than the limit load of 13,000 pounds before yielding.

A negative margin of safety indicates that the structure is weaker than required.

The Civil Aeronautics Authority specifies the following minimum margins of safety. All fittings, 20%; castings, 100%; parts subjected to shock loads, 100%; aluminum alloys and steel parts in bearing with repeated reversed loading, 50%.

Problems

3.1. Determine the elongation of a steel rod 20 inches long if the tensile stress is 20,000 psi.

3.2. The elongation of an aluminum rod $\frac{1}{2}$ inch in diameter and 30 inches long is found to be 0.012 inches owing to the action of tensile load. Determine the value of the load.
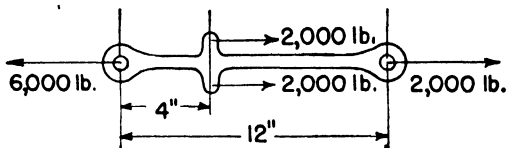
Fig. 3.4. Tension Link.

3.3. Determine the elongation of the steel bar shown in Figure 3.4 if the area of the cross section is 0.5 square inch.

3.4. A 17ST aluminum alloy fitting with a cross-section area of 0.30 square inch is subjected to a tensile load of 15,000 pounds. Determine

(a) the margin of safety if
$$F_{tu} = 55,000 \text{ psi}$$

(b) the load required to produce yielding.
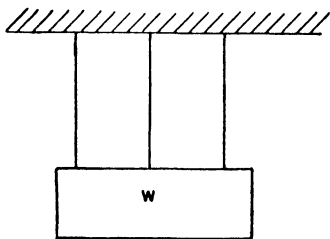
Fig. 3.5. Wire Suspension.

3.5. A rigid body of weight W hangs from three equally spaced wires as shown in Figure 3.5.

(a) If all the wires are steel and the cross-sectional area of each wire is 0.0625 square inches, determine the stress in each wire.

(b) If the outer wires are aluminum and the center wire steel, determine the stresses in each wire. (*Note:* All wires elongate same amount.)

(c) If one outer wire and the center wire are aluminum and the other outer wire is steel, determine the stresses.

3.6. Of three materials, 4130 steel, 17ST aluminum, and magnesium alloy, determine the lightest of three rods carrying a tensile load of 20,000 pounds which causes a yield stress in each.

References

ANC-5, "Strength of Metal Aircraft Elements," Army-Navy Civil Committee on Aircraft Design Criteria. Revised Edition, December 1942; with Amendment No. 2, August 1946.

CHAPTER 4

Load Transmission in Single Span Beams
and Cantilever Beams

4.1 Introduction. The transmission of load through the structure may depend upon the behavior of the material during the application of the load. In many cases, however, the distribution of the loads in the members of the structure depends only on force equilibrium of the structure and not at all on the stiffness or other characteristics of the material. If the distribution of loads can be determined from conditions of statical equilibrium alone, namely the summation of moments and forces equal to zero, it is said to be *statically determinate;* and, if other conditions such as the deformations of the structure are required for the determination of the load distribution, the structure is said to be *statically indeterminate.*

Of the various members carrying loads of tension, compression, shear, torsion, and bending, the members subjected to some bending action
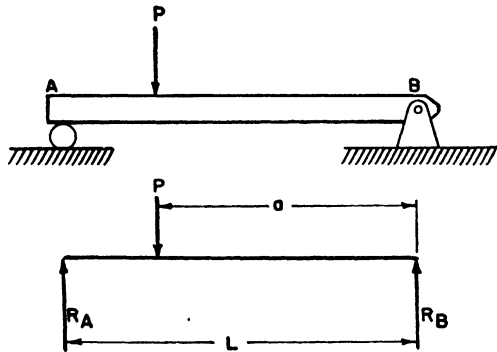
Fig. 4.1. Simple Beam with Concentrated Load.

(although this action is usually accompanied by the other actions of shear, torsion, and so forth), are usually called *beams.* Many components of the airframe can be thought of as beam components. For example, the wing, the fuselage, or the longitudinal members supporting the floor are beams. When beams extend between only two supports, they are called *single-span beams;* and depending on the conditions at the supports they can be either statically determinate or statically indeterminate. Multiple-span beams, beams with more than two supports, are always statically indeterminate.

The determination of the reactions, deflections and distribution of

shears and bending moments in single-span beams and cantilever beams will be discuss

4.2 External reactions. If a beam is statically determinate, the reactions at the supports can be determined from the equations of statical equilibrium, $\Sigma M = 0$, $\Sigma F = 0$. From the free body diagram of the simple beam shown in Figure 4.1, it is apparent that there are two unknown reactions, R_A and R_B. If moments about any convenient point, say B, are summed,
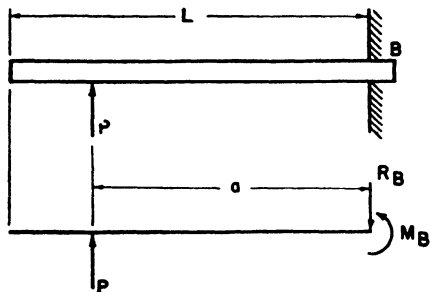
Fig. 4.2. Cantilever Beam with Concentrated Load.

$$\Sigma M_B = 0 = R_A L - Pa$$

$$R_A = \frac{a}{L} P$$

Since the sum of the forces in the vertical direction must be zero,

$$\Sigma F_V = 0 = R_A - P + R_B$$

$$R_B = P - R_A = P\left(1 - \frac{a}{L}\right)$$

In the case of the cantilever beam shown in Figure 4.2, it is apparent
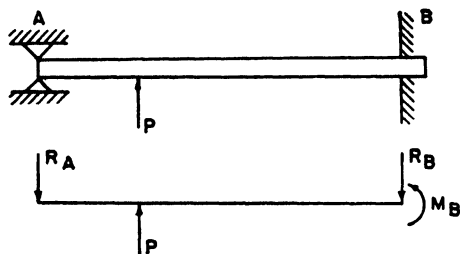
Fig. 4.3. Supported Cantilever.

again that the equations of statics are sufficient for determining the reactions.

Thus,

$$\Sigma F_V = 0 = R_B - P$$

$$R_B = P$$

$$\Sigma M_B = 0 = M_B - Pa$$

$$M_B = Pa$$

However, if the end of the cantilever is supported as shown in Figure 4.3, there are three unknown reactions R_A, R_B, and M_B and only two equations for determining the reactions, namely, the summation of moments in the plane of the forces equal to zero and the summation of the forces

in the vertical direction equal to zero. Summing forces in the horizontal direction does not give any additional information since there are no forces in the horizontal direction. This beam is therefore statically indeterminate, and one additional condition is required for the solution which will be considered in a later article.

4.3 Internal forces. The external loads and reactions on a beam cause internal forces in the beam. These internal actions can be divided into a *shearing force*, V, and a *bend-ing moment*, M. Consider the canti-lever beam shown in Figure 4.4, cut at section *a-b*; then consider the beam forces required on the cut sec-tion to hold the left portion of the beam in equilibrium. Since this portion is in equilibrium, the sum of the vertical forces and the sum of the moments must be zero. If we assume that the internal force V is downward on the right end of the left portion, then we see that

$$\Sigma F = 0 = P - V$$
$$V = P$$

If we take moments about the cut section, it is apparent to us that

$$\Sigma M = 0 = M - Px$$
$$M = Px$$

Since there are no external forces acting on the cut between the two

Fig. 4.4. Shear and Bending in Cantilever Beam.

portions, the internal forces must be balanced on the two faces, or the moments and forces on the two sides must be equal and opposite.

The distribution of shear and moment will be as shown in Figure 4.4. The sign convention for the positive directions of shear and bending moment will be as follows. The shearing force is positive if the left portion of the beam tends to move upward relative to the right portion. The bending moment is positive if it tends to curve the beam concave upward. It should be noticed particularly that positive beam bending moments can be clockwise or counterclockwise depending upon the side of the cut being investigated.

The distribution of shear force and bending moment for a beam carry-ing more than one load can be determined by adding together or super-imposing the effect of each load acting separately. This is an application of the *principle of superposition* that will be more completely discussed

in the next chapter. An example of superimposed systems is shown in Figure 4.5.

If more and more loads are applied closer and closer together, the condition of a continuously distributed load will be approached. The intensity of the distributed load will be in force per unit length of beam. As more and more equal loads equally spaced are added in Figure 4.5, the

LOADING

SHEAR FORCE

BENDING MOMENT
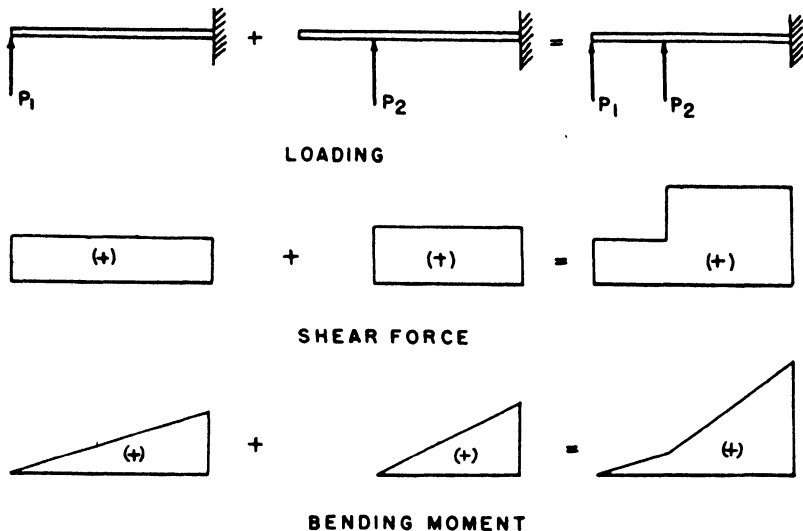
Fig. 4.5. Cantilever Beam with Two Concentrated Loads.

more uniform the load tends to become, and the shear and moment curves become smooth without discontinuities.

4.4 Load, shear, and moment relations. Some general relations between load, shear, and moment can be established that will be useful for determining the shear and moment distributions and their characteristics.

Consider the simply supported beam shown in Figure 4.6 carrying a distributed load p where p is the intensity of load in force per unit length of beam.

Then $$p = f(x)$$

For a small element of the length of beam Δx, the loading can be considered uniform with good approximation as long as the loading for the interval is continuous. If we assume that the shear force changes by an amount ΔV from the left side of the element to the right and similarly that the moment changes by an amount ΔM, then we find that, since the total external load for the element is $p \, \Delta x$, where p is the average intensity for the interval,

$$\Sigma F = 0 = V - (V + \Delta V) + p\,\Delta x$$

$$\frac{\Delta V}{\Delta x} = p \tag{4.1}$$

$$\Sigma M = 0 = M + V\,\Delta x + p\,\Delta x\,\frac{\Delta x}{2} - (M + \Delta M)$$

$$\frac{\Delta M}{\Delta x} = V + p\,\frac{\Delta x}{2} \tag{4.2}$$
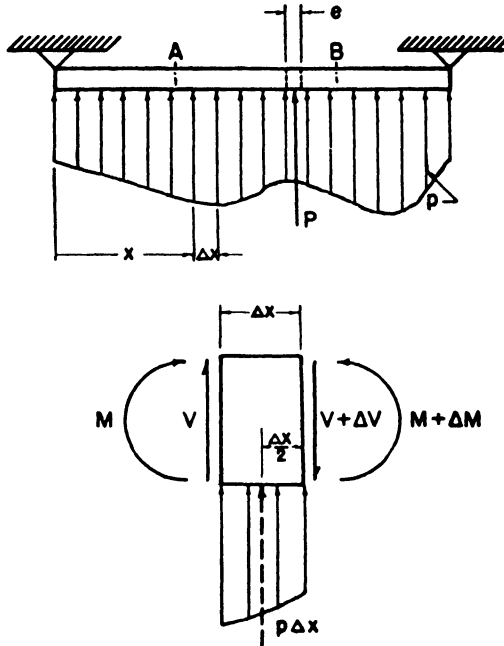
Fig. 4.6.   Beam with Distributed Load.

The limit of the ratios as $\Delta x \to 0$ are the well-known relations

$$\frac{dV}{dx} = p \tag{4.3}$$

$$\frac{dM}{dx} = V \tag{4.4}$$

also
$$p = \frac{dV}{dx} = \frac{d^2M}{dx^2}$$

Geometrically, Equation 4.3 indicates that the slope of the shear curve at any point is equal to the intensity of the load at that point.   A sudden change in the intensity of the load, such as for a concentrated load, indicates a sudden change in the slope of the shear curve.   In a similar manner, the slope of the moment curve is equal to the value of the shear force at a point.   A sudden change in the shear force corresponds to a sudden change in the slope of the moment curve.   It should further

be noted that when the shear is zero the slope of the moment curve is zero, which thereby indicates a possible position of maximum or minimum moment.

The change in shear force between any two points, such as A and B of the beam shown in Figure 4.6, can be determined from Equation 4.3. Solving for dV and integrating both sides, we have

$$\int_A^B dV = \int_A^B p\, dx$$

or $V_B - V_A = \int_A^B p\, dx = $ (area of load curve between A and B)   (4.5)

Hence, if the distribution of load p is a known function of x, the change in shear forces between any two sections of the beam can be determined. It is useful also to remember that the integral on the right side of Equation 4.5 can be interpreted as the area of the load curve between A and B. In many cases where the integration would be difficult, summation processes, when this latter interpretation is used, can be employed advantageously.

A difficulty in using Equation 4.5 may occur when the interval A, B contains a concentrated load. Supposing such a concentrated load does exist, then the integration can be divided into two parts, one containing the concentrated load and the other the distributed loading. The concentrated load can be thought of as a distributed load of higher intensity p_1 spread over a small beam length c. The load then can be defined as

$$P = \int_0^c p_1\, dx_1$$

the change in shear is therefore

$$V_B - V_A = \int_A^B p\, dx + \int_0^c p_1\, dx_1 = \int_A^B p\, dx + P \qquad (4.6)$$

Similar relations exist for the shear and moment so that

$$M_B - M_A = \int_A^B V\, dx = \text{(area of shear curve between } A \text{ and } B) \qquad (4.7)$$

EXAMPLE 4.1.   Determine the shear force and bending moment distribution for the idealized wing with an external strut brace and a uniform airload as shown in Figure 4.7. Neglect the effect of axial thrust on bending.

$$w = 10 \text{ lb/in}; L = 100 \text{ in}; a = 70 \text{ in}; \alpha = 20°$$

Solution.

Reactions: $\Sigma M_B = 0 = P_y a - \dfrac{wL^2}{2}$

$$P_y = \frac{wL^2}{2a} = \frac{10 \times 100^2}{2 \times 70} = 714 \text{ lb}$$

$$\Sigma F_y = 0 = R_y + P_y - wL$$
$$R_y = wL - P_y = 10 \times 100 - 714 = 286 \text{ lb}$$
$$\Sigma F_x = 0 = P_y \cot \alpha - R_x$$
$$R_x = 714 \cot 20 = 1960 \text{ lb}$$

Shear: The shear force distribution will be determined by the three methods: equilibrium, relation between load and shear, and area of load curve.
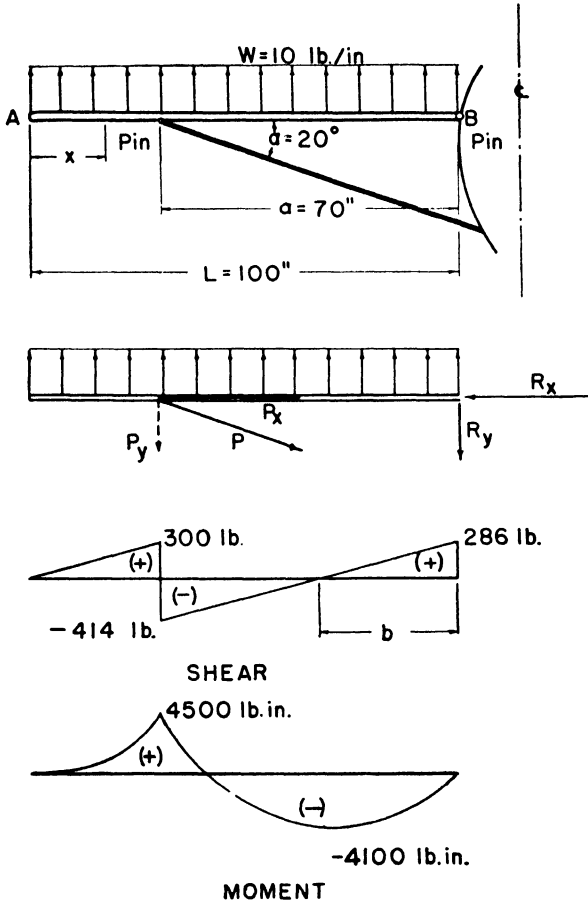
Fig. 4.7.   Shear Force and Bending Moment for a Simplified Wing.

From the conditions of equilibrium for a portion of beam of length x

$$\Sigma F_y = 0 = V - wx$$
$$V = wx = 10x \qquad \text{for } 0 \leqq x < (L - a)$$
$$\Sigma F_y = 0 = V - wx + P_y$$
$$V = wx - P_y = 10x - 714 \qquad \text{for } (L - a) < x \leqq L$$

From the shear load relation

$$V_B - V_A = \int_A^B p \, dx + \text{concentrated loads}$$

Since the shear force at the left end of the beam is zero and $p = w$,

$$V = \int_0^x w \, dx = wx = 10x \qquad \text{for } 0 \leqq x < (L - a)$$

$$V = \int_0^x w \, dx - P_y = wx - P_y = 10x - 714 \qquad \text{for } (L - a) < x \leqq L$$

By use of area of load curve relation when the shear at the left end is zero,

$$V = \text{area of load curve}$$
$$= wx = 10x \qquad \text{for } 0 \leqq x < (L - a)$$
$$V = wx - P_y = 10x - 714 \qquad \text{for } (L - a) < x \leqq L$$

Moments: When the equilibrium of an element of length x is considered and moments are taken about the right end of the element,

$$\Sigma M = 0 = M - \frac{wx^2}{2}$$

$$M = \frac{wx^2}{2} = \frac{10x^2}{2} = 5x^2 \qquad \text{for } 0 \leqq x \leqq (L - a)$$

$$\Sigma M = 0 = M - \frac{wx^2}{2} + P_y[x - (L - a)]$$

$$M = \frac{wx^2}{2} - P_y[x - (L - a)] = 5x^2 - 714x + 21{,}400$$
$$\text{for } (L - a) \leqq x \leqq L$$

By use of the relation between shear and moment when the moment on the left end is zero,

$$M = \int_0^x V \, dx = \int_0^x wx \, dx = \frac{wx^2}{2} = 5x^2 \qquad \text{for } 0 \leqq x \leqq (L - a)$$

$$M = \int_0^x V \, dx + \text{moment due to concentrated loads}$$

$$M = \int_0^x V \, dx - P_y[x - (L - a)] = 5x^2 - 714x + 21{,}400$$
$$\text{for } (L - a) \leqq x \leqq L$$

When the fact that area of the shear curve is equal to the change in moment is used,

$$M = \frac{wx^2}{2} = 5x^2 \qquad \text{for } 0 \leqq x \leqq (L - a)$$

$$M = 4500 + \frac{(-414 + 10x - 714)}{2}(x - 30)$$

$$= 5x^2 - 714x + 21{,}400 \qquad \text{for } (L - a) \leqq x \leqq L$$

The shear force and bending moment curves are shown in Figure 4.7.

The place where the slope of the moment curve is zero is a possible maximum point. This point can be determined by differentiation of the moment or from the relation of the moment and shear curves. Thus,

$$\frac{dM}{dx} = 0 = \frac{d}{dx}(5x^2 - 714x + 21{,}400) = 10x - 714$$
$$= 71.4 \text{ in}$$

Then $M = 5(71.4)^2 - 714(71.4) + 21{,}400 = -4{,}100 \text{ lb in}$

Actually, the moment is maximum at the load P_y where the slope of the moment curve varies discontinuously. The point of zero slope of the moment curve also can be determined from the moment shear relation since the zero slope of the moment curve corresponds to zero shear from the relation

$$\frac{dM}{dx} = V = 0$$

Then from similar triangles of the shear curve

$$\frac{b}{286} = \frac{a - b}{414}$$
$$b = 28.6$$

Then $x = L - b = 100 - 28.6 = 71.4 \text{ in as before.}$

It will be left as an exercise for the student to show that the slopes of the shear curve to the left and right of the load P_y are equal and that the slope of the moment curve suddenly changes at the load P_y.

4.5 Distributed torque loads. Many structural members are subjected to loads that cause twisting about their longitudinal axes. A simple example is a rod with a torque applied at each end, in which the torque distribution is a constant. The torque distribution for a wing, and many other structures, is not usually constant; therefore, the analysis of members carrying distributed torque should be considered.

Consider a rod fixed at one end with loads eccentrically placed with respect to the longitudinal axis of the rod so that the distributed loads can be considered as acting on a shelf extending out from the rod as shown in Figure 4.8. If a torque T is assumed to act at one side of an element of the rod of length Δx, then the torque at the other end will differ by some amount ΔT. If the distributed loading is of intensity p then the torque per linear inch of rod is

$$pr = m$$

and the total increase in torque for a section of length Δx is $m \Delta x$. From equilibrium

$$\Sigma T = 0 = T + m \Delta x - (T + \Delta T)$$

or $$\frac{\Delta T}{\Delta x} = m$$

which taken in the limit is

$$\frac{dT}{dx} = m \tag{4.8}$$

This is analogous to $dV/dx = p$ for the beam bending case and hence the same methods for evaluation can be used as those developed in Article 4.4.
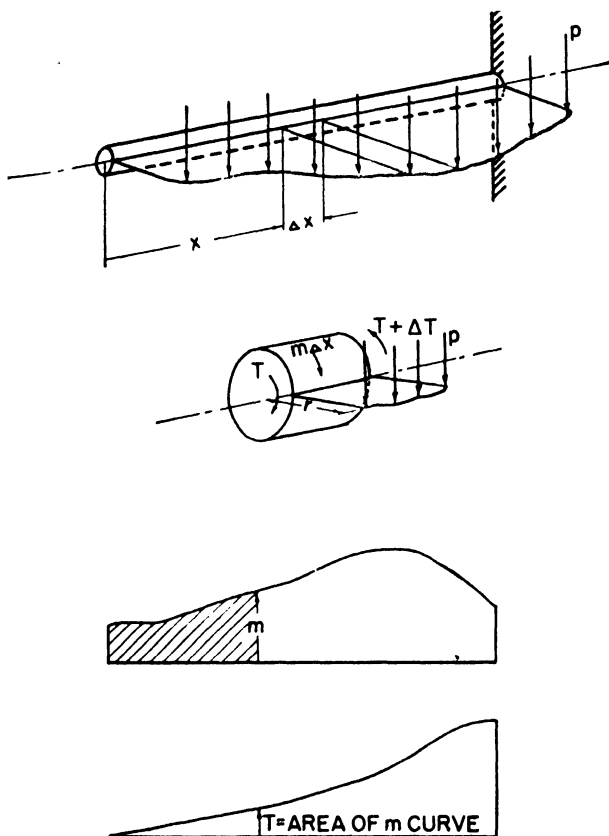
Fig. 4.8.   Torque Distribution.

4.6 Shear, moment, and torque distribution for a wing with dihedral and sweepback. Wings are usually built with dihedral and sweepback for aerodynamic reasons and for the maintenance of the stability of the airplane. A measure of sweepback is the angle between the lateral axis, which is a line perpendicular to the longitudinal axis of the airplane lying in the horizontal plane, and a reference line in the wing. The wing reference line can be specified differently for various uses; however, for purposes of load analysis, the elastic axis of the wing is convenient. In

a similar manner the dihedral can be specified in terms of an angle between the plane of the longitudinal and lateral axes, and the elastic axis of the wing.

The intersection of the elastic axis with each cross section of the wing determines the point, called the *center of twist*, about which each cross section will rotate if the wing is twisted by a torque.   In the preliminary
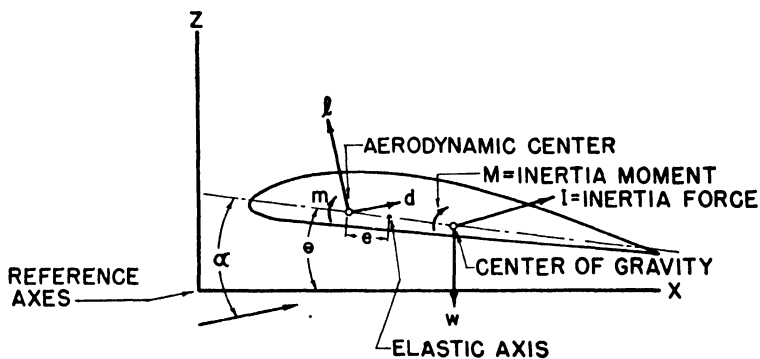
(a)
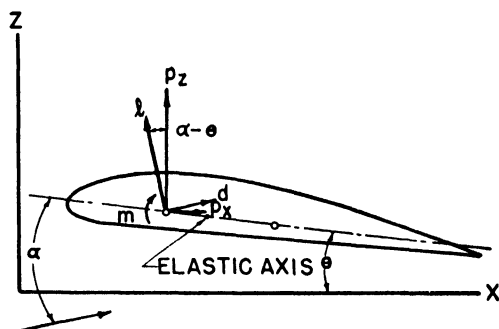
(b)

Fig. 4.9.   Aerodynamic Forces in Reference Directions.

design stages the location of the elastic axis is not known; therefore, analyses must be made for a possible range of locations of the elastic axes and eventually the position used that most closely corresponds to the final location.   For one transport airplane the preliminary location of the elastic axis was chosen between 24% and 32% of the chord.   This range being selected on the basis of similar previous designs.

Consider a portion of a wing, Figure 4.9, between two cross sections a

unit distance apart along the span. The forces acting on this element will be composed of (1) lift, (2) drag, (3) aerodynamic moment, (4) weight, and (5) inertia forces. The forces can be resolved into forces in the direction of the reference axes, x and z. If only the aerodynamic forces are considered, it is apparent that the forces acting at the aerodynamic center are

$$p_z = l \cos (\alpha - \theta) + d \sin (\alpha - \theta)$$
$$p_x = -l \sin (\alpha - \theta) + d \cos (\alpha - \theta) \quad (4.9)$$

where θ = the angle of incidence between the chord line of the wing and the reference line x

α = angle of attack

l = lift per unit length of span (lb/ft)

d = drag per unit length of span (lb/ft)

p_z = force per unit length of span in z direction (lb/ft)

p_x = force per unit length of span in x direction (lb/ft).

When $\theta = 0$, the forces p_z and p_x are the forces perpendicular to the chord and parallel to the chord. The other forces can be resolved in a similar manner.

If we refer to Figure 4.10, we see that the aerodynamic forces in the x and z directions at any wing section of length Δu_n will be $p_{xn} \Delta u_n$ and $p_{zn} \Delta u_n$. The shear forces in the x and z directions at any section a distance y from wing root will be the sum of all the airloads outboard of that section. If the section of width Δu_n at the tip is denoted by Δu_1 and the section on which the shear is being determined is denoted by i, then

$$V_x = \sum_{n=1}^{i} p_{xn} \Delta u_n$$
$$V_z = \sum_{n=1}^{i} p_{zn} \Delta u_n \quad (4.10)$$

The moments about lines parallel to the x and z axes at any section i can be determined from the area of the shear curve or by summing the moments of the airloads outboard of the section i

$$M_x = \sum_{n=1}^{i} V_{zn} \Delta u_n = \sum_{n=1}^{i} p_{zn} u_n \Delta u_n$$
$$M_z = \sum_{n=1}^{i} V_{xn} \Delta u_n = \sum_{n=1}^{i} p_{xn} u_n \Delta u_n \quad (4.11)$$

The shear forces V_{xn} and V_{zn} are measured at the center of the interval Δu_n, which may be considered as the average value of the shear forces on the two sides of the interval.

The torque about the elastic axis at section i can be obtained by summing the torques produced by all the forces outboard of section i. If we refer to Figure 4.10(b) we find that the moment of the forces of the

(a)

(b)
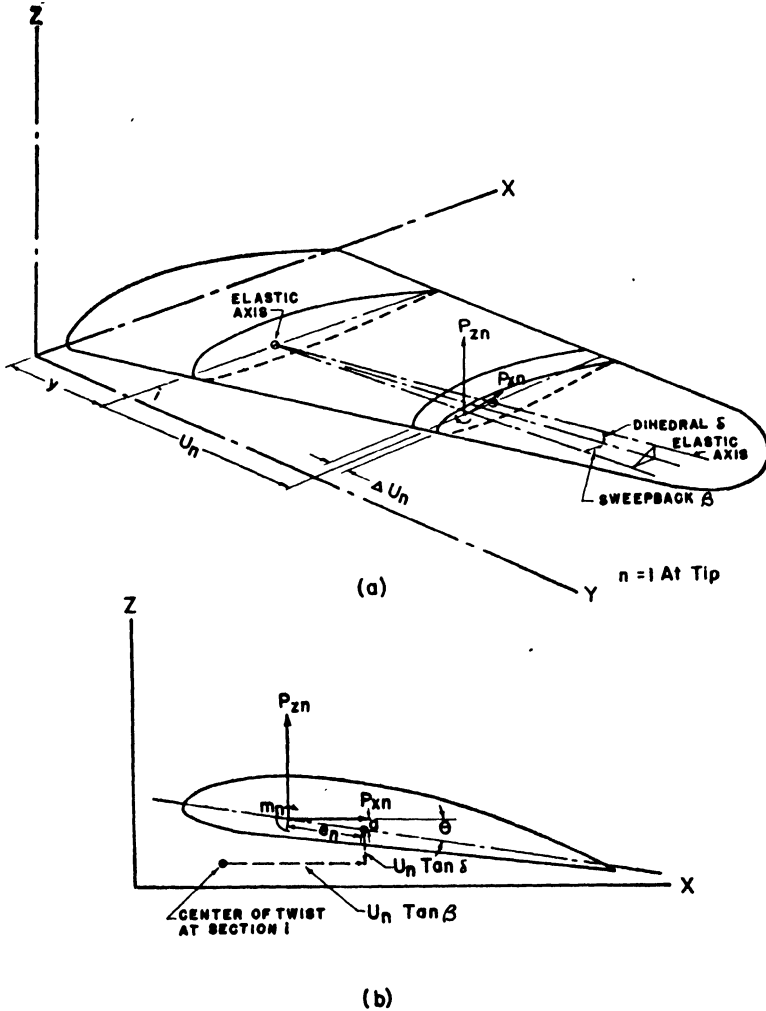
Fig. 4.10. Forces on Wing.

nth section about the center of twist of the ith section is

$$[m_n + p_{zn}(a + u_n \tan \delta) - p_{xn}(u_n \tan \beta - e_n \cos \theta)] \Delta u_n$$

If the angle of incidence θ is small (as it usually is), then the quantity a can be neglected and $\cos \theta = 1$ so that the total torque at the ith section is

$$T = \sum_{n=1}^{i} [m_n + p_{zn}u_n \tan \delta - p_{xn}(u_n \tan \beta - e_n)] \Delta u_n \qquad (4.12)$$

The shear, moment, and torque curves for the wing thus are completely determined. The actual values usually are obtained by substituting values in a table and performing the processes indicated in Equations 4.10, 4.11, and 4.12. The values of p_{xn} and p_{zn} are determined from the load curve, and values of Δu_n and u_n are measured from a wing drawing.

4.7 Beam deflection. The shear forces and bending moments cause the beam to deflect. This deflection consists of a curvature of the beam, which usually varies from point to point depending on the load distribution and manner in which the beam is supported. Both the bending moment and the shear force contribute to the deflection, but for most conventional beams (except for short deep ones) the contribution of the
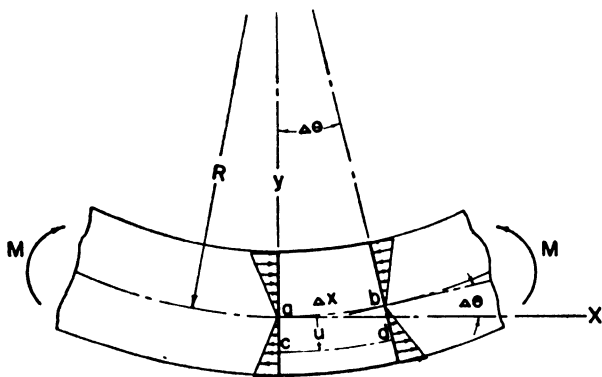
Fig. 4.11. Bending of Beam.

bending moment to the deflection is far greater than the effect of the shear force.

Consider a portion of a beam with bending moments at the ends as shown in Figure 4.11. The moment causes the material at the top of the beam to be compressed and the material at the bottom to be extended. Therefore, there will be a longitudinal portion of the beam denoted by the line ab, which undergoes neither elongation nor contraction. If the two lines passing through ac and bd were originally parallel and a distance Δx apart before the moments were applied, it can be shown experimentally that after the application of the moments the lines will remain straight but be rotated through an angle $\Delta\theta$ with respect to each other, as shown in Figure 4.11. This situation will exist for the assumptions that the material is homogeneous and that there is no lateral pressure across the beam.

If only the geometry of the deformation of the beam is considered, it is apparent that

$$\Delta x = R\,\Delta\theta$$

or

$$\frac{1}{R} = \frac{\Delta\theta}{\Delta x}$$

If $\Delta\theta$ is small, the arc length Δx is approximately equal to the projection of the arc length on the x axis so that as $\Delta x \to 0$

$$\frac{1}{R} = \frac{d\theta}{dx} \qquad (4.13)$$

where $\qquad\qquad R =$ the radius of curvature

$\qquad\qquad\qquad \dfrac{d\theta}{dx} =$ the rate of change of slope.

Since $\theta = \dfrac{dy}{dx}$ and $\dfrac{d\theta}{dx} = \dfrac{d}{dx}\left(\dfrac{dy}{dx}\right) = \dfrac{d^2y}{dx^2}$

therefore, $\qquad\qquad\qquad \dfrac{1}{R} = \dfrac{d^2y}{dx^2} \qquad (4.14)$

If the slope is not small enough so that the distances measured along the arc and the x axis are approximately equal, then it can be shown that

$$\frac{1}{R} = \frac{\dfrac{d^2y}{dx^2}}{\left[1 + \left(\dfrac{dy}{dx}\right)^2\right]^{\frac{3}{2}}} \qquad (4.15)$$

This is the exact equation for the curvature, but Equation 4.14 is sufficiently accurate for all engineering applications of ordinary beam deflections.

The strains in the material can be expressed in terms of the curvature of the beam. Consider a longitudinal line cd some distance u below the line of invariable length ab. The material along cd will elongate an amount proportional to the distance u, since the ends of the line are bounded by the straight radial lines ac and bd. The strain along cd is the elongation of cd divided by its original length ab, which is equivalent to Δx. Hence, the strain ϵ is

$$\epsilon = \frac{(R + u)\,\Delta\theta - \Delta x}{\Delta x} = u\,\frac{\Delta\theta}{\Delta x}$$

but $\qquad\qquad\qquad \dfrac{1}{R} = \dfrac{\Delta\theta}{\Delta x}$

therefore $\qquad\qquad\qquad \epsilon = \dfrac{u}{R} \qquad (4.16)$

This expression is useful in metal-forming problems where the allowable radius of bend R can be calculated if the limiting strain ϵ and thickness of the material $t = 2u$ are known.

In all the foregoing discussion nothing has been said about the material except that it is homogeneous, and therefore the equations developed apply to *elastic* as well as *inelastic* materials. If the material is elastic, the deformation can be expressed easily in terms of the applied

moments, the geometry of the beam, and the properties of the material. For elastic materials

$$f = E\epsilon$$

or, if Equation 4.16 is used,

$$f = E\frac{u}{R}$$

The stress distribution is therefore linear as indicated in Figure 4.11, and for equilibrium the moment of the forces caused by the stresses on the cross section of the beam is equal to the applied moment

$$M' = \int_A fu \, dA = \frac{E}{R}\int_A u^2 \, dA = \frac{EI}{R}$$

where $I = \int_A u^2 \, dA = $ a geometric property of the cross section.

This is usually written
$$\frac{1}{R} = \frac{M}{EI} \tag{4.17}$$

or
$$\frac{d^2y}{dx^2} = \frac{M}{EI} \tag{4.18}$$

where M = bending moment (lb in)
E = modulus of elasticity of material (psi)
$\cdot$ I = moment of inertia of cross section abou tcentroidal axis (in⁴).

The determination of the deflection of a beam for a given moment distribution, therefore, consists of solving Equation 4.18 for the proper end conditions of the beam. The deflection can be determined by the usual integration procedures or by the area-moment method.

4.8 Relations of load, shear, moment, slope, and deflection. The relations between load, shear, and moment were discussed in Article 4.4, and it was shown that

$$p = \frac{dV}{dx}$$

$$V = \frac{dM}{dx}$$

or
$$p = \frac{dV}{dx} = \frac{d^2M}{dx^2}$$

The relations between moment, slope, and deflection as given in the last article are

$$\frac{d\theta}{dx} = \frac{M}{EI}$$

$$\frac{d^2y}{dx^2} = \frac{M}{EI}$$

Therefore

$$p = \frac{d^2M}{dx^2} = EI\frac{d^4y}{dx^4}$$

$$V = \frac{dM}{dx} = EI\frac{d^3y}{dx^3} \tag{4.19}$$

$$M = EI\frac{d^2y}{dx^2}$$

$$\theta = \frac{dy}{dx}$$

$$y = y(x)$$

Each quantity of load, shear, moment, and slope can therefore be expressed in terms of the deflection y, or conversely, y can be expressed in
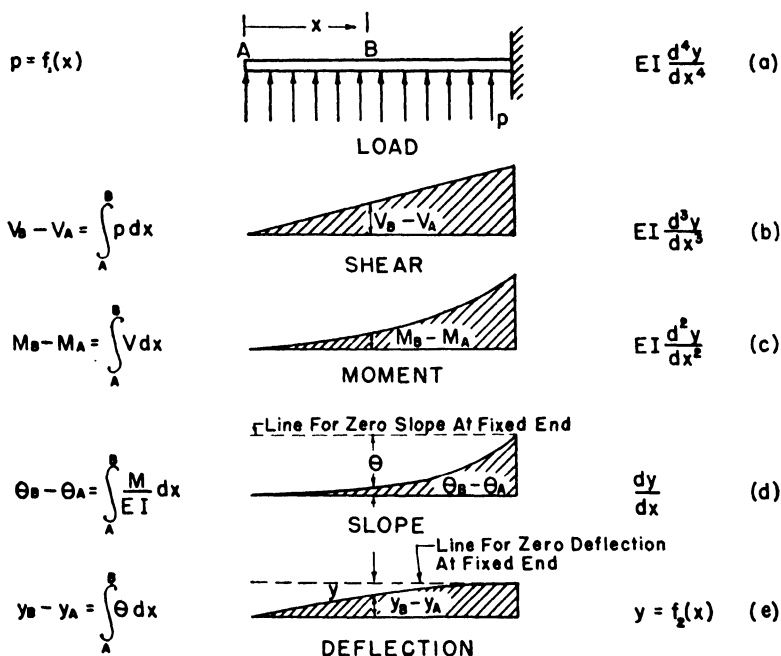
Fig. 4.12. Relations between Load, Shear, Moment, Slope, and Deflection.

terms of the load, shear, moment, or slope. In the former case of determining load, shear, and so on, from the deflection, differentiation is needed; whereas to determine the deflection from the load, shear, and so on, integration is required. Figure 4.12 shows the relation of the five curves of load, shear, moment, slope, and deflection. If we start with the load curve and travel downward, we find that each curve is the integral of the one immediately above; whereas if we start with the deflection curve and go upward, we find that each curve is the derivative of the one below.

The designer usually is expected to obtain the deflection from the load distribution, so that integration is required. Sometimes a direct integration is difficult, and the approximate value of the integral is determined by interpreting it as an area or a sum. For example, if the moment distribution and the values of the moment of inertia are known, and the slope of the beam is to be determined in the case where direct integration is difficult, then an approximation can be made by

$$\theta_B - \theta_A = \sum_{n=1}^{m} \left(\frac{M}{EI} \right)_n \Delta x_n \qquad (4.20)$$

It should be noted that the final slope and moment curve should include the consideration of the conditions at the ends of the beam. For example, although the difference between the slope at two points, A and B, is given by the ordinate of the shaded area of curve (d) in Figure 4.12, the actual slope must conform to the condition that the slope at the right end is zero. Therefore, the slope should be measured from the dotted line sketched in on curve (d).

4.9 Area-moment method. Before an example of the determination of the deflection of a beam is given, another interesting relation between the curves in Figure 4.12 should be pointed out. Each curve is related in the same way to its neighboring curve. Thus, the moment curve is obtained from the load curve by two integrations, and the deflection curve is obtained from the M/EI curve by two integrations. Since it is possible to determine the moment from the load by direct summation of moments of the load curve, the possibility of determining the deflection from the M/EI curve by a similar process of taking the moments of the M/EI curve is suggested. This can be done, and the process is known as the *area-moment method*.

Fig. 4.13.   Area-Moment Diagram.

Consider two points, A and B, on a beam. Suppose the M/EI distribution has been determined. Then if we refer to Figure 4.13, we find that the top diagram represents the M/EI values between the two points A and B on the beam and the lower diagram represents the deflection of the neutral axis of the beam between the two points A and B. Of course,

the deformation has been greatly exaggerated in the figure. A vertical line through A intercepts the tangent to B at A'. The tangents for two points a distance Δx apart have tangent slopes differing by $\Delta\theta$; and, since $\Delta\theta$ is small, the tangents intercept a length on AA' of approximately $\Delta\theta_n x_n$. Therefore, y_{AB}, the distance between point A and the tangent at B is

$$y_{AB} = \sum_{n=1}^{m} x_n \, \Delta\theta_n$$

The summation is taken for the whole interval from A to B. According to Equation 4.20 the change in slope between two points a distance Δx apart is simply

$$\Delta\theta_n = \left(\frac{M}{EI}\right)_n \Delta x_n \tag{4.21}$$

Therefore,

$$y_{AB} = \sum_{n=1}^{m} \left(\frac{M}{EI}\right)_n x_n \, \Delta x_n \tag{4.22}$$

or as $\Delta x \to 0$ the exact expression is

$$y_{AB} = \int_A^B \frac{M}{EI} \, x \, dx$$

Since the product $\frac{M}{EI} \Delta x$ is the area of the M/EI diagram for an interval Δx and since $\left(\frac{M}{EI} \Delta x\right) x$ is the moment of this area, Equation 4.22 can be interpreted in terms of the moment of the area of the M/EI diagram.

The distance between point A on a beam and the tangent at any other point B is the moment of the area of the M/EI curve about point A.

EXAMPLE 4.2. Determine the slope and deflection at the free end of a tapered cantilever beam carrying a uniform load if the material of the beam is aluminum and the cross section of the beam consists of two flanges connected by a web, as shown in Figure 4.14. Assume the web does not buckle.

$$L = 120 \text{ in} \qquad\qquad w = 12 \text{ lb/in}$$
$$h_1 = 5 \text{ in} \qquad\qquad\;\; A = 1 \text{ sq in}$$
$$h_2 = 10 \text{ in}$$

Solution. Since the slope at the fixed end is zero, the slope at the free end can be obtained from Equation 4.20.

$$\theta_B - \theta_A = 0 - \theta_A = \int_A^B \frac{M}{EI}\,dx$$

The approximate slope can be expressed as a summation process that can be interpreted geometrically as the area of the M/EI diagram

$$\theta_A = -\sum_{n=1}^{m}\left(\frac{M}{EI}\right)_n \Delta x_n$$

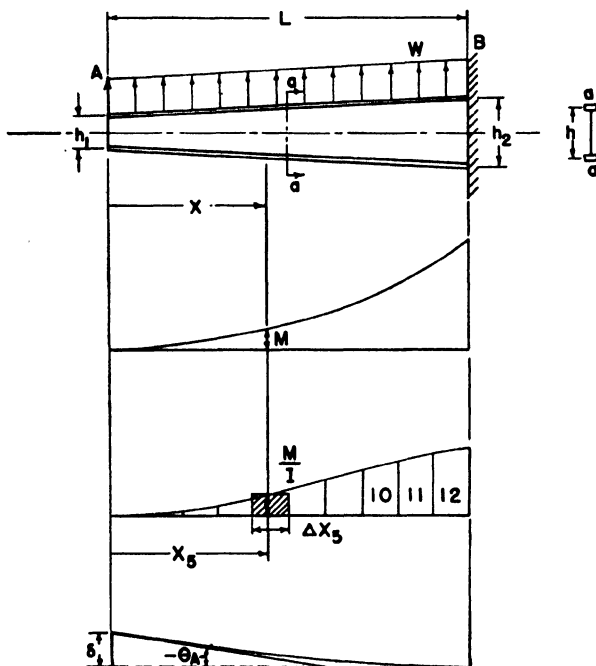Similarly, the deflection y_{AB} is the deflection measured from a hori-

Fig. 4.14.   Deflection of Tapered Beam.

zontal axis through the fixed end.   From Equation 4.22

$$y_{AB} = \delta = \int_A^B \left(\frac{M}{EI}\right) x\,dx$$

or

$$\delta = \sum_{n=1}^{m}\left(\frac{M}{EI}\right)_n x_n\,\Delta x_n$$

Both the integral and summation processes will be used to illustrate the methods.   In any case it is necessary to determine the bending

moment and moment of inertia of the cross section at various stations along the beam.

The bending moment at any section x is

$$M = \frac{wx^2}{2} = 6x^2$$

The moment of inertia about the principal axis also is a function of x. The depth h at any section can be determined by proportionality.

$$h = h_1 + (h_2 - h_1)\frac{x}{L}$$

$$= 5 + (10 - 5)\frac{x}{120} = 5 + 0.0417x$$

Then
$$I = 2I_f + 2\left(\frac{h}{2}\right)^2 A + I_w$$

where I = moment of inertia of complete section
I_w = moment of inertia of web
I_f = moment of inertia of flange about its own centroidal axis
A = area of flange.

For sections of this type, I_f and I_w usually can be neglected in comparison with $2\left(\frac{h}{2}\right)^2 A$.   Therefore,

$$I = \frac{h^2}{2} A = 0.5(5 + 0.0417x)^2$$

Since E is a constant,

$$\theta_A = -\frac{1}{E}\int_0^L \frac{M}{I}\,dx = \frac{-1}{10.5 \times 10^6}\int_0^{120} \frac{6x^2}{0.5(5 + 0.0417x)^2}\,dx$$

By referring to integral tables we can show that

$$\theta_A = -0.00895 \text{ rad} = -0.513°$$

The negative sign corresponds to the sign convention adopted earlier.

The deflection δ is

$$\delta = \frac{1}{E}\int_0^L \frac{M}{I} x\,dx = \frac{1}{10.5 \times 10^6}\int_0^{120} \frac{6x^3}{0.5(5 + 0.0417x)^2}\,dx = 0.784 \text{ inches}$$

The values determined by the summation process are obtained from the following table.

Sta.	Δx (in)	x (in)	M (lb in)	I (in^4)	$\dfrac{M}{I}\,\Delta x$	$\dfrac{M}{I}\,x\,\Delta x$
1	10	5	0.15×10^3	13.56	1.11×10^2	0.06×10^4
2	10	15	1.35	15.82	8.53	1.28
3	10	25	3.75	18.26	20.53	5.13
4	10	35	7.35	20.86	35.23	12.33
5	10	45	12.15	23.65	51.37	23.12
6	10	55	18.15	26.60	68.23	37.53
7	10	65	25.35	29.73	85.26	55.42
8	10	75	33.75	33.03	102.18	76.63
9	10	85	43.35	36.51	118.73	100.92
10	10	95	54.15	40.16	134.83	128.09
11	10	105	66.15	43.97	150.44	157.96
12	10	115	79.35	47.98	165.38	190.19
				$\Sigma =$	941.81×10^2	788.66×10^4

Then

$$\theta_A = -\frac{1}{E}\sum \frac{M}{I}\,\Delta x = -\frac{941.81 \times 10^2}{10.5 \times 10^6} = -0.00897 \text{ rad} = -0.514°$$

$$\delta_A = \frac{1}{E}\sum \frac{M}{I}\,x\,\Delta x = \frac{788.66 \times 10^4}{10.5 \times 10^6} = 0.751 \text{ inches}$$

The accuracy of the given data and the physical nature of the problem do not justify the number of significant figures carried in the above analysis. This was done only to compare methods and should not be interpreted as the accuracy to which the deformation is known.

4.10 Supported cantilever. The supported uniform cantilever beam with a concentrated load shown in Figure 4.15 represents a statically indeterminate structure because there are three unknown forces, R_A, R_B, and M_B, and only two equations of statical equilibrium, $\Sigma M = 0$ and $\Sigma F_v = 0$, relating the three unknowns. Since the value of the forces cannot be obtained from the force equilibrium alone, another condition must be used. This additional condition involves the consideration of the deformation of the structure.

The final configuration of the supported cantilever may be obtained first by applying the load P to the cantilever without the support at A, in which case the end A deflects upward some distance δ, and then by applying a downward force at A until the deflection of the end is zero. The beam can therefore be thought of as being composed of two statically determinate systems, (1) and (2) in Figure 4.15, in which the deflection at A due to P acting alone is exactly equal and opposite to the deflection at A due to R_A acting alone. This relation gives the additional condition required for determining the values of the forces. Symbolically

$$\Sigma M = 0$$
$$\Sigma F = 0$$
$$\delta_P = \delta_R \text{ or } \delta = 0 \qquad (4.23)$$

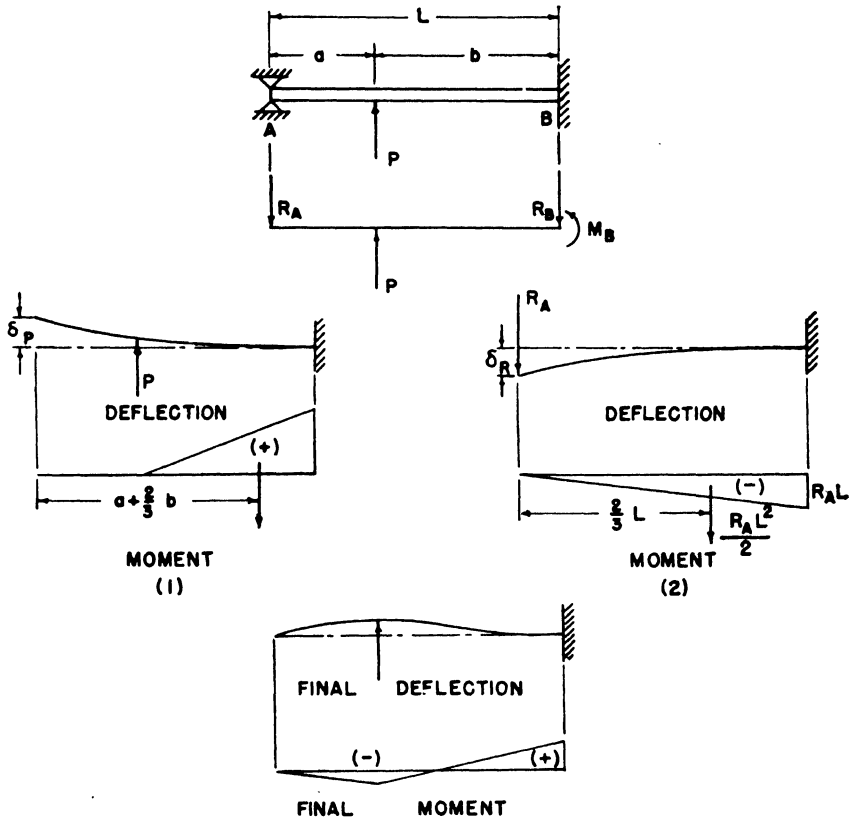The deflection δ_P of system (1) can be determined easily by use of

Fig. 4.15. Supported Cantilever with Concentrated Load.

the area-moment method. According to this method, the deflection is the moment of the area of the M/EI diagram about A. Since E and I are constants,

$$\delta_P = \frac{Pb^2}{2}\left(a + \frac{2}{3}b\right)\frac{1}{EI} \qquad (4.24)$$

Similarly, for system (2) $\delta_R = \frac{R_A L^2}{2}\frac{2}{3}L\frac{1}{EI} = \frac{R_A L^3}{3EI} \qquad (4.25)$

Now since $\delta_P = \delta_R$, $R_A = \frac{3Pb^2}{2L^3}\left(a + \frac{2}{3}b\right)$

Or, because $b = L - a$, $R_A = \frac{P}{2L^3}(L - a)^2(2L + a) \qquad (4.26)$

The remaining unknowns, R_B and M_B, now can be determined by use of the equations of equilibrium

$$\Sigma F_v = 0 = R_A - P + R_B$$
$$R_B = P - R_A \tag{4.27}$$
$$\Sigma M_B = 0 = P(L - a) - R_A L - M_B$$

$$M_B = P(L - a) - R_A L = \frac{Pa}{2L^2}(L^2 - a^2) \tag{4.28}$$

The complete moment diagram is shown in Figure 4.15.

The results of the analysis for the case of the supported cantilever with a concentrated load can be generalized to include that of a distributed load. Consider a distributed load with intensity p as shown in Figure 4.16. For a small interval Δx on the beam, the load will be $p\,\Delta x$. By consideration of only this load, the reaction at A is determined by Equation 4.26 where $P = p\,\Delta x$ and x replaces a. If we call the reaction ΔR_A, then
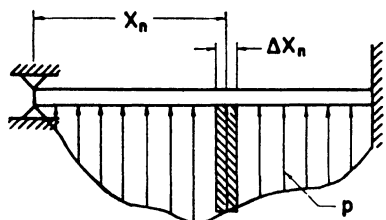
Fig. 4.16. Supported Cantilever with Distributed Load.

$$\Delta R_A = \frac{p\,\Delta x}{2L^3}(L - x)^2(2L + x)$$

If all the loads of this type are superimposed for the whole beam,

$$R_A = \frac{1}{2L^3}\sum_{n=1}^{m} p_n(L - x_n)^2(2L + x_n)\,\Delta x_n$$

or, as $\Delta x \to 0$, $R_A = \frac{1}{2L^3}\int_0^L p(L - x)^2(2L + x)\,dx \tag{4.29}$

Similarly, the moment M_B becomes

$$M_B = \frac{1}{2L^2}\sum_{n=1}^{m} p_n x_n(L^2 - x_n^2)\,\Delta x_n$$

or $M_B = \frac{1}{2L^2}\int_0^L px(L^2 - x^2)\,dx \tag{4.30}$

EXAMPLE 4.3.   Determine the fixed end moment for a uniform supported cantilever beam carrying a uniform load w.

Solution. $p = w = $ constant

Then from Equation 4.30 $M_B = \frac{1}{2L^2}\int_0^L wx(L^2 - x^2)\,dx$

$$= \frac{w}{2L^2}\left[\frac{x^2}{2}L^2 - \frac{x^4}{4}\right]_0^L = \frac{wL^2}{8}$$

4.11 Supported cantilever with end moment. The results of an analysis of a supported cantilever with a moment applied at the pinned end will be useful in later analyses.

The analysis of the supported uniform cantilever with end moment will be made in a manner similar to that used in the previous article. The beam is considered to be composed of two statically determinate systems, one consisting of a cantilever beam with the end moment applied, which thus produces an end deflection, and the other consisting
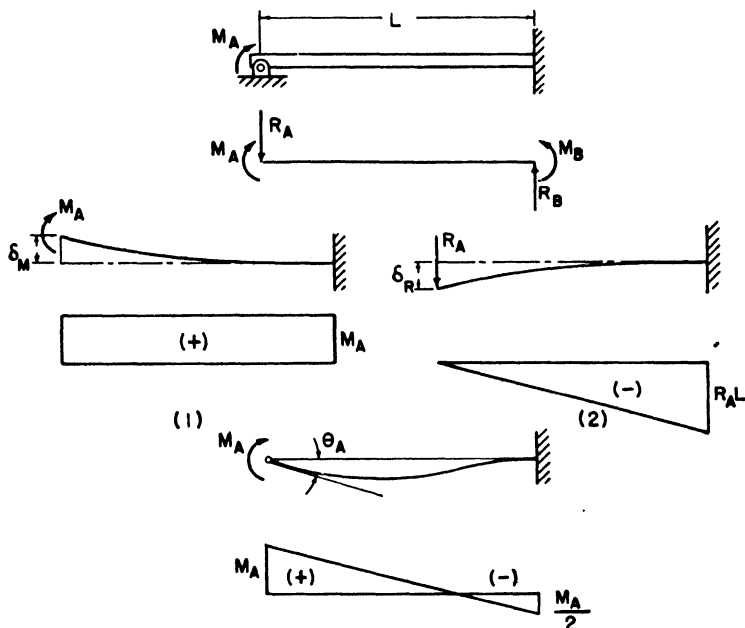
Fig. 4.17.   Supported Cantilever with End Moment.

of a cantilever beam with an end reaction which causes an end deflection just sufficient to cancel the deflection produced by the moment.

Referring to Figure 4.17 and remembering that the deflection at the end of the beam for system (1) is the moment of the area of the M/EI diagram, we have

$$\delta_M = \frac{M_A L}{EI} \frac{L}{2} = \frac{M_A L^2}{2EI} \tag{4.31}$$

The deflection of a cantilever with end load is given by Equation 4.25.

$$\delta_R = \frac{R_A L^3}{3EI}$$

Since the end deflection must be zero,

$$\delta_M = \delta_R$$

$$\frac{M_A L^2}{2EI} = \frac{R_A L^3}{3EI}$$

$$R_A = \frac{3}{2}\frac{M_A}{L} \tag{4.32}$$

The bending moment at the fixed end of the original supported cantilever is therefore

$$M_B = M_A - R_A L = M_A - \frac{3}{2}\frac{M_A L}{L}$$

$$M_B = -\frac{M_A}{2} \tag{4.33}$$

and the bending moment distribution is as shown in Figure 4.17.

To summarize, a bending moment applied at the supported end and producing *compression* in the top fibers of the beam causes a moment at the fixed end equal in magnitude to one half the applied moment and in the direction to cause *tension* in the top fibers of the beam.

4.12 Beam with both ends fixed. The solution of a uniform beam with both ends fixed can be obtained by imposing another condition on the analysis of the supported cantilever beam. This additional condition recognizes the fact that the rotations at *both* ends of the beam are zero.

Consider the fixed-end beam shown in Figure 4.18 composed of two systems: (1) a supported cantilever with concentrated load applied anywhere along the span; (2) a supported cantilever with a moment applied at the supported end. The moment applied in the second system is then adjusted so that the rotation produced by it exactly cancels the rotation caused by the applied load in the first system. Since one end is fixed, the rotation at *A* for each system will be the area of the respective M/EI diagrams. These areas can be determined best from their original components. Thus, when reference is made to Figure 4.15, the rotation due to the load *P* in system (1) is

$$\theta_P = \frac{1}{EI}\left[-\frac{P}{2}(L-a)^2 + \frac{P}{4L}(L-a)^2(2L+a)\right]$$

$$= \frac{Pa}{4EIL}(L-a)^2 \tag{4.34}$$

and from Figure 4.17 $\quad \theta_{MA} = \frac{1}{EI}\left(M_A L - \frac{3}{4}M_A L\right) = \frac{M_A L}{4EI} \tag{4.35}$

Then, since $\quad\quad\quad \theta_{MA} = \theta_P$

$$\frac{M_A L}{4EI} = \frac{Pa}{4EI}\frac{(L-a)^2}{L}$$

$$M_A = \frac{Pa}{L^2}(L-a)^2 \tag{4.36}$$

The reaction R_A may be determined by adding the reactions at A of systems (1) and (2) as given by Equations 4.26 and 4.32.

$$R_A = \frac{P}{2L^3}(L-a)^2(2L+a) + \frac{3Pa}{2L^3}(L-a)^2$$

$$= \frac{P}{L^3}(L-a)^2(L+2a)$$

$$= \frac{P}{L^3}(L^3 - 3a^2L + 2a^3) \tag{4.37}$$

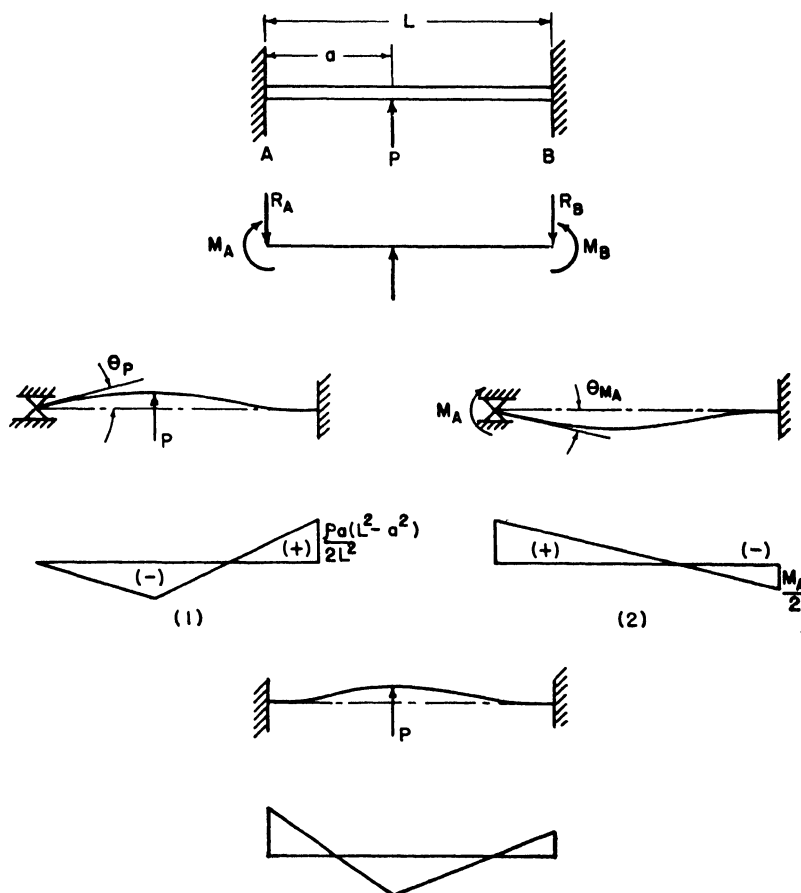Having one moment and one reaction, the other two can be deter-

Fig. 4.18. Fixed-End Beam.

mined from the equations of equilibrium, and the complete moment distribution and shear distribution can be obtained.

The results for the fixed-end beam now can be generalized for a

distributed load of intensity p. In a manner similar to that used in Article 4.10 the concentrated load is replaced by $p\,\Delta x$ and the elements summed for the length of the beam. Thus,

$$M_A = \frac{1}{L^2} \sum_{n=1}^{m} p x_n (L - x_n)^2 \,\Delta x_n$$

or

$$M_A = \frac{1}{L^2} \int_0^L p x (L - x)^2 \, dx \tag{4.38}$$

and

$$R_A = \frac{1}{L^3} \sum_{n=1}^{m} p(L^3 - 3x_n^2 L + 2x_n^3) \,\Delta x_n$$

$$R_A = \frac{1}{L^3} \int_0^L p(L^3 - 3x^2 L + 2x^3) \, dx \tag{4.39}$$

Determining M_B from the equations of equilibrium gives

$$M_B = \frac{1}{L^2} \sum_{n=1}^{m} p x_n^2 (L - x_n) \,\Delta x_n$$

$$M_B = \frac{1}{L^2} \int_0^L p x^2 (L - x) \, dx \tag{4.40}$$
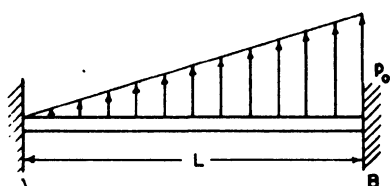
Fig. 4.19. Uniformly Varying Load.

EXAMPLE 4.4. Determine the bending moments at the fixed ends of a uniform fixed-end beam carrying a uniformly increasing load, as shown in Figure 4.19.

Solution. If the intensity of the load at B is p_0, the intensity at any point x obtained by proportion will be

$$p = \frac{p_0 x}{L}$$

From Equation 4.38

$$M_A = \frac{1}{L^2} \int_0^L p x (L - x)^2 \, dx = \frac{p_0}{L^3} \int_0^L x^2 (L - x)^2 \, dx$$

$$= \frac{p_0}{L^3} \left[\frac{x^3 L^2}{3} - \frac{2x^4 L}{4} + \frac{x^5}{5} \right]_0^L = \frac{p_0 L^2}{30}$$

From Equation 4.40

$$M_B = \frac{1}{L^2} \int_0^L p x^2 (L - x) \, dx = \frac{p_0}{L^3} \int_0^L x^3 (L - x) \, dx$$

$$= \frac{p_0}{L^3} \left[\frac{x^4 L}{4} - \frac{x^5}{5} \right]_0^L = \frac{p_0 L^2}{20}$$

Problems

4.1. A small airplane with a 40 foot wing span has two gasoline tanks holding 50 gallons of gasoline each, located 3 feet outboard of the fuselage center line. If an airload distribution as shown in Figure 4.20 is assumed and gasoline weighs
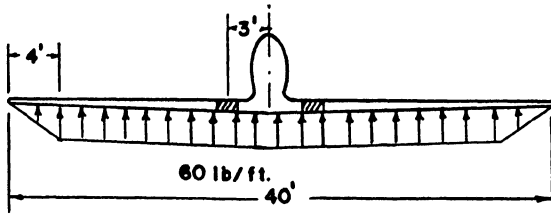

Fig. 4.20.   Airplane Wing.

6 pounds per gallon, determine the shear and bending moment distribution of the wing, and draw the distribution diagrams.

4.2. For a rudder with pressure distribution as shown in Figure 4.21, determine

(a) hinge moment
(b) shear distribution
(c) bending moment distribution.
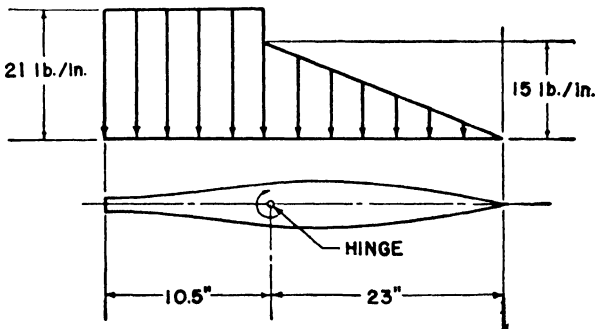
Fig. 4.21.   Rudder.

The hinge moment represents a control force sufficient to hold the rudder in equilibrium.
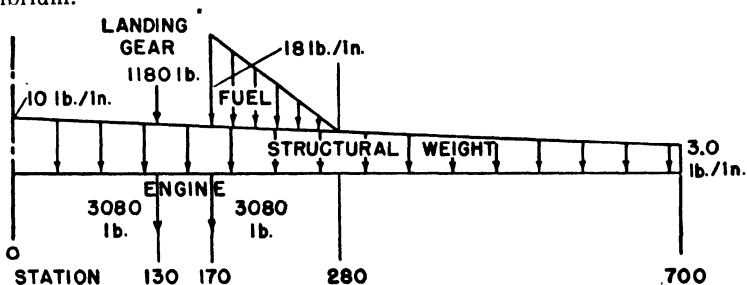
Fig. 4.22.   Wing Dead Weight.

4.3. The dead weight loading on a wing is shown in Figure 4.22; determine the shear and bending moment distribution.

4.4. A circular rod, similar to the one shown in Figure 4.8, has a triangular shelf extending horizontally from the rod. This shelf has a base at the fixed end of length c and tapers uniformly to a point at the free end. Along the hypotenuse of the triangle is a uniform downward load of w lb/in. Determine the torque distribution along the rod.

4.5. For an airplane weighing 21,000 pounds and with a wing as specified in the wing loading Problem 2.8, determine the loads, shears, and bending moments for a set of axes parallel and perpendicular to the chord. Also determine the torque about the elastic axis at each section if the dihedral of the elastic axis is 6°, the sweepback is zero, and the elastic axis is 30% of the chord aft of the leading edge.

4.6. Determine the shear and bending moment distribution, due to lift only, of the rigid blade shown in Figure 4.23 of a hovering (zero velocity) helicopter,
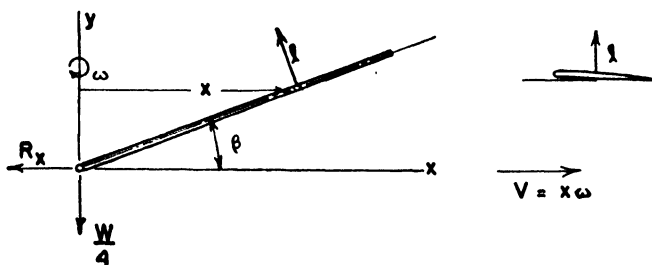

Fig. 4.23. Helicopter Blade.

assuming that the blade is pinned to the motor shaft so that it can move in the vertical plane. The problem will be simplified by assuming also a constant chord and a constant section coefficient of lift. Four blades support the total weight W of the helicopter.

4.7. For the beam shown in Figure 4.14, determine the deflection of the free end if the beam is carrying a uniformly increasing load having zero intensity at the free end and 20 lb/in at the fixed end.

4.8. Determine the deflection and rotation of the free end of the aluminum cantilever beam shown in Figure 4.24. The cross section of the beam is rectangular, and the width of the beam is two inches.
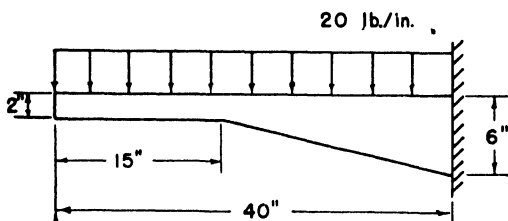

Fig. 4.24. Haunched Cantilever.

4.9. For the supported cantilever with concentrated load shown in Figure 4.15, determine the position of the load P that causes the fixed-end moment to be a maximum for a given beam. Determine the maximum fixed-end moment and compare it with the moment at the load position when the load is in a position to make the moment under the load a maximum.

4.10. Answer the same questions stated in Problem 4.9 for a beam with both ends fixed and carrying a concentrated load, Figure 4.18.

4.11. Determine the moment at the fixed end of the uniform supported cantilever beam shown in Figure 4.25.
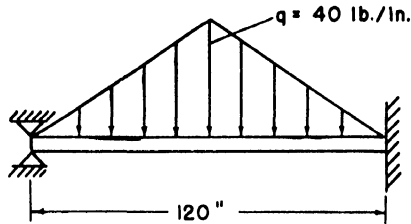

Fig. 4.25. Supported Cantilever.

4.12. A fixed-end beam has a fitting at mid span, through which a bending moment is applied. Determine

(a) moments at fixed ends
(b) reactions at fixed ends
(c) bending moment distribution.

CHAPTER 5

General Structural Relationships
and Elastic Energy

5.1 Introduction. A few simple structural components were discussed in the previous chapter. Before proceeding to the analysis of more complicated structures we will consider some general structural relationships, which will be useful in developing other methods of analysis and which will increase the understanding of the fundamental principles underlying all structural analyses.

Two assumptions will be made in the developments which follow in this chapter. They are:

(1) The structure is elastic.

(2) The law of conservation of energy is valid.

5.2 Hooke's law. Hooke's law is a statement of the behavior of most materials for a limited range of loading; namely, the deflections produced by the loads are proportionate to the loads. This is a general statement without restrictions as to the size or shape of the body, but it does infer that the material is elastic. In the previous chapters it has been shown that Hooke's law applies to a few cases. For example, the elongation of a tensile member is

$$\delta = \frac{PL}{AE}$$

and the end deflection for a cantilever beam with an end load is

$$\delta = \frac{PL^3}{3EI}$$

In each of the preceding instances the deflection is proportionate to the load; in one case the constant of proportionality is L/AE and in the other it is $L^3/3EI$. In general then, the relation between load and deflection can be written

$$\delta_2 = k_{21}P_1$$

where $\delta_2 =$ deflection in a *given direction* at point 2

$P_1 =$ load at point 1

$k_{21} =$ the constant of proportionality such that when multiplied by the load at point 1 it gives the deflection at point 2. This is called an *influence coefficient.*

If it is permissible to superimpose the deflections at a point by adding

the deflections in a given direction at that point because of several loads acting simultaneously, then

$$\delta_2 = k_{21}P_1 + k_{22}P_2 + \cdots k_{2n}P_n \tag{5.1}$$

5.3 Principle of superposition. Consider a structure such as a cantilever beam, and for the sake of simplicity assume that two loads are supported at the free end. If one load P'_1 is first applied, then

$$\delta'_1 = P'_1 \frac{L^3}{3EI} = k'_{11}P'_1$$

If only the second load is applied,

$$\delta''_1 = P''_1 \frac{L^3}{3EI} = k''_{11}P''_1$$

The total deflection can be obtained by adding δ'_1 and δ''_1 only so long as each of the separate deflections are proportionate to the loads producing them. In other words, changing the load should not change the load deflection relationship. If this condition is fulfilled, then

$$\delta_1 = \delta'_1 + \delta''_1 = (P'_1 + P''_1)\frac{L^3}{3EI}$$

In order to superimpose deflections, it is necessary only that the *deflection be proportionate to the load*. This condition is not fulfilled when the material is inelastic or when the geometry of the structure is such that the deflection is not proportionate to the load as for example in beam columns.

5.4 Elastic energy. Consider a structure on which several loads are simultaneously and gradually applied to avoid vibration. If the deflections in the direction of the loads P_1, P_2 are δ_1, δ_2, and so on, then since only the force in the direction of the displacement will do work and since the work done by each load is the average force times the displacement, the work done on the structure is

$$W = \tfrac{1}{2}[P_1\delta_1 + P_2\delta_2 + \cdots P_n\delta_n]$$

This work is stored in the structure in the form of *elastic energy* or strain energy, which is recoverable when the loads are removed since the strucure is elastic. Therefore,

$$U = \tfrac{1}{2}[P_1\delta_1 + P_2\delta_2 + \cdots P_n\delta_n] \tag{5.2}$$

where U = elastic energy (in lb)

It should be noted that the reactions at the *fixed* supports do no work because there are no displacements at the supports.

Although P and δ in the above equations have been taken to represent a force and linear displacement, the expressions can be generalized to include moment and rotation.

The elastic energy in a structure can be considered as being composed of the elastic energy due to

(1) tension-compression   (3) torsion
(2) bending   (4) shear.

(1) *Tension-compression.* The elastic energy stored in an element of a tensile member of length dx is

$$u = \frac{P\delta}{2}$$

but

$$\delta = \frac{P\,dx}{EA}$$

so

$$u = \frac{P^2\,dx}{2EA}$$

The total energy is the sum of the energies for each element of length dx; therefore,

$$U = \int \frac{P^2\,dx}{2EA} \tag{5.3}$$

where the integration is made throughout the whole member.

(2) *Bending.* Consider an element of length dx of a member in pure bending about one of the principal axes of the cross section as shown in Figure 5.1. The work done by the applied moment is the product of the average moment times the angle through which it rotates, or
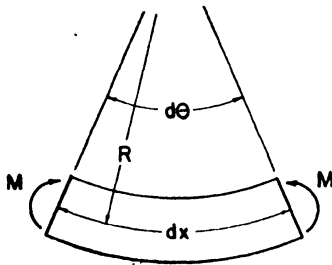

Fig. 5.1. Bending.

$$u = \frac{M\,d\theta}{2} = \frac{M\,dx}{2R}$$

But from Equation 4.17

$$\frac{1}{R} = \frac{M}{EI}$$

So

$$u = \frac{M^2\,dx}{2EI}$$

The total elastic energy in the member is therefore

$$U = \int \frac{M^2\,dx}{2EI} \tag{5.4}$$

EXAMPLE 5.1. Determine the elastic energy stored in a uniform cantilever beam of length L with a concentrated load P at the free end.

From Equation 5.4 $\qquad U = \int_0^L \frac{M^2\,dx}{2EI}$

Measuring the coordinate x from the free end, we find that

$$M = Px$$

Therefore, $\qquad U = \int_0^L \frac{P^2 x^2\,dx}{2EI} = \frac{P^2 L^3}{6EI}$ $\hspace{2cm}$ (5.5)

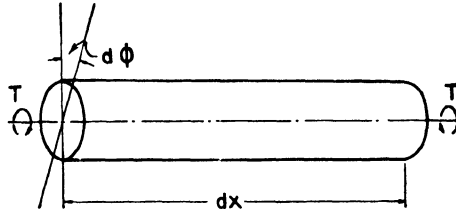(3) *Torsion.* If a torque T is applied to each end of a rod of length

Fig. 5.2. Torsion.

dx, as shown in Figure 5.2, the angle of twist $d\phi$ of one end relative to the other can be shown to be

$$d\phi = \frac{T\,dx}{GC}$$

where G = modulus of rigidity (psi)

$\qquad C$ = geometric property of the cross section which becomes the polar moment of inertia for *circular* sections (in⁴).

This expression is analogous to $d\theta = \frac{M}{EI}\,dx$ for the bending case. The elastic energy stored in the rod is

$$u = \frac{T\,d\phi}{2} = \frac{T^2\,dx}{2GC}$$

Therefore, the total energy for a rod is

$$U = \int \frac{T^2\,dx}{2GC} \hspace{2cm} (5.6)$$

(4) *Shear.* The elastic energy of shear will be derived from the consideration of a small element of length dx subjected to a shear force V, as shown in Figure 5.3. If we assume that the shear force on the right moves a distance δ, then
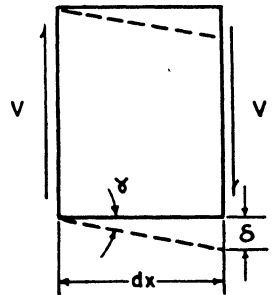

Fig. 5.3. Shear.

$$u = \frac{V\delta}{2}$$

But $\hspace{2cm}$ $\delta = \gamma\,dx$

and it will be shown later that $\gamma = \dfrac{V}{GA}$

where $A =$ area of cross section on which V acts (in^2).

Therefore, $$u = \frac{V^2\,dx}{2GA}$$

and the total energy is $$U = \int \frac{V^2\,dx}{2GA} \tag{5.7}$$

The elastic energy of a structure subjected to tension, bending, torsion, and shear is the sum of the energies given in Equations 5.3, 5.4, 5.6, and 5.7, or

$$U = \int \frac{P^2\,dx}{2EA} + \int \frac{M^2\,dx}{2EI} + \int \frac{T^2\,dx}{2GC} + \int \frac{V^2\,dx}{2GA} \tag{5.8}$$

Fortunately, in the analysis of most structures, not all these energies are present at the same time; therefore, the problem is considerably simplified. It will be shown, for example, that the energy of shear can be neglected for most beams.

5.5 Relation of influence coefficients. Consider a body such as a cantilever beam with two concentrated loads applied at two different positions along the span. If only the load P_1 is applied, then the deflection at point 1 is

$$\delta_1 = k_{11}P_1$$

and the elastic energy is $$U_1 = \frac{k_{11}P_1^2}{2}$$

When the load P_2 is applied, the work added, because of the deflection at point 2, is

$$U_2 = \frac{k_{22}P_2^2}{2}$$

However, in applying the load at 2, the deflection at point 1 is changed by an amount $k_{12}P_2$; and, since the load at 1 remains constant during this process, the additional work done by the load P_1 is the force times the displacement $k_{12}P_2$,

or $$U_{12} = k_{12}P_2P_1$$

The total energy for the system with both loads applied is therefore

$$U = \frac{k_{11}P_1^2}{2} + \frac{k_{22}P_2^2}{2} + k_{12}P_2P_1$$

If the loads are applied in the reverse order so that P_2 is applied first, then the elastic energy is

$$U = \frac{k_{11}P_1^2}{2} + \frac{k_{22}P_2^2}{2} + k_{21}P_1P_2$$

It is apparent that these energies must be equal; for, if they are not equal, it is necessary only to apply the loads in such a manner as to require the least work and remove them in the proper sequence to recover the maximum work and thus create energy.   In order to have the energies equal,

$$k_{12} = k_{21} \tag{5.9}$$

Physically, this equality means that the deflection at point 1 in the direction of a unit load at 1 due to a unit load at point 2, is equal in magnitude to the deflection at point 2 in the direction of a unit load at 2 due to a unit load at point 1.

5.6 Castigliano's theorem.   The elastic energy in structures has been expressed in terms of the loads and deflections of the structure, as indicated in Equation 5.2; and in terms of the loads, the geometry of the structure, and the elastic property of the material, as specified in Equation 5.8.   The equivalence of these expressions suggests a method for determining deflections.   For example, equating the work done by the end load on a cantilever beam to the elastic energy stored as given by Equation 5.5, we have

$$\frac{P\delta}{2} = \frac{P^2 L^3}{6EI}$$

or
$$\delta = \frac{PL^3}{3EI}$$

It is easily shown that the displacement in the direction of a force is obtained also by taking the partial derivative of the strain energy with respect to the force.   Since

$$U = \frac{P^2 L^3}{6EI}$$

therefore
$$\frac{\partial U}{\partial P} = \frac{PL^3}{3EI} = \delta \text{ as before.} \tag{5.10}$$

This latter result can be proved for the general case.   For simplicity the analysis of a structure having two applied loads will be made from which the general case of a system with any number of loads can be inferred.

$$U = \tfrac{1}{2}[P_1\delta_1 + P_2\delta_2]$$

where
$$\delta_1 = k_{11}P_1 + k_{12}P_2$$
$$\delta_2 = k_{21}P_1 + k_{22}P_2$$

Then
$$U = \tfrac{1}{2}[P_1(k_{11}P_1 + k_{12}P_2) + P_2(k_{21}P_1 + k_{22}P_2)]$$
$$U = \tfrac{1}{2}[k_{11}P_1^2 + k_{22}P_2^2 + k_{12}P_1P_2 + k_{21}P_1P_2]$$

but
$$k_{12} = k_{21}$$

therefore,
$$U = \tfrac{1}{2}[k_{11}P_1^2 + k_{22}P_2^2 + 2k_{12}P_1P_2] \tag{5.11}$$

and
$$\frac{\partial U}{\partial P_1} = (k_{11}P_1 + k_{12}P_2) = \delta_1 \tag{5.12}$$

Castigliano's theorem states that the deflection in the direction and at the location of any external force on an elastic structure is the partial derivative of the elastic energy of the structure with respect to the force. Since the results apply equally to moments and rotations, there is an analogous expression

$$\frac{\partial U}{\partial M} = \theta \qquad (5.13)$$

This result may be summarized as follows: The rotation in the direction and at the location of an external moment on an elastic structure is the partial derivative of the elastic energy of the structure with respect to the moment.

The application of Castigliano's theorem to a particular case now may be considered. At the beginning of this article the end deflection of a uniform cantilever beam with a concentrated end load was found to be (Equation 5.10)

$$\delta = \frac{\partial U}{\partial P} = \frac{\partial}{\partial P} \left(\frac{P^2 L^3}{6EI} \right) = \frac{PL^3}{3EI}$$

However, the elastic energy was found by an integration process (Equation 5.5) so that it may be simpler to differentiate before integrating and thus make it unnecessary to obtain the elastic energy in order to determine the deflection. If this is done,

$$\delta = \frac{\partial U}{\partial P} = \frac{\partial}{\partial P} \int_0^L \frac{M^2 \, dx}{2EI}$$

and, since only M is a function of P,

$$\delta = \int_0^L M \frac{\partial M}{\partial P} \frac{dx}{EI}$$

Therefore, since in this case $M = Px$, $\dfrac{\partial M}{\partial P} = x$, then

$$\delta = \int_0^L \frac{Px^2 \, dx}{EI} = \frac{PL^3}{3EI} \text{ as before.}$$

If the deflection in the direction of a load P_0 is required in a structure having the various forms of elastic energy as given by Equation 5.8, it is necessary only to differentiate the expression term by term:

$$\delta = \int P \frac{\partial P}{\partial P_0} \frac{dx}{EA} + \int M \frac{\partial M}{\partial P_0} \frac{dx}{EI} + \int T \frac{\partial T}{\partial P_0} \frac{dx}{GC} + \int V \frac{\partial V}{\partial P_0} \frac{dx}{GA}$$

$$(5.14)$$

The analogous expression for the rotation at a point where a moment M_0 is applied is

$$\theta = \int P \frac{\partial P}{\partial M_0} \frac{dx}{EA} + \int M \frac{\partial M}{\partial M_0} \frac{dx}{EI} + \int T \frac{\partial T}{\partial M_0} \frac{dx}{GC} + \int V \frac{\partial V}{\partial M_0} \frac{dx}{GA}$$

$$(5.15)$$

The use of elastic energy simplifies some deflection problems because visualization of the deformation is not necessary. In other words, a knowledge of the geometry of the deflection of the structure is not required.

EXAMPLE 5.2. Determine the deflection due to shear and bending of a uniform cantilever beam of length L with a symmetrical rectangular cross section of moment of inertia I and area A, and with a concentrated end load P. Also determine the rotation of the end due to bending only.

Solution. Since shear and bending are to be considered, it will be necessary to use Equation 5.14 including the elastic energy of shear and bending. Then

$$\delta = \int_0^L M \frac{\partial M}{\partial P} \frac{dx}{EI} + \int_0^L V \frac{\partial V}{\partial P} \frac{dx}{GA}$$

Measuring x from the free end, we see that

$$M = Px; \qquad V = P$$

so that

$$\frac{\partial M}{\partial P} = x; \qquad \frac{\partial V}{\partial P} = 1$$

$$\delta = \int_0^L \frac{Px^2 \, dx}{EI} + \int_0^L \frac{P \, dx}{GA} = \frac{PL^3}{3EI} + \frac{PL}{GA}$$

Therefore,

$$\delta = \frac{PL^3}{3EI} \left[1 + \frac{3EI}{GAL^2} \right]$$

The second part of this expression represents the effect of shear.

If we let

$$I = Ar^2 = \frac{bh^3}{12}$$

where r = radius of gyration which in this case is equal to the depth of the cross section h divided by $2 \sqrt{3}$,

then

$$\delta = \frac{PL^3}{3EI} \left[1 + \frac{h^2}{4L^2} \frac{E}{G} \right]$$

For aluminum for which $\frac{E}{G} = 2.6$

$$\delta = \frac{PL^3}{3EI} \left[1 + 0.65 \frac{h^2}{L^2} \right]$$

For a short beam for which $L = 5h$,

$$\delta = \frac{PL^3}{3EI} [1 + 0.026]$$

Therefore, if the effect of the shear is neglected in determining the deflection, the results are in error about 3% in this case. It has been assumed in this analysis that the shear is uniformly distributed over the cross section. This is not actually the case, but the results indicate the order of magnitude of the effect of shear.

To determine the rotation of the free end, an applied moment at that point is required. Since there is no applied moment, a moment M_0 is assumed although we know that eventually it will be made equal to zero. If we consider only the bending energy, then from Equation 5.15

$$\theta = \int_0^L M \frac{\partial M}{\partial M_0} \frac{dx}{EI}$$

But
$$M = Px + M_0 \text{ so that } \frac{\partial M}{\partial M_0} = 1$$

Therefore,
$$\theta = \int_0^L (Px + M_0) \frac{dx}{EI}$$

But
$$M_0 = 0$$

Therefore,
$$\theta = \int_0^L Px \frac{dx}{EI} = \frac{PL^2}{2EI}$$

EXAMPLE 5.3. Determine the deflection of point A in the z direction of the simplified landing strut shown in Figure 5.4. The following data apply:

$$P = 50 \text{ lb} \qquad\qquad L_1 = 5 \text{ in}$$
$$\alpha = 20° \qquad\qquad L_2 = 36 \text{ in}$$

The structure is made of $1\frac{1}{4} - 0.035$ 4130 chrome-moly steel tubing, The properties of the tubing as given in the ANC-5 are

$$I = 0.02467 \text{ in}^4 \qquad\qquad E = 29 \times 10^6 \text{ psi}$$
$$J = 2I = 0.04934 \text{ in}^4 \qquad\qquad G = 11 \times 10^6 \text{ psi}$$
$$A = 0.13360 \text{ in}^2$$

Solution. If the effect of shear is neglected, the elastic energy of bending exists in the horizontal tube (1), and a combination of bending and torsion exists in tube (2). The bending moment in tube (1) will be represented by a double-headed vector as shown in Figure 5.4. From equilibrium

$$M_1 = Px_1$$

The force P and moment PL_1 will be applied at the lower end of tube (2) as shown in the figure. At a distance x_2, the torque and bending moment can be determined from equilibrium.

$$\Sigma T = 0 = T_2 - PL_1 \cos \alpha$$
$$T_2 = PL_1 \cos \alpha$$
$$\Sigma M = 0 = M_2 - PL_1 \sin \alpha - Px_2$$
$$M_2 = PL_1 \sin \alpha + Px_2$$

Then
$$\frac{\partial M_1}{\partial P} = x_1; \quad \frac{\partial M_2}{\partial P} = x_2 + L_1 \sin \alpha; \quad \frac{\partial T_2}{\partial P} = L_1 \cos \alpha$$

and
$$\delta = \int_0^{L_1} M_1 \frac{\partial M_1}{\partial P} \frac{dx_1}{EI} + \int_0^{L_2} M_2 \frac{\partial M_2}{\partial P} \frac{dx_2}{EI} + \int_0^{L_2} T_2 \frac{\partial T_2}{\partial P} \frac{dx_2}{GJ}$$

$$\delta = \int_0^{L_1} P x_1^2 \frac{dx_1}{EI} + \int_0^{L_2} P(L_1 \sin \alpha + x_2)^2 \frac{dx_2}{EI} + \int_0^{L_2} P L_1^2 \cos^2 \alpha \frac{dx_2}{GJ}$$

$$\delta = \frac{P}{3EI} (L_1^3 + L_2^3 + 3L_1^2 L_2 \sin^2 \alpha + 3L_1 L_2^2 \sin \alpha) + \frac{P}{GJ} L_1^2 L_2 \cos^2 \alpha$$
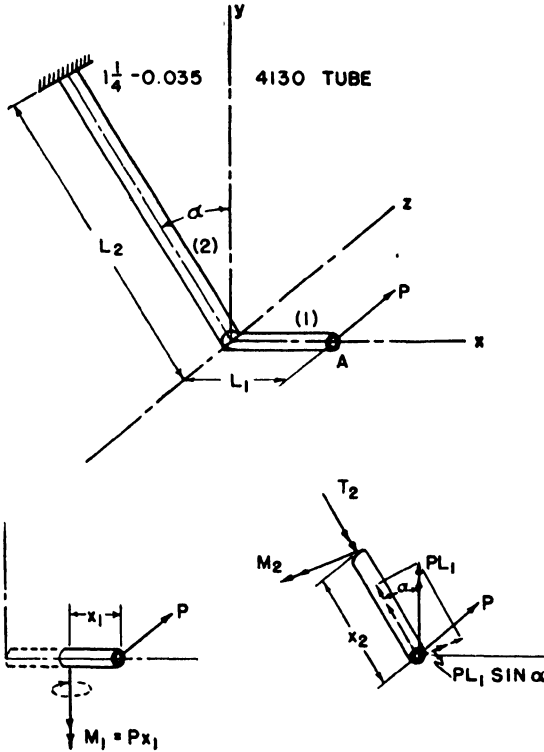
Fig. 5.4.   Simplified Tubular Frame.

If we substitute numerical values,

$$\delta = 1.33 \text{ in}$$

• **5.7 Castigliano's second theorem.**   An extension can be made of the theorem developed in the last article that is particularly useful in solving statically indeterminate structures.

In Article 4.10 a supported cantilever beam was considered, and it was shown that three unknowns were determined from two equations of equilibrium and one condition of deflection; namely, that the deflection at the supported end was zero.   When we know the relation between

elastic energy and deflection, this latter condition can be expressed in terms of the elastic energy of the system. Thus, for any unyielding support (fixed), where R is the reaction at the support which may be either a force or moment,

$$\frac{\partial U}{\partial R} = \delta = 0 \tag{5.16}$$

Equation 5.16 gives the relation of the elastic energy and the *external* reaction at any support where the deflection is zero. A relation now will be developed involving the elastic energy and an *internal* force or moment. Consider a statically indeterminate framework, such as that shown in Figure 5.5. If we assume that one of the diagonal members is cut and that forces are applied as shown, the elastic energy of the system can
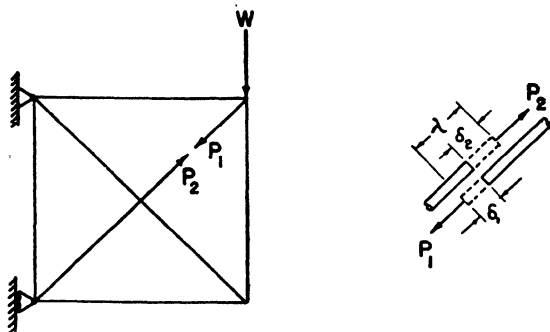
Fig. 5.5. Statically Indeterminate Frame.

be expressed in a manner similar to Equation 5.11. In this case, however, more than two loads must be considered since there are other members of the structure having elastic energy. Then

$$U = \tfrac{1}{2}[k_{11}P_1^2 + k_{22}P_2^2 + 2k_{12}P_1P_2 + \text{other similar terms}]$$

Assuming the same relations to exist for the "other similar terms" and considering in detail only the first three terms of the elastic energy, we see that

$$\frac{\partial U}{\partial P_1} = k_{11}P_1 + k_{12}P_2 + \cdots = \delta_1$$

$$\frac{\partial U}{\partial P_2} = k_{22}P_2 + k_{12}P_1 + \cdots = \delta_2$$

Therefore $\qquad \lambda = \delta_1 + \delta_2 = \dfrac{\partial U}{\partial P_1} + \dfrac{\partial U}{\partial P_2} \tag{5.17}$

Since P_1 and P_2 are internal forces in the same member, they must be equal in magnitude. Therefore, if $P_1 = P_2 = P$

$$U = \tfrac{1}{2}[k_{11}P^2 + k_{22}P^2 + 2k_{12}P^2 + \cdots \text{ other similar terms}]$$

and $\qquad \dfrac{\partial U}{\partial P} = k_{11}P + k_{22}P + 2k_{12}P + \cdots = \delta_1 + \delta_2 \tag{5.18}$

By comparing Equations 5.17 and 5.18, it is evident that

$$\frac{\partial U}{\partial P} = \lambda \tag{5.19}$$

If the structure is continuous so that there are no overlaps or gaps in the members, then

$$\frac{\partial U}{\partial P} = 0 \tag{5.20}$$

Equation 5.20 states that the rate of change of the elastic energy of a structure with respect to an internal force or moment is zero. Since the vanishing of this derivative is a condition for maximum or minimum energy, it can be shown that an elastic structure in stable equilibrium will assume a configuration so as to make the elastic energy a minimum. This is known as the *principle of least work*.

EXAMPLE 5.4.   Determine the force in a cable supporting the end of a cantilever carrying a uniform load, as shown in Figure 5.6.

Solution. The force in the cable will be assumed to be P_2. Referring to the properties of the beam by subscript 1 and using subscript 2 for the cable, then from Equations 5.14 and 5.20, we have

Fig. 5.6.   Beam with Elastic End Support.

$$\frac{\partial U}{\partial P_2} = 0 = \int_0^L M \frac{\partial M}{\partial P_2} \frac{dx}{E_1 I_1} + \int_0^a P \frac{\partial P}{\partial P_2} \frac{dy}{E_2 A_2}$$

But $M = P_2 x - \dfrac{wx^2}{2}$

and $P = P_2$

Therefore, $\dfrac{\partial M}{\partial P_2} = x$ and $\dfrac{\partial P}{\partial P_2} = 1$

Then

$$0 = \int_0^L \left[P_2 x - \frac{wx^2}{2} \right] x \frac{dx}{E_1 I_1} + \int_0^a P_2 \frac{dy}{E_2 A_2}$$

$$0 = \frac{1}{E_1 I_1} \left[\frac{P_2 L^3}{3} - \frac{wL^4}{8} \right] + \frac{P_2 a}{E_2 A_2}$$

or

$$P_2 = \frac{3}{8} \left[\frac{wL^4}{L^3 + \dfrac{3a E_1 I_1}{E_2 A_2}} \right]$$

If the cable is considered as infinitely rigid, the system reduces to the one of the supported cantilever. Thus, as $E_2 A_2 \to \infty$, $P_2 \to \frac{3}{8} wL$.

As the cable is made less and less stiff, more and more of the load w is carried by the beam until $E_2 A_2 \to 0$ and $P_2 \to 0$.

When we know the end force on the cantilever, we can determine the bending moment and shear force distribution of the beam.

Problems

5.1. An elastic cable is strung between two supports and carries a load at the midpoint, as shown in Figure 5.7. If the cable is initially straight and horizontal

Fig. 5.7. Cable with Load.

and if the deflection after the load is applied is δ, show that the principle of superposition cannot be applied to this structure.
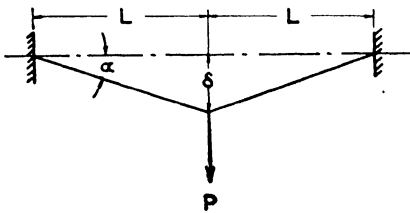
5.2. A nonuniform cantilever beam such as a wing is loaded at its end, and the deflections are measured at various points along the length of the beam so that the deflection curve may be plotted. What additional information can be determined readily from the curve?

5.3. Show that for a cantilever beam such as a wing the *average* deflection produced by a load at the end is the same as the deflection at the end produced by the same load uniformly distributed.

5.4. Determine the deflection and rotation at the mid span of a uniform cantilever beam carrying a uniformly distributed load.

5.5. Solve Problem 4.7 by elastic energy methods.

5.6. A torque of 1000 lb in about the x axis is applied at point A of the structure shown in Figure 5.4. Determine the deflection in the z direction and the angle of twist in the yz plane of the end of the tube at point A.

5.7. Determine the fixed-end moments for the beam shown in Figure 4.18 by elastic energy methods.

5.8. Determine the reaction at the simply supported end of the beam shown in Figure 5.8, and draw the moment diagram.
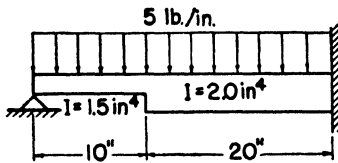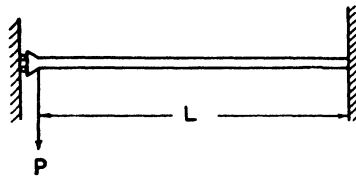

Fig. 5.8. Supported Cantilever.

Fig. 5.9. Cantilever.

5.9. An aluminum beam as shown in Figure 5.9 has both ends fixed against rotation although the left end is free to displace vertically. With the beam loaded as shown determine,

(a) moments at ends of beam
(b) deflection at end.

References

Southwell, R. V., *An Introduction to the Theory of Elasticity*. Oxford Press, 1936.
Timoshenko, S., *Theory of Elasticity*. McGraw-Hill, 1934.
Timoshenko, S., *Theory of Structures*. McGraw-Hill, 1945.
Van Den Broek, J. A., *Elastic Energy Theory*. John Wiley and Sons, 1942.

CHAPTER 6

Load Transmission in Multiple
Span Beams

$\bullet$

6.1 Introduction. The single-span beams discussed in Chapter 4 had either fixed ends, in which case the ends were completely restrained against rotation, or supported ends, in which the ends were unrestrained with regard to rotation. *Multiple-span* or *continuous beams* are beams having several supports such as, for example, floor beams which are supported at several points by bulkhead rings. The restraint against rotation of the ends of each span depends upon the stiffnesses of the connecting spans. The interconnection between spans means that the stiffness of any span influences to some extent the moment distribution of every other span.

Two methods will be developed for analyzing multiple span beams. One method, which uses the *equation of three moments*, requires the solution of a set of simultaneous equations for beams with more than two spans. Another method, called the *moment distribution* or *Hardy Cross method*, is a method of successive approximations in which all the unknowns are obtained directly without the solutions of simultaneous equations. In general, the equation of three moments is simpler to use on beams of three spans or less, whereas the moment distribution method is easier to use for beams of more than three spans.

6.2 Equation of three moments. Consider a beam resting on three supports, as shown in Figure 6.1. If the beam is cut at the center support B, the internal moment, M_B, acting on the cut ends will be equal in magnitude and in the direction shown. The left span (1) and right span (2) now can be considered as single-span beams with the condition that the moment M_B must be adjusted so that the rotation of span (1) at B is equal to the rotation of span (2) at B, which thus makes the beam continuous over the support.

The forces and moments for the left span have been resolved into their components. If M_{p1} is the moment due to the distributed loading p_1 span (1) being assumed as simply supported, then the moment at any point a distance x_1 from the *left* end of span (1) is

$$M_1 = M_{p1} + \frac{M_A}{L_1}(L_1 - x_1) + M_B \frac{x_1}{L_1} \qquad (6.1)$$

and
$$\frac{\partial M_1}{\partial M_B} = \frac{x_1}{L_1}$$

Similarly, if we measure x_2 from the *right* end of span (2),

$$M_2 = M_{p2} + \frac{M_C}{L_2}(L_2 - x_2) + M_B\frac{x_2}{L_2} \qquad (6.2)$$

and $\qquad \dfrac{\partial M_2}{\partial M_B} = \dfrac{x_2}{L_2}$

DEFLECTION

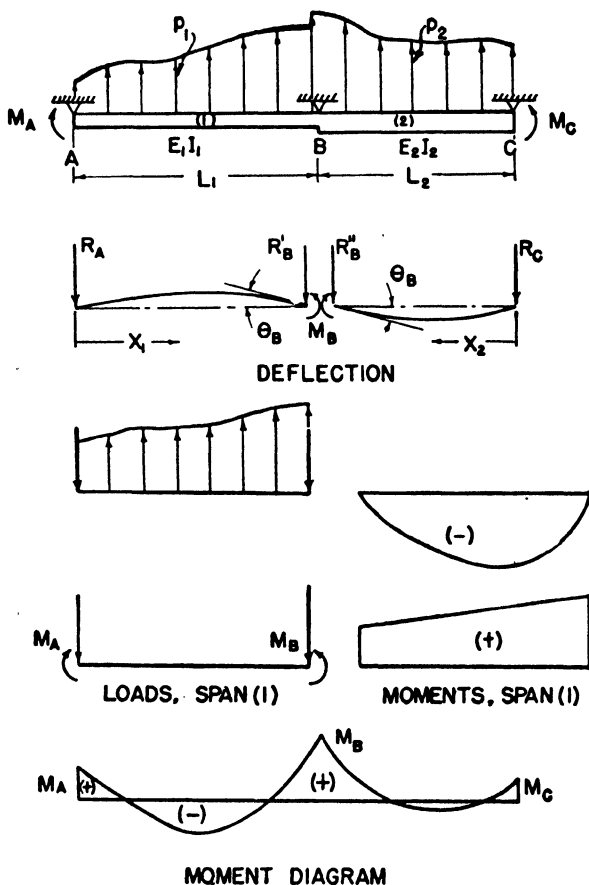LOADS, SPAN (I)   MOMENTS, SPAN (I)

MOMENT DIAGRAM

Fig. 6.1.   Two-Span Beam with Distributed Load.

According to the principle of least work (Equation 5.20), which is equivalent to equating the slopes on each side of support B,

$$\frac{\partial U}{\partial M_B} = 0 = \int_0^{L_1} M_1 \frac{\partial M_1}{\partial M_B}\frac{dx_1}{E_1 I_1} + \int_0^{L_2} M_2 \frac{\partial M_2}{\partial M_B}\frac{dx_2}{E_2 I_2}$$

$$0 = \int_0^{L_1}\left[M_{p1} + \frac{M_A}{L_1}(L_1 - x_1) + M_B\frac{x_1}{L_1}\right]\frac{x_1}{L_1}\frac{dx_1}{E_1 I_1} \quad .$$

$$\cdot \quad + \int_0^{L_2}\left[M_{p2} + \frac{M_C}{L_2}(L_2 - x_2) + M_B\frac{x_2}{L_2}\right]\frac{x_2}{L_2}\frac{dx_2}{E_2 I_2}$$

For EI constant in each span,

$$M_A \frac{L_1}{E_1 I_1} + 2M_B \left(\frac{L_1}{E_1 I_1} + \frac{L_2}{E_2 I_2} \right) + M_C \frac{L_2}{E_2 I_2}$$
$$= - \frac{6}{E_1 I_1 L_1} \int_0^{L_1} M_{p1} x_1 \, dx_1 - \frac{6}{E_2 I_2 L_2} \int_0^{L_2} M_{p2} x_2 \, dx_2 \quad (6.3)$$

where M_{p1} = the moment due to the load p_1 at any section a distance x_1 from the *left* end of span (1) when the span is assumed to be simply supported,

and M_{p2} = the moment due to the load p_2 at any section a distance x_2 from the *right* end of span (2) when the span is assumed to be simply supported.

Equation 6.3 is called the *equation of three moments*. The integrals on the right may be interpreted geometrically as the moments of the areas of the moment diagrams.

If M_B is known, the reactions at the supports can be determined by statics. Thus, if the moment due to the load p_1 *only* about A is called M_{p1A}, then

$$\Sigma M_A = M_A - M_B - M_{p1A} + R'_B L_1 = 0$$

Therefore, $$R'_B = \frac{M_B - M_A + M_{p1A}}{L_1}$$

Similarly, $$R''_B = \frac{M_B - M_C + M_{p2C}}{L_2}$$

The final reaction at B is therefore

$$R_B = R'_B + R''_B$$
$$R_B = \frac{M_B - M_A + M_{p1A}}{L_1} + \frac{M_B - M_C + M_{p2C}}{L_2} \quad (6.4)$$

EXAMPLE 6.1. Determine the moments at the supports, the support reactions, and the moment diagram for the two-span beam shown in Figure 6.2 when the material of the beam is aluminum and

$w = 10$ lb/in	$a = 5$ in	$\dfrac{L_1}{I_1} = 30$
$P = 300$ lb	$I_1 = 1$ in^4	
$L_1 = 30$ in	$I_2 = 1.5$ in^4	$\dfrac{L_2}{I_2} = 24$
$L_2 = 36$ in	$E_1 = E_2 = 10.5 \times 10^6$ psi	

Solution. The moment at B will be obtained from Equation 6.3. For $E = $ constant

$$M_A \frac{L_1}{I_1} + 2M_B \left(\frac{L_1}{I_1} + \frac{L_2}{I_2} \right) + M_C \frac{L_2}{I_2}$$
$$= - \frac{6}{I_1 L_1} \int_0^{L_1} M_{p1} x_1 \, dx_1 - \frac{6}{I_2 L_2} \int_0^{L_2} M_{p2} x_2 \, dx_2$$

The moment M_A is the moment of the overhang

$$M_A = \frac{wa^2}{2} = \frac{10(5)^2}{2} = 125 \text{ lb in}$$

and $M_C = 0$
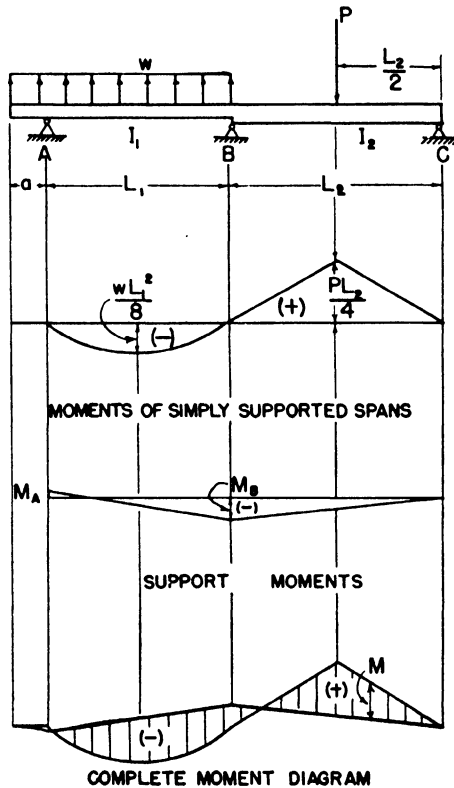
Fig. 6.2. Two-Span Beam.

The moment on the left span due to the load w, assuming a simply supported beam, is

$$M_{p1} = \frac{wx_1^2}{2} - \frac{wL_1x_1}{2} = \frac{w}{2}(x_1^2 - L_1x_1)$$

Thus, $$\int_0^{L_1} M_{p1}x_1\,dx_1 = \int_0^{L_1} \frac{w}{2}(x_1^3 - L_1x_1^2)\,dx_1 = -\frac{wL_1^4}{24}$$

The first load term on the right of the equation of three moments is therefore

$$-\frac{6}{I_1L_1}\int_0^{L_1} M_{p1}x_1\,dx_1 = -\frac{6}{I_1L_1}\left(\frac{-wL_1^4}{24}\right) = \frac{wL_1^3}{4I_1} = \frac{10(30)^3}{(4)(1)}$$

$$= 67,500 \text{ lb/in}^2$$

The second load term on the right will be determined geometrically. Thus,

$$\int_0^{L_2} M_{p2}x_2\, dx_2 = \text{moment of the area of the moment curve about point } C$$

$$= \frac{PL_2}{4}\frac{L_2}{2}\frac{L_2}{2} = \frac{PL_2^3}{16}$$

and

$$-\frac{6}{I_2 L_2}\int_0^{L_2} M_{p2}x_2\, dx_2 = -\frac{6}{16}\frac{PL_2^2}{I_2} = \frac{-6(300)(36)^2}{(16)(1.5)} = -97{,}200 \text{ lb/in}^2$$

By substituting the above values into the equation of three moments,

$$(125 \times 30) + 2M_B(30 + 24) = 67{,}500 - 97{,}200$$
$$M_B = -310 \text{ lb in (tension in top fiber)}.$$

The final moment distribution is shown in Figure 6.2.

The reactions are determined from equilibrium and Equation 6.4:

$$R_B = \frac{M_B - M_A + M_{p1A}}{L_1} + \frac{M_B - M_C + M_{p2C}}{L_2}$$

$$= \frac{-310 - 125 + 4500}{30} + \frac{-310 - 0 - 5400}{36}$$

$$= -23 \text{ lb (upward)}.$$

Also for the right span

$$\Sigma M_B = -310 + 5400 + R_C 36 = 0$$
$$R_C = -141 \text{ lb (upward)}$$

and

$$\Sigma F_v = 0 = R_A - 350 - 23 + 300 - 141$$
$$R_A = 214 \text{ lb (downward)}.$$

6.3 Beam with more than two spans. The equation of three moments can be used for the analysis of beams of more than two spans by repeating the equation for two spans at a time until the entire length of the beam has been considered.
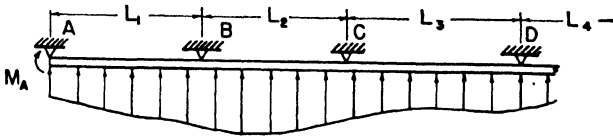
Fig. 6.3. Multiple-Span Beam.

Figure 6.3 shows a multiple span beam with the spans numbered 1, 2, 3, and so forth. The equation of three moments for the first two spans is

$$M_A \frac{L_1}{E_1 I_1} + 2M_B\left(\frac{L_1}{E_1 I_1} + \frac{L_2}{E_2 I_2}\right) + M_C \frac{L_2}{E_2 I_2}$$
$$= \text{loading terms for spans 1 and 2.} \quad (6.5)$$

For spans 2 and 3,

$$M_B \frac{L_2}{E_2 I_2} + 2M_C \left(\frac{L_2}{E_2 I_2} + \frac{L_3}{E_3 I_3} \right) + M_D \frac{L_3}{E_3 I_3}$$
$$= \text{loading terms for spans 2 and 3.} \quad (6.6)$$

Continuing in this manner gives a set of simultaneous equations with as many equations as unknowns. The moments at the supports thus can be determined, and the reactions at the supports can be determined from the statical equilibrium conditions.

6.4 Effect of end fixity. In the previous analyses of multi-span beams it had been assumed that the beam was free to rotate at the supports. If one or both ends of the beam are fixed against rotation, the moments can be determined by the equation of three moments.

Consider a two-span beam with the right end fixed. This would correspond to restraining the beam shown in Figure 6.3 at the support C. Since the beam at C cannot rotate, the restraint can be thought of being produced by having span 3 so stiff that no rotation at C is possible. With $I_3 = \infty$ Equations 6.5 and 6.6 become

$$M_A \frac{L_1}{E_1 I_1} + 2M_B \left(\frac{L_1}{E_1 I_1} + \frac{L_2}{E_2 I_2} \right) + M_C \frac{L_2}{E_2 I_2}$$
$$= \text{loading terms for spans 1 and 2.}$$

$$M_B \frac{L_2}{E_2 I_2} + 2M_C \frac{L_2}{E_2 I_2} = \text{loading terms for span 2.} \quad (6.7)$$

These two equations can be solved simultaneously for the unknowns M_B and M_C.

6.5 Moment distribution method. The equation of three moments is most suitable for the analyses of beams having less than two or three unknowns. For the determination of more unknown moments, the solution of the necessary simultaneous equations becomes burdensome; therefore, another method involving successive approximations is more suitable. The method of successive approximations is sometimes called the *Hardy Cross method*, after its originator, or more generally the *moment distribution method*. The philosophy of the method has been extended to many structures other than beams or frames with considerable success; and the general method, of which the moment distribution method is a special case, is called the *relaxation method*.

Briefly stated, the moment distribution method consists of fixing the beam at each support so that the slopes at the supports are all zero when the loads are applied. The restraints are then released one by one. Allowing the beam to rotate at one support changes the moments at the adjacent supports. After one end of the beam has been released and the

beam has reached equilibrium, the end is fixed again, and the restraints at the other supports are released one by one. This process continues until the releasing of the beam at the supports does not change the moments at the adjacent supports and does not change the slope of the beam at any support with an accuracy sufficient for engineering purposes. When this condition is obtained the conditions of continuity and equilibrium have been satisfied.

Consider the continuous beam shown in Figure 6.4. If the beam is fixed at each support A, B, and C, then the fixed-end moments for the
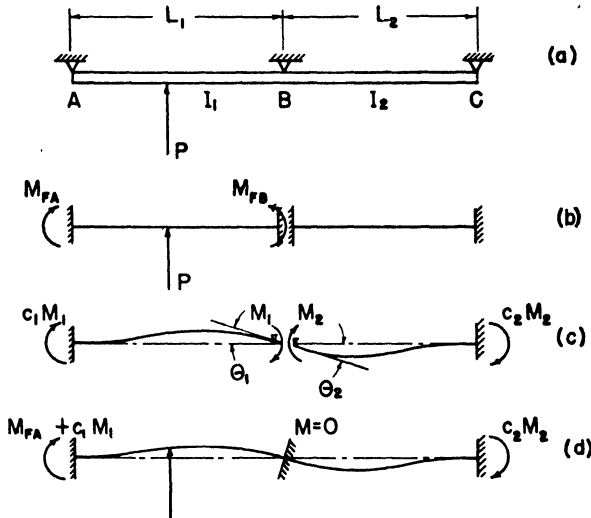
Fig. 6.4.   Moment Distribution.

left span are M_{FA} and M_{FB}, as shown in (b). However, the counterclockwise moment at B represents an unbalanced external moment. This unbalanced moment may be balanced out by applying moments M_1 and M_2 in such a way that the slopes on each side of support B are equal and by making the sum of the balancing moments equal to the unbalanced moment, as shown in Figure 6.4(b), (c), and (d).

If we take *clockwise moments positive*, then

$$\Sigma M_B = 0 = M_1 + M_2 - M_{FB} \qquad (6.8)$$

For continuity $\theta_1 = \theta_2$

but from Equation 4.35 $\theta_1 = \dfrac{M_1 L_1}{4E_1 I_1}; \ \theta_2 = \dfrac{M_2 L_2}{4E_2 I_2} \qquad (6.9)$

Therefore, if $E_1 = E_2$

$$M_1 = M_2 \frac{L_2 I_1}{L_1 I_2}$$

Substituting this value into the equilibrium Equation 6.8 and solving for M_2 gives

$$M_2 = M_{FB} \frac{\dfrac{I_2}{L_2}}{\dfrac{I_2}{L_2} + \dfrac{I_1}{L_1}} = M_{FB} R_2 \tag{6.10}$$

where $\dfrac{I}{L}$ = stiffness factor

R = distribution factor.

Distributing the unbalanced moment M_{FB} into a moment M_1 on the left span and M_2 on the right, changes the moments at A and C. It has been shown (Article 4.11) that a supported cantilever with an end moment induces a *beam* moment at the fixed end equal to half the applied moment and in the opposite direction. Using a *clockwise sign convention* as shown in Figure 6.4(c), a moment M_2 on the right span at support B, makes the moment at C

$$M_C = \frac{M_2}{2} = c_2 M_2 \tag{6.11}$$

where $c_2 = \frac{1}{2}$ = the carry-over factor.

The moments at the supports A and C are changed by the distributed moments at B by an amount $c_1 M_1$ and $c_2 M_2$ respectively. The new moments at A and C are now distributed similarly. Distributing the unbalanced moment at A and C in turn, changes the moment at B, and the process is continued until the unbalanced moments converge to a negligible value.

EXAMPLE 6.2. Determine the moments at the supports by the moment distribution method for the method beam analyzed in Example 6.1.

The stiffness factors are

$$\frac{I_1}{L_1} = \frac{1}{30} = 0.0333; \frac{I_2}{L_2} = \frac{1.5}{36} = 0.0417$$

The overhang on the left of support A offers no restraint against rotation; so the stiffness is zero.

$$\frac{I}{a} = 0$$

Similarly to the right of C, $\dfrac{I}{L} = 0$

The distribution factor at support B is obtained from Equation 6.10:

$$R_1 = \frac{\dfrac{I}{L_1}}{\dfrac{I_1}{L_1} + \dfrac{I_2}{L_2}} = \frac{0.0333}{0.0333 + 0.0417} = 0.444$$

$$R_2 = 1 - R_1 = 1 - 0.444 = 0.556$$

At A and C the distribution factors on each side are

$$R = \frac{0}{\dfrac{I_1}{L_1}} = 0$$

$$R = \frac{\dfrac{I_1}{L_1}}{0 + \dfrac{I_1}{L_1}} = 1$$

The fixed-end moments for span (1) are given by Equation 4.40:

$$M = \frac{1}{L_1^2} \int_0^{L_1} wx^2(L_1 - x)\, dx = \frac{1}{12}\, wL_1^2 = \frac{1}{12} \times 10 \times (30)^2 = 750 \text{ lb in}$$

For span (2), using Equation 4.36 gives

$$M = \frac{PL_2}{2L_2^2}\left(L_2 - \frac{L_2}{2}\right)^2 = \frac{PL_2}{8} = \frac{300 \times 36}{8} = 1350 \text{ lb in}$$

For cantilever on the left

$$M = \frac{wa^2}{2} = \frac{10(5)^2}{2} = 125 \text{ lb in}$$

The solution of the problem is shown in Figure 6.5. The stiffness factors and distribution factors have been tabulated in the first two lines of the table. The fixed-end moments are given on the third line, and it should be noticed that the moments correspond to the clockwise sign convention. The fourth line shows the distributed moments. For example, at support B there is a counterclockwise moment of 1350 lb in to the right of the support and a counterclockwise moment of 750 lb in to the left. The total unbalanced moment is $750 + 1350 = 2100$ lb in counterclockwise. This must be balanced out by a clockwise moment $(+)$ distributed according to the distribution factors on line 2. These balancing moments are shown on line 4. The carry-over moments are shown on the fifth line. These moments are obtained by multiplying the distributed moments by the carry-over factor of $\frac{1}{2}$ and applying the resulting moments at the opposite ends of the span. This completes the cycle of operation, and then the process is repeated.

Since there was no change in the distributions of lines 7 and 8, the process could have been stopped at line 8. However, in this case the distribution was carried one more step to show the rate of decrease of the values. If you are in doubt, continue the distribution until the values on a line at the completion of a step become small compared with the values of the initial fixed-end moments.

The moments at the supports are obtained by adding separately the columns to the left and right of the supports. If no errors have been made, the sums should be numerically equal with opposite sign. Thus, at support B the sum of the left column is 308 lb in and the sum of the right is -308 lb in. This means a *clockwise* moment inducing tension in the top fiber of the beam on the left and a counterclockwise moment
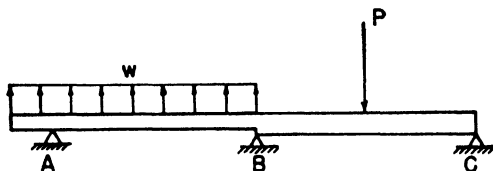
STIFFNESS FACTOR	0	0.0333		0.0417		0	(1)
DISTRIBUTION FACTOR	0	1	0.444	0.556		1	0	(2)
FIXED-END MOM.	-125	750	-750	-1350	1350	0	(3)
DISTRIBUTED MOM.	0	625	932	1168	-1350	0	(4)
CARRY-OVER MOM.	0	466	-312	-675	584	0	(5)
DISTRIBUTED MOM.	0	466	438	549	-584	0	(6)
	0	219	-233	-292	274	0	(7)
	0	219	233	292	-274	0	(8)
	0	116	-109	-137	146	0	(9)
	0	116	109	137	-146	0	(10)
MOM. AT SUPPORTS	-125	125	308	-308	0	0	(11)

Fig. 6.5. Moment Distribution for Two-Span Beam.

inducing tension in the top fiber on the right. The moment determined from the equation of three moments at this support was found to be 310 lb in.

6.6 Effect of support deflection. In many instances multiple-span beams are supported on structures which themselves are elastic and may therefore deform. An example of a beam on deflecting supports would be an elevator which is supported by connecting hinges to the horizontal stabilizer. The effect of the displacements of the supports can be considered by superimposing the fixed-end moments caused by the deflection of the supports and the fixed-end moments due to the regular loading and then proceeding with the usual moment distribution.

Figure 6.6 shows a beam for which the three supports have moved a distance δ_A, δ_B and δ_C. The left span between supports A and B is

shown with the fixed-end moments M_δ induced by the relative support deflection $\delta_A - \delta_B$. The moment at any point x is

$$M = Rx - M_\delta$$

From Castigliano's theorem

$$\delta_A - \delta_B = \frac{\partial U}{\partial R} = \int_0^L M \frac{\partial M}{\partial R} \frac{dx}{EI} = \int_0^L (Rx - M_\delta)x \frac{dx}{EI}$$

$$= \frac{1}{EI}\left(\frac{RL^3}{3} - \frac{M_\delta L^2}{2}\right)$$
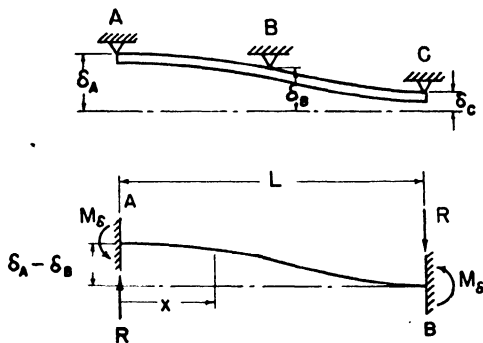
Fig. 6.6. Support Deflection.

If we take moments about B, for equilibrium

$$\Sigma M_B = 0 = RL - 2M_\delta$$

$$R = \frac{2M_\delta}{L}$$

Therefore, $$\delta_A - \delta_B = \frac{M_\delta L^2}{6EI}$$

$$M_\delta = \frac{6EI}{L^2}(\delta_A - \delta_B) \tag{6.12}$$

This fixed-end moment caused by the deflection of the support should be added with proper regard for sign to the fixed-end moment due to the load.   This sum takes the place of the values on line 3 of Figure 6.5.

6.7 Discussion of end restraints.   In the examples, the moment distribution method has been applied only to multiple-span beams with the beams externally unrestrained against rotation at the supports.   One of the most useful applications of the moment distribution method is for beams with one or both ends fixed.   The fixing of the end influences the distribution factor at that point.   For example, if the end C of the beam in Figure 6.5 is fixed, then the effect of the fixity can be considered as being produced by a span to the right of C with an infinitely large stiffness factor.   Since the stiffness factor to the left of C is 0.0417, the distribution factor on this

side is $\dfrac{0.0417}{0.0417 + \infty} = 0$.   This means that all the moment going to C is absorbed and the convergence of the values is greater than before so that fewer steps are required for a solution.

It is possible for the ends of a beam to be only partially restrained against rotation, as would be the case if the end of the beam were connected to an elastic structure.   Since the distribution factor for a beam with a pin-connected end is unity and the factor for a beam with a completely fixed end is zero, it follows that for a beam with the end 75% fixed the distribution factor is 0.25 on the beam side and 0.75 on the restrained side of the support.   This scheme provides an easy way of considering various end restraints.

6.8 Determination of distribution factors and carry-over factors for nonuniform beams.   The moment distribution method has been applied to beams for which the modulus of elasticity and moment of inertia are constant throughout each span.   There are cases, such as when the beam is tapered, when this latter assumption does not hold.   The carry-over factors and distribution factors for nonuniform spans are different from those for uniform spans.

The values of the distribution factors and carry-over factors for nonuniform beams may be determined from a consideration of their definition as given by Equations 6.10 and 6.11.   According to Equation 6.11 the carry-over factor is defined as the ratio of the moment induced at the fixed end of a supported cantilever beam to the moment applied at the supported end.   This ratio can be determined by the methods given in Chapters 4 and 5.   It is apparent that the carry-over factor in going from left to right on the beam may be different from that for going from right to left.

From the derivation of the distribution factor given in Equation 6.10 it can be shown that the distribution factor is defined as the ratio of the moment to produce unit rotation of the span to one side of the support when the span is assumed to be a supported cantilever, to the sum of the moments required to produce unit rotation on the spans to both sides of the support.

6.9 Short cuts of moment distribution method.   Only the fundamentals of the moment distribution method have been discussed in the foregoing articles.   Many short cuts have been devised which greatly simplify the solution of many problems.   It is suggested that the student study the references for further information.

Problems

6.1. Figure 6.7 shows the distribution of possible floor loadings for a modern transport.   If the numbers represent the load in pounds per linear inch, and if I is the moment of inertia of the floor beam for the various spans, determine

(1) bending moments at the supports
(2) bending moment diagrams
(3) reactions at the supports.
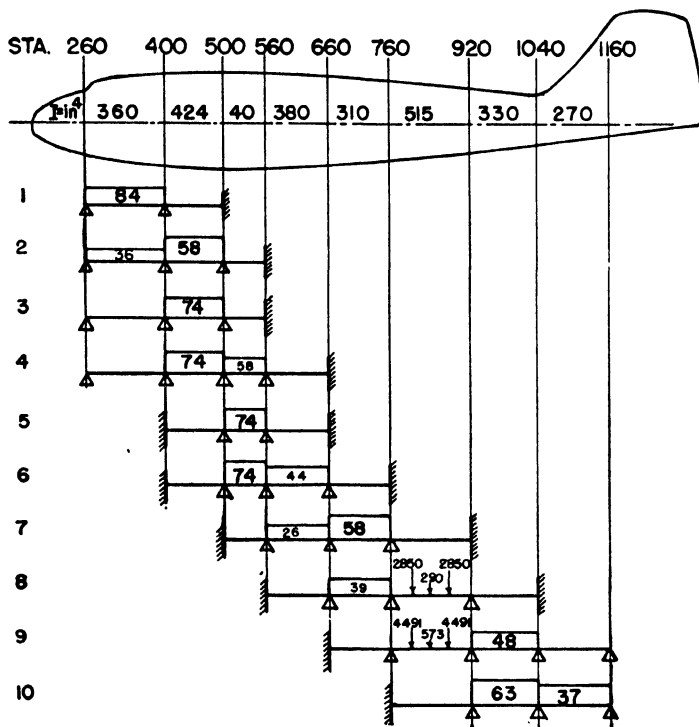
Fig. 6.7.   Floor Loading.

6.2. An elevator spar supported at six hinge points is loaded as shown in Figure 6.8.   Assume that the moment of inertia of the cross section of the spar
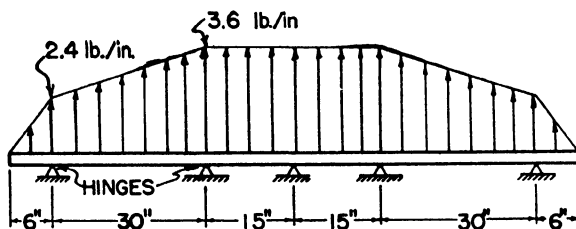
Fig. 6.8.   Elevator Spar.

is constant, and determine

(1) moments at hinges
(2) moment diagram.

(*Hint:* The problem can be simplified if it is realized that the structure is symmetrical about the center hinge so that the slope of the beam at the center hinge is zero.)

6.3. One half of an aluminum elevator spar is shown in Figure 6.9. If the hinge supports deflect as shown, determine the beam moments at the supports.
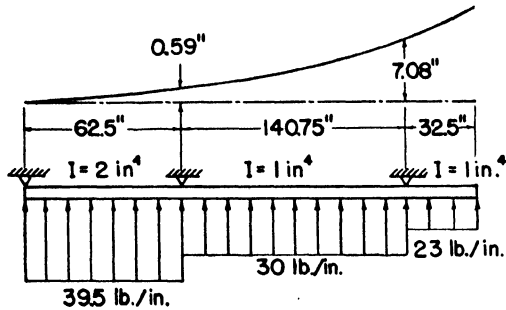
Fig. 6.9. Deflected Elevator.

6.4. Determine the bending moments and shear forces for the uniform floor beam shown in Figure 6.10, assuming that the fuselage wall restrains the rotation of the ends of the floor beam 50%.
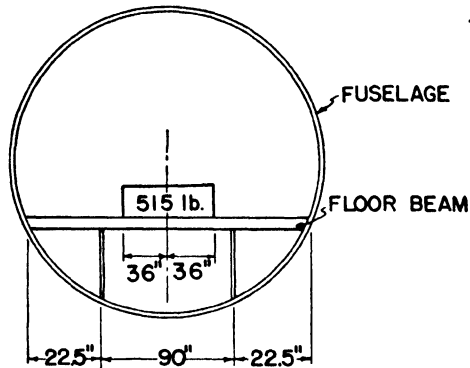
Fig. 6.10. Loading on Floor Beam.

References

Cross, Hardy, "Analysis of Continuous Frames by Distributing Fixed-end Moments." Transactions ASCE, 1932.

Southwell, R. V., *Relaxation Methods in Engineering Science.* Oxford Press, 1940.

Williams, H. A., "The Application of the Hardy Cross Method of Moment Distribution." Transactions ASME, 1934.

CHAPTER 7

Frames and Rings

....

7.1 Introduction. For the multiple-span beams discussed in the previous chapter it was shown that the moments and forces in the beams depended on the stiffness distribution and the support restraint as well as the loading. In all cases, however, the beam axis was essentially a straight line so that the analysis was not complicated by the necessity of considering the geometry of curved members or bent sections. Some structures such as bulkhead rings or fuselage frames are composed of curved members or a complicated arrangement of members which makes the geometry of the structure complex.

A few of these more complicated structures will be discussed in this chapter. The fundamental principles of analysis will be the same as those used before.
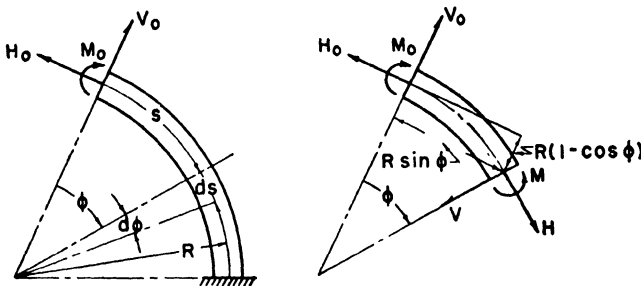
Fig. 7.1. Curved Beam.

7.2 Deflection of curved beams. One of the most useful applications of Castigliano's theorem is for the solutions of the deflections and forces in curved members. Since the derivation of these theorems is in no way restricted by the geometry of the structure, they can be applied directly to curved members.

Consider a curved beam for which the locus of the center of gravities of the cross sections is a portion of an arc of a circle and with a bending moment, a thrust, and a shear force applied to the end, as shown in Figure 7.1. It has been shown already in Example 5.2 that the effect of the shear force on deflection is negligible for most beams and depends on the length to depth ratio and the type of cross section of the beam. Similar conclusions can be made for the effect of the thrust on the deflection of the curved beam. Therefore, if the energy of thrust and shear is assumed to be negligible, the elastic energy is given by

$$U = \int M^2 \frac{ds}{2EI} \tag{7.1}$$

where ds is an element of length along the beam. In the case of the circular bar it is more suitable to use polar coordinates. Therefore, substituting $ds = R\,d\phi$ gives

$$U = \int_0^\beta M^2 \frac{R\,d\phi}{2EI}$$

But $M = M_0 - H_0 R(1 - \cos \phi) + V_0 R \sin \phi$

and $\frac{\partial M}{\partial M_0} = 1; \; \frac{\partial M}{\partial H_0} = -R(1 - \cos \phi); \; \frac{\partial M}{\partial V_0} = R \sin \phi$

According to Castigliano's theorem,

$$\delta_R = \frac{\partial U}{\partial V_0} = \int_0^\beta M \frac{\partial M}{\partial V_0} \frac{R\,d\phi}{EI}$$

$$= \frac{R^2}{EI} \left\{ M_0(1 - \cos \beta) + H_0 R \left(\frac{3}{4} - \cos \beta + \frac{1}{4} \cos 2\beta \right) \right.$$
$$\left. + \frac{V_0 R}{2} \left(\beta - \frac{1}{2} \sin 2\beta \right) \right\} \tag{7.2}$$

$$\delta_T = \frac{\partial U}{\partial H_0} = \int_0^\beta M \frac{\partial M}{\partial H_0} \frac{R\,d\phi}{EI}$$

$$= \frac{R^2}{EI} \left\{ M_0(\sin \beta - \beta) + H_0 R \left(\frac{3}{2}\beta - 2 \sin \beta + \frac{1}{4} \sin 2\beta \right) \right.$$
$$\left. - V_0 R \left(\frac{3}{4} - \cos \beta + \frac{1}{4} \cos 2\beta \right) \right\} \tag{7.3}$$

$$\theta = \frac{\partial U}{\partial M_0} = \int_0^\beta M \frac{\partial M}{\partial M_0} \frac{R\,d\phi}{EI}$$

$$= \frac{R}{EI} \left\{ (M_0 - H_0 R)\beta + H_0 R \sin \beta + V_0 R(1 - \cos \beta) \right\} \tag{7.4}$$

where δ_R = deflection in radial direction, positive away from center (in)

δ_T = deflection in tangential direction, extension positive (in)

θ = clockwise rotation (rad).

The expressions for the deflections become simplified for $\beta = 90°$ and $180°$.

7.3 Circular frame with diametrically opposed loads. Elastic energy methods are useful also in analyzing statically indeterminate frames. The unknown forces and moments in these structures that cannot be determined from static equilibrium conditions are called *redundants*.

A complete circular ring with diametrically opposed loads is shown in Figure 7.2. Such a ring is similar to a proving ring used for calibrating testing machines. A cut can be made in the ring at any point. However, if the cut is made at the top, the structure is symmetrical in loading

and geometry with respect to the cut. The forces in the ring at the cut are the redundant force H_1 and the bending moment M_1. Since these are internal forces they can have no external resultant so that the forces acting on the sides of the cut are equal and opposite. Since H_1 and M_1

MOMENT   SHEAR   THRUST
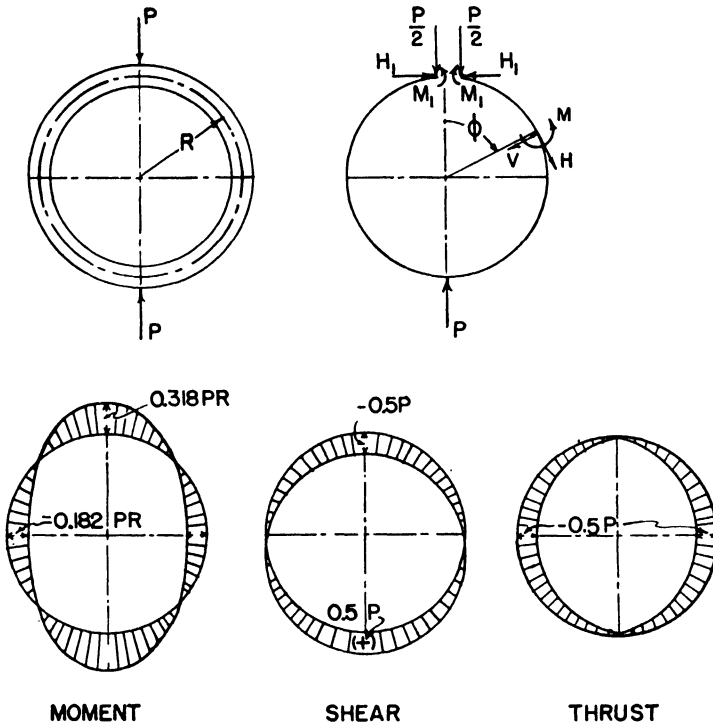
Fig. 7.2. Circular Frame.

are internal forces, then according to Castigliano's theorem, in order to make the ring continuous,

$$\frac{\partial U}{\partial M_1} = 0 = \int M \frac{\partial M}{\partial M_1} \frac{ds}{EI} \text{ and } \frac{\partial U}{\partial H_1} = 0 = \int M \frac{\partial M}{\partial H_1} \frac{ds}{EI} \quad (7.5)$$

The integrals are to be evaluated over the entire structure. However, since the structure and loading are symmetrical about the vertical axis, the values of the integrals for the left and right sides of the ring are the same so that the total value of the integral is equal to twice the value of the integral for one side. The partial derivatives of the elastic energy may therefore be considered as twice the value of the integral for one side, and since this is equated to zero, the factor two can be cancelled out.

The bending moment at any angle ϕ, for $0 < \phi < \pi$, is

$$M = M_1 - H_1R(1 - \cos \phi) - \frac{PR}{2} \sin \phi \qquad (7.6)$$

Therefore, $\dfrac{\partial M}{\partial M_1} = 1; \dfrac{\partial M}{\partial H_1} = -R(1 - \cos \phi)$

and, since $\quad ds = R\,d\phi$

Equations 7.5 become

$$\frac{\partial U}{\partial M_1} = 0 = \int_0^\pi \left[M_1 - H_1R(1 - \cos \phi) - \frac{PR}{2} \sin \phi \right] \frac{R\,d\phi}{EI}$$
$$= M_1\pi - H_1R\pi - PR$$

$$\frac{\partial U}{\partial H_1} = 0 = \int_0^\pi \left[M_1 - H_1R(1 - \cos \phi) - \frac{PR}{2} \sin \phi \right] \left[-R(1 - \cos \phi) \right] \frac{R\,d\phi}{EI}$$
$$= M_1\pi - H_1R\tfrac{3}{2}\pi - PR$$

Solving these equations simultaneously, we have

$$H_1 = 0$$
$$M_1 = \frac{PR}{\pi}$$

Therefore, the moment at any angle ϕ given by Equations 7.6 is

$$M = \frac{PR}{\pi} - \frac{PR}{2} \sin \phi = PR(0.318 - 0.5 \sin \phi) \text{ for } 0 < \phi < \pi \quad (7.7)$$

The thrust and shear at any section can be found from a consideration of the static equilibrium of the forces in the horizontal and vertical directions. Thus,

$$\Sigma F_H = 0 = H_1 + V \sin \phi - H \cos \phi$$
$$\Sigma F_V = 0 = \frac{P}{2} + V \cos \phi + H \sin \phi$$

and
$$V = -\frac{P}{2} \cos \phi$$

$$H = -\frac{P}{2} \sin \phi \qquad \text{for } 0 < \phi < \pi \qquad (7.8)$$

The force and moment distributions are shown in Figure 7.2.

In this particular example it is possible to show immediately that $H_1 = 0$. If the ring is cut at the top and bottom, a thrust H_1 is required at each point because of symmetry. These forces are not balanced by any external force and therefore in order to satisfy equilibrium conditions the thrusts must be zero.

7.4 Redundant center. In the previous analyses the solution of two simultaneous equations were required to determine the two unknowns of moment and thrust. It will be shown that if the redundants are applied at a point called the *redundant center* each redundant can be determined

directly without the use of simultaneous equations.   This is an advantage when there are several unknowns.

Consider a structure of any shape with a cut at some point and the redundants applied at the ends of rigid arms which are incapable of absorbing energy, as shown in Figure 7.3.   Select a coordinate system with the origin at the point where the redundants are applied.   The moment at any section of the structure can be considered as equal to the
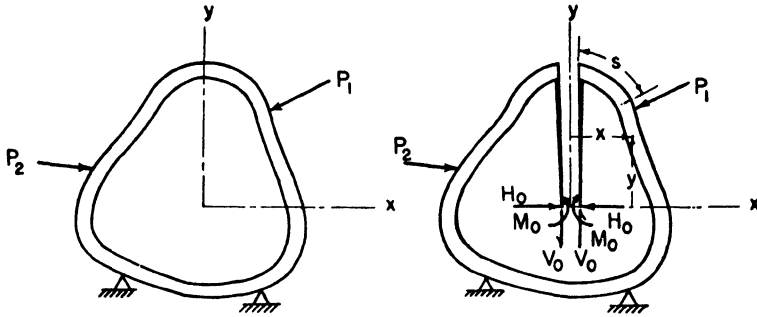
Fig. 7.3.   Redundant Center.

moment due to the redundants plus the moments due to the external loads.   Thus,

$$M = M_R + M_L \qquad (7.9)$$

where M_L = moment at any section due to external loads with the redundant forces zero.

$$M_R = M_0 + H_0 y + V_0 x = \text{moment due to reduntants only.} \quad (7.10)$$

Now $\dfrac{\partial M}{\partial M_0} = 1$; $\dfrac{\partial M}{\partial H_0} = y$; $\dfrac{\partial M}{\partial V_0} = x$; since M_L does not contain the redundants.   From Castigliano's theorem

$$\frac{\partial U}{\partial M_0} = 0 = \int M \frac{\partial M}{\partial M_0} \frac{ds}{EI}$$

$$\frac{\partial U}{\partial H_0} = 0 = \int M \frac{dM}{\partial H_0} \frac{ds}{EI}$$

$$\frac{\partial U}{\partial V_0} = 0 = \int M \frac{\partial M}{\partial V_0} \frac{ds}{EI}$$

Therefore,

$$\int (M_0 + H_0 y + V_0 x + M_L) \frac{ds}{EI} = M_0 \int \frac{ds}{EI} + H_0 \int y \frac{ds}{EI}$$

$$+ V_0 \int x \frac{ds}{EI} + \int M_L \frac{ds}{EI} = 0 \quad (7.11)$$

$$\int (M_0 + H_0 y + V_0 x + M_L) y \frac{ds}{EI} = M_0 \int y \frac{ds}{EI} + H_0 \int y^2 \frac{ds}{EI}$$

$$+ V_0 \int xy \frac{ds}{EI} + \int M_L y \frac{ds}{EI} = 0$$

$$\int (M_0 + H_0 y + V_0 x + M_L) x \frac{ds}{EI} = M_0 \int x \frac{ds}{EI} + H_0 \int yx \frac{ds}{EI}$$

$$+ V_0 \int x^2 \frac{ds}{EI} + \int M_L x \frac{ds}{EI} = 0$$

If the axes are selected so that

$$\int y \frac{ds}{EI} = \int x \frac{ds}{EI} = \int xy \frac{ds}{EI} = 0 \tag{7.12}$$

then it is evident that each of the above equations can be solved directly for one unknown each. These axes may be thought of as the principal
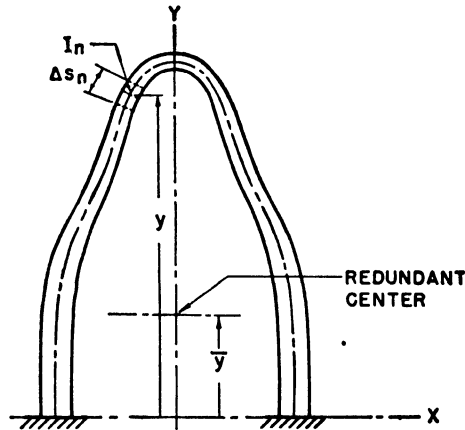
Fig. 7.4. Turnover Bulkhead.

axes of the ds/EI's. The redundant center always will lie on an axis of symmetry; and, if there are two axes of symmetry, the redundant center will be at their intersection.

The redundant center is determined much like the center of gravity except that the value ds/EI is used in place of dA. For example, for a structure such as the turnover bulkhead, with one axis of symmetry, shown in Figure 7.4, a convenient reference axis is used and the structure divided into a number of parts. The distance $\bar{y}$ from the reference axis to the redundant center is given by

$$\bar{y} \sum_{n=1}^{m} \frac{\Delta s_n}{E_n I_n} = \sum_{n=1}^{m} y_n \frac{\Delta s_n}{E_n I_n} \qquad (7.13)$$

If E is a constant, it can be cancelled out of the calculations.

EXAMPLE 7.1. Determine the forces and moments at the supports and the distribution of bending moments in the frame shown in Figure 7.5. Assume that $I_2 = I_1/2$.

FRAME   REDUNDANTS
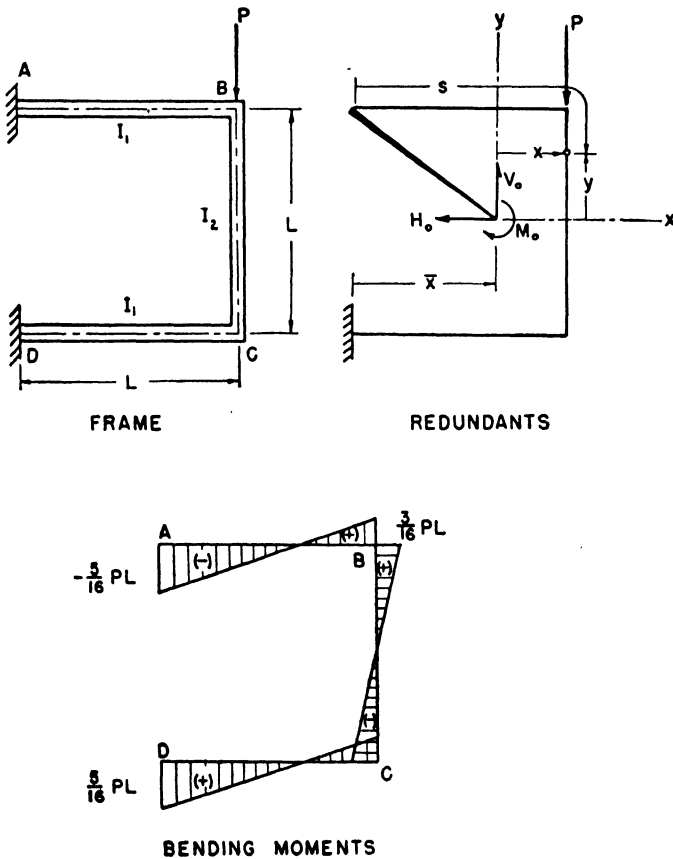
BENDING MOMENTS

Fig. 7.5. Square Frame.

Solution. The redundant center will be on the axis of symmetry, x. The distance $\bar{x}$ from the line of the supports to the redundant center will be determined by equating moments of the ds/EI's as given in Equation 7.13. In this case the integral form is used. Since E is a constant, it can be cancelled out.

$$\bar{x} \int \frac{ds}{I} = \int x \frac{ds}{I}$$

$$\bar{x} \left[2 \int_0^L \frac{dx}{I_1} + \int_0^L \frac{dy}{I_2} \right] = 2 \int_0^L x \frac{dx}{I_1} + \int_0^L L \frac{dy}{I_2}$$

$$\bar{x} = L \left[\frac{\dfrac{1}{I_1} + \dfrac{1}{I_2}}{\dfrac{2}{I_1} + \dfrac{1}{I_2}} \right] = \frac{3}{4} L$$

The moment at any point x, y, due to the redundants is

$$M_R = M_0 + H_0 y + V_0 x$$

The moment of the applied load P is zero everywhere except on the lower leg,

$$M_L = 0 \qquad \text{for } AB \text{ and } BC$$

$$M_L = P \left(\frac{L}{4} - x \right) \qquad \text{for leg } CD$$

Since $\displaystyle \int x \frac{ds}{EI} = \int y \frac{ds}{EI} = \int xy \frac{ds}{EI} = 0$, the first of Equations 7.11

reduces to $\qquad \displaystyle M_0 \int_A^D \frac{ds}{EI} = - \int_A^D M_L \frac{ds}{EI}$

or $\qquad \displaystyle M_0 \left[\int_A^B \frac{ds}{EI_1} + \int_B^C \frac{ds}{EI_2} + \int_C^D \frac{ds}{EI_1} \right] = - \int_C^D M_L \frac{ds}{EI_1}$

$$M_0 \int_A^D \frac{ds}{EI} = M_0 \left(\frac{2L}{EI_1} + \frac{L}{EI_2} \right) = 4 \frac{M_0 L}{EI_1}$$

If we remember that for leg CD the s direction is the negative x direction, we find that

$$\int_A^D M_L \frac{ds}{EI} = - \int_{\frac{1}{4}L}^{-\frac{1}{4}L} P \left(\frac{L}{4} - x \right) \left(- \frac{dx}{EI} \right) = \frac{PL^2}{2EI_1}$$

Therefore, $\qquad\qquad\qquad\qquad M_0 = - \dfrac{PL}{8}$

By using the second of equations 7.11

$$H_0 \int_A^D y^2 \frac{ds}{EI} = - \int_A^D M_L y \frac{ds}{EI}$$

$$H_0 \left[\int_{-\frac{1}{4}L}^{\frac{1}{4}L} \left(\frac{L}{2} \right)^2 \frac{dx}{I_1} + \int_{\frac{1}{4}L}^{-\frac{1}{4}L} y^2 \left(- \frac{dy}{I_2} \right) + \int_{\frac{1}{4}L}^{-\frac{1}{4}L} \left(\frac{L}{2} \right)^2 \left(- \frac{dx}{I_1} \right) \right]$$

$$= - \int_{\frac{1}{4}L}^{-\frac{1}{4}L} P \left(\frac{L}{4} - x \right) \left(- \frac{L}{2} \right) \left(- \frac{dx}{I_1} \right)$$

Therefore, $\qquad\qquad\qquad\qquad H_0 = \tfrac{3}{8} P$

From the third of Equations 7.11

$$V_0 \int_A^D x^2 \frac{ds}{EI} = -\int_A^D M_L x \frac{ds}{EI}$$

$$V_0 \left[\int_{-\frac{1}{4}L}^{\frac{1}{4}L} x^2 \frac{dx}{I_1} + \int_{\frac{1}{4}L}^{-\frac{1}{4}L} \left(\frac{L}{4}\right)^2 \left(-\frac{dy}{I_2}\right) + \int_{\frac{1}{4}L}^{-\frac{1}{4}L} x^2 \left(-\frac{dx}{I_1}\right) \right]$$

$$= -\int_{\frac{1}{4}L}^{-\frac{1}{4}L} P\left(\frac{L}{4} - x\right) x \left(-\frac{dx}{I_1}\right)$$

Thus,
$$V_0 = \frac{P}{2}$$

The complete moment is therefore

$$M = M_R + M_L$$

$$M = P\left[-\frac{L}{8} + \frac{3}{8}y + \frac{x}{2} \right] \qquad \text{for } A \text{ to } C$$

$$M = P\left[\frac{L}{8} + \frac{3}{8}y - \frac{x}{2} \right] \qquad \text{for } C \text{ to } D$$

The moment distribution is shown in Figure 7.5. Positive moment produces compression in outside fibers of frame.

7.5 Pressure cabin bulkhead ring. If there are additional members attached to a closed frame, it is not always possible to apply all the redundant forces at the redundant center. The analysis of the pressure cabin which follows is an example of a structure of this type. It will be shown, however, that the use of a redundant center to which some of the redundants can be applied simplifies the resulting simultaneous equations.

Figure 7.6 shows a fuselage bulkhead ring with an applied internal pressure load coming from the skin adjacent to the ring. A wing spar or floor beam intersects the lower portion of the ring and for simplicity it is assumed that this beam is pin-connected to the ring. The ring is shown with a circular plan form although the analysis is suitable for any shape. If a ring of uniform section is assumed, the redundant center for the ring coincides with the center of the circle. It is assumed further that the floor tie is relatively stiff so that its elongation can be neglected.

If V_0 has a value other than zero, the deflection on the two halves of the symmetrical ring will be unsymmetrical and the ends at the cut will not join. Therefore, $V_0 = 0$ from symmetry. The conditions for determining the unknown redundants are therefore

$$\frac{\partial U}{\partial M_0} = 0$$

$$\frac{\partial U}{\partial H_0} = 0 \qquad\qquad (7.14)$$

$$\frac{\partial U}{\partial F} = \delta_F = 0$$

A rectangular coordinate system will be used so that the extension of the method to noncircular frames will be apparent. This particular case would be simplified by the use of polar coordinates. By using the coordinates x, y, the moments due to the redundants are

$$M_R = M_0 + H_0 y \qquad\qquad a > y > -b$$
$$M_R = M_0 + H_0 y + F(y + b) \qquad -b > y > -(c + b)$$

The moment caused by the pressure loading where p is the load per linear inch of ring arc is obtained from a consideration of the equilibrium
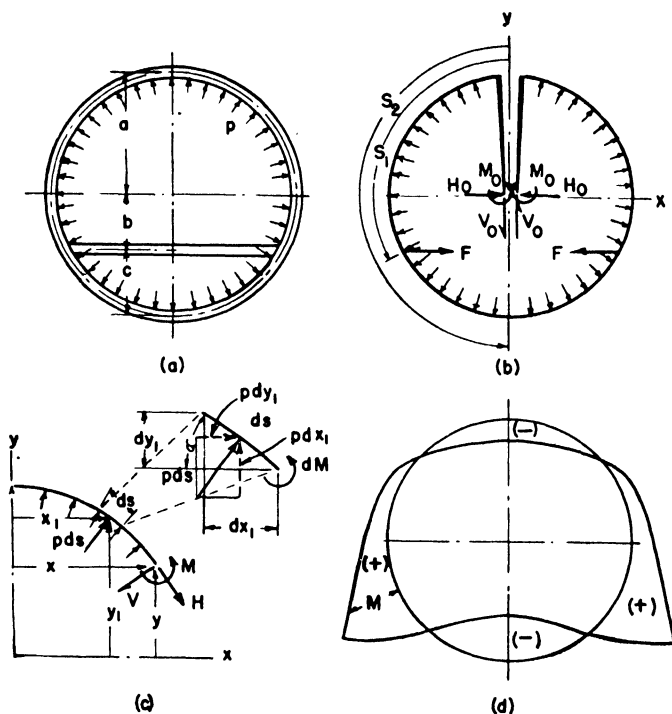
Fig. 7.6. Pressure Cabin.

of a portion of the ring, Figure 7.5(c). The force acting on a small element of length ds located at position x_1, y_1 is $p\,ds$. The components of force in the x_1, y_1, directions are

$$p\,ds \sin \alpha = p\,ds\,\frac{dy_1}{ds} = p\,dy_1$$

$$p\,ds \cos \alpha = p\,ds\,\frac{dx_1}{ds} = p\,dx_1$$

The moment of these forces at the point x, y, is

$$dM = p\,dy_1(y_1 - y) + p\,dx_1(x - x_1)$$

The total moment at y due to the pressure will therefore be

$$M_L = \int_y^a p(y_1 - y)\, dy_1 + \int_0^x p(x - x_1)\, dx_1$$

$$= \frac{p}{2}(y - a)^2 + \frac{px^2}{2}$$

The moments for the ring due to the redundants and pressure are therefore

$$M = M_0 + H_0 y + \frac{p}{2}(y - a)^2 + \frac{px^2}{2}$$

$$\text{for } a > y > -b \qquad (7.15)$$

$$M = M_0 + H_0 y + \frac{p}{2}(y - a)^2 + \frac{px^2}{2} + F(y + b)$$

$$\text{for } -b > y > -(c + b)$$

Also $\quad \dfrac{\partial M}{\partial M_0} = 1; \dfrac{\partial M}{\partial H_0} = y; \dfrac{\partial M}{\partial F} = 0 \quad \text{for } a > y > -b$

$$\dfrac{\partial M}{\partial M_0} = 1; \dfrac{\partial M}{\partial H_0} = y; \dfrac{\partial M}{\partial F} = y + b$$

$$\text{for } -b > y > -(c + b)$$

The redundants are therefore determined from Equation 7.14 where s_1 is a distance measured along the ring from the top to force F, and s_2 is distance measured along ring from top to bottom. If we remember

$$\int_0^{s_2} y\, \frac{ds}{EI} = \int_0^{s_2} x\, \frac{ds}{EI} = 0$$

then we see that

$$\frac{\partial U}{\partial M_0} = 0 = M_0 \int_0^{s_2} \frac{ds}{EI} + \frac{p}{2} \int_0^{s_2} (y-a)^2 \frac{ds}{EI} + \frac{p}{2} \int_0^{s_2} x^2 \frac{ds}{EI} + F \int_{s_1}^{s_2} (y+b) \frac{ds}{EI}$$

$$(7.16)$$

$$\frac{\partial U}{\partial H_0} = 0 = H_0 \int_0^{s_2} y^2 \frac{ds}{EI} + \frac{p}{2} \int_0^{s_2} (y - a)^2 y \frac{ds}{EI} + \frac{p}{2} \int_0^{s_1} x^2 y \frac{ds}{EI}$$

$$+ F \int_{s_1}^{s_2} (y + b) y \frac{ds}{EI}$$

$$\frac{\partial U}{\partial F} = 0 = M_0 \int_{s_1}^{s_2} (y + b) \frac{ds}{EI} + H_0 \int_{s_1}^{s_2} y(y + b) \frac{ds}{EI}$$

$$+ \frac{p}{2} \int_{s_1}^{s_2} (y - a)^2 (y + b) \frac{ds}{EI}$$

$$+ \frac{p}{2} \int_{s_1}^{s_2} x^2 (y + b) \frac{ds}{EI} + F \int_{s_1}^{s_2} (y + b)^2 \frac{ds}{EI}$$

The values of the integrals of the equations can be determined by a tabulation method and the simultaneous equations solved for M_0, H_0, and F.

The solution for a circular ring with constant moment of inertia of the cross section, radius of 40 inches, and an internal pressure of four pounds per inch is shown in Figure 7.6(d).

Problems

7.1. A semicircular arch of radius R has a radial load P directed toward the center at the crown. If the cross section of the arch is constant and if one end of the arch is fixed and the other free, determine the horizontal deflection, vertical deflection, and rotation of the free end.

7.2. If the free end of the arch in Problem 7.1 is pivoted, determine the reactions at the pivot support.

7.3. A steel wire retainer ring shown in Figure 7.7 is designed so that when the gap δ is closed the maximum stress is just equal to the yield stress of the material. Neglecting the deformation of the portion e and assuming that the maximum stress is given by $f = \dfrac{Md}{2I}$, determine the gap δ.
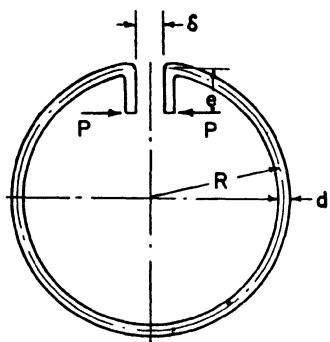
Fig. 7.7. Snap Retainer Ring.

$$d = \tfrac{1}{16} \text{ in} \qquad\qquad R = 1 \text{ in}$$
$$e = \tfrac{1}{4} \text{ in} \qquad\qquad f_y = 100{,}000 \text{ psi}$$

7.4. Determine the bending moments for a frame similar to the one shown in Figure 7.5 if the leg AB carries a uniformly distributed load w (lb/in). The frame is pin-connected at A, and the moment of inertia of the members of the frame are constant and equal.
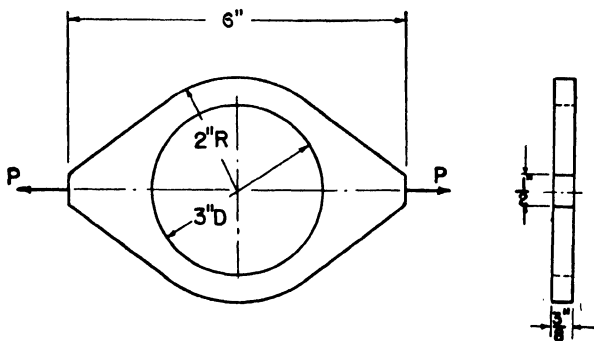
Fig. 7.8. Tie Rod Fitting.

7.5. A tension member is constructed with an access opening, as shown in Figure 7.8. Determine the load P that will just cause yielding if the member is an aluminum alloy forging with $F_{ty} = 30{,}000$ psi.

7.6. Determine the bending moment distribution in the fuselage bulkhead

frame and spar shown in Figure 7.9.   The bulkhead distributes the wing reactions into the fuselage skin by means of the assumed linear shear distribution.

I of bottom spar $=$ 16,500 in⁴
I of frame $=$ 10.2 in⁴   for $0 < \alpha < 90°$
I of frame $=$ 20 in⁴   for $\alpha > 90°$.
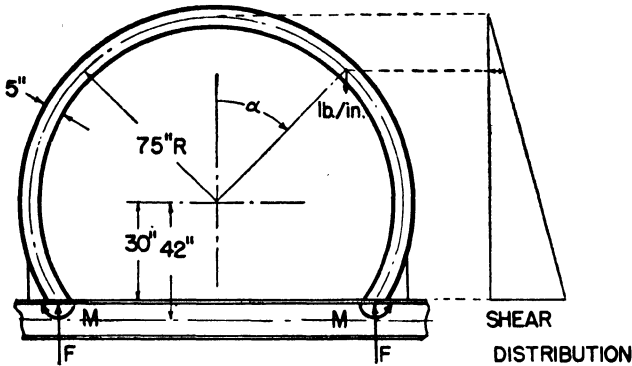
F = 178,000 lb.
M = 750,000 lb. in.

Fig. 7.9.   Fuselage Ring and Spar.

References

Timoshenko, S., *Strength of Materials*, Part II.   D. Van Nostrand Company, Inc., 1940.
Van Den Broek, J. A., *Elastic Energy Theory*.   John Wiley and Sons, 1942.

Part III
STRUCTURAL STABILITY

CHAPTER 8

Columns and Beam Columns

••

8.1 Introduction. Structural members carrying direct compressive loads along their longitudinal axes are called *columns* or *struts*. If the member is subjected to a transverse load as well as to the axial compression, it is called a *beam column*. Members transmitting axial compression, such as wing stiffeners, fuselage longerons, and landing gear struts, are common in the airplane structure. The failure of columns is not necessarily determined by the stress becoming a limiting value based on the strength properties of the material as it is for many other members; but it depends upon a phenomenon called *buckling*, which may or may not involve the strength properties of the material. The criterion for buckling failure is the fact that the member will carry only a limited load and that any attempt to increase the load merely increases the deflection even though the stresses may be relatively low.

There are two main classifications of column failure: (1) general stability failure or primary failure in which the whole member takes part in the failure and (2) local stability failure in which a localized part of the member fails. In the general stability failure the cross section of the column retains its initial shape; and, although the cross sections may move relative ·to one another, they do not distort. In local stability failure, the cross sections themselves distort and change shape. Both types of failure may be classified further into two groups: (a) elastic stability failure in which buckling occurs when the material is elastic; namely, the stresses do not exceed the proportional limit of the material and (b) inelastic stability failure in which the stresses do exceed the proportional limit when buckling occurs.

The problem of column failure is complicated, and the theory is not yet sufficiently developed so that all conditions can be predicted analytically. For this reason and for convenience many semi-empirical methods are used in analyzing columns. Some of these methods will be discussed in this chapter.

8.2 Elastic stability of strut with ·one end fixed. The failure of a strut for which the material is elastic, and for which, therefore, the stresses are below the proportional limit, will be considered first. Further assumptions made in analyzing the strut shown in Figure 8.1 are: (1) The strut is initially straight of uniform cross section and homogeneous material. (2) Deflections are small so that the ordinary flexural theory may be used. (3) Weight of the strut is neglected.

For some small axial load P applied on the strut it will be found

that if the top of the strut is deflected some slight amount sideways, the strut will resume its initial straight condition when the sidewise pressure is released. It is possible to apply a load so that when the strut is slightly deflected sideways the strut will either stay in the deflected position or its deflection will increase rapidly so that the strut collapses. The load required just to maintain the slight deflection is called the *Euler* or *critical load*.

If the critical load is assumed to be applied to the strut so that the deflection δ is maintained, then the bending moment at any section a distance x from the fixed end is

$$M = P(\delta - y)$$

or, since from Equation 4.18 $M = EI \dfrac{d^2y}{dx^2}$

$$\frac{d^2y}{dx^2} + k^2y = k^2\delta \tag{8.1}$$

where $$k^2 = \frac{P}{EI}.$$

The solution of this equation is

$$y = A \cos kx + B \sin kx + \delta \tag{8.2}$$

Fig. 8.1. Strut with One End Fixed.

which may be verified by substitution. The conditions at the ends of the strut are

$$y = \frac{dy}{dx} = 0 \text{ at } x = 0$$

Substituting these conditions into Equation 8.2, we obtain

$$y = \delta(1 - \cos kx) \tag{8.3}$$

The shape of the deflection curve is therefore a cosine curve, and the end deflection δ is indeterminate. A further condition is

$$y = \delta \text{ at } x = L$$
$$\delta = \delta(1 - \cos kL)$$

As long as δ is not zero we may divide through by it, and therefore

$$\cos kL = 0$$

This condition is satisfied if $kL = \dfrac{\pi}{2}, \dfrac{3}{2}\pi$ and so on. If we take the smallest of these to obtain the least load, then

$$P = \frac{\pi^2 EI}{4L^2} \tag{8.4}$$

This is the load required to hold the strut in a slightly deflected position, and it is called the *critical load* or *allowable column load*. The stress is essentially the load divided by the cross-section area, and therefore

$$F_c = \frac{P}{A} = \frac{\pi^2 E}{4\left(\dfrac{L}{\rho}\right)^2}$$

Where F_c = the allowable column stress (psi)

$\rho = \sqrt{\dfrac{I}{A}}$, the radius of gyration of the cross section (in)

$\dfrac{L}{\rho}$ = slenderness ratio.

For values of P less than the critical load the strut remains straight. For values of P greater than the criti-cal load the deflection is indeter-minate because of the approximation $M = EI\dfrac{d^2y}{dx^2}$ used in the analysis. The load deflection curves for the assump-tion used in the analysis are shown by the dashed line in Figure 8.2. Actually however, if the initial crookedness and large deflections are considered, the load deflection curve will be shown by the solid line of Figure 8.2.
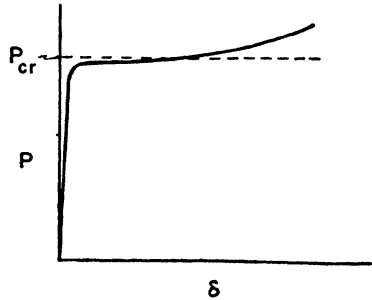
Fig. 8.2. Load Deflection Curve.

8.3 Elastic stability of struts with various end conditions. The critical load and allowable column stress for a pin-ended strut and a strut with both ends fixed can be determined from the results of the previous analysis.

Since the slope at the center of the pin-ended strut shown in Figure 8.3(a) is zero, the strut can be considered as being made up of two fixed-free struts having half the length of the pin-ended strut. The critical load for the pin-ended strut is therefore the same as for a strut of half the length and with one end fixed. Therefore,

$$P = \frac{\pi^2 EI}{4\left(\dfrac{L}{2}\right)^2} = \frac{\pi^2 EI}{L^2}$$

The strut with both ends fixed against rotation will deflect as shown in Figure 8.3(b). The points of counterflexure are positions of zero bending moment so that the critical load may be considered the same as that for the strut with one end fixed for which the length is $L/4$. Thus,

$$P = \frac{\pi^2 EI}{4\left(\dfrac{L}{4}\right)^2} = \frac{4\pi^2 EI}{L^2}$$

The strut shown in Figure 8.3(c) with one end fixed and one end hinged cannot be analyzed in the same manner as the previous two struts since the line between the point of counterflexure and the pinned-end is not parallel to the line of action of the load. The *form* of equation for the critical load, however, is the same.
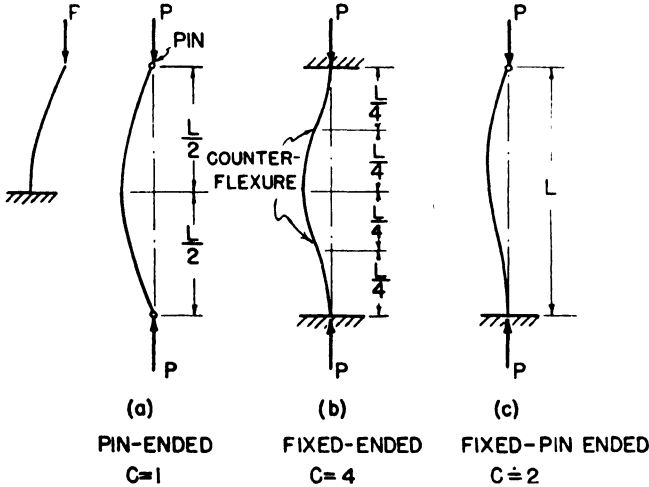
Fig. 8.3. Struts with Various End Conditions.

For each strut it is evident that the critical load and allowable column stress can be expressed in the forms

$$P = C\pi^2 \frac{EI}{L^2} \tag{8.5}$$

and

$$F_c = C\pi^2 \frac{E}{\left(\dfrac{L}{\rho}\right)^2} \tag{8.6}$$

where $\qquad C$ = end fixity coefficient

$\dfrac{L}{\rho}$ = slenderness ratio.

The end fixity coefficient is sometimes included in the expression for the slenderness ratio as follows:

$$\frac{L'}{\rho} = \frac{L}{\rho \sqrt{C}} \tag{8.7}$$

Therefore,

$$F_c = \frac{\pi^2 E}{\left(\dfrac{L'}{\rho}\right)^2} \tag{8.8}$$

8.4 Struts with variable cross section. In the previous strut analyses the moment of inertia of the cross section has been considered constant. If the moment of inertia varies from section to section, then the differential equation for the equilibrium of the strut, Equation 8.1, is difficult to solve.   By using an energy method, it is possible to express the critical load in terms of integrals, so that even if the variation of moment of inertia cannot be expressed analytically, the critical load can be determined approximately by summation processes.

Consider the strut shown in Figure 8.4. Suppose an axial load *P* is applied and then the end of the strut is displaced some distance δ. As the strut bends, the end moves vertically downward a distance λ; and, since the load remains constant during this process, the work done by the load is *P*λ. The
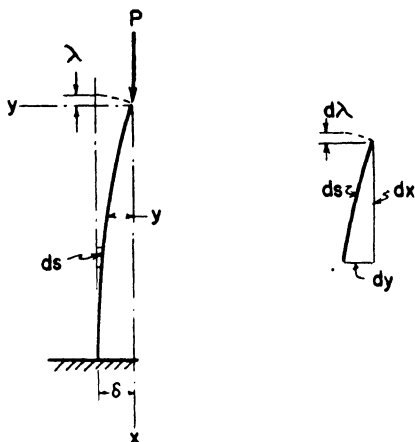
Fig. 8.4.   Strut Shortening.

elastic energy stored in the strut during bending is $\int \dfrac{M^2\,dx}{2EI}$.   If the work done by the force is greater than the elastic energy stored in the strut, the strut continues to deflect.   If the work done by the force is less than the elastic energy, the strut straightens.   The deflection is maintained when

$$P\lambda = \int_0^L \frac{M^2\,dx}{2EI} \tag{8.9}$$

From the geometry of an element of the strut

$$d\lambda = ds - dx$$

and

$$ds = \sqrt{(dx)^2 + (dy)^2} = dx\sqrt{1 + \left(\frac{dy}{dx}\right)^2}$$

Expanding this according to the binomial theorem and assuming that $\dfrac{dy}{dx}$ is small so that higher powers of the slope may be neglected, we obtain

$$d\lambda = \frac{dx}{2}\left(\frac{dy}{dx}\right)^2$$

$$\lambda = \frac{1}{2}\int_0^L \left(\frac{dy}{dx}\right)^2 dx \tag{8.10}$$

Substituting this value of λ into Equation 8.9 gives

$$P = \frac{\int_0^L \frac{M^2\,dx}{EI}}{\int_0^L \left(\frac{dy}{dx}\right)^2\,dx}$$

Since $M = EI\,\dfrac{d^2y}{dx^2}$, this may be written

$$P = \frac{\int_0^L \left(\frac{d^2y}{dx^2}\right)^2 EI\,dx}{\int_0^L \left(\frac{dy}{dx}\right)^2\,dx}$$

For the special case where the coordinate axes are selected so that $M = Py$ as in Figure 8.4, then

$$P = \frac{\int_0^L \left(\frac{dy}{dx}\right)^2\,dx}{\int_0^L y^2\,\frac{dx}{EI}} \tag{8.11}$$

This latter form is usually the most accurate.

If the shape of the elastic curve of the strut and the distribution of the rigidity EI are known, the critical load P can be determined exactly by use of Equation 8.11. For the case of the strut with one end fixed and with constant cross-section moment of inertia, it was shown in Article 8.2 that the deflection curve is a trigonometric function. It is easy to verify that Equation 8.11 gives the correct load if this function is used. The power of this method, however, lies in the fact that even if the exact deflection curve is not known the critical load can be determined approximately as long as the curve selected satisfies the end conditions. If a parabola is used as a deflection curve of the pin-ended strut, in place of the trigonometric function, the critical load determined by means of Equation 8.11 is only about $1\tfrac{1}{3}\%$ greater than the true critical load.

This method makes it possible to determine also the approximate critical load for struts with variable moments of inertia. Of course, if the variation of I cannot be expressed conveniently as a function of x, the integrals of Equation 8.11 can be evaluated approximately by a summation process.

EXAMPLE 8.1. Determine the critical load for the pin-ended steel shaft shown in Figure 8.5: $E = 30 \times 10^6$ psi.

Solution. The moments of inertia of the cross sections are

$$I_1 = \frac{\pi d_1^4}{64} = \frac{\pi(\tfrac{1}{2})^4}{64} = 0.00307 \text{ in}^4$$

$$I_2 = \frac{\pi d_2^4}{64} = \frac{\pi(\tfrac{3}{4})^4}{64} = 0.0155 \text{ in}^4$$

Assume a deflection curve

$$y = \delta \sin \frac{\pi x}{L}$$

This curve satisfies the conditions that the deflections at the ends are zero and the slope at the center is zero. At any section

$$\frac{dy}{dx} = \delta \frac{\pi}{L} \cos \frac{\pi x}{L}$$

Since the strut is symmetrical about the center, the integrations need be evaluated for only half the length. Evaluating for the whole length
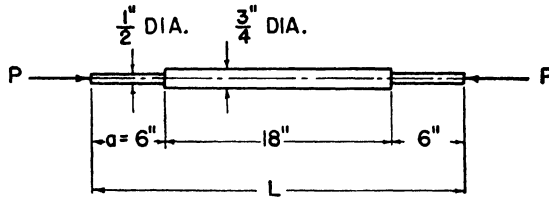
Fig. 8.5. Nonuniform Strut.

merely doubles the numerator and denominator of Equation 8.11 as compared with the half-length evaluation. Therefore,

$$P = \frac{E \displaystyle\int_0^{\frac{L}{2}} \left(\frac{dy}{dx}\right)^2 dx}{\displaystyle\int_0^{\frac{L}{2}} y^2 \frac{dx}{I}}$$

$$P = \frac{E \displaystyle\int_0^{\frac{L}{2}} \delta^2 \frac{\pi^2}{L^2} \cos^2 \frac{\pi x}{L}\, dx}{\displaystyle\int_0^{a} \delta^2 \sin^2 \frac{\pi x}{L} \frac{dx}{I_1} + \displaystyle\int_a^{\frac{L}{2}} \delta^2 \sin^2 \frac{\pi x}{L} \frac{dx}{I_2}}$$

$$= \frac{E\pi^2}{4L} \left[\frac{1}{\dfrac{1}{I_1}\left(\dfrac{a}{2} - \dfrac{L}{4\pi}\sin\dfrac{2\pi a}{L}\right) + \dfrac{1}{I_2}\left(\dfrac{L}{4} - \dfrac{a}{2} + \dfrac{L}{4\pi}\sin\dfrac{2\pi a}{L}\right)} \right]$$

$$P = 3660 \text{ lb}$$

The allowable column stress is

$$F_c = \frac{P}{A} = \frac{3660}{\dfrac{\pi}{4}\left(\dfrac{1}{2}\right)^2} = 18{,}640 \text{ psi}$$

This is below the proportional limit of the material so that the strut fails elastically and it is correct to use Equation 8.11.

8.5 Buckling of columns stressed beyond the proportional limit. In the previous analyses it has been assumed that the stresses in the column are less than the proportional limit of the material. The results are correct for relatively slender columns. Most columns, however, are of such size that the stresses at buckling exceed the proportional limit.

Consider a strut made of a material with a stress-strain curve as shown in Figure 3.2(b). If the axial compressive load is applied gradually to the strut and if the strut is properly proportioned, the normal stress P/A may become greater than the proportional limit before the strut buckles. Therefore, the modulus of elasticity is no longer a constant as previously assumed, but it is a variable and a function of the stress. The modulus above the proportional limit is represented by the tangent modulus shown in Figure 3.3. Engesser suggested that the constant modulus of elasticity in the Euler Equation 8.6 be replaced by the variable tangent modulus E_T, for columns that buckle in the inelastic range. Therefore,

$$F_c = \frac{C\pi^2 E_T}{\left(\dfrac{L}{\rho}\right)^2} \qquad (8.12)$$

where E_T = tangent modulus (psi).

It is apparent that E_T is a function of F_c, so that a curve showing the relation between these two quantities must be known before the equality expressed by Equation 8.12 can be established. The solution of this expression is obtained by a trial and error process.

At about the same time Considère pointed out that, if the strut is loaded first to a stress greater than the proportional limit and then deflected sideways, a bending moment will be induced which will cause the stress to increase on one side of the strut and decrease on the other. The ratio of the stress to strain on the side where the stress is increased is given by the tangent modulus. However, on the other side where the stress is decreased, the material will unload along a line parallel to the initial straight line of the stress-strain curve so that the ratio is the ordinary modulus of elasticity. Consideration of this effect leads to what is known as the *double modulus theory*. It has been shown that the allowable column stress is a function of the *shape* of the cross section as well as of the material. The allowable column stress therefore becomes,

$$F_c = \frac{C\pi^2 E_R}{\left(\dfrac{L}{\rho}\right)^2} \qquad (8.13)$$

where E_R = reduced modulus (psi)

$$= \frac{4EE_T}{(\sqrt{E} + \sqrt{E_T})^2} \text{ for rectangular cross sections.}$$

Subsequent carefully conducted tests made by Von Kármán showed that the double modulus theory approached the test values.   However, for most ordinary tests the tangent modulus theory gives satisfactory agree-
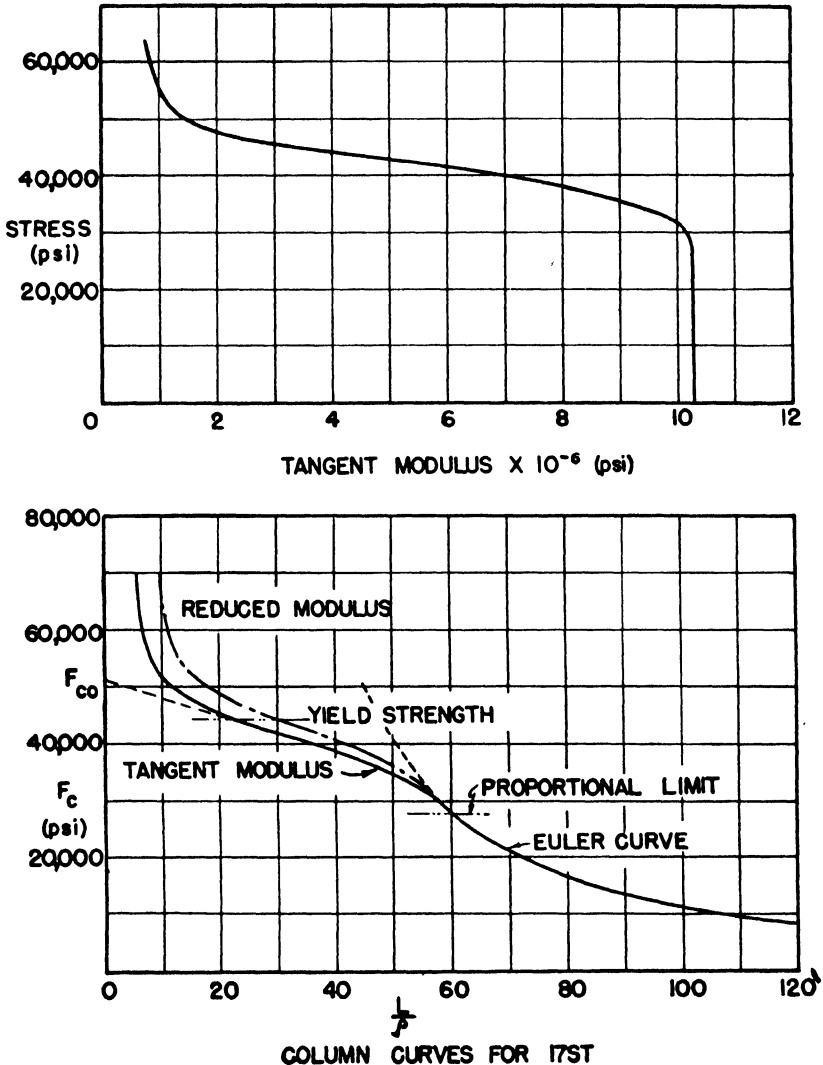
Fig. 8.6.   Column Curves.

ment; and, since it is simpler and gives the lower limit of the buckling load, it is more commonly used.

Figure 8.6 shows the tangent modulus stress relation and the column curves for the tangent modulus theory and reduced modulus theory for a column of 17ST material having a rectangular cross section.

8.6 Column yield stress. If we refer to Figure 8.6 we notice that both the reduced modulus curve and the tangent modulus curve show rapid increase in allowable column stress for small slenderness ratios. The stress required to buckle the column for small slenderness ratios exceeds the yield strength of the material. Since stresses much in excess of the yield strength are undesirable and since it is convenient to have a stress for zero slenderness ratio for the development of some semi-empirical column formulas, a quantity called the *column yield stress, F_{co},* is defined.

The column yield stress is obtained from column tests by extrapolating the test curve to $L/\rho = 0$ and disregarding the tendency for the curve to rise for very small slenderness ratios. See Figure 8.6. According to the ANC-5, the column yield stress for aluminum is

$$F_{co} = F_{cy}\left(1 + \frac{F_{cy}}{200{,}000}\right) \tag{8.14}$$

and for 4130 steel it is

$$F_{co} = 1.06 F_{cy} \tag{8.15}$$

8.7 Empirical column formulas. Various formulas have been proposed for the region of column failure in which the stresses are greater than the proportional limit. All these curves should join the Euler curve at the proportional limit since the Euler curve is valid for column failure when the stress is less than the proportional limit. The joining of the curves at the proportional limit is not always realized, but the empirical curves developed are suitable for preliminary design.

The family of curves that are tangent to the Euler curve at one end and that have a value of F_{co} for $L/\rho = 0$ may be written:

$$F_c = F_{co} - K\left(\frac{L}{\rho}\right)^n$$

For $n = 1$ the curve is a straight line. For $n = 2$ the curve is a parabola. These two curves are the ones most commonly used. The straight line is sometimes used for columns of aluminum alloy; and the parabola, for steel. These curves together with the tangent modulus curve are shown in Figure 8.7.

It is simply a matter of geometry to show that the Euler curve joins the straight line curve at a slenderness ratio

$$\left(\frac{L}{\rho}\right)_t = \pi\sqrt{\frac{3CE}{F_{co}}}$$

Similarly, it can be shown for the parabola that

$$\left(\frac{L}{\rho}\right)_t = \pi\sqrt{\frac{2CE}{F_{co}}}$$

The values of K for the two curves are

$$K = \frac{2C\pi^2 E}{\left(\dfrac{L}{\rho}\right)_t^3} \text{ for straight line}$$

and

$$K = \frac{C\pi^2 E}{\left(\dfrac{L}{\rho}\right)_t^4} \text{ for the parabola}$$
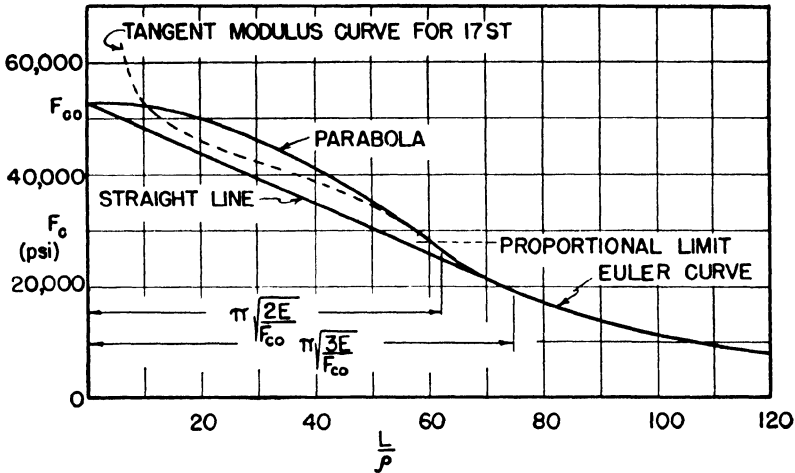
Fig. 8.7. Empirical Column Curves for $C = 1$.

Therefore, the column equations for the stresses in the inelastic range are

Straight line: $\quad F_c = F_{co}\left[1 - \dfrac{0.385}{\pi\sqrt{\dfrac{CE}{F_{co}}}}\dfrac{L}{\rho}\right]$ for $\dfrac{L}{\rho} < \pi\sqrt{\dfrac{3CE}{F_{co}}}$ $\quad$ (8.16)

Parabola: $\quad F_c = F_{co}\left[1 - \dfrac{F_{co}}{4\pi^2 EC}\left(\dfrac{L}{\rho}\right)^2\right]$ for $\dfrac{L}{\rho} < \pi\sqrt{\dfrac{2CE}{F_{co}}}$ $\quad$ (8.17)

The Euler equation should be used for slenderness ratios greater than the transition slenderness ratio, $(L/\rho)_t$.

8.8 Torsional-bending stability of columns. The type of columns discussed thus far have all been assumed to fail by general instability. The cross sections of the columns have been assumed stable so that localized failure is prevented. Since local stability failure is often concerned with cross sections made up of thin sheet material, a discussion of this type of failure will be postponed until later when sheet failure is discussed.

There is another type of general failure, however, known as *torsional-bending stability*, which is extremely important. It is a known fact that

some columns when subjected to axial compression do not fail only by deflecting sideways but by twisting about a longitudinal axis as well. That is, the central sections of the column rotate relative to the end sections. This torsional type of failure is most likely to occur in columns having cross sections of thin material that do not form completely closed tubes, such as channel sections or other open sections.

It has been shown that some bending occurs in a column when subjected to an axial compression. The magnitude of the bending moment varies along the column since it depends on the amount of deflection which is not constant. The variation of the bending moment implies
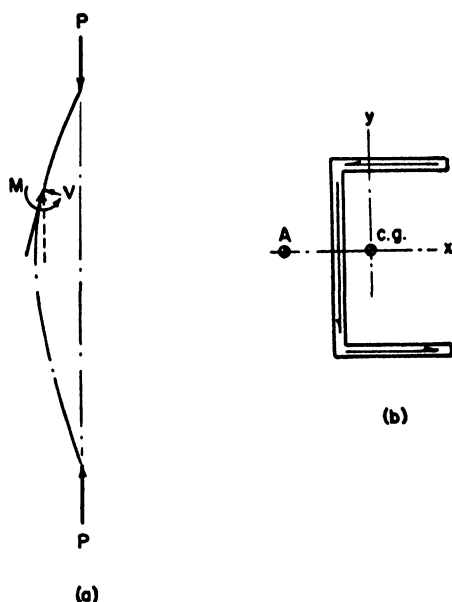
Fig. 8.8. Torsional-Bending Stability.

that there is a shear force on the cross sections of the column since $\frac{dM}{ds} = V$. The shear force and bending moment at a cross section of a pin-ended column are shown in Figure 8.8(a).

It will be shown later (Article 11.7) that, if the resultant shear force does not pass through a point in the cross section known as the *shear center*, the member will twist. In the case of the channel section shown in Figure 8.8(b) the shear center is to the left of the channel at point A. Suppose the column is loaded in such a manner that it bends about the x axis of the cross section and so that the resulting shear force is parallel to the y axis but does not pass through the shear center. In this case, shear stresses will be induced in the flanges which result in flange shear

forces in the directions shown in the figure. These flange forces produce a couple which tends to rotate the section about the shear center. If the section is torsionally weak, the column may fail by twisting before it fails by bending.

The analytical development of the critical conditions for a torsionally weak column are too complicated to be presented here. This problem has been solved successfully by Wagner and others, and the results will be indicated.

The allowable column stress for a pin-ended strut with stresses below the proportional limit is given by

$$F_c = \frac{1}{I_p} \left(GC + \frac{\pi^2}{L^2} E\Gamma \right) \tag{8.18}$$

where L = length of column (in)

   I_p = polar moment of inertia of the cross section about the axis of rotation (shear center) (in⁴)

   C = geometric property of the cross section involving its torsional stiffness (see Article 12.5) (in⁴)

   Γ = torsion-bending constant (see Article 12.9) (in⁶)

   E, G = usual elastic constants (psi).

For a channel section

$$\Gamma = \frac{h^2 t}{12} \left[e^2(h + 6b) + 2b^2(b - 3e) \right]$$

where h = distance between flanges (in)

   b = flange width (in)

   e = distance between shear center and center of web (in)

   t = sheet thickness (in).

If the column is attached to a sheet, such as a stringer attached to the surface of a wing, the sheet tends to restrain the torsional buckling. See references.

8.9 Beam column with uniform load. A beam column is a member subjected to a transverse load similar to an ordinary beam and simultaneously carrying an axial compression like a column. Many members in the airplane structure, such as fuselage longerons, are beam columns.

The analysis of the beam column is complicated because the transverse load produces a deflection which in turn induces a moment due to the eccentricity of the axial compression. The moment thus produced induces further deflection, and the process continues until equilibrium is reached.

For simplicity, a beam column carrying a uniform distributed transverse load will be analyzed first. It is assumed that the material remains elastic. From equilibrium of the forces the vertical reactions at the ends

of the beam shown in Figure 8.9 can be determined. By taking equilibrium of moments for a portion of the beam of length x where the deflection is y the moment can be determined. Therefore,

$$M = \frac{wx^2}{2} - \frac{wLx}{2} - Py$$

Differentiating gives $\quad \dfrac{d^2M}{dx^2} = w - P\dfrac{d^2y}{dx^2}$

But for small deflections, $\dfrac{M}{EI} = \dfrac{d^2y}{dx^2}$

so that $\qquad \dfrac{d^2M}{dx^2} + k^2M = w$ \hfill (8.19)

where $\qquad k^2 = \dfrac{P}{EI}$
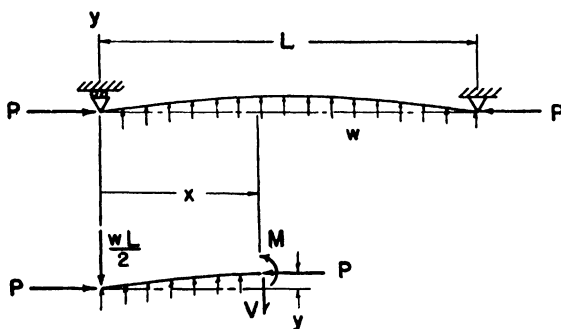
Fig. 8.9. Beam Column with Uniform Load.

The solution of Equation 8.19 is

$$M = A \cos kx + B \sin kx + \frac{w}{k^2} \tag{8.20}$$

The conditions at the ends of the beam are

$$M = 0 \text{ at } x = 0$$
$$M = 0 \text{ at } x = L$$

By substituting these conditions in Equation 8.19 and solving for A and B, Equation 8.20 becomes

$$M = -\frac{w}{k^2}\left[\cos kx - \left(\frac{\cos kL - 1}{\sin kL}\right)\sin kx - 1\right] \tag{8.21}$$

The position of maximum moment can be obtained by equating the derivative of the moment to zero. However, from symmetry it is evi-

dent that the maximum moment is at the center of the beam where $x = L/2$. Thus,

$$M_{max} = -\frac{w}{k^2}\left[\cos\frac{kL}{2} - \left(\frac{\cos kL - 1}{\sin kL}\right)\sin\frac{kL}{2} - 1\right]$$

This moment may be expressed in terms of the half angle $kL/2$ by using the trigonometric relations

$$\sin kL = 2\sin\frac{kL}{2}\cos\frac{kL}{2}$$

$$\cos kL = 2\cos^2\frac{kL}{2} - 1$$

Therefore, $$M_{max} = -\frac{w}{k^2}\left(\sec\frac{kL}{2} - 1\right) \qquad (8.22)$$

The maximum moment for a constant w is now a function of P so if we let

$$k^2 = \frac{P}{EI} \rightarrow \frac{\pi^2}{L^2}$$

then $$\sec\frac{kL}{2} = \frac{1}{\cos\frac{kL}{2}} \rightarrow \frac{1}{0} = \infty$$

and $M_{max} \rightarrow \infty$. This indicates that the beam has buckled, and the axial load required to buckle the beam is

$$\frac{P}{EL} = \frac{\pi^2}{L^2}$$

or $$P = \frac{\pi^2 EI}{L^2}, \text{ the Euler load.}$$

Therefore, if the stresses remain lower than the proportional limit, the compressive load required to buckle the beam with a uniform beam load is the same as the load to buckle the column without the transverse load.   This result is generally true for beam columns.

Expanding the expression for the maximum moment into a series and remembering that the maximum bending moment for a simply supported beam carrying *only* a uniform load is

$$M_{w(max)} = -\frac{wL^2}{8}$$

we find that the ratio of $\dfrac{M_{max}}{M_{w(max)}}$ can be expressed in terms of the ratio of the applied axial load and the buckling load P_{cr}.   These ratios have been plotted in Figure 8.10, and the curve indicates clearly the rapid increase in bending moment with increase in axial load.

The shear force in the beam is determined by means of the relation

$$V = \frac{dM}{dx}$$

or

$$V = \frac{w}{k}\left[\sin kx + \left(\frac{\cos kL - 1}{\sin kL}\right)\cos kx\right] \qquad (8.23)$$

If we know the bending moments and the axial load, we can deter-
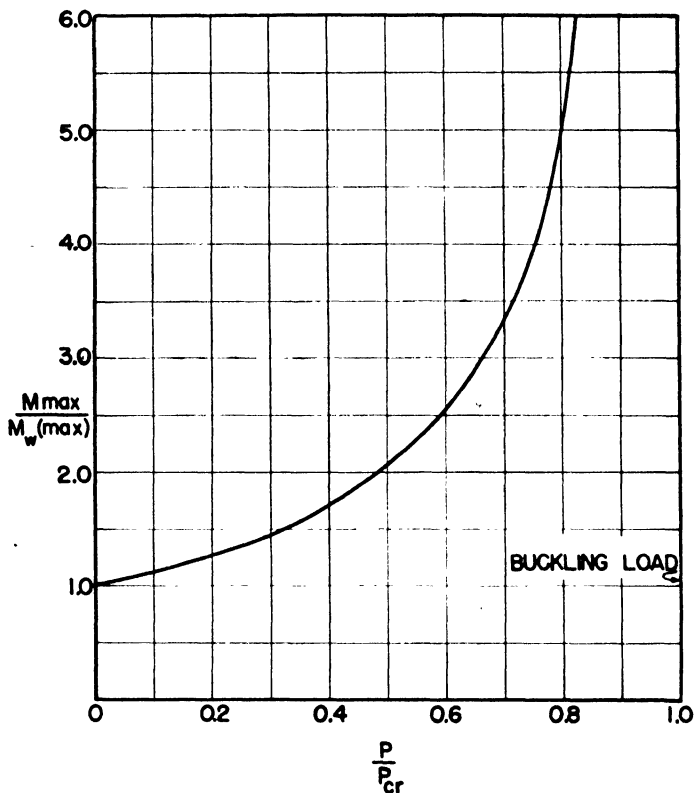
Fig. 8.10. Effect of Axial Load on Maximum Bending Moment.

mine the stresses in the beam column from the relation

$$f = \frac{P}{A} \pm \frac{Mc}{I} \qquad (8.24)$$

where c = the distance from the neutral axis of the beam to the fiber for which the stress is being determined (in).

This formula is rigorously valid only for stresses below the proportional limit, although sometimes it can be used up to the yield strength with small error. It should be remembered, however, that the axial load to produce buckling is not the Euler load if the stresses are greater than the proportional limit.

8.10 General case of beam column with distributed transverse load.
The equation for the bending moment in a beam column with any distribution of transverse loading is set up easily although the solution of the equation may be difficult in particular cases of specified distributions of load.

From the previous analysis of the beam column in Article 8.9 it is apparent that the bending moment in the beam column can be expressed in terms of the usual beam bending moment due to the transverse load and the moment due to the axial load. Thus,

$$M = M_L - Py \tag{8.25}$$

where M_L = beam bending moment caused by transverse load and neglecting the effect of the axial load, P.

Differentiating Equation 8.25, we have

$$\frac{d^2M}{dx^2} = \frac{d^2M_L}{dx^2} - P\frac{d^2y}{dx^2}$$

But

$$\frac{d^2M_L}{dx^2} = p$$

where p is the intensity of the distributed load at any section x

and

$$P\frac{d^2y}{dx^2} = \frac{P}{EI}M = k^2M$$

Therefore,

$$\frac{d^2M}{dx^2} + k^2M = p \tag{8.26}$$

This equation then is solved when p as a function of x is known and the conditions at the ends of the beam are used to determine the arbitrary constants resulting in the solution of the equation. If, for example, there is a moment on the left end of M_1 and a moment on the right end of M_2, then the end conditions will be

$$M = M_1 \text{ at } x = 0$$
$$M = M_2 \text{ at } x = L$$

EXAMPLE 8.2. For the wing shown in Figure 8.11 determine the bending moment distribution, taking into account the effect of the axial load. Assume that the wing spar carrying the load has a cross section with a moment of inertia of 16.5 in^4 and that the spar is made of spruce with the modulus of elasticity of 1.3×10^6 psi. Determine the maximum compressive stress if the distance from the neutral axis of the spar to the outer compressive fiber is 3 inches and the area of the beam is 7 square inches.

Solution. The reactions on the wing are determined similarly to

those in Example 4.1.   The axial load acting on the inboard portion of the wing is

$$P = \frac{wL^2}{2l} \cot \alpha = \frac{12 \times (216)^2}{2 \times 144} \cot 20° = 5{,}340 \text{ lb}$$

The moment due to the load on the outer portion of the wing at the
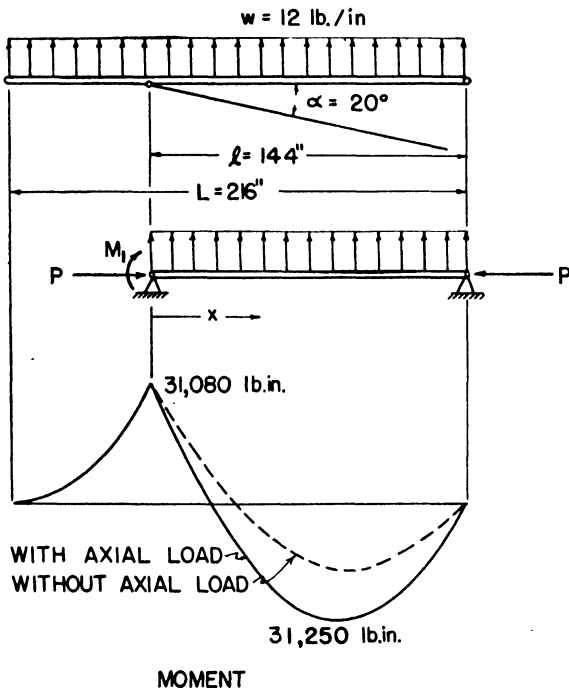
Fig. 8.11.   Bending Moments for Wing.

point where the strut joins the wing is

$$M_1 = \frac{w(L - l)^2}{2} = \frac{12 \times (72)^2}{2} = 31{,}080 \text{ lb in}$$

Since the distributed load is uniform, the relation for the moment according to Equation 8.26 is

$$\frac{d^2M}{dx^2} + k^2M = w$$

The solution is $M = A \cos kx + B \sin kx + \dfrac{w}{k^2}$

Since $M = M_1$ at $x = 0$

$M = 0$ at $x = L$

Therefore,

$$M = \frac{w}{k^2}\left\{\left(\frac{M_1 k^2}{w} - 1\right)\cos kx - \frac{\left[\left(\frac{M_1 k^2}{w} - 1\right)\cos kl + 1\right]}{\sin kl}\sin kx + 1\right\}$$

Substituting numerical values, we find that

$$k^2 = \frac{P}{EI} = \frac{5340}{1.3 \times 10^6 \times 16.5} = 0.2489 \times 10^{-3}$$

$$k = 0.01578$$

$$kl = 0.01578 \times 144 = 2.272 \text{ rad} = 130.2°$$

$$\frac{w}{k^2} = \frac{12}{0.2489 \times 10^{-3}} = 48,200$$

$$\frac{M_1 k^2}{w} = \frac{31,080}{48,200} = 0.645$$

$$\cos kl = -0.6455 \qquad \sin kl = 0.7638$$

Therefore,

$$M = 48,200[-0.355 \cos (0.01578x) - 1.610 \sin (0.01578x) + 1]$$

The moment diagram is shown in Figure 8.11.

The maximum compressive stress is

$$f = \frac{P}{A} + \frac{Mc}{I} = \frac{5340}{7} + \frac{31,250 \times 3}{16.5} = 6440 \text{ psi}$$

8.11 Principle of superposition for beam columns. The principle of superposition does not apply in the sense that the moments for one system of loading including the axial load can be superimposed or added to the moments for a different system of loading with a *different* axial load in order to get the combined moments. It can be shown, however, that the moments for two systems can be superimposed if the axial load is the *same for both.*

Consider a beam to which an axial load P_1 and a distributed load p_1 are applied and then from which the loads are removed and to which an axial load P_2 and a distributed load p_2 are applied. The moments in each case are

$$M_1 = M_{L1} - P_1 y_1$$
$$M_2 = M_{L2} - P_2 y_2$$

If the moments are superimposed, then

$$M = M_1 + M_2 = M_{L1} - P_1 y_1 + M_{L2} - P_2 y_2$$

and

$$\frac{d^2 M}{dx^2} = \frac{d^2}{dx^2}(M_{L1} + M_{L2}) - P_1 \frac{d^2 y_1}{dx^2} - P_2 \frac{d^2 y_2}{dx^2}$$

But

$$\frac{d^2}{dx^2}(M_{L1} + M_{L2}) = p_1 + p_2 = p$$

and, if $P_1 = P_2$ and $y = y_1 + y_2$ so that $\dfrac{d^2}{dx^2}(y_1 + y_2) = \dfrac{M}{EI}$

then $$\frac{d^2M}{dx^2} + \frac{P}{EI}M = p$$

which is the equation for the beam column with loads superimposed.

This principle is very useful since, if the moment distribution is known for two different loadings of beam columns, the moments for the combined loading can be obtained by superposition.

It should be emphasized that bending moments for two geometrically similar beam columns can be superimposed only when the axial loads are the same for each. The final axial load is the *original* axial load acting on *either* beam column.

8.12 Deflection of beam columns. The deflection of a beam column can be determined from the equation for the equilibrium of the beam column expressed in terms of the deflection. Therefore, if the moment in the beam column is given by

$$M = M_L - Py$$

then since $M = EI\dfrac{d^2y}{dx^2}$ it can be expressed as

$$\frac{d^2y}{dx^2} + \frac{P}{EI}y = \frac{M_L}{EI} \tag{8.27}$$

This equation is then solved for y in a manner similar to the way Equation 8.26 is solved for M.

If the moment distribution has already been determined, however, it is usually easier to solve for the deflection from the equation for the moments:

$$M = M_L - Py$$

so that $$y = \frac{M_L - M}{P} \tag{8.28}$$

By using this method the deflection for the wing of Example 8.2 is the moment represented by difference between the dashed and solid line curves of Figure 8.11 divided by the axial load P.

8.13 Beam column with end moments. In order to develop some expressions that will be useful in solving statically indeterminate beam column problems, the rotations at the ends of a simply supported beam column with end moments will be determined.

Consider the beam column shown in Figure 8.12. Since there is no transverse load, the equation for the beam column is

$$\frac{d^2M}{dx^2} + k^2M = 0$$

Therefore, $\qquad M = A \cos kx + B \sin kx$

Now at $x = 0,$ $\qquad M = M_A$

and at $x = L,$ $\qquad M = 0$

therefore, $\qquad M = M_A(\cos kx - \cot kL \sin kx)$

The moment in the simply supported beam neglecting the axial load is

$$M_L = M_A \left(1 - \frac{x}{L} \right)$$

and from Equation 8.28

$$y = \frac{M_L - M}{P} = -\frac{M_A}{P} \left(-1 + \frac{x}{L} + \cos kx - \cot kL \sin kx \right)$$

Therefore, $\dfrac{dy}{dx} = -\dfrac{M_A}{P} \left(\dfrac{1}{L} - k \sin kx - k \cot kL \cos kx \right)$

The rotation of each end of the beam can be determined from the
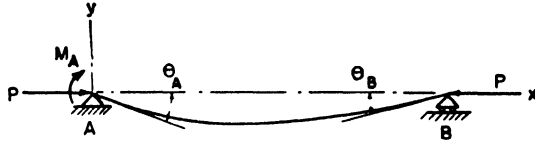
Fig. 8.12. Beam Column with End Moment.

equation for the slope. Thus, since the slope is negative at the left end,

$$\theta_A = -\left(\frac{dy}{dx} \right)_{x=0} = \frac{M_A}{P} \left(\frac{1}{L} - k \cot kL \right)$$

$$\theta_B = \left(\frac{dy}{dx} \right)_{x=L} = -\frac{M_A}{P} \left(\frac{1}{L} - \frac{k}{\sin kL} \right) \qquad (8.29)$$

These rotations may be written in the form

$$\theta_A = \frac{M_A L}{3EI} \, \psi$$

$$\theta_B = \frac{M_A L}{6EI} \, \phi \qquad (8.30)$$

where $\qquad \psi = \dfrac{3}{(kL)^2} (1 - kL \cot kL)$

$$\phi = \frac{6}{(kL)^2} \left(\frac{kL}{\sin kL} - 1 \right)$$

If a positive beam bending moment M_B is applied at the end B and $M_A = 0$, then

$$\theta_A = \frac{M_B L}{6EI} \, \phi$$

$$\theta_B = \frac{M_B L}{3EI} \, \psi$$

Therefore, if both end moments are applied simultaneously, then according to the principle of superposition we have

$$\theta_A = \frac{L}{6EI}\,(2M_A\psi + M_B\phi)$$

$$\theta_B = \frac{L}{6EI}\,(M_A\phi + 2M_B\psi) \qquad (8.31)$$

8.14 Beam column with end moment and one end fixed. Consider the beam column shown in Figure 8.13 with an end moment at A of M_A and the other end fixed against rotation.
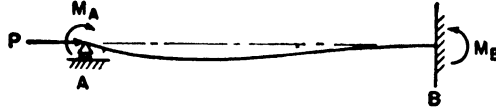
Fig. 8.13.   Beam Column with One End Fixed.

Since the rotation at B is zero, then by means of Equation 8.31 we have

$$\theta_B = 0 = \frac{L}{6EI}\,(2M_B\psi + M_A\phi)$$

or

$$M_B = -\frac{1}{2}\,M_A\frac{\phi}{\psi} \qquad (8.32)$$

It will be recalled in the development of the moment distribution method .(Article 6.5) that for an ordinary beam the moment induced at the fixed end of a beam is one half the magnitude and opposite in direction to the moment applied at the simply supported end. The carry-over factor in this case is one half. In like manner, the carry-over factor for the beam column as determined by Equation 8.32 is

$$c = \frac{1}{2}\frac{\phi}{\psi} \qquad (8.33)$$

It is interesting to note that M_B becomes very large for the beam shown in Figure 8.13 when $\psi \to 0$.

Let $\psi = 0 = \dfrac{3}{(kL)^2}(1 - kL\cot kL)$

or $\tan kL = kL$

The smallest value of kL satisfying this condition, other than for $kL = 0$, .is

$$kL = 4.49$$

Hence, $k^2 = \dfrac{P}{EI} = \dfrac{20.16}{L^2}$

and $P = 2.025\,\dfrac{\pi^2 EI}{L^2} \qquad (8.34)$

This is the initial buckling load. The corresponding end fixity factor for a column with one-end fixed and the other end pinned is 2.025.

8.15 Fixed-end beam column with uniform transverse load. The fixed-end beam column with a uniform transverse load of intensity w is resolved into two statically determinate systems, as shown in Figure 8.14. The end moments will be determined by superimposing the two systems so that the rotations at the ends are zero.
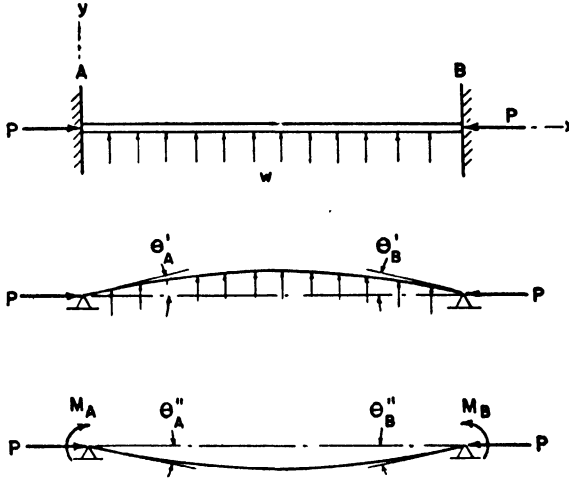
Fig. 8.14. Beam Column with Uniform Load.

The bending moment for a simply supported beam column with a uniform transverse load was determined in Article 8.9 and found to be

$$M = -\frac{w}{k^2}\left[\cos kx - \left(\frac{\cos kL - 1}{\sin kL}\right)\sin kx - 1\right]$$

The moment in the simply supported span, if the axial load is neglected, is

$$M_L = -\frac{wLx}{2} + \frac{wx^2}{2}$$

Therefore,

$$y = \frac{M_L - M}{P}$$

$$= \frac{1}{P}\left\{-\frac{wL}{2}x + \frac{wx^2}{2} + \frac{w}{k^2}\left[\cos kx - \left(\frac{\cos kL - 1}{\sin kL}\right)\sin kx - 1\right]\right\}$$

Then $\quad \dfrac{dy}{dx} = \dfrac{w}{P}\left\{-\dfrac{L}{2} + x - \dfrac{1}{k}\left[\sin kx + \left(\dfrac{\cos kL - 1}{\sin kL}\right)\cos kx\right]\right\}$

and $\quad \theta'_A = \left(\dfrac{dy}{dx}\right)_{x=0} = -\dfrac{w}{P}\left[\dfrac{L}{2} + \dfrac{1}{k}\left(\dfrac{\cos kL - 1}{\sin kL}\right)\right]$

$$= -\frac{wL^3}{EI}\alpha \tag{8.35}$$

where $\quad \alpha = \dfrac{1}{(kL)^2}\left[\dfrac{1}{2} + \dfrac{1}{kL}\left(\dfrac{\cos kL - 1}{\sin kL}\right)\right]$

From symmetry $\qquad\qquad\qquad \theta'_A = \theta'_B$

The rotation of the end of the simply supported beam column with end moments as determined in Article 8.13 is

$$\theta''_A = \frac{M_A L}{6EI} (2\psi + \phi)$$

In order to have the slope at the end of the beam zero corresponding to a fixed end

$$\theta'_A = \theta''_A$$

or $\qquad\qquad\qquad M_A = - wL^2 \frac{6\alpha}{2\psi + \phi}$

By means of the trigonometric half-angle relations this can be expressed as

$$M_A = M_B = \frac{w}{k^2} \left(1 - \frac{kL}{2} \cot \frac{kL}{2} \right) \qquad (8.36)$$

If we know the moments at the ends of the beam we can determine readily the moment at any section.

8.16 Equation of three moments for beam columns. The development of the equation of three moments for beam columns is similar in
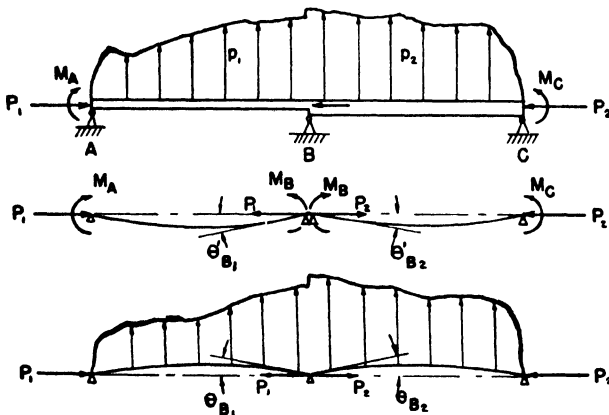
Fig. 8.15. Continuous Beam Column.

procedure to that for ordinary beams, as discussed in Article 6.2. The continuous beam column is considered cut at the supports, and the support moments are evaluated for the conditions that make the beam continuous over the supports. The beam column resolved into two statically determinate systems is shown in Figure 8.15.

Let θ_{B1} and θ_{B2} be equal to the rotations of the simply supported spans to the left and right of the support B due to only the axial loads and transverse loads. These rotations can be evaluated in a manner

similar to those in Article 8.15 for the beam column with the uniform transverse load.

If θ'_{B1} and θ'_{B2} are the rotations to the left and right of support B because of the moments M_A, M_B, and M_C, when the spans are assumed to be simply supported, then from Article 8.13,

$$\theta'_{B1} = \frac{L_1}{6E_1 I_1}(2M_B \psi_1 + M_A \phi_1)$$

$$\theta'_{B2} = \frac{L_2}{6E_2 I_2}(2M_B \psi_2 + M_C \phi_2)$$

For continuity across the support B

$$\theta'_{B1} - \theta_{B1} = -(\theta'_{B2} - \theta_{B2})$$

or
$$\theta'_{B1} + \theta'_{B2} = \theta_{B1} + \theta_{B2}$$

Assuming E is a constant for all spans and substituting the values for θ'_{B1} and θ'_{B2} into the above equation, we have

$$M_A \frac{L_1}{I_1}\phi_1 + 2M_B\left(\frac{L_1}{I_1}\psi_1 + \frac{L_2}{I_2}\psi_2\right) + M_C \frac{L_2}{I_2}\phi_2 = 6E(\theta_{B1} + \theta_{B2}) \quad (8.37)$$

where θ_{B1} = rotation to left of B assuming span 1 is simply supported and carries a transverse load and axial load only. This is the equation
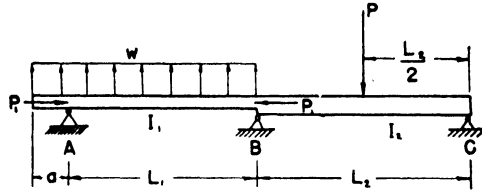
Fig. 8.16. Two Span Beam Column.

of three moments for beam columns. It may be used in the same way that the ordinary equation of three moments is used for solving multi-span beams.

EXAMPLE 8.3. Determine the moments at the supports for the beam analyzed in Example 6.1 except that an axial compressive load P_1 of 24,000 pounds is added to the left span. The beam is shown in Figure 8.16.

Solution. The data given in Example 6.1 are

$w = 10$ lb/in	$a = 5$ in	$\dfrac{L_1}{I_1} = 30$
$P = 300$ lb	$I_1 = 1$ in^4	
$L_1 = 30$ in	$I_2 = 1.5$ in^4	$\dfrac{L_2}{I_2} = 24$
$L_2 = 36$ in	$E_1 = E_2 = 10.5 \times 10^6$ psi	
In addition,	$P_1 = 24,000$ lb	

For span AB

$$k^2 = \frac{P_1}{EI_1} = \frac{24,000}{10.5 \times 10^6 \times 1} = 0.00228$$

$$k = 0.0477$$

$$kL = 0.0477 \times 30 = 1.431 \text{ rad} = 82°$$

$$\phi_1 = \frac{6}{(kL)^2}\left(\frac{kL}{\sin kL} - 1\right) = \frac{6}{(1.431)^2}\left(\frac{1.431}{0.9903} - 1\right) = 1.304$$

$$\psi_1 = \frac{3}{(kL)^2}(1 - kL \cot kL) = \frac{3}{(1.431)^2}(1 - 1.431 \times 0.1405) = 1.171$$

$\phi_2 = \psi_2 = 1$ since there is no axial load on span BC.

The rotation at B of span (1), if we consider that it is simply supported, is given by Equation 8.35:

$$\theta_{B1} = -\frac{wL^3}{EI}\frac{1}{(kL)^2}\left[\frac{1}{2} + \frac{1}{kL}\left(\frac{\cos kL - 1}{\sin kL}\right)\right]$$

$$= -\frac{10 \times (30)^3}{E \times 1}\frac{1}{(1.431)^2}\left[\frac{1}{2} + \frac{1}{1.431}\left(\frac{0.1392 - 1}{0.9903}\right)\right] = \frac{14,160}{E}$$

The rotation at B of span (2) can be determined by means of the methods given in Chapter 4.

$$\theta_{B2} = -\frac{PL_2^2}{16EI_2} = -\frac{300 \times (36)^2}{16E \times 1.5} = -\frac{16,200}{E}$$

Therefore, $$6E(\theta_{B1} + \theta_{B2}) = 6E\left(\frac{14,160}{E} - \frac{16,200}{E}\right) = -12,240$$

and $$M_A\frac{L_1}{I_1}\phi_1 + 2M_B\left(\frac{L_1}{I_1}\psi_1 + \frac{L_2}{I_2}\psi_2\right) + M_C\frac{L_2}{I_2}\phi_2 = -12,240$$

$$(125 \times 30 \times 1.304) + 2M_B[(30 \times 1.171) + 24] + 0 = -12,240$$

$$M_B = -145 \text{ lb in}$$

The bending moments at the supports are therefore

$$M_A = 125 \text{ lb in}$$
$$M_B = -145 \text{ lb in}$$
$$M_C = 0$$

8.17 Additional considerations of beam columns. Only a few simplified cases of beam columns have been analyzed in the preceding articles. It is seen easily that the solutions can become mathematically involved for complicated loading conditions. For this reason it will be well for the student who intends to work more intensively in this field to look up the methods for graphically solving beam columns in the references given at the end of the chapter.

Only the equation of three moments for solving continuous beam columns has been considered here. Actually a method exists which is an

extension of the moment distribution method and in which the modifica-
tion of the distribution factors and carry-over factors due to the axial
compression load is considered. For further information consult the
references at the end of the chapter.

Problems

8.1. Assuming that the deflection curve of the strut shown in Figure 8.4 is a
parabola, determine the elastic buckling load by the elastic energy method.

8.2. Determine the Euler load for the aluminum pin-ended strut with vertical
end pins shown in Figure 8.17.
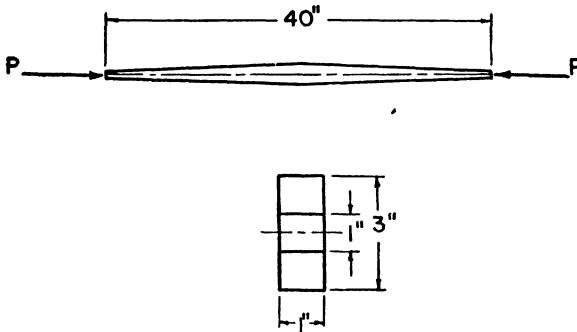
END VIEW

Fig. 8.17.   Strut with Variable Cross Section.

8.3. Using one of the tangent modulus curves for stainless steel given in the
ANC-5, determine the column curve for a pin-ended stainless steel column having
a cross-section area of 0.1194 in², a radius of gyration of 0.386 in, and a moment of
inertia of 0.0178 in⁴.

8.4. A pin-ended 1-0.035 24ST aluminum alloy tube 20 inches long carries
a compressive load of 2000 pounds. Determine the margin of safety. (*Note:*
refer to the ANC-5 for column formulas, curves, and tube data.)

8.5. If there is a compressive load of 60,000 pounds on an engine mount strut
that has ends welded into the connecting structure so that the end fixity coefficient
is 2, determine the margin of safety for a $2\frac{1}{2}$ − 0.095 4130 tubular strut 60 inches
long. $F_{ty} = 100,000$ psi.

8.6. Determine the allowable load for the 17ST link shown in Figure 8.18.
(*Note:* The ends of the link are pin-connected in one plane and completely
restrained against rotation in the other.)

8.7. A 17ST aluminum alloy round tube 20 inches long is required to carry a
compressive load of 5000 pounds. If $C = 1$ and $F_{ty} = 40,000$ psi, determine the
size of the tube for a small positive margin of safety. (Use standard sizes given
in the ANC-5.)

8.8. Determine the maximum bending moment for a uniform strut fixed at
one end and carrying a compressive load P at the other end along with a trans-
verse load of mP in which m is a constant.
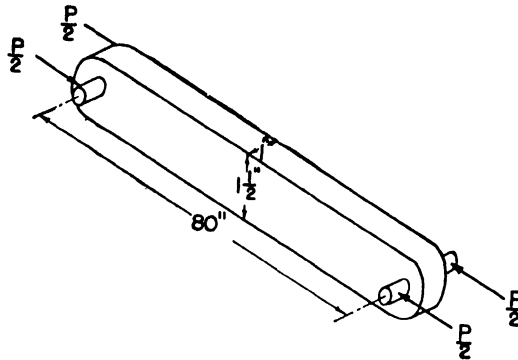
Fig. 8.18. Compression Link.

8.9. A simply supported steel beam column 80 inches long, with a cross-sectional moment of inertia of 0.4 in⁴ has an end moment at the left support of 10,000 lb in. If the direct axial compression is 3000 pounds, determine

(1) location of maximum moment
(2) magnitude of maximum moment.

8.10. Determine the moment at the center of a pin-ended beam column with an axial compressive load P applied at each end and a transverse concentrated load Q at midspan. (*Note:* the slope is zero at the midspan.) If the beam is a $1\frac{1}{2}$-0.058 alloy steel tube 40 inches long, determine the maximum stress when $P = 1000$ pounds and $Q = 750$ pounds.
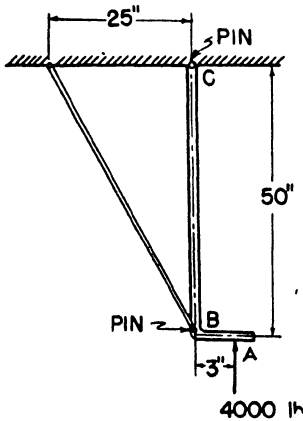
Fig. 8.19. Landing Gear.

8.11. Using the formulas for beam columns, given in Roark *Formulas for Stress and Strain*, and the principle of superposition, determine the equation for the bending moment for a simply supported beam column with a distributed transverse load varying linearly from a value of w at one end to $2w$ at the other.

8.12. A simplified landing gear strut shown in Figure 8.19 is made of a continuous $2\frac{1}{2}$-0.083 alloy steel tube pin connected at C and heat treated to $F_{cy} = 165,000$ psi. Determine

(1) reaction at ends of strut BC
(2) maximum bending moment in strut
(3) margin of safety based on yielding.

8.13. Under what conditions can the strength of a compression strut be increased by heat treatment?

8.14. Determine the fixed-end moments for a beam column with a uniformly varying transverse load which is zero at one end and has a value q_0 at the other.

References

Goodier, J. N., "The Buckling of Compressed Bars by Torsion and Flexure." Cornell University Engineering Experiment Station, Bulletin No. 27, December 1941.

Goodier, J. N., "Flexural-Torsional Buckling of Bars of Open Section." Cornell University Engineering Experiment Station, Bulletin No. 28, January 1942.

James, B. W., "Principal Effects of Axial Load on the Moment Distribution Analyses of Rigid Structures." NACA Tech. Note 534, 1935.

Kappus, R., "Twisting Failure of Centrally Loaded Open-Section Columns in the Elastic Range." NACA Tech. Memo. 851, 1938.

Roark, R. J., *Formulas for Stress and Strain*. McGraw-Hill, 1938.

Timoshenko, S., *Theory of Elastic Stability*. McGraw-Hill, 1936.

Wagner, Herbert, "Torsion and Buckling of Open Sections." NACA Tech. Memo. 807, October 1936.

Westergarrd, H. B. and W. R. Osgood, "Strength of Steel Columns." Appl. Mech. ASME, 1928.

Young, D. H., "Rational Design of Steel Columns." Trans. ASCE, 1936.

Young, Dana, "Inelastic Buckling of Variable-Section Columns." *Journal of Applied Mechanics*, September 1945.

CHAPTER 9

Compressive Strength of Thin Sheet Members

....

9.1 Introduction. Many columns and struts, as well as the covering of the surface of the airplane, are composed of thin metallic sheets. The combinations of surface sheets reinforced by longitudinal stiffener members commonly used in present design are called *sheet-stiffener panels*. There is a trend in design away from the use of the *sheet-stiffener type* of construction and toward a truly monocoque or shell-like construction. The strength of all of these various members depends, in varying degrees, on the compressive strength of thin metallic sheet.

It was indicated in the previous chapter that many columns may fail by local instability. This type of failure is most likely to occur in columns with cross sections composed of thin sheet so that collapse of the thin wall is possible. It is also likely that the surface of a wing or fuselage will wrinkle locally, owing to the loads carried by the member. The designer should be able to predict the loads required to buckle a column locally or to wrinkle a surface, as well as to be able to determine the maximum loads such members can carry.

Most of the methods used in calculating the compressive strength of sections made up of thin material are semi-empirical because of the complexity of the problem. However, the methods given in this chapter have been correlated with tests and are considered to be sufficiently accurate for preliminary design.

9.2 Flat sheet with edge compression. As in the analysis of columns, the analysis of the buckling of sheet is divided into two groups: (1) elastic stability and (2) inelastic stability. Elastic stability will be considered first.

The closest correlation between flat sheet in compression and the columns previously analyzed occurs when the sheet is unsupported along its unloaded edges. In this case the only difference between the sheet and the column is that the width of the sheet may be of the same order of magnitude as the length, whereas in the column the cross section is small as compared with the length. A sheet with edge compression is shown in Figure 9.1.

Assume a uniformly distributed load, p, along the top and bottom edges of the sheet. Consider a strip of sheet of unit width. As the compression load causes the sheet to bend, the fibers on the compressive side of the sheet tend to expand laterally because of Poisson's effect, and the fibers contract laterally on the tension side for the same reason. The sheet therefore tends to dish inward, with a curvature in the vertical

- **144**

plane due to the direct bending, and a curvature in the horizontal plane
due to the Poisson effect. The latter is called *anticlastic curvature*.
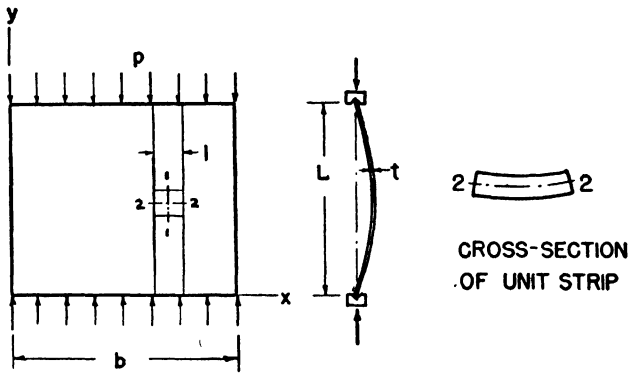
Fig. 9.1. Compression of Sheet with Unloaded Edges Free.
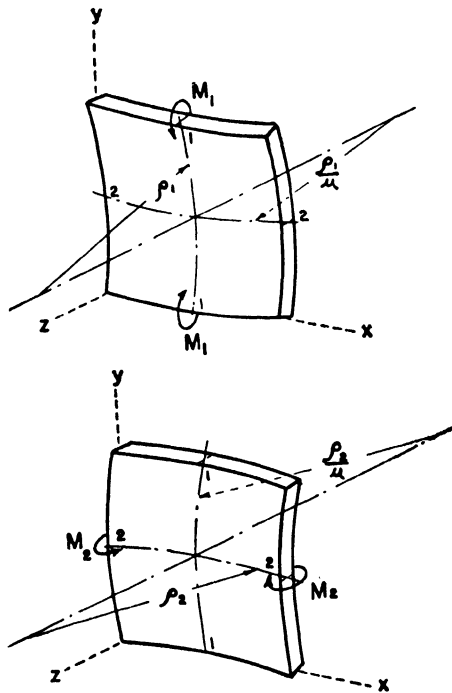
Fig. 9.2. Deformation of Flat Sheet Element.

However, since the sheet is wide, the material adjacent to the strip
tends to restrain the anticlastic curvature, so that a moment about the
vertical edges of the strip is induced.

Consider a unit square cut from the strip with a direct moment M_1 applied to the horizontal edges and an induced moment M_2 on the vertical edges, as shown in Figure 9.2. By applying M_1 alone first, the curvature in the plane of the moment is $1/\rho_1$, and the induced curvature in the horizontal plane is $-\mu/\rho_1$. The minus sign denotes that the center of curvature is on the side of the sheet opposite to the other center of curvature. The same thing holds for M_2 only; the curvatures in the same directions are $-\mu/\rho_2$ and $1/\rho_2$. The curvature in the 1-1 direction with both moments acting simultaneously is by superposition

$$\frac{1}{R_1} = \frac{1}{\rho_1} - \frac{\mu}{\rho_2}$$

and in the 2-2 direction

$$\frac{1}{R_2} = \frac{1}{\rho_2} - \frac{\mu}{\rho_1}$$

According to the flexure formula $\dfrac{1}{\rho_1} = \dfrac{M_1}{EI_1}$

Since $I_1 = \dfrac{t^3}{12}$, then $\quad \dfrac{1}{\rho_1} = \dfrac{12M_1}{Et^3}$

and $\qquad\qquad\qquad\quad \dfrac{1}{\rho_2} = \dfrac{12M_2}{Et^3}$

Therefore, $\qquad\qquad\quad \dfrac{1}{R_1} = \dfrac{12}{Et^3}(M_1 - \mu M_2)$

$$\frac{1}{R_2} = \frac{12}{Et^3}(M_2 - \mu M_1)$$

If the restraint of the sheet is sufficient to prevent the curvature in the 2-2 direction, then

$$\frac{1}{R_2} = 0 \text{ and } M_2 = \mu M_1$$

Therefore, $\qquad\qquad\quad \dfrac{1}{R_1} = \dfrac{12}{Et^3}(1 - \mu^2)M_1 \qquad\qquad (9.1)$

or $\qquad\qquad\qquad\quad \dfrac{1}{R_1} = \dfrac{M_1}{D}$

where $\qquad\qquad\qquad\quad D = \dfrac{Et^3}{12(1 - \mu^2)}$

D for the sheet therefore replaces EI for the ordinary bending case so that Euler's equation becomes

$$p = \frac{\pi^2 D}{L^2} = \frac{\pi^2 Et^3}{12(1 - \mu^2)L^2} \qquad\qquad (9.2)$$

where $\quad\quad p$ = load per unit length of loaded edge (lb/in)
$\qquad\qquad \mu$ = Poisson's ratio.

If the sheet has a width b, then the total load is

$$P = \frac{\pi^2 E t^3 b}{12(1 - \mu^2)L^2} \qquad (9.3)$$

and
$$\frac{P}{A} = F_c = \frac{\pi^2 E}{12(1 - \mu^2)} \frac{t^2}{L^2} \qquad (9.4)$$

9.3 Flat sheet in compression with unloaded edges supported.   If the unloaded edges of the flat sheet shown in Figure 9.1 are guided in V-grooves so that the edges of the sheet can rotate but not deflect, the edges are said to be *simply supported* or *guided*.   Edges in slots that completely restrain the rotation of the edge are *fixed*.   The edge conditions influence the curvature across the sheet so that the compressive load required to produce buckling depends on the edge conditions. .

The analysis of a sheet with various edge conditions considers the moment in the sheet in two directions as well as a twist.   This analysis is too complicated to be discussed here, but the results will be indicated.

Fig. 9.3.   Sheet Buckled into Three Half-Waves.

Consider a sheet with all edges simply supported.   As in the case of columns, the buckling load can be expressed in terms of a fixity coefficient. Equation 9.4 can thus be written

$$F_c = \frac{K_1 \pi^2 E}{12(1 - \mu^2)} \frac{t^2}{L^2} \qquad (9.5)$$

where $K_1 = \left(m + \dfrac{L^2}{mb^2} \right)^2$ = fixity coefficient

m = an integer number of half-waves in buckled plate in direction of load (see Figure 9.3).

The magnitude of K_1 and hence of F_c depends on the ratio of L/b. When L/b is less than one, that is when the sheet is wider than it is long, then L^2/mb^2 is always less than m and the smallest value of K_1 is when m equals one.   The sheet therefore buckles into one half-wave, and the stress is

$$F_c = \left(1 + \frac{L^2}{b^2} \right)^2 \frac{\pi^2 E}{12(1 - \mu^2)} \frac{t^2}{L^2}$$

$$= \left(\frac{1}{L} + \frac{L}{b^2} \right)^2 \frac{\pi^2 E}{12(1 - \mu^2)} t^2$$

By differentiation it can be shown that the factor in parentheses is a minimum when $L = b$. Therefore, a square sheet will require the least stress to buckle it, and conversely a sheet that is not square will tend to buckle into squares, as shown in Figure 9.3.

If Equation 9.5 is rewritten as

$$F_c = K_2 E \frac{t^2}{b^2} \qquad (9.6)$$

where

$$K_2 = \left(\frac{L}{mb} + \frac{mb}{L}\right)^2 \frac{\pi^2}{12(1 - \mu^2)}$$

the value of K_2 for μ equal to 0.3 and for various L/b ratios can be plotted as shown in Figure 9.4. From these curves it is evident that a
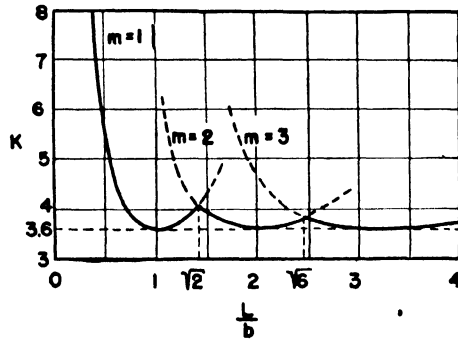
Fig. 9.4. Fixity Factor for Sheet with All Edges Guided.

sheet with an L/b ratio slightly greater than one will buckle into one half-wave because the load is less for forming one half-wave than two half-waves. The variation of K_2, and hence the stress, is therefore given by the solid curve.

It is common to include all the factors except E and t/b in the fixity coefficient. Thus, for a value of $\mu = 0.3$, which is approximately correct for steel and aluminum, the allowable stress for a sheet with any edge condition is given as

$$F_c = KE \left(\frac{t}{b}\right)^2 \qquad (9.7)$$

where
$\qquad K$ = fixity coefficient
$\qquad t$ = thickness of sheet (in)
$\qquad b$ = length of loaded side (in).

Values of K for various edge conditions are shown in Figure 9.5. The peaks indicating the change in modes of buckling corresponding to the change in the number of half-waves have been omitted. Coefficients for other conditions are given in the ANC-5.

The form of the equation for a panel in shear, that is, with shear forces applied along the edges of the flat panel, has the same form as for the panel in compression. The value of K for a flat panel in shear with all edges guided is given by the dashed line in Figure 9.5.

EXAMPLE 9.1. Compare the loads required to buckle elastically, similar sheets of steel and aluminum of the same weight.
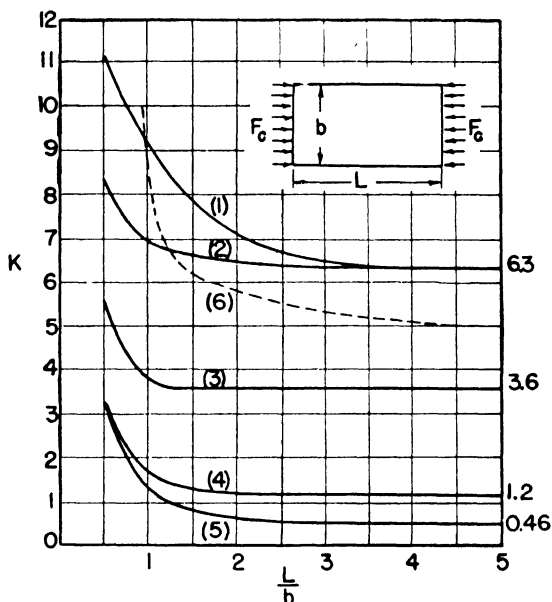
Fig. 9.5. Fixity Coefficients for Flat Sheet. 1. All edges fixed; 2. loaded edges guided, unloaded edges fixed; 3. all edges guided; 4. loaded edges guided, one unloaded edge fixed and one free; 5. loaded edges guided; one unloaded edge guided and one free; 6. shear panel with all edges guided.

Solution. For panels of the same length, width, and weight, the thicknesses will vary inversely with the densities, w.

Equating weights gives $Lbt_s w_s = Lbt_a w_a$

then

$$\frac{t_a}{t_s} = \frac{w_s}{w_a} = \frac{0.283}{0.100} = 2.83$$

The load required to buckle the steel sheet is

$$P_s = F_c bt_s = KE_s \left(\frac{t_s}{b}\right)^2 bt_s = KE_s \frac{t_s^3}{b}$$

and similarly for aluminum

$$P_a = KE_a \frac{t_a^3}{b}$$

Then

$$\frac{P_a}{P_s} = \frac{E_a}{E_s}\left(\frac{t_a}{t_s}\right)^3 = \frac{10.5 \times 10^6}{30 \times 10^6}(2.83)^3 = 7.93$$

The aluminum sheet will carry about 8 times as much compressive load before buckling as a similar sheet of steel of the same weight. Since the aluminum is lighter per unit volume than steel, it is possible to use it in greater thicknesses and thus obtain more stability strength.

9.4 Buckling of sheet stressed beyond the proportional limit. As for the column, if the stresses exceed the proportional limit of the sheet, the modulus of elasticity is no longer a constant and its variation with the stress must be considered in determining the buckling load. The buckling of the sheet is more complicated than the column since the sheet involves restraint along four edges and curvatures in two directions. The same idea of expressing the allowable compressive stress in terms of a "reduced modulus" is used for the sheet as was used in the column so that Equation 9.7 is modified for the inelastic range as follows:

$$F_c = KE_r \left(\frac{t}{b}\right)^2 \tag{9.8}$$

where $E_r = \eta E$

η = a factor for modifying E when the stress is greater than the proportional limit.

Many investigators have suggested forms for η based on test and theory. Several of these forms involve the tangent modulus of the material, and most are complicated and difficult to use. Hoff has suggested a method for determining η which although conservative is quite simple to use. Because of the simplicity and conservativeness of the method, its use is recommended for preliminary design. Regardless of what method is used, tests should be made on the structure before the final design is determined. If test curves exist they should be used.

Hoff's method is based on the fact that since the regular column curves for a material really give the relation of E to E_r as specified by the licensing authority, the column curves can be used for determining the allowable compressive stresses in flat sheet in the inelastic range. Figure 9.6 shows a column curve as given in the ANC-5 for tubes of 24ST. For an ordinary column in which local failure is not considered, the allowable stresses in the inelastic and elastic ranges are given by

$$F_{c1} = \frac{\pi^2 E_r}{\left(\dfrac{L'}{\rho}\right)^2} \text{ inelastic range}$$

$$F_{c2} = \frac{\pi^2 E}{\left(\dfrac{L'}{\rho}\right)^2} \text{ elastic range}$$

Therefore, for the same $\dfrac{L'}{\rho}$

$$\frac{F_{c1}}{F_{c2}} = \frac{E_r}{E} = \eta$$

It follows therefore that if the stress is calculated on the assumption that the material is elastic, the actual stress will be reduced by a factor η from the calculated elastic stress.   If the stress in the sheet is assumed in the elastic range and equated to the Euler column stress, then

$$F_c = KE\left(\frac{t}{b}\right)^2 = \frac{\pi^2 E}{\left(\dfrac{L'}{\rho}\right)^2}$$

or

$$\frac{L'}{\rho} = \frac{\pi}{\sqrt{K}}\frac{b}{t} \qquad (9.9)$$

The stress corresponding to this L'/ρ is then determined from the column curve of the material.   This stress is the allowable stress for the sheet.

$$\frac{L'}{\rho} = \frac{\pi}{\sqrt{K}}\frac{b}{t}$$
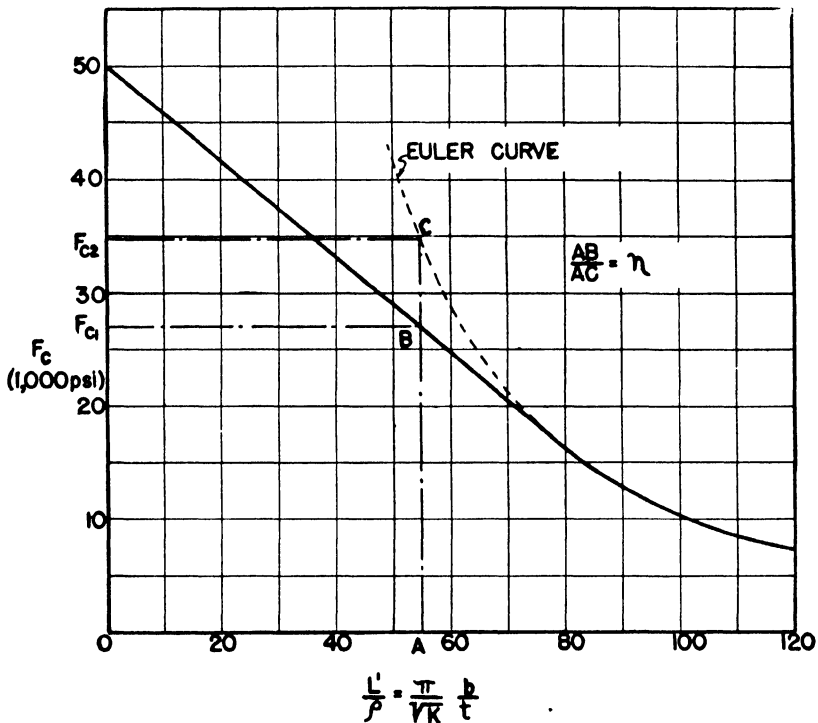
Fig. 9.6.   Column Curve for 24ST Round Tubing.

The method is best illustrated by an example.

EXAMPLE 9.2.   Determine the buckling stress for a $3'' \times 3'' \times 0.091''$ flat 24ST sheet, assuming that two edges are carrying a compressive load and that all edges are guided.

Solution. Assume that the material is elastic. Then

$$F_c = KE\left(\frac{t}{b}\right)^2 = 3.6 \times 10.5 \times 10^6 \left(\frac{0.091}{3}\right)^2 = 34{,}800 \text{ psi}$$

This stress is higher than the proportional limit; therefore the sheet will buckle inelastically. Substituting this stress into the Euler equation gives

$$F_c = KE\left(\frac{t}{b}\right)^2 = \frac{\pi^2 E}{\left(\dfrac{L'}{\rho}\right)^2}$$

or

$$\frac{L'}{\rho} = \frac{\pi}{\sqrt{K}}\frac{b}{t} = \frac{\pi}{\sqrt{3.6}}\frac{3}{0.091} = 54.6$$

The column stress corresponding to this L'/ρ can be determined from the column curves for the material, Figure 9.6, or from the equation given in the ANC-5 for this material. Hence,

$$F_c = 50{,}000 - 421\frac{L'}{\rho} = 50{,}000 - 421 \times 54.6 = 27{,}020 \text{ psi}$$

9.5 Crippling strength—open sections of flat sheet elements. Sections such as angles, channels, and so on, that do not form completely closed sections, such as cylinders, are called *open sections.*
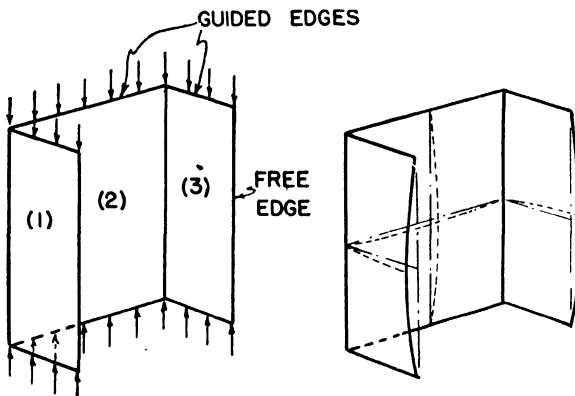
Fig. 9.7. Buckling of Channel.

It has been found that the load required to buckle short lengths of open sections made up of flat sheet elements can be approximated closely by summing up the loads required to buckle each element independently. The total load thus determined divided by the area of the section is called the *crippling stress* and corresponds to the stress required for local buckling of the column. It has been substantiated also that the bend,

where two elements join, supports the adjacent sheet elements as if the edges of the sheet were guided.

The assumption that the buckling loads for the separate sheet elements can be added to obtain the total load has some logic.   Consider a channel section as shown in Figure 9.7.   If a compressive load is applied to the ends of the channel by two parallel crossheads in the testing machine, the legs, being the weaker elements, will buckle first and thus shirk taking additional load until the back finally buckles and general collapse occurs.

If the legs of the channel, elements 1 and 3, are analyzed as flat sheets with three guided edges and one free edge for which the allowable stresses are F_{c1} and F_{c3}, and if the back of the channel is analyzed as a flat sheet with four edges guided with an allowable stress F_{c2}, then the total load carried by the section is

$$P = F_1 b_1 t_1 + F_2 b_2 t_2 + F_3 b_3 t_3 \qquad (9.10)$$

and the crippling stress is

$$F_{cc} = \frac{P}{A} = \frac{F_{c1} b_1 t_1 + F_{c2} b_2 t_2 + F_{c3} b_3 t_3}{b_1 t_1 + b_2 t_2 + b_3 t_3} \qquad (9.11)$$

where b_1, etc. = centerline width of sheet element (in)

   t_1, etc. = thickness of sheet element (in).

It is apparent that putting bends on the outstanding legs increases the strength of the section since this tends to change the restraint of the edge from a free condition to a guided condition which thereby increases the value of K used in the analysis.

EXAMPLE 9.3.   Determine the crippling stress for the 24ST channel shown in Figure 9.8.

Solution.   It will be assumed that L/b for each sheet element is greater than three so that the fixity factor K is essentially a constant.

Fig. 9.8.   Channel Section.

Using centerline distances gives

$$\frac{b_1}{t_1} = \frac{0.484}{0.032} = 15.1; \qquad \frac{b_2}{t_2} = \frac{0.718}{0.032} = 22.4$$

For the outstanding legs 1 and 3

$$F_{c1} = K_1 E \left(\frac{t_1}{b_1}\right)^2 = 0.46 \times 10.5 \times 10^6 \times \left(\frac{1}{15.1}\right)^2 = 21{,}200 \text{ psi}$$

This stress is approximately the proportional limit so that it does not have to be adjusted for change in modulus.

For the back element 2, the stresses will be higher than the proportional limit.   Using Equation 9.9
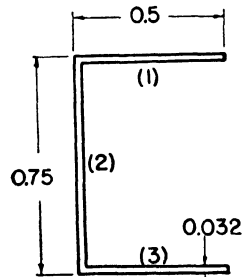
$$\frac{L'}{\rho} = \frac{\pi}{\sqrt{K_2}} \frac{b_2}{t_2} = \frac{\pi}{\sqrt{3.6}} 22.4 = 37.1$$

Therefore, from Figure 9.6

$$F_{c2} = 34,500 \text{ psi}$$

and

$$\begin{aligned}
F_{cc} &= \frac{2F_{c1}b_1t_1 + F_{c2}b_2t_2}{2b_1t_1 + b_2t_2} \\
&= \frac{(2 \times 21,200 \times 0.485 \times 0.032) + (34,500 \times 0.718 \times 0.032)}{(2 \times 0.485 \times 0.032) + (0.718 \times 0.032)} \\
&= 26,800 \text{ psi}
\end{aligned}$$

The test stress for this section was 28,000 psi. Ratio of calculated to test stress is $\frac{26,800}{28,000} = 0.957$.

9.6 Crippling strength—open-section extrusions. Open-section extrusions are analyzed similarly to the thin-sheet open sections. How-
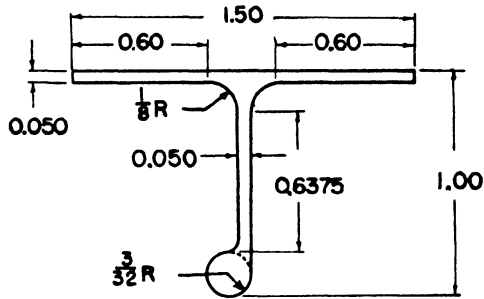
Fig. 9.9. Extruded Bulb Tee-Section.

ever, since the elements of the extrusion are usually thicker as compared with their width and since the place where the elements join are usually generously filleted, the effect of the extra metal is considered by measuring the width of the flat element up to the beginning of the fillet radius. This allows for a slightly smaller b/t ratio and therefore a higher allowable stress on the element.

EXAMPLE 9.4. Determine the crippling load and crippling stress for the 24ST bulb Tee-section shown in Figure 9.9.

Solution. The b/t ratios are

$$\frac{b_1}{t_1} = \frac{0.60}{0.05} = 12.0; \qquad \frac{b_2}{t_2} = \frac{0.6375}{0.05} = 12.75$$

The elements 1 have one free edge; therefore,

$$\frac{L'}{-\rho} = \frac{\pi}{\sqrt{K_1}} \frac{b_1}{t_1} = \frac{\pi 12}{\sqrt{0.46}} = 55.6$$

and from **Figure 9.6**

$$F_{c1} = 26,500 \text{ psi}$$

To be conservative, we assume that the bulb offers no additional restraint to the edge of element 2. Therefore,

$$\frac{L'}{\rho} = \frac{\pi}{\sqrt{K_2}} \frac{b_2}{t_2} = \frac{\pi}{\sqrt{0.46}} \times 12.75 = 59.1$$

and $\qquad F_{c2} = 25,200 \text{ psi}$

The crippling stress is therefore

$$F_{cc} = \frac{2F_{c1}b_1t_1 + F_{c2}b_2t_2}{2b_1t_1 + b_2t_2}$$

$$= \frac{(2 \times 26,500 \times 0.60) + (25,200 \times 0.6375)}{(2 \times 0.6) + 0.6375} = 26,100 \text{ psi}$$

The crippling load is based on the whole area.

$$P = F_{cc}A = 26,100 \times 0.145 = 3,780 \text{ lb}$$

The test crippling stress for this section is 28,000 psi. Therefore, the ratio of predicted stress to test stress is

$$\frac{26,100}{28,000} = 0.932$$

9.7 Strength of columns of thin-walled open sections. Columns with open sections made of thin sheet fail locally if the length of the column is small. The upper limit of the column failure in the inelastic range is therefore the crippling strength of the section. The problem of the failure of such columns in the inelastic range is difficult to solve so that an empirical method is often used. A semi-empirical method widely used is to assume the allowable crippling stress F_{cc} as the upper limit of the allowable column stress for small L'/ρ. This is equivalent to replacing the column yield stress, F_{co}, used for solid sections, by the crippling stress, F_{cc}, since the section will buckle locally for small L'/ρ's. The column curve in the inelastic range is assumed to be a parabola, and the Euler curve is valid in the elastic range as before. Therefore, replacing F_{co} by F_{cc} in Equation 8.17, we have

$$F_c = F_{cc}\left[1 - \frac{F_{cc}}{4\pi^2EC}\left(\frac{L}{\rho}\right)^2\right] \text{ for } \frac{L}{\rho} < \pi\sqrt{\frac{2CE}{F_{cc}}} \qquad (9.12)$$

and $\qquad F_c = \dfrac{C\pi^2E}{\left(\dfrac{L}{\rho}\right)^2} \text{ for } \dfrac{L}{\rho} > \pi\sqrt{\dfrac{2CE}{F_{cc}}} \qquad (9.13)$

Tests performed on open-section columns with flat ends resting on the crossheads of a testing machine indicate an average fixity factor of $C = 2$ to 3.

EXAMPLE 9.5. Determine the allowable column stress for a 24ST column 12 inches long and with a channel cross section similar to the one analyzed in Example 9.3.

Solution. The moment of inertia of the channel section will be least about a principal axis parallel to the back. The distance from the center line of the back to the principal axis can be determined by summing moments of areas. If we call this distance $\bar{y}$, then

$$\bar{y} = \frac{\Sigma yA}{A}$$

$$= \frac{0.468 \left(\frac{0.468}{2} + 0.016\right) 2 \times 0.032}{(2 \times 0.468 \times 0.032) + (0.75 \times 0.32)}$$

$$= 0.139 \text{ in}$$

The moment of inertia about the centroidal axis is

$$I = (0.718 \times 0.032)(0.139)^2$$
$$+ 2\left[(0.484 \times 0.032)\left(\frac{0.484}{2} - 0.139\right)^2 + \frac{1}{12}(0.484)^3\, 0.032\right]$$
$$= 0.00137 \text{ in}^4$$

and $A = 0.0540 \text{ in}^2$

Therefore, $\rho = \sqrt{\dfrac{I}{A}} = \sqrt{\dfrac{0.00137}{0.0540}} = 0.159 \text{ in}$

$$\frac{L}{\rho} = \frac{12}{0.159} = 75.5$$

But from Example 9.3, $F_{cc} = 26{,}800$ psi so that

$$\pi \sqrt{\frac{2CE}{F_{cc}}} = \pi \sqrt{\frac{2 \times 2 \times 10.5 \times 10^6}{26{,}800}} = 124$$

Since $\dfrac{L}{\rho} = 75.5 < 124$

the parabolic column Equation 9.12 will be used:

$$F_c = F_{cc}\left[1 - \frac{F_{cc}}{4\pi^2 EC}\left(\frac{L}{\rho}\right)^2\right]$$

For $C = 2$ $F_c = 26{,}800 - 0.868\left(\frac{L}{\rho}\right)^2$

$$= 26{,}800 - 0.868 \times (75.5)^2 = 21{,}900 \text{ psi}$$

9.8 Ultimate strength of flat sheet. It has been determined experimentally that flat sheet with guided or fixed edges will carry a higher compressive load than the buckling load. Since the edges are restrained by the supports, the sheet adjacent to the supports is in effect stiffer than the middle portion of the sheet, and in some cases failure does not occur

until the material along the supports reaches the yield point. Tests conducted on flat sheet indicate that the stress distribution along the loaded edges has a sinusoidal character, as shown in Figure 9.10. After buckling occurs, the stress in the center of the loaded edges does not increase and shirks taking additional load. The stiffer edge portions take the additional load after buckling occurs.

Kármán suggested that an approach to predicting the ultimate load for flat sheet could be made by considering all the load to be carried by the sheet adjacent to the restrained edges. The stress in this portion of the sheet is assumed uniform and equal to the stress at the edge. The

AT BUCKLING   AFTER BUCKLING
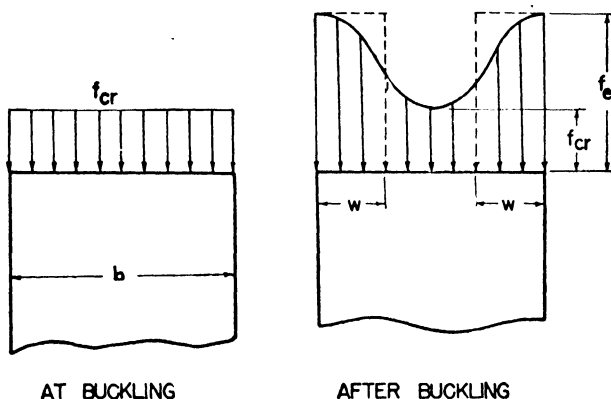
Fig. 9.10. Effective Width.

width of the sheet having the edge stress is called the *effective width*. If we assume that the edge stress is given by an equation having the same form as the buckling equation, then

$$f_e = KE \left(\frac{t}{b_1} \right)^2$$

where f_e = edge stress (psi).

For a panel as shown in Figure 9.10 there are two widths effective in carrying the load. If we call the effective width w so that $b_1 = 2w$ and assume that the edges are guided so that $K = 3.6$, then

$$f_e = 3.6E \frac{t^2}{4w^2}$$

$$w = 0.949t \sqrt{\frac{E}{f_e}}$$

It has been found that a factor of 0.85 agrees better with experimental data. Therefore,

$$w = 0.85t \sqrt{\frac{E}{f_e}} \tag{9.14}$$

This is the design equation used in the ANC-5. If failure occurs when the edge stress is equal to the compressive yield stress of the material F_{cy}, then the ultimate load of the sheet is

$$P = 2wtF_{cy} = 1.70t^2 \sqrt{EF_{cy}} \qquad (9.15)$$

The effective width can be expressed in terms of the critical stress f_{cr} since

$$f_{cr} = KE \left(\frac{t}{b}\right)^2 \qquad \text{`}$$

Solving for E and substituting into Equation 9.14 for $K = 3.6$, we have

$$w = 0.448b \sqrt{\frac{f_{cr}}{f_e}} \qquad (9.16)$$

where $\qquad b =$ width of panel (in)

$f_{cr} =$ buckling stress for sheet (psi).

More recent experiments show that a closer approximation to the effective width is given by

$$w = 0.50b \sqrt[3]{\frac{f_{cr}}{f_e}} \qquad (9.17)$$

This is known as *Marguerre's equation.*

9.9 Strength of columns of thin-walled closed sections. In the case of open sections, such as channels or angles, the buckling of the sheet sections limits the maximum load that the column can carry because the section is not sufficiently stabilized to take an increased load. In the case of closed sections, however, the walls will carry more load than the load required to buckle the walls so that the upper limit for the column load, as L'/ρ approaches zero, is the ultimate strength of the column cross section. The allowable column stress for columns with closed sections can be approximated by substituting the ultimate stress of the section for the crippling stress used in Equation 9.12.

9.10 Strength of curved sheet. There seems to be no completely satisfactory analysis of curved sheet available which will predict the buckling stress or crushing stress of curved sheet. Many empirical formulas do exist which are suitable for calculating these stresses for given ranges of values of radius, thickness, length, and edge fixity conditions. Some of these equations are discussed in the references given at the end of the chapter.

Tests have indicated some general results for sections made up of straight and curved elements, as shown in Figure 9.11. For example, it has been shown that if the edges of a curved sheet are supported, the edge stress which can be carried is not much greater than the stress required to buckle the center portion of the sheet. The following suggestions have

been made by Sechler for estimating the crushing stress of sections having curved sheet elements.

(1) If the buckling stress for the curved element is reached before any straight element buckles, then the crippling stress for the entire section is taken as equal to the buckling stress for the curved element.

(2) If the buckling stress for the weakest curved element is reached after a flat element buckles, then the total load carried by the section is
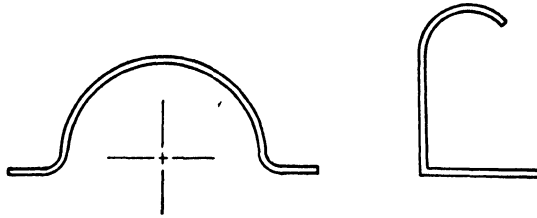
Fig. 9.11.   Sections with Curved Elements.

equal to the sum of the buckling loads of the buckled flat elements, and the product of the buckling stress for the weakest curved element and the area of the unbuckled element.

Since the buckling stresses of the curved elements must be known in order to apply this method to sections with curved elements, it is desirable to test the curved section directly unless experimental data for the curved elements are available.

A method has been suggested for predicting the ultimate crushing stress for a curved sheet having a large radius of curvature as might be used for covering on a fuselage. By assuming that the edges are guided by stiffeners or other means, the ultimate stress is based on the effective width concept similar to that used for flat sheet. However, since the curvature tends to strengthen the sheet, the center portion between the effective widths is assumed to carry a stress

$$f_c \doteq 0.3E\,\frac{t}{R} \qquad (9.18)$$

where R = radius of curvature of sheet (in)

t = thickness of sheet (in).

Fig. 9.12.   Curved Sheet.

If we refer to Figure 9.12, we can express the ultimate compressive strength for the curved sheet by
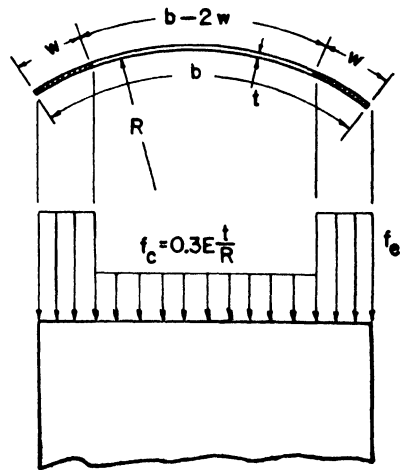
$$F_c = \frac{P}{A} = \frac{2f_e wt + 0.3E\dfrac{t^2}{R}(b - 2w)}{bt}$$

$$= \frac{2f_e w + \dfrac{0.3E}{R}(b - 2w)t}{b} \tag{9.19}$$

where w = effective width calculated in the same manner as for flat sheet (in).

9.11 Compressive strength of sheet-stringer panels. It is common practice in the design of modern aircraft structures to strengthen the sheet carrying compressive loads by attaching stringers to the sheet
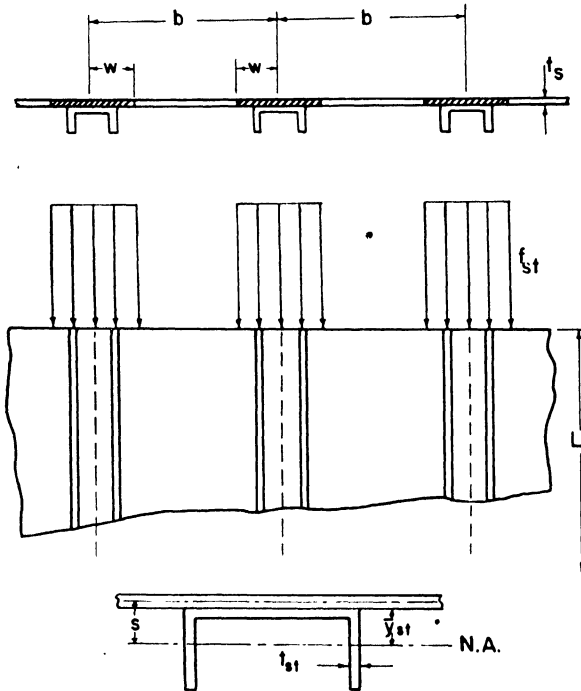
Fig. 9.13. Sheet-Stringer Panel.

that act as columns. Since the sheet usually buckles at a lower stress than the stringers, only the effective width of the sheet is assumed to act with the stringers as load carrying elements, Figure 9.13. The load carried by each stringer and its adjacent sheet is therefore

$$P_{st} = f_{st}(A_{st} + 2wt_s) \tag{9.20}$$

where f_{st} = allowable stringer stress (psi)
                  A_{st} = area of stringer (in²).

Since the effective width is determined by the edge stress on the sheet that is now the stringer stress and since the allowable stringer stress depends on the sheet acting with it, the solution of this problem is one of trial and error. The steps in the solution are:

(1) Determine the allowable column stress for the stringer alone.

(2) On the basis of this stringer stress, determine the effective width of sheet acting with the stringer. This changes the radius of gyration ρ of the column.

(3) Determine the allowable column stress for the new section composed of the stringer and effective sheet acting with it.

(4) Determine new effective width as in step (2) and repeat procedure.

An example will be used to illustrate the method.

EXAMPLE 9.6. Determine the ultimate load carried by each stringer and effective 24ST sheet adjacent to it for the panel shown in Figure 9.13 if the stringer has a channel section similar to the one analyzed in Examples 9.3 and 9.5 and if

$$b = 3.75 \text{ in} \qquad A_{st} = 0.0540 \text{ in}^2$$
$$t_s = 0.032 \text{ in} \qquad I_{st} = 0.00137 \text{ in}^4$$
$$L = 12 \text{ in} \qquad \bar{y}_{st} = 0.155 \text{ in}$$
$$\rho_{st} = 0.159 \text{ in}$$

Solution. Assume an end fixity coefficient $C = 2$. The column equation for the stringer is given in Example 9.5 as

$$F_c = 26,800 - 0.868 \left(\frac{L}{\rho}\right)^2$$

For the stringer alone $\dfrac{L}{\rho} = \dfrac{12}{0.159} = 75.5$; therefore,

$$F_c = 26,800 - 0.868(75.5)^2 = 21,900 \text{ psi}$$

The buckling stress for the sheet is

$$f_{cr} = KE \left(\frac{t}{b}\right)^2$$

and, since the stringer is an open section and torsionally weak, the edge conditions of the sheet at the stringer will be assumed guided so that $K = 3.6$. Then

$$f_{cr} = 3.6 \times 10.5 \times 10^6 \left(\frac{0.032}{3.75}\right)^2 = 2,760 \text{ psi}$$

The effective width of sheet from Equation 9.17 is

$$l = 2w = b \sqrt[3]{\frac{f_{cr}}{f_c}} = 3.75 \sqrt[3]{\frac{2,760}{21,900}}$$
$$= 1.880 \text{ in}$$

The new column section is therefore composed of the stringer with 1.880 inches of sheet. Figure 9.14 shows the relation between the radius of gyration of any stringer to the radius of gyration of the stringer plus
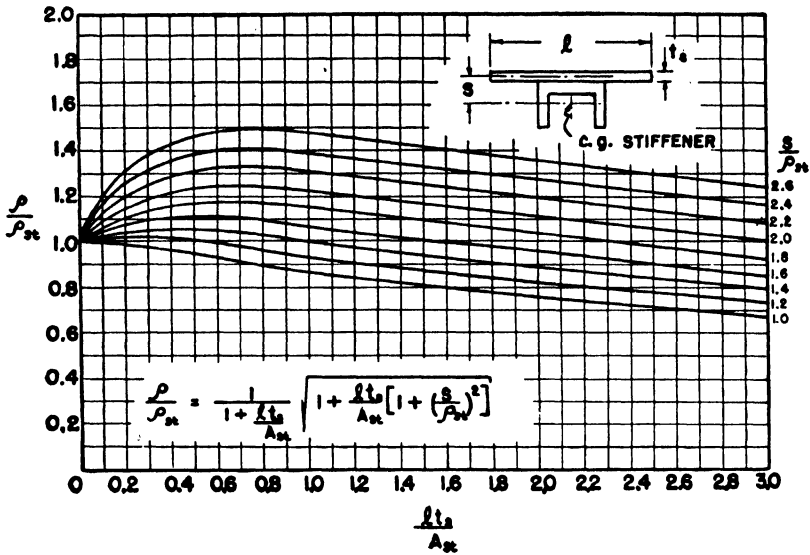
Fig. 9.14. Determination of ρ/ρ_{st}.

the effective sheet acting with it. By using these curves when

$$S = \bar{y}_{st} + \frac{t_s}{2} = 0.155 + \frac{0.032}{2} = 0.171 \text{ in}$$

$$\frac{S}{\rho_{st}} = \frac{0.171}{0.159} = 1.075$$

$$\frac{lt_s}{A_{st}} = \frac{1.880 \times 0.032}{0.0540} = 1.11$$

then

$$\frac{\rho_1}{\rho_{st}} = 0.88$$

and

$$\rho_1 = 0.159 \times 0.88 = 0.140 \text{ in}$$

The new $\dfrac{L}{\rho_1}$ is

$$\frac{L}{\rho_1} = \frac{12}{0.140} = 85.7$$

and the column stress is

$$f_{st} = 26{,}800 - 0.868(85.7)^2 = 20{,}400 \text{ psi}$$

The effective width is therefore

$$l = 3.75 \sqrt[3]{\frac{2{,}760}{20{,}400}} = 1.93 \text{ in}$$

By repeating previous steps,

$$\frac{\rho_2}{\rho_{st}} = 0.875$$

$$\rho_2 = 0.139$$

$$\frac{L}{\rho_2} = 86.3$$

$$f_{st} = 26,800 - 0.868(86.3)^2 = 20,300 \text{ psi}$$

Since the last step did not materially change the allowable column stress, the process can be stopped. The load on each stringer and adjacent sheet is therefore

$$P = f_{st}(A_{st} + lt_s)$$
$$= 20,300(0.054 + 1.93 \times 0.032) = 2,350 \text{ lb}$$

9.12 Inter-rivet buckling. It has been assumed that there is a continuous line of attachment between the stringers and sheet for the panels analyzed in the preceding article. When rivets are used for the attachment, this assumption is true only as long as the sheet does not buckle between rivets. Some idea of the rivet spacing required to prevent sheet buckling between rivets can be determined from a consideration of the column action of the sheet between rivets.

The sheet adjacent to the stringer and the stringer act together and have the same strain. The stress in the sheet and stringer is the same as long as the sheet and the stringer are the same material and the sheet does not buckle between rivets. If buckling between rivets occurs, then the sheet does not take its share of the increasing load as the strain is increased. If we consider the sheet between rivets as a column of unit width and of length equal to the rivet spacing, then if the sheet buckles at a stringer stress f_{st} we can give the relation by

$$f_{st} = \frac{C\pi^2 E_r}{\left(\dfrac{d}{\rho}\right)^2}$$

where d = rivet spacing (in)

$$\rho = \sqrt{\frac{I}{A}} = \sqrt{\frac{t_s^2}{12}} \text{ (in)}$$

C = end fixity coefficient of sheet at rivets = 4, since sheet cannot rotate at rivets.

Therefore, $$f_{st} = \frac{4\pi^2 E_r}{12d^2} t_s^2$$

and $$d = 1.81 t_s \sqrt{\frac{E_r}{f_{st}}}$$

If the stringer stress is less than the proportional limit, then $E_r = E$. If the stringer stress is greater than the proportional limit, the reduced modulus E_r must be used.

If we assume that the stringer stress of 20,300 psi as determined in Example 9.6 is sufficiently close to the proportional limit, then $E = 10.5 \times 10^6$ psi can be used. The maximum distance between rivets if inter-rivet buckling is to be prevented is

$$d = 1.81 \times 0.032 \sqrt{\frac{10.5 \times 10^6}{20,300}} = 1.32 \text{ in}$$

Fischel, in the reference given at the end of the chapter, describes how the ultimate load for a sheet-stringer panel can be estimated when inter-rivet buckling occurs.

9.13 Additional considerations of sheet-stringer panels. Stringers with open sections are torsionally weak and do not offer much restraint to the tendency for the sheet to rotate as it buckles. The probable mode of deformation for a sheet-stringer panel with open-section stringers

(a)

(b)

Fig. 9.15. Panels with Open-Section and Closed-Section Stringers.

is shown in Figure 9.15(a). For this reason when we calculate the buckling stress for the sheet used in determining the effective width, we assume that the sheet has guided edge conditions at the stringers, and that an edge fixity coefficient of $K = 3.6$ is used. Closed-section stringers or stringers that form a closed section when attached to the sheet are torsionally rigid and tend to restrain the sheet from rotating at the stringers, as shown in Figure 9.15(b). For this reason it is better probably to determine the buckling stress of the sheet on the basis that the edges attached to the stringers are restrained from rotating and are therefore fixed. The edge fixity coefficient for this case, as determined from Figure 9.5(2), is $K = 6.3$.

Sometimes the proportions of the sheet-stringer panel are such that the effective widths of two adjacent stringers overlap. In such a case it is apparent that the entire sheet between the stringers is effective in carrying the stringer stress.

It is difficult sometimes to correlate test data for sheet-stringer panels with calculated values because of the unknown fixity conditions at the ends of the panel where the loads are applied. Measured stresses on panels with flat milled edges resting against the flat surfaces of the testing machine crossheads indicate that a fixity factor of about 3 gives good agreement between test and calculated values. Panels supported at the ends by ribs or other elastic structures are not as rigidly supported as in the test machine. In such cases a fixity factor of 2 sometimes is used.

The analyses of the panels in the foregoing articles have been made on the assumption that the stress-strain characteristics of the stringer and sheet are the same. This is not always the case, however, since a variation in the materials may mean that the proportional limit of the sheet is reached before the proportional limit of the stringer. The two materials then have different compressive load-carrying characteristics after one of the materials has reached the proportional limit. This problem is considered in Fischel's article referred to at the end of the chapter.

Nothing has been said about curved sheet-stringer panels. The analysis of a curved panel is most difficult because the curvature of the sheet tends to support the stringer by the tangential tension or compression stresses in the sheet. The interaction of the sheet and stringer is very complicated, and an analysis of a curved panel cannot be considered here. The student is referred to articles on the subject.

It should be apparent from the analyses of sheet and sheet-stringer panels and from the discussions, that there is still much to be learned concerning the behavior of such structures. It should be emphasized that the analysis for any given structure can be very inaccurate so that whenever possible tests should be made to verify the analysis.

Problems

9.1. A flat aluminum 17ST sheet 10 inches wide, 20 inches long, and 0.032 inches thick has all edges guided. Compressive loads are applied to the 10-inch sides. Determine

(1) buckling stress
(2) number of buckling waves lengthwise
(3) load carried by the sheet if the stress at the two supported unloaded edges is 25,000 psi.

9.2. A 24ST clad sheet 3 inches wide, 10 inches long, and 0.064 inches thick has the 3-inch edges guided and the 10-inch edges fixed. Determine the buckling load for the sheet if the 3-inch edges carry a compressive load.

9.3. Determine the crippling stress for the 24SRT Z section shown in Figure 9.16.

9.4. Determine the crippling stress for the Z section of Problem 9.3, if the $\frac{1}{4}$-inch tips on the legs are missing.
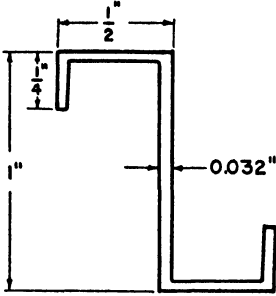
Fig. 9.16. Z Section.
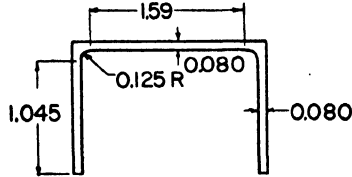
TOTAL AREA = 0.354 in.²

Fig. 9.17. Channel Extrusion.

9.5. For the 24ST extrusion shown in Figure 9.17, determine

(1) crippling stress
(2) allowable load for a section of short length
(3) allowable column stress for a column 16 inches long having an end fixity coefficient of 2.

9.6. Determine the ultimate load for a 24ST curved panel 3 inches wide, 12 inches long, 0.020 inches thick, with a radius of curvature of 20 inches, assuming that all edges are guided and the long edges fail by yielding. The 3-inch sides carry a compressive load.
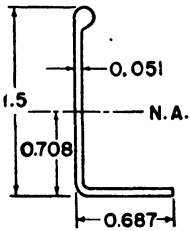
$A_{st} = 0.150$ in.²

$\rho_{st} = 0.565$ in.

Fig. 9.18. Bulb Angle Stiffener.

9.7. A 24ST sheet-stringer panel was tested, and the strain of the stringer at failure was 0.0019 in/in. If the thickness of the sheet was 0.032 inches and it was attached to torsionally weak stringers spaced at 6 inches, determine

(1) area of sheet carrying same stress as stringers
(2) maximum allowable rivet spacing to prevent inter-rivet buckling.

9.8. 24ST stiffeners with section shown in Figure 9.18 are attached at 5-inch intervals to 0.040-inch 24ST sheet. If the sheet-stiffener panel is 16 inches long, determine the allowable load for each stiffener with its effective sheet. The crippling stress for the stiffener alone is 30,500 psi. Assume an end fixity $C = 2$.

9.9. A hat-stiffened panel is shown in Figure 9.19. If the hat stiffeners are
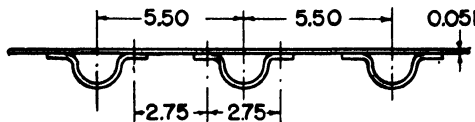
Fig. 9.19. Hat-Stiffened Panel.

24ST clad with a crippling stress of 43,900 psi, a moment of inertia = 0.218 in^4, an area of 0.280 in^2, and a center of gravity located 0.466 inches from the flat sides, determine the allowable stress for a panel 20 inches long when the skin is 0.051 24ST clad sheet. Assume an end fixity $C = 2$.

References

Ebner, H., "The Strength of Shell Bodies—Theory and Practice." NACA Tech. Memo. No. 838, September 1937.

Fischel, J. R., "Effective Widths in Stiffened Panels under Compression." *Journal of Aeronautical Sciences*, Vol. 7, No. 5, March 1940.

Hoff, N. J., "Instability of Monocoque Structures in Pure Bending." *Journal of Royal Aeronautical Sciences*, April 1938.

Hoff, N. J., "A Note on Inelastic Buckling." *Journal of Aeronautical Sciences*, Vol. 11, No. 2, April 1944.

Holt, M., and J. R. Leary, "The Column Strength of Aluminum Alloy 75ST Extruded Shapes." NACA Tech. Note, No. 1004, January 1946.

Howland, L., "Effect of Rivet Spacing on Stiffened Thin Sheet in Compression." *Journal of Aeronautical Sciences*, Vol. 3, No. 12, October 1936.

Lundguist, E. E., "Comparison of Three Methods for Calculating the Compressive Strength of Flat and Slightly Curved Sheet and Stiffener Combinations." NACA Tech. Note, No. 455, March 1933.

Marguerre, K., "The Apparent Width of the Plate in Compression." NACA Tech. Memo. No. 833, July 1937.

Timoshenko, S., *Theory of Elastic Stability*. McGraw-Hill, 1936.

Von Kármán, T., E. E. Sechler, and L. H. Donnel, "The Strength of Thin Plates in Compression." ASME Trans., Vol. 54, No. 2, January 1932.

Part IV
STRESS ANALYSIS

CHAPTER 10

Bending

●●●

10.1 Introduction. All previous analyses, with the possible exception of some of the buckling problems, have been concerned with the forces and moments acting at various sections of the structure. A study will be made now of the details of the distribution of the forces and moments on the sections of the structure in order to correlate them with the strength properties of the material.

Whereas before, our interest was focused on the overall sections of the structure, now we will be concerned with the conditions at each point of the sections. The conditions at a point in a material are usually given in terms of stress or the force per unit area, and therefore the analytical procedures are called *stress analyses*.

Since bending is an important consideration in designing a structure which involves the bending moments, the associated stress conditions will be investigated in the following articles.

10.2 Bending stress. The bending stress distribution on the cross section of a straight homogeneous elastic beam was discussed briefly in Article 4.7. In this case the strain distribution is linear, and the stress at any point a distance u from the line of zero strain is

$$f = E \frac{u}{R}$$

where according to Equation 4.17

$$\frac{1}{R} = \frac{M}{EI}$$

Therefore,

$$f = \frac{Mu}{I}$$

In most texts the symbol y is used in place of u. This was not done before because of the possible confusion with the deflection which was denoted by y. Since there is not much possibility of confusion now, the bending stress will be specified as

$$f = \frac{My}{I} \tag{10.1}$$

where f = bending stress (psi)
$\quad M$ = bending moment (lb in)
$\quad y$ = distance from neutral axis to point where stress is to be determined (y positive downward) (in)
$\quad E$ = modulus of elasticity (psi)
$\quad I$ = moment of inertia of cross section about centroidal axis (in⁴).

The bending stress distribution on the cross section of a beam is shown in Figure 10.1. It should be noted that, when the moment is positive and y is positive, the stress is positive, which denotes tension.

The moment of the forces acting on the cross section of the beam must be equal to the applied moment for equilibrium. This is illustrated best by considering a small element of the area of the cross section of depth Δy and breadth b as illustrated in Figure 10.1(a). The force acting on this area is

$$\Delta P = fb\, \Delta y = \frac{My}{I}\, b\, \Delta y = \frac{M}{I}\, y\, \Delta A$$

The effect of the stresses therefore can be replaced by forces acting on small increments of areas, as shown in Figure 10.1(b). Since in this case
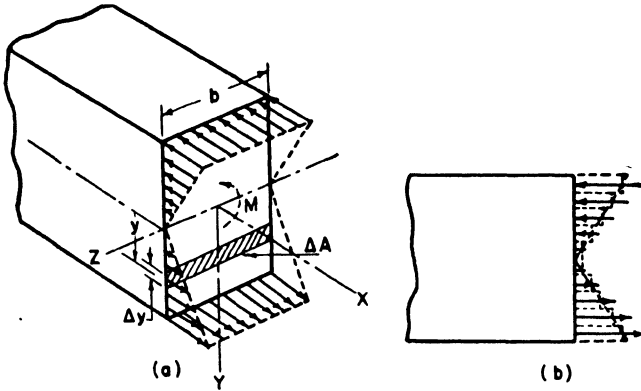
Fig. 10.1. Bending Stresses. (a) Bending stress distribution; (b) forces acting on elements of area.

only a pure bending moment is considered, there is no axial resultant force and therefore the sum of the forces on the section must equal zero.

$$\sum \Delta P = 0 = \frac{M}{I} \sum y\, \Delta A$$

or in the limit $\displaystyle\int_A y\, dA = 0$. This condition is satisfied when the axis from which y is measured is a centroidal axis.

The moment of the internal forces should equal the applied moment or

$$M = \sum y\, \Delta P = \frac{M}{I} \sum y^2\, \Delta A$$
$$= \frac{M}{I} \int_A y^2\, dA$$

but $\displaystyle\int_A y^2\, dA = I$ by definition so that

$$M = M$$

It is convenient sometimes to use the concept of the forces acting on the elements of areas in order to approximate the values of the bending stresses. For example, consider a beam with heavy flanges and a thin web, as shown in Figure 10.2. Since the web is thin, the forces acting

(a)
BENDING STRESS DISTRIBUTION

(b)
FLANGE FORCES
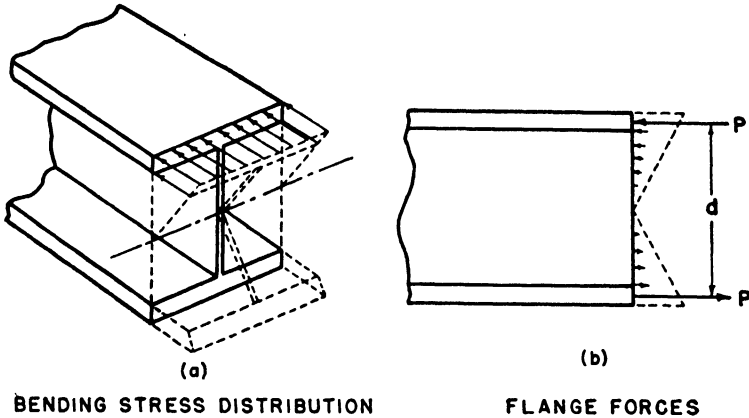
Fig. 10.2. Flanged Beam.

on the web are small as compared with the flange forces as shown in Figure 10.2(b). In this case

$$M \doteq Pd$$

where d = distance between centroids of flanges (in)
P = force on flange (lb)

and $$f \doteq \frac{P}{A} = \frac{M}{Ad} \tag{10.2}$$

where A = area of flange (in²)
f = flange stress (psi).

10.3 Unsymmetrical bending. It has been assumed in the previous analyses of bending stresses that the bending moment is applied about a centroidal axis that is a *principal* axis of the cross section. The bending moment is not always applied in this manner; and, when it is not, additional considerations must be made to determine the bending stresses. To illustrate the difficulty, consider the four-flange beam shown in Figure 10.3(a) with a bending moment applied for which the direction is to be interpreted by the right-hand rule. It will be assumed that only the

flanges resist the bending moment. The load on flange number one is therefore

$$P_1 = \frac{M}{I_z} y_1 A_1$$

and a similar expression is valid for the other flanges. Apparently, flanges 1 and 2 are in tension and flanges 3 and 4 are in compression. If the moments of the flange loads are determined about the y axis, we find

$$M_y = P_1 z_1 + P_2 z_2 + P_3 z_3 + P_4 z_4$$
$$= \frac{M}{I_z} (y_1 z_1 A_1 + y_2 z_2 A_2 + y_3 z_3 A_3 + y_4 z_4 A_4)$$

However, there is no applied moment about the y axis; therefore, this

(a)
MOMENTS ABOUT
SKEW AXES

(b)
MOMENTS ABOUT
PRINCIPAL AXES
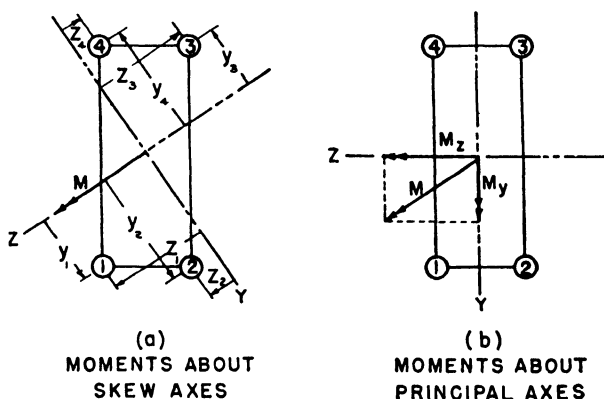
Fig. 10.3. Unsymmetrical Bending of Four-Flange Beam.

method is not correct unless the moment is applied about axes for which

$$y_1 z_1 A_1 + y_2 z_2 A_2 + y_3 z_3 A_3 + y_4 z_4 A_4 = 0$$

Such a set of axes always can be determined. The sum

$$\sum_A yz \, \Delta A \text{ or } \int_A yz \, dA$$

is called the *product of inertia* and denoted by I_{yz}. The results of previous analyses can be used when the moments are applied about axes for which the product of inertia is zero. Such axes are called *principal axes*. Any two perpendicular centroidal axes of symmetry are principal axes.

To illustrate how the difficulties can be overcome in this case, suppose for simplicity that the flange areas are equal and that the y and z axes are rotated to the position shown in Figure 10.3(b). It can be shown easily that these are principal axes because for every area a given positive distance to one side of the axes, there is a similar area a negative distance to the other side of the axes. If we remember that, because of symmetry,

$y_1 = y_2 = -y_3 = -y_4$ and $z_1 = -z_2 = -z_3 = z_4$ and $A_1 = A_2 = A_3$ $= A_4$, then

$$\Sigma yz \, \Delta A = y_1 z_1 A_1 + y_2 z_2 A_2 + y_3 z_3 A_3 + y_4 z_4 A_4 = 0$$

A moment applied about one of these axes will not induce a moment about the axis perpendicular to it. It is convenient therefore to resolve the moment M into two components M_z and M_y. The stress at flange 1, due to M_z, is therefore

$$f_1' = \frac{M_z y_1}{I_z}$$

and the stress at flange 1, due to the moment about the y axis, is

$$f_1'' = -\frac{M_y z_1}{I_y}$$

The stress on flange 1 is therefore

$$f_1 = f_1' + f_1'' = \frac{M_z y_1}{I_z} - \frac{M_y z_1}{I_y} \tag{10.3}$$

To illustrate the use of Equation 10.3 consider a beam of rectangular cross section with bending moment M applied as shown in Figure 10.4.
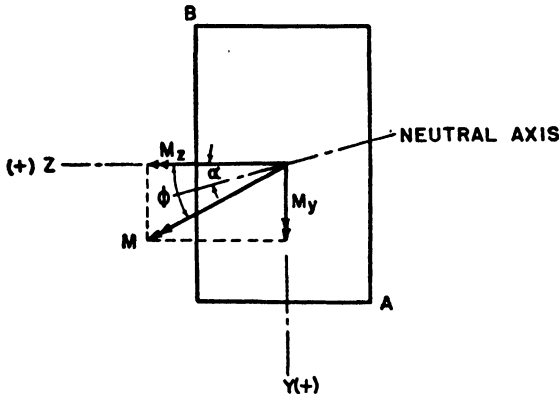
Fig. 10.4. Unsymmetrical Bending of Rectangular Section.

Because of symmetry the y and z axes are principal axes. The components of the moment in the y and z directions are

$$M_z = M \cos \phi$$
$$M_y = M \sin \phi$$

Then according to Equation 10.3 the stress at any point yz is

$$f = \frac{M_z y}{I_z} - \frac{M_y z}{I_y} \tag{10.4}$$

$$= M \left(y \frac{\cos \phi}{I_z} - z \frac{\sin \phi}{I_y} \right)$$

The stress distribution is composed of two parts: one, a stress distribution due to M_z as shown in Figure 10.1(a); the other, a stress distribution due to M_y which causes a similar condition about the y axis as M_z does about the z axis.

The line along which the stress is zero is called the *neutral axis*. The neutral axis can be determined easily by equating the stress given by Equation 10.4 to zero and solving for the line in terms of y and z. Thus,

$$f = 0 = \frac{M_z y}{I_z} - \frac{M_y z}{I_y}$$

$$\frac{y}{z} = \frac{M_y}{I_y} \frac{I_z}{M_z}$$

This determines a straight line through the center of gravity of the section which makes an angle α measured counterclockwise with the positive z axis where

$$\tan \alpha = \frac{y}{z} = \frac{M_y}{I_y} \frac{I_z}{M_z} \tag{10.5}$$

It is necessary to know the location of the neutral axis in order to determine the fibers with the highest stresses. The most stressed fiber will be farthest from the neutral axis. In the case of the rectangular section shown in Figure 10.4, the highest tensile stress will be at A and the highest compressive stress at B.

It is difficult or inconvenient sometimes to determine the principal axes of a section so that Equation 10.4 may be used directly. The stresses in terms of the moment of inertia about any two perpendicular centroidal axes and the product of inertia may be determined by transforming the expression for stress in terms of the principal axes to the corresponding expression in terms of axes which are not principal axes. If this is done, then

$$f = \frac{(M_z I_y + M_y I_{yz})}{I_y I_z - (I_{yz})^2} y - \frac{(M_y I_z + M_z I_{yz})}{I_y I_z - (I_{yz})^2} z \tag{10.6}$$

The vectors representing positive moments are taken in the positive y and z directions as indicated in Figure 10.4. The angle of the neutral axis measured counterclockwise from the positive z direction is given by

$$\tan \alpha = \frac{M_y I_z + M_z I_{yz}}{M_z I_y + M_y I_{yz}} \tag{10.7}$$

EXAMPLE 10.1. Determine the maximum bending stress for an aluminum beam with a Z section as shown in Figure 10.5 if the bending moment about the z axis is 3600 lb in and $d = 1\frac{3}{4}$ in, $b = 1\frac{3}{4}$ in, $t = \frac{3}{16}$ in.

Solution. The solution will be made by two methods; one in which the positions of the principal axes are not known and the other in which the principal axes' positions are known.

The moment of inertia of the section about the z axis is determined by summing the moments of inertia of the component rectangles consisting of the top and bottom flange of length b and thickness t, and the web of length $d - 2t$ and thickness t. The moments of inertia of the flanges about their own centroidal axes will be neglected since they are small.
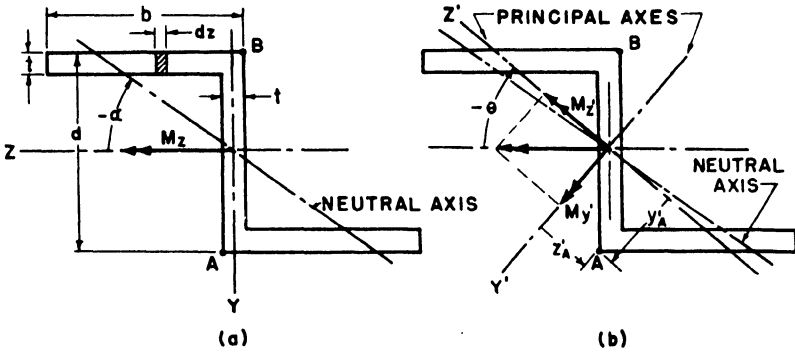
Fig. 10.5. Unsymmetrical Bending of Z Section.

$$I_z = 2bt\left(\frac{d-t}{2}\right)^2 + \frac{t}{12}(d-2t)^3$$

$$= 2 \times 1.75 \times 0.188 \times \left(\frac{1.562}{2}\right)^2 + \frac{0.188}{12}(1.375)^3 = 0.442 \text{ in}^4$$

$$I_y = \frac{2t}{12}b^3 + 2bt\left(\frac{b-t}{2}\right)^2$$

$$= \frac{0.188 \times (1.75)^3}{12} + 1.75 \times 0.188 \times \left(\frac{1.562}{2}\right)^2 = 0.569 \text{ in}^4$$

The product of inertia will be determined from the definition

$$I_{yz} = \int_A yz\, dA$$

Since the web is symmetrical about the y and z axes, it will have no product of inertia. The flanges will be taken as rectangles of length $b - t$ and thickness t. If we take an element of area in the upper flange of length dz and thickness t, then since the y distance for this flange is $-(d-t)/2 = -0.781$ and $+0.781$ for the lower flange

$$I_{yz} = \int_{\frac{t}{2}}^{b-\frac{t}{2}} -0.781zt\, dz + \int_{b-\frac{t}{2}}^{\frac{t}{2}} 0.781zt\, dz$$

$$= -2\int_{\frac{t}{2}}^{b-\frac{t}{2}} (0.781)(0.188)z\, dz = -0.401 \text{ in}^4$$

The location of the neutral axis is given by Equation 10.7. For the case $M_y = 0$

$$\tan \alpha = \frac{I_{yz}}{I_y} = -\frac{0.401}{0.569} = -0.705$$

$$\alpha = -35.2°$$

The axis is shown in the figure. The most stressed fibers are therefore at A and B. The coordinates of point A are $z = +t/2 = 0.094$ inches and $y = +d/2 = 0.875$ inches. Therefore, since $M_y = 0$,

$$f_A = \frac{M_z I_y y}{I_y I_z - (I_{yz})^2} - \frac{M_z I_{yz} z}{I_z I_y - (I_{yz})^2}$$

$$= \frac{3600[(0.569 \times 0.875) + (0.401 \times 0.094)]}{(0.569 \times 0.442) - (0.401)^2} = 21,250 \text{ psi (tension)}$$

The stress at B will have the same value in compression.

The second method of solution involves the use of the principal axes. The moments of inertia about the principal axes of a section in terms of the moments of inertia about any other two perpendicular axes with origin at the centroid are given by

$$I_{\substack{z' \\ y'}} = \frac{I_z + I_y}{2} \pm \sqrt{\left(\frac{I_z - I_y}{2}\right)^2 + I_{yz}^2} \qquad (10.8)$$

where the angle between the z axis and the principal axis measured counterclockwise from the z axis is

$$\tan 2\theta = \frac{2I_{yz}}{I_y - I_z} \qquad (10.9)$$

If the moment of inertia about the z axis is greater than that about the y axis, then the angle θ is measured to the principal axis about which the moment of inertia is a maximum.

Substitution into Equations 10.8 and 10.9 of the values for I_z, I_y, and I_{yz} gives

$$I_{z'} = 0.0996 \text{ in}^4$$
$$I_{y'} = 0.911 \text{ in}^4$$
$$\theta = -40.5°$$

In order to determine the stress at A, the coordinates of point A in terms of the new axes y' and z' must be known. These values and the components of the moment along the y' and z' axes are determined by trigonometry and found to be

$$M_{z'} = 2740 \text{ lb in}$$
$$M_{y'} = 2340 \text{ lb in}$$
$$z'_A = -0.496 \text{ in}$$
$$y'_A = 0.726 \text{ in.}$$

The stress at point A according to Equation 10.3 is

$$f = \frac{M_{z'}y'}{I_{z'}} - \frac{M_{y'}z'}{I_{y'}}$$

$$= \frac{2740 \times 0.726}{0.0996} + \frac{2340 \times 0.496}{0.911} = 21{,}250 \text{ psi}$$

It is apparent that the second method is more difficult to use if the location of the principal axes cannot be determined by inspection. The product of inertia must be determined for both methods, and the second method requires some additional calculations.

10.4 Nonlinear stress distribution. The condition of linear stress distribution in bending depends on two assumptions

(a) linear strain distribution
(b) stress proportional to strain.

These assumptions are valid for the straight homogeneous elastic beams analyzed previously but there are other cases of importance in design where one or both of these assumptions cannot be made, such as for

(1) composite beams
(2) inelastic bending
(3) curved beams.

Each of these will be discussed.

(1) *Composite beams.* A beam with a section composed of two or more different materials is called a *composite beam.* Plane sections remain plane during bending; and, if the beam is initially straight, the strain distribution will be linear. However, since the modulus of elasticity may vary from point to point on the section due to the variation in material, the stress distribution will be nonlinear.

Consider a beam with cross section as shown in Figure 10.6(a) composed of a plastic core to which is bounded an aluminum sheet on the bottom surface. Since the plastic is more flexible than the aluminum, it is apparent that if the plastic is replaced by aluminum so as to give the equivalent resistance to bending, a smaller area of aluminum is required than the original area of the plastic. Figure 10.6(b) shows the plastic replaced by aluminum; this section is called the *transformed section.* This transformed section must fulfill the conditions of the original section, namely that the strain distribution be linear and that the bending moment be the same for the original and the transformed section. In order to meet these requirements the strain at the same distance from the neutral axes of the two sections must be equal and the force acting on an element of area must remain the same in magnitude and distance from the neutral axis. Using the subscript 1 for referring to the original

section and subscript 2 for the transformed section, then for the region of the plastic, we obtain

$$y \, \Delta P_1 = y \, \Delta P_2$$

$$yE_1 eb_1 \, \Delta y = yE_2 eb_2 \, \Delta y$$

$$b_2 = \frac{E_1}{E_2} b_1 = nb_1 \tag{10.10}$$

where $n = \dfrac{\text{modulus of elasticity of plastic}}{\text{modulus of elasticity of aluminum}}$

The problem thus is reduced to determining the stresses in a homogeneous section. It should be remembered, however, that after the stress
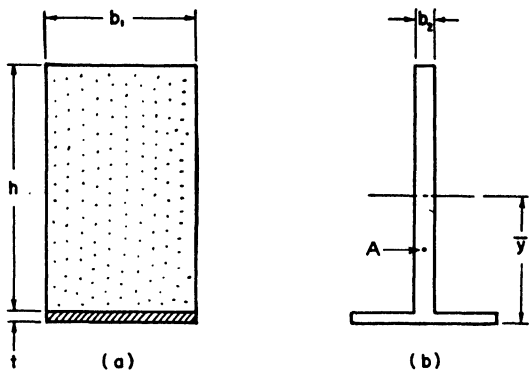
ORIGINAL SECTION   TRANSFORMED SECTION

Fig. 10.6. Composite Section.

is determined in the transformed section, say at point A, the stress in the original section corresponds to a stress in the plastic material. Since the strain at corresponding points of the two sections is the same, the stress in 2 must be multiplied by the ratio n to determine the stress in 1.

$$f_1 = nf_2 \tag{10.11}$$

for the region transformed.

ı EXAMPLE 10.2. Determine the maximum tension stress and compression stress in a section similar to that shown in Figure 10.6(a) if the beam is subjected to a bending moment of 10^5 lb in, $b = 5$ in, $h = 10$ in, and $t = 0.064$ in. The modulus of elasticity for the plastic is $E_p = 500,000$ psi and for the aluminum, $E_A = 10 \times 10^6$ psi. The moment is applied so as to produce compression in the top fiber.

Solution. $n = \dfrac{500,000}{10 \times 10^6} = 0.05$

$$b_2 = nb_1 = 0.05 \times 5 = 0.25 \text{ in}$$

The centroidal axis of the transformed section is obtained by taking the moments of the areas about the base.

$$\bar{y} = \frac{(10 \times 0.25)(5 + 0.064) + (5 \times 0.064)0.032}{(10 \times 0.25) + (5 \times 0.064)} = 4.49 \text{ in}$$

The moment of inertia is

$$I = \frac{(10)^3 \times 0.25}{12} + (5 - 4.49)^2(10 \times 0.25) + (4.49 - 0.032)^2(5 \times 0.064)$$
$$= 27.84 \text{ in}^4$$

The maximum tensile stress is

$$f_t = \frac{Mc_t}{I} = \frac{10^5 \times 4.49}{27.84} = 16,100 \text{ psi}$$

The maximum compressive stress is

$$f_c = n\frac{Mc_c}{I} = \frac{0.05 \times 10^5 \times (10.064 - 4.49)}{27.84} = 1000 \text{ psi}$$

(2) *Inelastic bending.* Another example of nonlinear stress distribution in bending occurs when the stress at any point of the cross section of the beam exceeds the proportional limit of the material. Thus, although the strain distribution is linear, the stress is not directly proportional to the strain so that the stress distribution is nonlinear. This is called *inelastic bending* and is important in determining the moment carried by a beam when the stresses are greater than the proportional limit.

For the beam with rectangular cross section shown in Figure 10.7 assume that the strain distribution is linear. Suppose the strain at point a on the cross section corresponds to the strain oa on the stress-strain diagram of the material. The stress corresponding to this strain is greater than the proportional limit of the material and is denoted by f_a. The stress at each point therefore can be determined, and the shape of the stress distribution will be similar to the shape of the stress-strain curve.

The same conditions of equilibrium must apply for the case of inelastic bending as for ordinary bending; namely, the axial load must be zero

$$\int_A f \, dA = 0$$

and the moment of the stresses must equal the applied moment

$$\int_A fy \, dA = M$$

It is apparent that the stress is now a nonlinear function of y so that it is difficult to determine analytically the stress conditions to satisfy the

above relations.   Many schemes have been proposed for solving this difficulty, such as empirically expressing the stress as a function of strain. However, the method most commonly used for determining the moment to produce the ultimate stress of the material is the one which uses a quantity called the *bending modulus of rupture*.
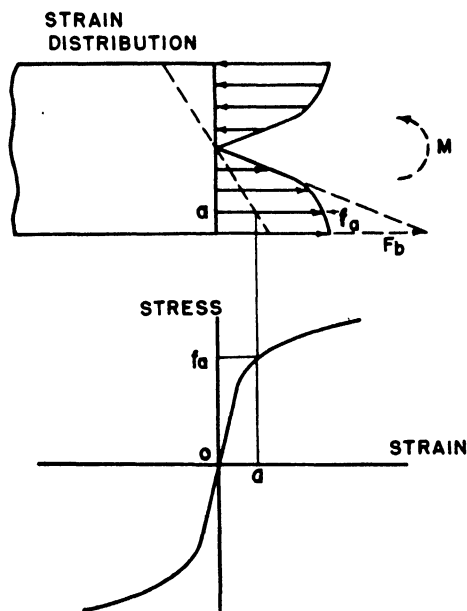
Fig. 10.7.   Inelastic Bending.

The bending modulus of rupture is a fictitious stress based on the assumption that the stress distribution is linear up to the rupture point. Hence, if the moment applied to the beam in Figure 10.7 is the ultimate moment, the bending modulus of rupture corresponds to the stress F_b. The bending modulus of rupture is determined experimentally for beams of various material and cross section, and the data usually is presented in the form of curves, as shown in Figure 10.8.   The ultimate bending moment that the beam can withstand is simply

$$M = F_b \frac{I}{c} \qquad (10.12)$$

For sections not subject to buckling the bending modulus of rupture is usually greater than the allowable ultimate stress.   Since tubes may fail by buckling if the walls are too thin, the bending modulus of rupture given in Figure 10.8 is less than the allowable ultimate stress of the material for high D/t ratios.

(3) *Bending of curved beams.* The stress distribution caused by the bending of a beam with an initial curvature such as the one shown in Figure 10.9 is nonlinear, and the departure from linearity increases as the curvature of the beam increases. Although plane sections of the beam remain plane during bending, the strain distribution is not linear because
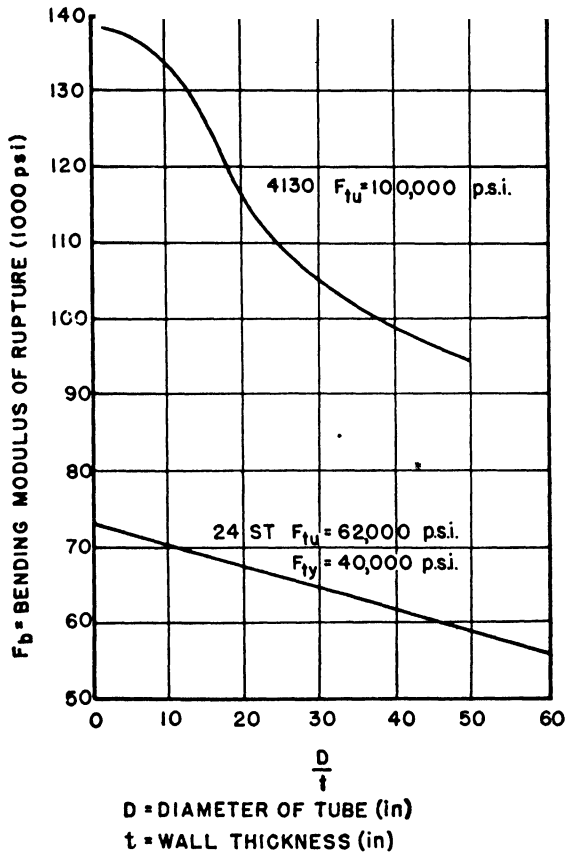
Fig. 10.8. Bending Modulus of Rupture for Circular Tubing. (Courtesy, Army-Navy Civil Committee on Aircraft Design Criteria of the Aeronautical Board.)

of the initial difference in length between the inner and outer fibers of the beam.

Since plane sections remain plane, the *elongation* of any point a distance y from the neutral axes is given by

$$\delta = K_1 y$$

The distance between two points on the original undistorted sections measured along a curve a distance y from the neutral axis is

$$L = (r - y)\theta$$

The strain is therefore

$$e = \frac{\delta}{L} = K_1\theta \frac{y}{r-y} = K_2 \frac{y}{r-y}$$

which corresponds to a hyperbolic distribution. If the proportional limit of the material is not exceeded, then the stress is proportional to the

DISPLACEMENT OF C
RELATIVE TO b

STRESS
DISTRIBUTION

CROSS-
SECTION
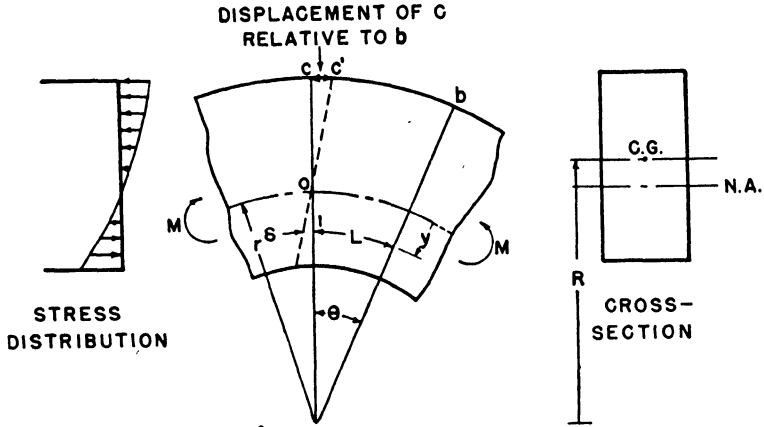
Fig. 10.9. Curved Beam.

strain and

$$f = Ee = EK_2 \frac{y}{r-y}$$

The two conditions of equilibrium, namely

$$\int_A f \, dA = 0$$

$$\int_A fy \, dA = M$$

are sufficient to locate the position of the neutral axis and to determine the stress in terms of the bending moment, the geometric properties of the cross section, and the radius of curvature of the neutral surface of the cross section. Since it is usually difficult to evaluate the stress in particular cases, the student is referred to the references for graphical and analytical methods. The general effect of the curvature, however, is to displace the neutral axis from the centroidal axis toward the center of curvature and to increase the stress on the concave side and decrease the stress on the convex side of the curve as compared with the corresponding stresses for a straight beam.

It is possible to express the stress in the curved beam in terms of the stress that would exist in the corresponding straight beam by multiplying the expression for the stress in the straight beam by a stress factor.

Thus,

$$f = K \frac{Mc}{I}$$ (10.13)

where K = curved beam stress factor
M = applied moment (lb in)
c = distance from centroidal axis to outer fiber (in)
I = moment of inertia of cross section about centroidal axis (in⁴).

Some stress factors K for the stresses at the extreme fibers of various sections are shown in Figure 10.10. It should be noticed that for beams for which the depth of the section is greater than 10 times the radius of curvature of the centroidal surface, the factor K is approximately unity,
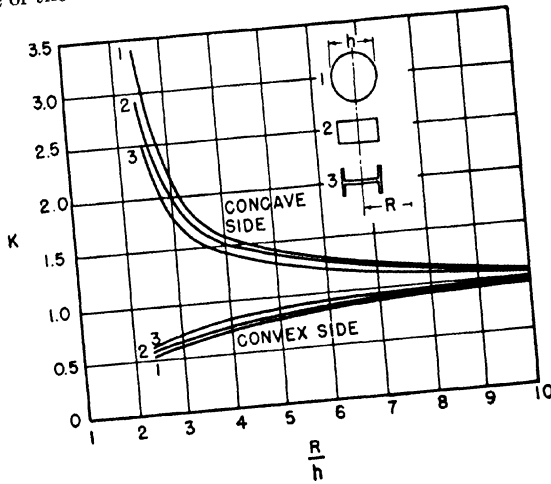
Fig. 10.10. Stress Factors for Curved Beams.

which indicates that the equation for the stress in straight beams can be used with little error.

10.5 Section efficiency. The designer sometimes is able to choose between various types of sections to use for a beam in bending. It is desirable therefore to know the relative efficiency of various sections so that the best may be selected. If the relative efficiency is defined as the comparative ability to resist bending moment for a given weight and maximum stress, then the efficiency will depend on the *section modulus* of the beam.

For a beam in which the stress distribution is linear, the maximum stress according to Equation 10.1 is

$$f = \frac{Mc}{I}$$

where c is the distance from the neutral axis to the most stressed fiber. The bending moment the beam can resist for a given stress is therefore

$$M = f\frac{I}{c} \tag{10.14}$$

where I/c is the section modulus. It is apparent therefore that the higher the section modulus the higher the bending moment for an allowable stress.

Figure 10.11 shows 3 sections having the same area and height. It is assumed that all the area for the flanged beam is concentrated at the

$$\frac{I}{c} = 1.00 \qquad \frac{I}{c} = 0.50 \qquad \frac{I}{c} = 0.33$$
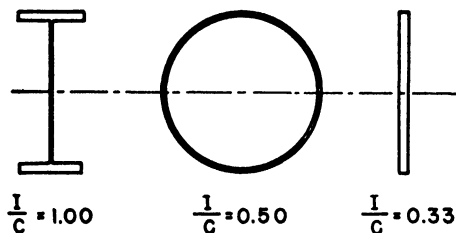
Fig. 10.11.   Section Moduli for Sections of Same Area.

flanges. If the section modulus for the flanged beam is unity, then the section modulus for the circular tube is 0.5 and the section modulus for the rectangle is 0.33. In other words, for the same bending stress and weight the flanged beam can resist twice as much moment as the tube and three times as much as the rectangle.

Other factors such as buckling and shear will modify the efficiencies of the sections. These factors will be discussed later.

Problems

10.1. A standard aluminum channel section has a depth from top to bottom flange of 7 inches and a moment of inertia about the axis of symmetry z of 21.27 in⁴. Determine the maximum tension stress if a bending moment of 100,000 lb in is applied about the z axis.

10.2. Assuming each flange of the channel section in Problem 10.1 is 2.09 inches wide and 0.210 inches thick, determine the tensile load carried by the flange.

10.3. A 5 × 3 aluminum angle section as shown in Figure 10.12 has a moment of 4000 lb in applied about the centroidal axis. Determine the location and magnitude of the maximum tension and compression stresses.

10.4. Determine the maximum tension and compression stresses in the box beam shown in Figure 10.13, assuming that only the angles are effective in resisting bending and that a moment of 144,000 lb in is acting about an axis parallel to the base of the box so as to produce compression in the bottom angles. The distances given are to the centroids of the angles. $A_1 = 2$ sq in, $A_2 = 1.5$ sq in, $A_3 = A_4 = 0.45$ sq in, $A_5 = 0.75$ sq in, $A_6 = 1.2$ sq in.
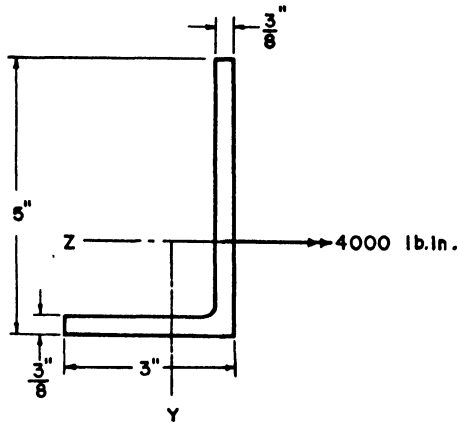
Fig. 10.12.   Angle Section.
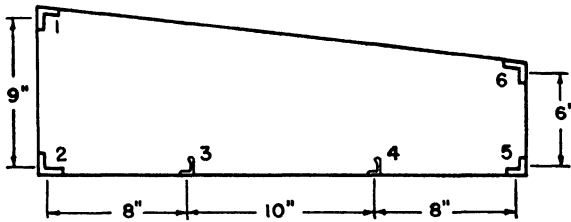
Fig. 10.13.   Box Section.

10.5. An aluminum beam with cross section as shown in Figure 10.14 acts as a guide for a flap extension mechanism. The flap mechanism rolls along the top of the bottom flange, and a steel surface is provided to prevent wear of the rollers on the aluminum beam. If the moment of inertia of the symmetrical aluminum beam section about its own horizontal centroidal axis is 12.26 in^4, the area is 2.92 sq in, and the other dimensions are as shown in the figure, determine the maximum tension stress in the steel and aluminum when the bending moment about the horizontal axis is 95,000 lb in so as to produce tension in the bottom fibers.

10.6. Compare the ultimate bending moment that a uniform straight beam with a rectangular cross section can carry, with the moment required to produce yielding in the same beam, assuming that the stress-strain curve of the material is linear up to the yield point and then that the stress is constant with strain until the ultimate strain is reached.

Fig. 10.14.   Composite Beam.

The strain at the yield point is to be considered negligible compared with the ultimate strain.
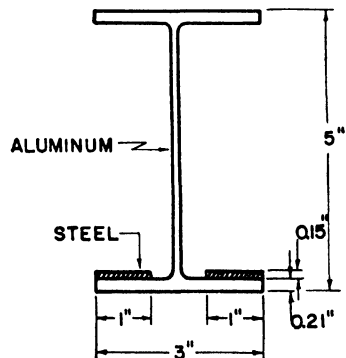
10.7. Compare the weight of the lightest standard 2-inch outside diameter tube of 4130 with the lightest standard 2-inch O.D. tube of 24ST if each is to carry an ultimate bending moment of 13,900 lb in. Use table on page 8-1 of the ANC-5 for determining standard sizes and weights.

10.8. Considering only bending stresses, determine the size of the section at A-A for a small margin of safety on yielding of the nose fork shown in Figure 10.15 if the limit load P is 960 pounds. The cross section at A-A is circular, and the material is 24ST with a yield strength of 43,000 psi.
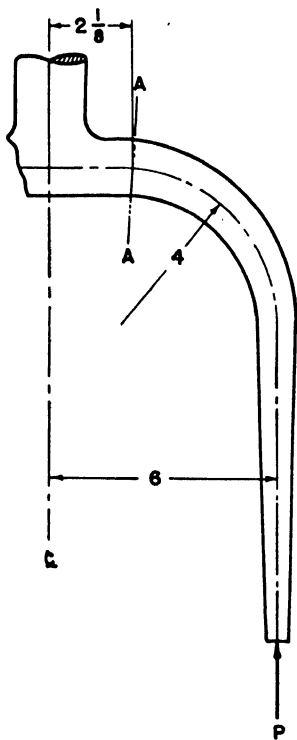
Fig. 10.15.   Nose-Wheel Fork.

References

Cozzone, Frank P., "Bending Strength in the Plastic Range." *Journal of Aeronautical Sciences*, Vol. 10, No. 5, May 1943.

Osgood, William R., "Plastic Bending Approximate Solution." *Journal of Aeronautical Sciences*, Vol. 12, No. 4, October 1945.

Perkins, H. C., "Stresses in Curved Bars." ASME Transactions, September–December 1931.

Shanley, F. R., *Basic Structures*. John Wiley and Sons, 1944.

Timoshenko, S., *Strength of Materials*, Part II: Advanced Theory and Problems. D. Van Nostrand Co., 1940.

Yachter, M., "A Note on Bending Beyond the Proportional Limit." *Journal of Aeronautical Sciences*, Vol. 12, No. 1, January 1945.

CHAPTER 11

Combined Bending and Shear

●●

11.1 Introduction. In the previous chapter the stresses in beams caused by bending moments were considered. However, in most structures the bending moments are usually accompanied by shear forces caused by the transverse forces acting on the beam. In fact, it has been shown that the rate of change of moment along a beam is equal to the shear force so that bending moments and shear forces usually occur simultaneously.

This chapter will be concerned with the distribution of the shear stresses on the cross sections of structural elements and the relation of these stresses with the shear forces producing them. The combination of bending stresses and shear stresses will be studied so as to be able to determine the effect of bending moments and shear forces on various types of structural members.

11.2 Shear stresses in webs. In order to start with the simplest type of shear-stress distribution, consider the portion of the symmetrical
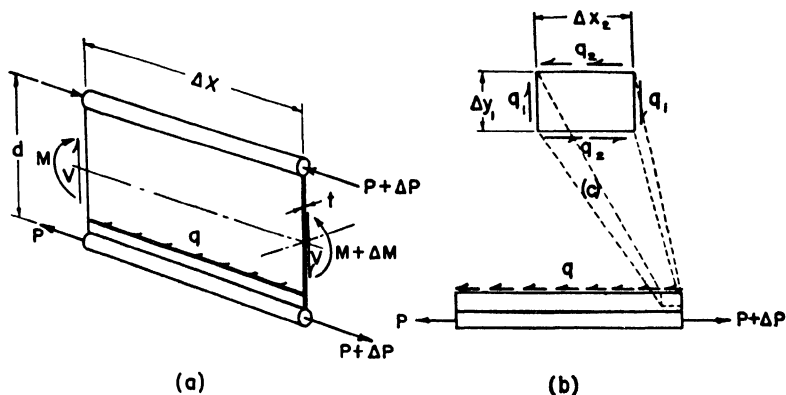
Fig. 11.1. Web Shear.

thin web beam with heavy flanges shown in Figure 11.1. Only a short portion of the beam of length Δx is shown. Since shear forces are present, the bending moments at the two sections Δx apart are not equal. The relation of shear force to bending moment has been shown previously to be

$$V = \frac{\Delta M}{\Delta x}$$

If we assume that the web will not buckle under the action of the forces

and that all the bending moment is carried by the flange forces, then the flange forces on the two ends of the bottom flange will differ by an amount ΔP. This unbalanced force is held in equilibrium by the horizontal shear force in the web adjacent to the flange. If the web is cut horizontally just above the flange, it is apparent that a horizontal force is needed for equilibrium. Assuming that the shear force in the web is uniformly distributed, we find then that the force per unit length of web is q; q is called the *shear flow*. For equilibrium

$$\Sigma F_x = 0 = P + \Delta P - P - q \Delta x$$

or

$$q = \frac{\Delta P}{\Delta x} = \frac{dP}{dx} \text{ in the limit} \tag{11.1}$$

where

$$q = \text{shear flow (lb/in)}.$$

In this case, the shear flow is the rate of change of the flange force with respect to x. The shear stress is simply the shear flow divided by the web thickness or

$$f_s = \frac{q}{t} \tag{11.2}$$

It is more useful usually to express the shear flow directly in terms of the shear force. The flange force is the flange stress times the area of the flange. Hence,

$$P = fA$$

But

$$f = \frac{My}{I}$$

so that

$$P = \frac{MyA}{I}$$

and

$$\frac{dP}{dx} = \frac{dM}{dx}\frac{yA}{I} = q$$

But

$$\frac{dM}{dx} = V$$

Therefore,

$$q = \frac{V}{I} yA \tag{11.3}$$

where
$y = $ distance from neutral axis to flange (in)
$V = $ shear force (lb)
$A = $ flange area (in²)
$I = $ moment of inertia of cross section (in⁴).

The question arises now of how this horizontal shear flow is related to the vertical shear flow. Consider the shear flows acting on a small rectangular element, as shown in Figure 11.1(c). In order to have equilibrium of the horizontal forces, it is apparent that the shear flow on the upper and lower sides of the element will have to be equal and opposite. The same reasoning applies to the two vertical sides. For

equilibrium of moments, the sum of the moments about any point, for example the lower right-hand corner, must be zero.

$$\Sigma M = 0 = -q_1 \, \Delta y_1 \, \Delta x_2 + q_2 \, \Delta x_2 \, \Delta y_1$$
$$q_1 = q_2$$

The shear flows on perpendicular planes at a point will always be equal in magnitude and will occur in equal and opposite pairs.

The sum of the forces due to the shear flows should be equal to the shear force producing them. Since we have assumed that the flange forces are the only axial forces acting, the horizontal and the vertical shear flows will be constant and

$$qd = V$$

Substituting the value of q from Equation 11.3, we obtain

$$\frac{V}{I} yAd = V$$

But for this case $y = \dfrac{d}{2}$ and $I = 2 \left(\dfrac{d}{2}\right)^2 A$, so that

$$V = V$$

The results of the analysis for the two-flange beam can be extended easily to a beam with many flanges or a beam with irregular cross section.
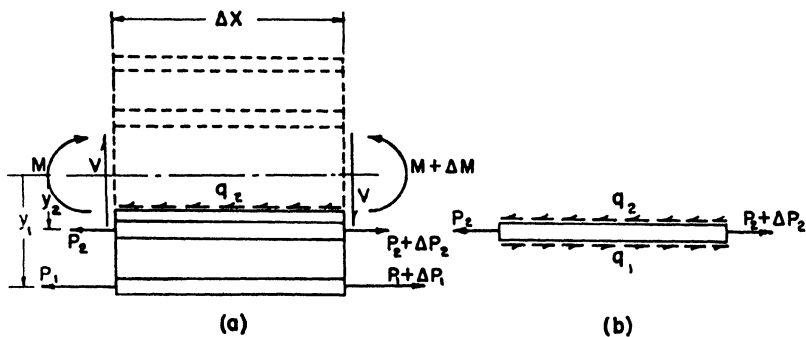
Fig. 11.2. Four-Flange Beam.

Consider the symmetrical four-flange beam shown in Figure 11.2. For equilibrium

$$q_2 \, \Delta x = \Delta P_1 + \Delta P_2$$

Then by direct analogy with the previous case, Equation 11.3 becomes

$$q_2 = \frac{V}{I} (y_1 A_1 + y_2 A_2)$$

In general, the shear flow adjacent to any flange n is

$$q_n = \frac{V}{I} \sum_{i=1}^{n} y_i A_i$$

The shear flow on a beam in which all the area is effective in resisting bending is therefore

$$q = \frac{V}{I} \int y \, dA \tag{11.4}$$

where $\int y \, dA$ is the moment of the area about the neutral axis of all the areas from the outside fiber of the beam to the point where the shear flow is to be determined.

I-BEAM   **SHEAR FLOW DISTRIBUTION**

IN WEB
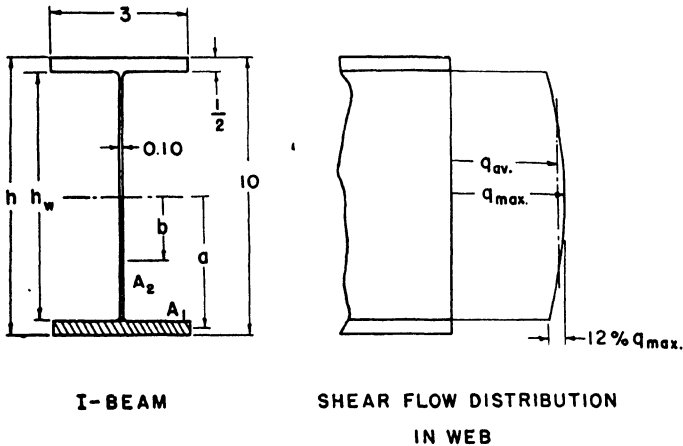
Fig. 11.3. Web Shear Flow.

Another useful relation exists between the shear flow on one side of an internal flange and the shear flow on the other side.   Flange number two is shown isolated in Figure 11.2(b).   If the shear flow on the bottom of the flange is q_1, it is evident that the shear flow on the top is

$$q_2 = q_1 + \frac{dP_2}{dx}$$

or, in general, $$q_n = q_{n-1} + \frac{dP_n}{dx} \tag{11.5}$$

EXAMPLE 11.1.   Determine the amount of variation of shear flow in the web of the symmetrical beam, shown in Figure 11.3, between the maximum value which occurs at the neutral axis and the value at a point adjacent to the flange.

Solution. Using Equation 11.4 gives

$$q = \frac{V}{I} \int y \, dA$$

The value of the integral for all the material below the neutral axis can be determined by taking the moment of the area below the neutral axis about the neutral axis.

Thus, $\qquad \int y \, dA = aA_1 + bA_2$
$$= 4.75(3 \times \tfrac{1}{2}) + 2.25(4.5 \times 0.10)$$
$$= 7.13 + 1.01 = 8.14 \text{ in}^3$$

The shear flow at the neutral axis is therefore

$$q_n = 8.14 \frac{V}{I}$$

The shear flow adjacent to the flange can be determined from the first term of evaluation of the integral or

$$q_f = 7.13 \frac{V}{I}$$

The variation in shear flow is therefore

$$\frac{q_n - q_f}{q_n} = \frac{8.14 - 7.13}{8.14} = 12\%$$

This solution does not take into account any stress increases caused by sharp corners.

11.3 Proportion of shear taken by web in thin-web beam. The assumption has been made previously that most of the shear force is carried by the web in thin-web non-tapering beams. This assumption should be investigated.

If the total shear force is divided into two parts, the web shear and the flange shear, then

$$V = V_w + V_f$$

By assuming that the shear flow in the web is constant, which seems justified when the section is proportioned as in the previous example, then

$$V_w = q_w h_w$$

where q_w is the average shear flow in the web

$$q_w = \frac{V}{I} \left(\int y \, dA \right)_{av}$$

Therefore, $\qquad V_w = \frac{V h_w}{I} \left(\int y \, dA \right)_{av}$

and $\qquad \frac{V_w}{V} = \frac{h_w}{I} \left(\int y \, dA \right)_{av}$

If we use the data from Example 11.1, we obtain

$$I = \frac{0.1 \times 9^3}{12} + 2\left[\left(3 \times \frac{1}{2}\right)(4.75)^2 + \frac{3 \times (\frac{1}{2})^3}{12}\right] = 73.8 \text{ in}^4$$

The average value of $\int y \, dA$ for the web will be approximated by taking the average of the maximum and minimum values from Example 11.1. Thus,

$$\left(\int y \, dA\right)_{av} = \frac{8.14 + 7.13}{2} = 7.63 \text{ in}^3$$

$$\frac{V_w}{V} = \frac{9 \times 7.63}{73.8} = 93\%$$

Therefore, 93% of the shear force is carried by the web and 7% by the flanges in this case.

It has been shown that for thin-web flanged beams the vertical shear flow in the web is essentially a constant and that the web carries most of the shear force. If it is assumed therefore that all the shear force is carried by the web and that the shear flow is constant, then the shear flow in the web is

$$q_w = \frac{V}{h_w} \tag{11.6}$$

and the shear stress is

$$f_s = \frac{V}{h_w t} \tag{11.7}$$

where
$$V = \text{total shear force (lb)}$$
$$h_w = \text{``effective'' height of web (in)}$$
$$t = \text{thickness of web (in)}.$$

11.4 Tapered beam. If a beam is tapered, the flanges will carry more of the shear load because the flange (bending) forces will have components in the direction of the shear force.

Consider a thin-web tapered beam as shown in Figure 11.4. The flange forces P_1 and P_2 are acting along the flanges as shown in the figure. These forces can be resolved into vertical and horizontal components P_V and P_H. For equilibrium in the horizontal direction

$$\Sigma F_H = 0 = P_{2H} - P_{1H}$$
$$P_{1H} = P_{2H} = P_H$$

For equilibrium of moments

$$\Sigma M = 0 = M - P_H h$$
$$P_H = \frac{M}{h}$$

Therefore,
$$P_1 = \frac{P_H}{\cos \alpha_1} = \frac{M}{h \cos \alpha_1}$$

$$P_2 = \frac{P_H}{\cos \alpha_2} = \frac{M}{h \cos \alpha_2}$$

and
$$P_{1V} = P_1 \sin \alpha_1 = \frac{M}{h} \tan \alpha_1$$

$$P_{2V} = P_2 \sin \alpha_2 = \frac{M}{h} \tan \alpha_2$$

The total shear force carried by the flanges because of the inclination of the flange loads is

$$V_f = P_{1V} + P_{2V} = \frac{M}{h} (\tan \alpha_1 + \tan \alpha_2) \qquad (11.8)$$

The shear carried by the web is

$$V_w = V - V_f = V - \frac{M}{h} (\tan \alpha_1 + \tan \alpha_2) \qquad (11.9)$$

This derivation is based on the assumptions that the web does not take any bending stresses and that the shear flow in the web is uniform.
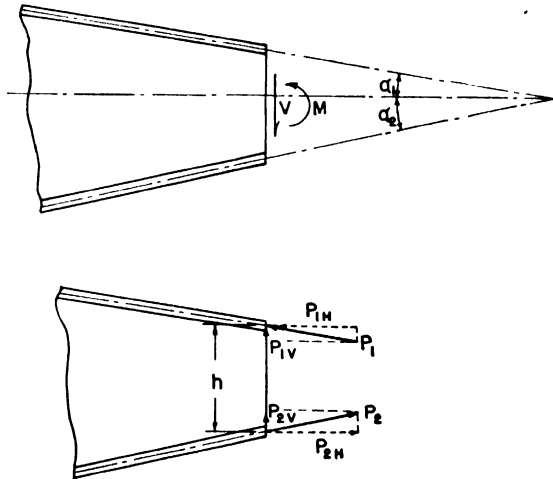
Fig. 11.4. Tapered Beam.

These assumptions are reasonable for moderately tapered beams with thin webs.

11.5 Beam with buckled web. For the thin-web beams previously studied, it has been assumed that the web did not buckle under the action of the loads. Such a web is said to be *shear resistant*. It is not unusual in aircraft construction to design a thin-web beam which is known to buckle when the load is applied. This is the so-called *tension-field web*. The reason such a beam is used is because under some conditions the tension-field web beam is lighter than the beam with shear resistant web for the same strength. Of the two types, however, the tension-field web beam is usually the more flexible.

Since the rigorous analysis and design of a tension-field beam is very complicated and still undergoing development, only a simplified analysis presenting the essentials will be discussed. The same assumptions will be made in considering the tension-field beam as for the thin-web beams studied previously, namely:

(1) The total bending moment is carried by the flanges.
(2) The total shear force is carried by the web.

Figure 11.5 shows a thin-web beam with heavy flanges supporting an end load V which produces a shear force and bending moment at each

(a)

(b)   (c)
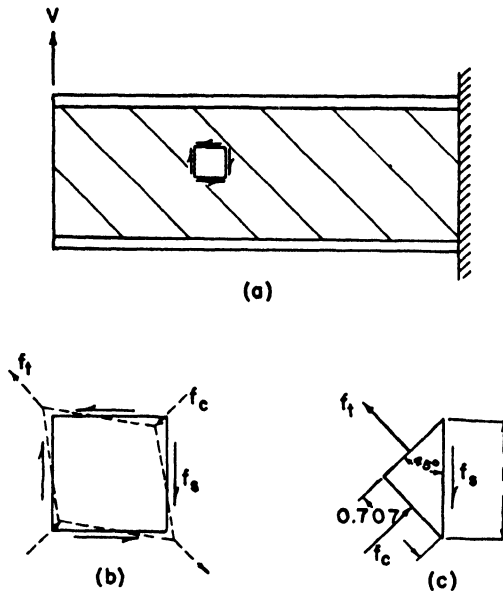
Fig. 11.5. Thin-Web Beam.

cross section of the beam. A square element of the web is shown isolated in Figure 11.5(b). The distortion of this element due to the shear stresses, as shown by the dashed lines, indicates that the same effect on the element could be produced by tension and compression stresses acting on the corners. As a matter of fact, it can be shown that such stresses do exist. Consider the equilibrium of the 45° isosceles triangular shaped element of Figure 11.5(c). From symmetry and equilibrium of the forces in the horizontal direction it is evident that $f_t = f_c$. There are no shear stresses on the sloping sides because equilibrium of moments must be maintained. By remembering that for a vertical side of unit length the sloping sides have a length of 0.707, then the force on a sloping side is $0.707 t f_t$ and the vertical component of this force is $(0.707)^2 t f_t = 0.5 t f_t$.

Therefore,

$$\Sigma F_V = 0 = f_s t - 0.5 f_t t - 0.5 f_c t$$

But $f_t = f_c$

Therefore, $f_t = f_c = f_s$ (11.10)

In other words, the tension and compression stresses on planes making an angle of 45° with the shear stress are equal in magnitude to the shear stress. These normal stresses are called the *principal stresses.*

If the diagonal compression stress exceeds the critical buckling stress of the web, the web will buckle. After the web buckles the compression stress will not increase materially, so that any restraint to increasing load must be resisted by an increase in the diagonal tension. The maximum amount of diagonal compression present depends on the proportions of the beam. Two cases in the design of beams with buckled webs are usually considered:

(1) pure diagonal tension-field web (The web is assumed to buckle at such a low load that the diagonal compression is neglected altogether.)

(2) incomplete diagonal tension-field web (The small amount of diagonal compression is considered in the analysis.)

Pure diagonal tension-field web. A beam in which only the diagonal tension is considered sometimes is called a *Wagner beam* because Professor Wagner was the first investigator of the phenomenon.

A portion of the beam with diagonal tension web is shown in Figure 11.6. The section on the right is a distance x from the end where the load V is applied. The total force P_w produced by the diagonal tension is equal to the stress times the area or
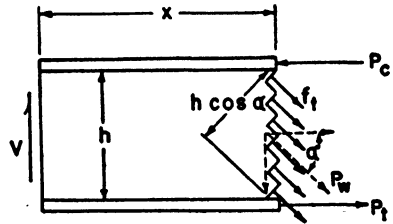
Fig. 11.6. Element Showing Diagonal Tension.

$$P_w = f_t t h \cos \alpha$$

For equilibrium in the vertical direction

$$\Sigma F_V = 0 = P_w \sin \alpha - V$$

or $$P_w = \frac{V}{\sin \alpha}$$

and $$f_t = \frac{V}{t h \sin \alpha \cos \alpha}$$ (11.11)

If α is assumed to be 45° (tests show it is between 40° and 42° due to the effect of the stiffeners), then

$$f_t = \frac{2V}{th}$$ (11.12)

where V = shear force (lb)

                               h = effective height (in)

                               t = web thickness (in).

The loads and stresses in the flanges are determined from moment equilibrium.

$$\Sigma M = 0 = Vx - P_c h + P_w \frac{h}{2} \cos \alpha$$

$$P_c = \frac{Vx}{h} - \frac{P_w}{2} \cos \alpha$$

But $$P_w = \frac{V}{\sin \alpha}$$

so that $$P_c = \frac{Vx}{h} + \frac{V}{2} \cot \alpha \tag{11.13}$$

Similarly, $$P_t = \frac{Vx}{h} - \frac{V}{2} \cot \alpha$$

For $\alpha = 45°$ $$P_c = V \left(\frac{x}{h} + \frac{1}{2} \right)$$

$$P_t = V \left(\frac{x}{h} - \frac{1}{2} \right) \tag{11.14}$$

The stresses on the flanges are determined by dividing the flange loads by the flange areas.
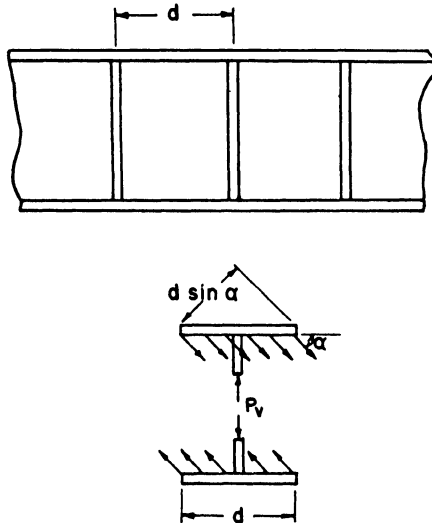
Fig. 11.7. Force on Stiffeners.

The diagonal tension acting along the flanges or spar caps tends to draw the top and bottom flanges together. In order to hold the flanges apart, vertical stiffeners must be provided at suitable intervals along

the beam. By assuming that each stiffener transmits the vertical load between the top and bottom flanges, the load being caused by the diagonal tension from the center of the interval to the left of the stiffener to the center of the interval to the right of the stiffener, then the forces acting will be as shown in Figure 11.7. The vertical force due to the diagonal tension acting along a length d of the flange is

$$P_v = f_t t d \sin^2 \alpha$$

But from Equation 11.11

$$f_t = \frac{V}{th \sin \alpha \cos \alpha}$$

Therefore, $$P_v = \frac{Vd}{h} \tan \alpha \qquad (11.15)$$

For $\alpha = 45°$ $$P_v = \frac{Vd}{h} \qquad (11.16)$$

This force produces a compressive stress in the stiffener. The allowable load for the stiffener usually is based on its column strength. The problem of the column strength of the stiffener is complicated, however, by the fact that the web adds some lateral restraint to the stiffener since it helps prevent the stiffener from buckling out of the plane of the web. Another factor influencing the design of the strut is the fact that the stiffener load P_v may be eccentrically applied at the ends of the strut which thus produces a bending moment. Professor Wagner in his paper (see references) developed some correction factors for evaluating the support of the web on the stiffener. The eccentric loading effect

Fig. 11.8. Bending Loads on Spar Cap.

is evaluated by considering the stiffener as a beam column.

The vertical component of the diagonal tension action along the flanges between the stiffeners tends to bend the flanges. If the stiffeners are spaced uniformly along the span and the vertical component of the diagonal tension is assumed uniformly distributed, then the flanges are similar to continuous beams carrying uniform loads as shown in Figure 11.8. As a matter of fact, the deflection of the flanges between stiffeners causes the diagonal tension to be nonuniform so that for a rigorous analysis this effect also must be considered. In the following analysis the diagonal tension will be considered uniform along the flange.

The vertical component of the diagonal tension per unit length of flange is determined by dividing the total force for an interval d, as given by Equation 11.15, by the length d. Hence,

$$p_v = \frac{V}{h} \tan \alpha$$

and for $\alpha = 45°$

$$p_v = \frac{V}{h} \tag{11.17}$$

Since we have assumed uniform stiffener spacing, the ends of the flange at the stringers will not rotate and the portion of the flange between stiffeners may be analyzed as a fixed-end beam carrying the uniform load p_v. The maximum bending moment for such a beam may be determined by means of the methods developed in Article 4.12. The maximum bending moment is

$$M_f = \frac{p_v d^2}{12} = \frac{V d^2}{12h} \tag{11.18}$$

This of course ignores any beam-column action. The maximum stress in the flange is determined then by adding the stress caused by the bending moment and the axial stress in the flange caused by the diagonal tension previously determined (Equation 11.14):

$$f_f = \frac{P_f}{A_f} \pm \frac{M_f c}{I_f} \tag{11.19}$$

where A_f = area of flange (in^2)

I_f = moment of inertia of flange about its own centroidal axis (in^4)

c = distance from neutral axis of flange to extreme fiber (in).

Incomplete tension-field web. It was assumed in the previous analysis of the tension-field beam that the diagonal compression in the web was so small that it could be neglected. The vertical component of the diagonal tension therefore carried all the shear load. Actually there is always some diagonal compression present, which as a minimum corresponds to the buckling strength of the web, so that some of the vertical shear load is carried by the vertical component of the diagonal compression. A web with an appreciable amount of diagonal compression is said to be an *incomplete tension-field web.*

The amount of shear force carried by the diagonal compression varies with the physical properties of the beam and the loading. Several investigations, both experimental and analytical, have been made to evaluate the influence of the diagonal compression (see references). The influence of the diagonal compression is taken into account usually by

reducing the shear force taken by the diagonal tension by the amount carried by diagonal compression. Thus, if V_{Dt} is the vertical component of the diagonal tension, then

$$V_{Dt} = KV \qquad (11.20)$$

When $K = 1$ all the shear force is carried by the diagonal tension as in the case previously analyzed, and when $K = 0$ the web is shear resistant (does not buckle). If the value of K is known, the results of the previous analysis can be used by replacing V by KV in most of the formulas. The actual value of K to use in a specific design is usually based on a semi-empirical relation, and the student is referred to the references for further information.

Additional comments on tension-field webs. At the beginning of Article 11.5 a statement was made to the effect that beams with tension-field
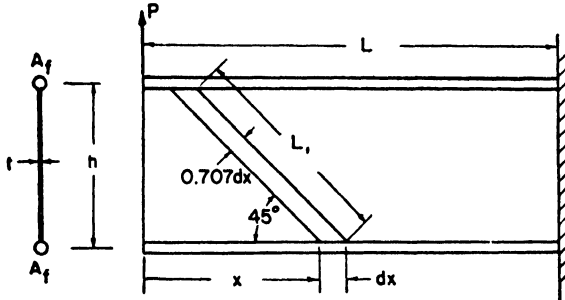
Fig. 11.9. Deflection of Beam with Tension-Field Web.

webs are more flexible than beams with shear-resistant webs. A comparison of the flexibilities of these two types of beams will now be made.

For the beam shown in Figure 11.9 it will be assumed that all the shear force is carried by the web and all the bending moment is resisted by the flanges. For simplicity the flange areas are assumed equal. The deflection of the end of the beam in the direction of the applied end load will be determined by considering the elastic energy of the flanges and the web.

The bending moment at any distance x from the end of the beam is Px, and the shear force is a constant equal to P. When we assume that the web does not buckle, the flange force in the top flange is

$$P_c = -\frac{Vx}{h} = -\frac{Px}{h} \text{ (compression)}$$

and in the bottom flange

$$P_t = \frac{Vx}{h} = \frac{Px}{h} \text{ (tension)}$$

According to Castigliano's theorem

$$\delta_1 = \frac{\partial U}{\partial P} = \int_0^L P_c \frac{\partial P_c}{\partial P} \frac{dx}{EA_f} + \int_0^L P_t \frac{\partial P_t}{\partial P} \frac{dx}{EA_f} + \int_0^L V \frac{\partial V}{\partial P} \frac{dx}{GA_w}$$

$$= \int_0^L \left(-\frac{Px}{h}\right)\left(-\frac{x}{h}\right) \frac{dx}{EA_f} + \int_0^L \left(\frac{Px}{h}\right) \frac{x}{h} \frac{dx}{EA_f} + \int_0^L P \frac{dx}{Ght}$$

$$\delta_1 = \frac{2PL^3}{3Eh^2 A_f} + \frac{PL}{Ght}$$

Since $\quad I = \dfrac{h^2 A_f}{2}$

$$\delta_1 = \frac{PL^3}{3EI} + \frac{PL}{Ght}$$

The first term represents the contribution of the bending moment to the deflection, and the second term shows the effect of the web shear.

If the web is assumed to be buckled, then the forces in the flanges are given by Equation 11.14 or

$$P_c = -V\left(\frac{x}{h} + \frac{1}{2}\right) = -P\left(\frac{x}{h} + \frac{1}{2}\right)$$

$$P_t = V\left(\frac{x}{h} - \frac{1}{2}\right) = P\left(\frac{x}{h} - \frac{1}{2}\right)$$

The diagonal tension in the web according to Equation 11.12 is

$$f_t = \frac{2V}{th} = \frac{2P}{th}$$

In order to determine the elastic energy in the web, consider a strip of web making an angle of 45° with the flanges and of width $0.707\,dx$. If P_1 is the tensile force in the strip so that $P_1 = f_t A_1$, where A_1 is the cross-section area of the strip and $L_1 = 1.41$, $h = $ length of strip, then

$$dU_1 = \frac{P_1^2 L_1}{2EA_1} = \frac{f_t^2 L_1 A_1}{2E} = \frac{2P^2}{Eht} dx$$

Therefore, the total energy of the web is

$$U_1 = \int_0^L \frac{2P^2}{Eht} dx$$

Considering the energy of the web and flanges, we have

$$\delta_2 = \frac{\partial U}{\partial P} = \int_0^L P_c \frac{\partial P_c}{\partial P} \frac{dx}{EA_f} + \int_0^L P_t \frac{\partial P_t}{\partial P} \frac{dx}{EA_f} + \frac{\partial}{\partial P} \int_0^L \frac{2P^2}{Eht} dx$$

$$= \int_0^L P\left(\frac{x}{h} + \frac{1}{2}\right)^2 \frac{dx}{EA_f} + \int_0^L P\left(\frac{x}{h} - \frac{1}{2}\right)^2 \frac{dx}{EA_f} + \int_0^L \frac{4P}{Eht} dx$$

$$= \frac{PL}{EA_f}\left(\frac{2L^2}{3h^2} + \frac{1}{2}\right) + \frac{4PL}{Eht}$$

$$\delta_2 = \frac{PL^3}{3EI} + \frac{PL}{2EA_f} + \frac{4PL}{Eht} \tag{11.21}$$

By comparing the value of deflection δ_2 of the beam with the buckled web and the beam with the shear-resistant web δ_1, it is evident that the beam with the buckled web has the greater deflection.   Both the flanges and the web of the buckled-web beam contribute more to the deflection than they do in the shear-resistant web beam.

If we consider the contribution of only the web in the two cases the ratio of deflections is

$$\frac{\delta_{2w}}{\delta_{1w}} = \frac{4PL}{Eht} \bigg/ \frac{PL}{Ght} = \frac{4G}{E}$$

For aluminum $\frac{G}{E}$ is about $\frac{2}{5}$; hence,

$$\frac{\delta_{2w}}{\delta_{1w}} = \frac{8}{5} \tag{11.22}$$

In other words, the shear flexibility of the buckled web is about $\frac{8}{5}$ the flexibility of the unbuckled web of the same dimension.   The thickness of a tension-field web would have to be about $\frac{8}{5}$ times the thickness of the unbuckled web in order to have the same rigidity.

The question often arises in design concerning the choice between a beam with a tension-field web and a beam with a shear-resistant web. From the standpoint of weight, Wagner has indicated that it is preferable to use the tension-field web if

$$\frac{\sqrt{V}}{h} < 7 \tag{11.23}$$

and, if

$$\frac{\sqrt{V}}{h} > 11$$

the shear web is better.   For the region between 7 and 11 there seems to be little choice.   If rigidity is a determining factor, the shear web should be used.

It should be emphasized again that the analyses of beams with tension-field webs presented here are of only the most elementary type.   Such factors as inclined stiffeners, beam taper, and allowance for rivet holes and lightening holes have not even been discussed.   The design of beams with tension-field webs is an art in itself and the student should acquaint himself with the design practice of the particular company with which he becomes associated.

EXAMPLE 11.2.   For the 24ST aluminum beam shown in Figure 11.10 carrying a limit load of 12,000 pounds at the end, determine

    (a) diagonal tension stress in web
    (b) margin of safety of web in tension
    (c) stiffener load
    (d) axial flange loads
    (e) stresses in flanges.

The web is assumed to be a pure tension-field web. The solution is to be considered only approximate.

The sum of the areas of the two angles comprising the top flange is 2.94 in², and the moment of inertia of the flange about its own centroidal

12,000 lb.
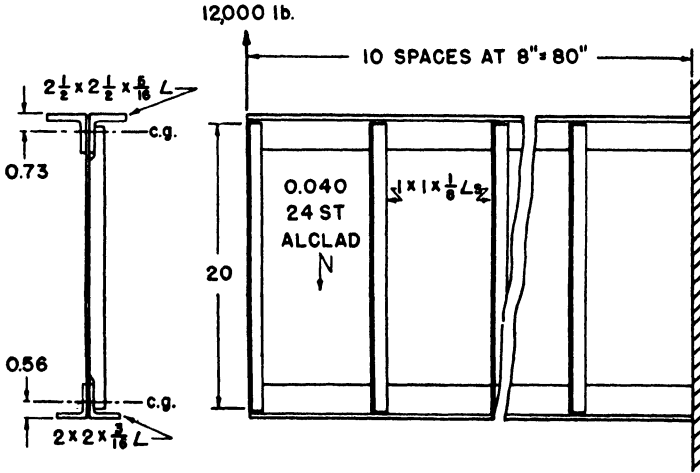
Fig. 11.10. Thin-Web Beam with End Load.

axis is 1.68 in⁴. Corresponding values for the bottom flange are $A = 1.44$ in² and $I = 0.54$ in⁴. The effective height of the web is 20 inches.

Solution.

Diagonal tension stress in web.

$$f_t = \frac{2V}{ht} = \frac{2 \times 12,000}{20 \times 0.040} = 30,000 \text{ psi}$$

Margin of safety of web. The allowable tension yield stress of clad 24ST sheet given in the ANC-5 is 37,000 psi. Therefore,

$$MS = \frac{F_{ty}}{f_t} - 1 = \frac{37,000}{30,000} - 1 = 23\%$$

Stiffener load.

$$P_v = \frac{Vd}{h} = \frac{12,000 \times 8}{20} = 4800 \text{ lb}$$

Axial force on flanges. The maximum forces in the flanges will occur at the fixed end where the moment is greatest.

For the tension flange

$$P_t = V\left(\frac{x}{h} - \frac{1}{2}\right) = 12,000\left(\frac{80}{20} - \frac{1}{2}\right) = 42,000 \text{ lb}$$

For the compression flange

$$P_c = V\left(\frac{x}{h} + \frac{1}{2}\right) = 12{,}000\left(\frac{80}{20} + \frac{1}{2}\right) = 54{,}000 \text{ lb}$$

. *Stresses in flanges.* The effect of the bending of the flanges between stiffeners will be considered in determining the maximum flange stresses.

The flange loads are a maximum at the fixed end, and the stresses will be determined there. The stress in the top fiber of the lower flange is

$$f_1 = \frac{P_t}{A_f} - \frac{M_f c_1}{I_f}$$

But
$$M_f = \frac{Vd^2}{12h} = \frac{12{,}000 \times (8)^2}{12 \times 20} = 3200 \text{ lb in}$$

and
$$c_1 = 2 - 0.56 = 1.44$$

Therefore,
$$f_1 = \frac{42{,}000}{1.44} - \frac{3200 \times 1.44}{0.54} = 20{,}650 \text{ psi (tension)}$$

The stress in the bottom fiber of the lower flange is

$$f_2 = \frac{P_t}{A_f} + \frac{M_f c_2}{I_f}$$
$$= \frac{42{,}000}{1.44} + \frac{3200 \times 0.56}{0.54} = 32{,}500 \text{ psi (tension)}$$

The stress in the bottom fiber of the upper flange is

$$f_3 = \frac{P_c}{A_f} + \frac{M_f c_3}{I_f}$$
$$= \frac{54{,}000}{2.94} + \frac{3200 \times (2.5 - 0.73)}{1.68} = 21{,}750 \text{ psi (compression)}$$

The stress in the top fiber of the upper flange is

$$f_4 = \frac{P_c}{A_f} - \frac{M_f c_4}{I_f}$$
$$= \frac{54{,}000}{2.94} - \frac{3200 \times 0.73}{1.68} = 16{,}950 \text{ psi (compression)}$$

11.6 Flange shear. It has been shown that for the flanged beam with thin web the amount of vertical shear force carried by the flange is small. The shear flow and the shear stress were determined on horizontal planes. A study now will be made of the shear conditions on the vertical planes of the flanges. Although the shear stress on the vertical planes of the flange of a conventional beam is seldom critical from the strength standpoint, we will see that it has implications which affect the design and manner of loading.

A portion of length dx of a thin-web I beam is shown in Figure 11.11. A vertical cut in the flange a distance s from the outside free edge is shown. Since the bending moment differs on the two end sections of the portion of length dx, the bending stresses will be different at the ends of the element $ab'cd$. The difference in the force on the end ab' and the end cd must be balanced by a force due to the shear flow along the edge $b'c$.

(a)

(b)   (c)

TOP VIEW   END VIEW
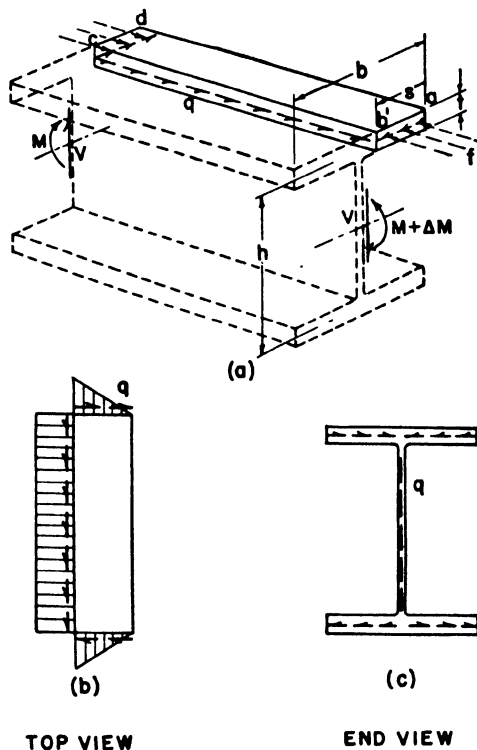
Fig. 11.11. Flange Shear.

This is analogous to the situation that existed in determining the shear flow in the web so that Equation 11.4 can be directly applied. Hence,

$$q = \frac{V}{I} \int y \, dA$$

By assuming a symmetrical beam of depth h, then the value of y is a constant and equal to $h/2$. The integral in the preceding equation is equal to the moment about the neutral axis of the area from the outside of the flange where the shear flow is zero to the cut section $b'c$. Thus,

$$\int y \, dA = \frac{h}{2} st$$

Substituting this value and the value for I in the equation for q gives

$$q = \frac{V}{h}\frac{s}{b} \tag{11.24}$$

The shear flow along the flange therefore varies linearly, as shown in Figure 11.11(b). The shear flow along the flanges and web of the cross section of the beam is shown in Figure 11.11(c). It should be noticed that for this case the shear seems to flow inward on the top flange and outward on the bottom.

The same reasoning applies in determining the shear flow in the curved web of the beam with cross section shown in Figure 11.12. In this case,

(a)   (b)

CURVED WEB   .   RESULTANT OF FORCES
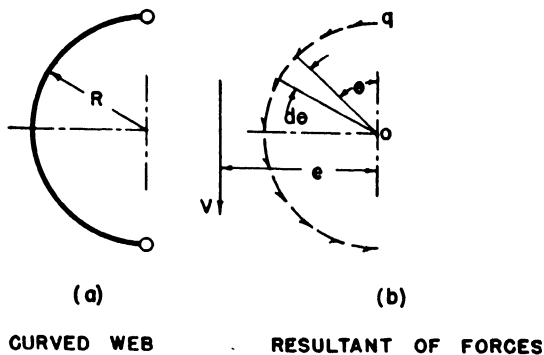
Fig. 11.12. Beam with Curved Web.

if the bending moment is resisted by the flange areas, then the shear flow in the web is

$$q = \frac{V}{I}\int y\,dA = \frac{V}{2A\frac{h^2}{4}}\frac{h}{2}A = \frac{V}{h}$$

In other words the shear flow for the case of the curved web is the same as for the straight web. The shear flow is shown in Figure 11.12(b). The component of shear force in the vertical direction can be determined by summing the vertical components of the shear forces caused by the shear flow along the curve. Force equilibrium shows that

$$qh = V$$

The horizontal forces are balanced since the shear flow starts and ends on the same vertical line. However, there is some question about the moment equilibrium, and this will be discussed in the following article.

11.7 Shear center. The shear flow in the flanges may have horizontal force resultants which produce a couple. This couple may cause a twisting of the beam about a longitudinal axis so that for equilibrium,

the location of the reactions supporting the beam may not lie necessarily on the longitudinal axis passing through the centers of gravity of the cross sections. The position of the reactions, and hence the position of the resultant shear forces on the cross section of the beam, is called the *shear center*.

The location of a shear center is shown best by a consideration of the shear forces acting on the cross section of the channel beam shown in Figure 11.13. The reaction at one end of the beam and the forces at a cross section are shown in the figure.

(a)   **(b)**
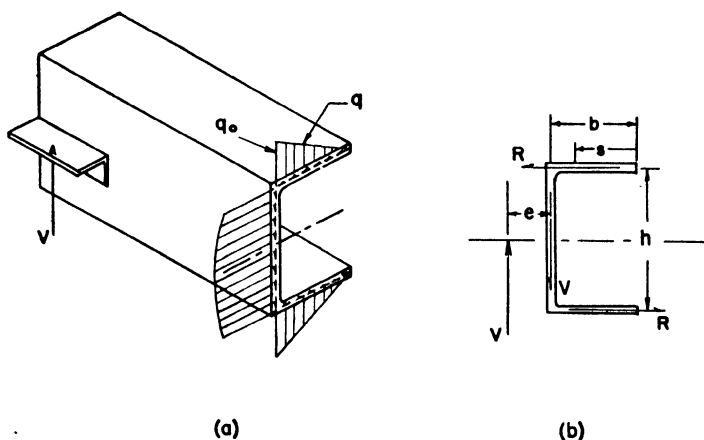
Fig. 11.13. Shear Flow in Channel Section.

The shear flow is obtained by the methods developed in the last article. The shear flow on the flange is

$$q = \frac{V}{I} \int y \, dA = \frac{V}{2I} hts$$

This is a maximum when $s = b$ or

$$q_0 = \frac{V}{2I} htb$$

Since this shear flow varies linearly from the outside edge of the flange to the web, the horizontal shear *force* in the top flange is

$$R = \frac{q_0 b}{2} = \frac{Vhtb^2}{4I}$$

There is a similar shear force on the bottom flange but in the opposite direction. These two shear forces form a couple

$$Rh = \frac{Vh^2tb^2}{4I}$$

For torque equilibrium of all the forces as shown in Figure 11.13(b) we have

$$\Sigma M = 0 = Ve - Rh$$

or
$$e = \frac{h^2 t b^2}{4I} \qquad (11.25)$$

Hence, the line of action of the resultant shear force which determines the location of the shear center is actually outside the section. The shear center is sometimes called *the elastic center* or *center of twist*. It can be shown, for example, that if a torque is applied about the center of twist, the beam will twist without bending. Conversely, if the transverse beam loading is applied so that the line of action of the loading is through the elastic center, the beam will bend without twisting. It follows therefore that, if it is desirable to have the channel beam bend without twisting, the loading will have to be applied on a shelf or fitting sticking out of the back of the section.

As another example of determining the shear center, consider the beam section with the curved web shown in Figure 11.12. If the beam section is symmetrical about a horizontal axis and the web is a semicircle of radius R, then the shear force for an arc length of $R\,d\theta$ is $qR\,d\theta$. The sum of the moments of these forces about 0 is

$$T = \int_0^\pi qR^2\,d\theta = qR^2\pi$$

If the reaction to the resultant shear force V is a distance e to the left of 0, then for equilibrium of moments

$$Ve = qR^2\pi$$

But
$$q = \frac{V}{h} = \frac{V}{2R}$$

so that
$$e = \frac{\pi R}{2} \qquad (11.26)$$
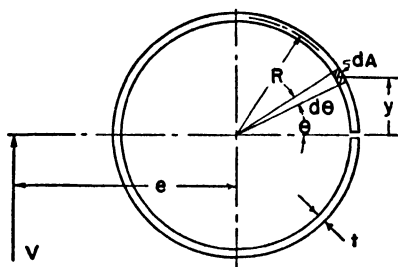
Fig. 11.14.   Split Tube.

EXAMPLE 11.3.   Determine the shear center of the circular split tube shown in Figure 11.14.

Solution. Since the tube is symmetrical about the horizontal axis passing through the center of the tube, the shear center will be somewhere on this axis. By assuming bending about this horizontal axis and a shear force applied perpendicular to the axis, the shear flow in the shell can be determined. It is apparent that the shear flow will not be constant since there are no heavy flanges to take the bending load.

The shear flow at any radial section of the shell is given by

$$q = \frac{V}{I} \int y\,dA$$

where $\int y\, dA$ is the moment about the horizontal axis of all the area from the split in the tube where the shear flow is zero to the section on which the shear flow is to be determined. Thus,

$$dA = Rt\, d\theta$$
$$y = R \sin\theta$$

so that
$$\int_0^\theta y\, dA = R^2 t(1 - \cos\theta)$$

Since
$$I = \int_0^{2\pi} y^2\, dA = \pi R^3 t$$

therefore
$$q = \frac{V(1 - \cos\theta)}{\pi R}$$

The torque of the shear flow about the center of the tube is

$$T = \int_0^{2\pi} qR^2\, d\theta = \frac{VR}{\pi} \int_0^{2\pi} (1 - \cos\theta)\, d\theta = 2RV$$

This must be balanced by the reacting torque Ve.

Hence,
$$e = 2R$$

A split tube would therefore have to be loaded a distance $2R$ from the center of the tube on the side opposite the split in order to have bending without twisting.

11.8 Shear lag. It has been assumed in determining the shear stresses and bending stresses on beam sections subjected to shear and bending that the bending stress at a fiber depends only on the distance of the fiber from the neutral axis and not on the position of the fiber along a line parallel to the neutral axis. Thus, the bending stress at the outside edge of the flange of an I beam has been considered equal to the bending stress on the flange at a point near the web when both of these positions are the same distance from the neutral axis. For a wide-flanged beam this assumption of constant flange bending stress along a line parallel to the neutral axis is not always valid. The flange shear stresses, being related to the bending stresses, do not correspond therefore to those calculated by means of the elementary theory. This phenomenon is known as *shear lag*. Fortunately, the effect of shear lag is usually minor except for very wide flanged beams or wide box beams.

The nature of shear lag is probably illustrated most easily by a consideration of a wide box beam of the type indicated in Figure 11.15. This beam is fixed solidly to a wall on the left end of the beam, and vertical loads are applied to the side spars at the right end. The loads cause the side spars to bend downwards, which thus elongates the top spar caps and contracts the bottom ones. Shear flows along the edges of the top sheet of the box adjacent to the spar caps will be induced

as illustrated in Figure 11.15(b). By considering the top of the box as a sheet loaded along its long edges by the shear flows, it is apparent that the elongation along the edges may be greater than the elongation in the central region of the sheet. The longitudinal strain near the center of the sheet therefore may be less than the longitudinal strain along the edges. By considering only the effect of the longitudinal strains, it is apparent that the longitudinal stresses will be lower at the center than at the sides, as indicated in the figure. Since the longitudinal stresses are not uniformly distributed as assumed in the elementary theory, the shear flows

(a)

(b)
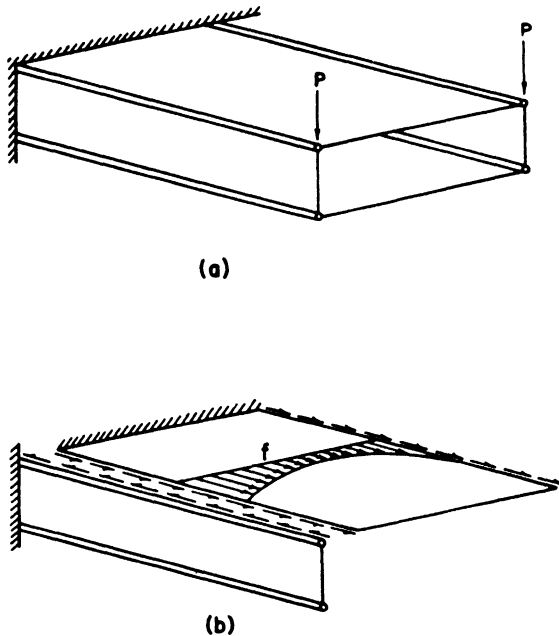
Fig. 11.15. Shear Lag.

do not correspond to those predicted by elementary theory. This phenomenon is called *shear lag*.

The analysis required to predict the actual stresses for structures in which shear lag occurs is too complicated to develop here. However, the general effect of the shear lag is to increase the stresses at the edges of the sheet and decrease the stresses in the central portion as compared with the stresses determined by ordinary beam theory.

Problems

11.1. A portion of a four-flange beam 10 inches long and similar to the one shown in Figure 11.2 has a bending moment on the left end of 50,000 lb in and a bending moment on the right end of 70,000 lb in. The flange areas are equal

and the flanges are equally spaced with 5 inches between centers.   Determine the flange forces and the shear flows in the web.   What is the vertical shear force?

11.2. The I section shown in Figure 11.3 carries a vertical shear load of 10,000 pounds and a horizontal shear load of 5,000 pounds.   Determine the shear flows in the web and flanges.   Determine the maximum shear stress in the web and the flanges, neglecting any stress concentrations.

11.3. A beam with a channel section as shown in Figure 11.16 is loaded with a shear force of 10,000 pounds so that bending occurs about the horizontal centroidal axis.   Assuming the web does not buckle, determine

(1) flange and web shear flow distributions
(2) percentage of vertical shear carried by web
(3) location of the line of action of vertical shear force.
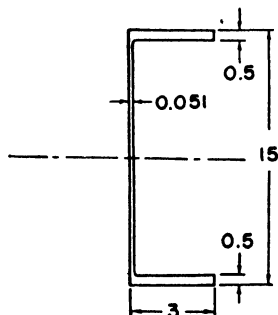
Fig. 11.16. Channel Section.

11.4. A thin circular tube with a mean radius R and a wall thickness t carries a transverse shear load V with line of action through the center of the tube. Determine the shear flow distribution.   (*Hint:* In determining $\int y\, dA$ use an area symmetrical about the line of V.)

11.5. A 24ST cantilever beam similar to the one shown in Figure 11.10 carries an end load of 10,000 pounds.   The beam is 50 inches long with stiffeners
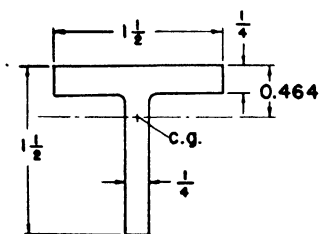
A = 0.740 in^2

I = 0.142 in^4
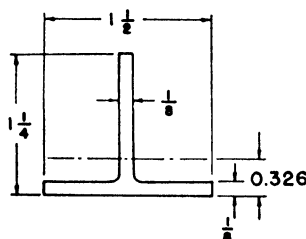
A = 0.373 in^2

I = 0.049 in^4

UPPER FLANGE   LOWER FLANGE

Fig. 11.17. Beam Flanges.

spaced at 10 inches.   The effective height of the web is 30 inches and the flanges are the 24ST extrusions shown in Figure 11.17.   Determine

(1) stress in web
(2) maximum stresses in flanges
(3) stiffener load.

If the allowable column strength of the stiffener is 12,200 psi and all other

allowable stresses are taken as the ultimate stress for the material given in the ANC-5, determine the margin of safety for each of the beam components.

11.6. A taper beam similar to the one shown in Figure 11.4 carries an end load of 10,000 pounds and has a cross section at the loaded end that is 12 inches between flanges, equal flange areas of 2.1 square inches, and a web thickness of 0.064 inches. If the flanges are uniform in area throughout their length but slope 1.5 inches per foot, determine the flange loads and shear stress in the web at a distance of 5 feet from the end where the load is applied. (Assume web does not buckle.)

11.7. Determine the location of the shear center for the beam sections shown in Figure 11.18. All flange areas $= A$ unless otherwise noted.
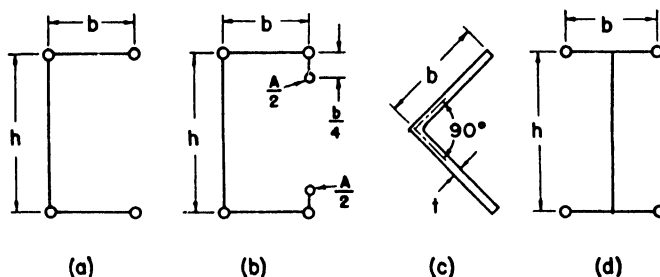
Fig. 11.18. Beam Sections.

11.8. If the section shown in Figure 11.18(b) carries a vertical shear load at the shear center of 5,000 pounds, and $b = 4$ inches, $h = 12$ inches, $A = 0.5$ inches^2, determine the shear flows.

11.9. What are the shear flows in the section used in Problem 11.8 if a horizontal shear load of 1,000 pounds acting at the shear center is added to the vertical shear load already present?

References

Hoff, J. N., "The Applicability of St. Venant's Principle to Airplane Structures." *Journal of Aeronautical Sciences*, October 1945.

Kuhn, Paul, "Investigations on the Incompletely Developed Plane Diagonal-Tension Field." NACA Tech. Report 697, 1940.

Kuhn, Paul, "A summary of Design Formulas for Beams having Thin Webs in Diagonal Tension." NACA Tech. Note 469, 1933.

Levin, L. Ross and David H. Nelson, "Comparison of Measured and Calculated Stresses in Built-up Beams." NACA Tech. Note 1063, May 1946.

Reissner, Eric, "On the Problem of Stress Distribution in Wide-Flanged Box-Beams." *Journal of Aeronautical Sciences*, Vol. 5, No. 8, June 1938.

Sibert, H. W., "Rational Analysis of Tension-Field Beams." *Journal of Aeronautical Sciences*, November 1942.

Wagner, Herbert, "Flat Sheet Metal Girders with Very Thin Webs." Part I. General Theories and Assumptions. NACA Tech. Memo 604, 1929. Part II. Sheet Metal Girders with Spars Resistant to Bending. NACA Tech. Memo. 605, 1929. Part III. Stress in Uprights. NACA Tech. Memo. 606, 1929.

CHAPTER 12

Torsion

....

12.1 Introduction. At the close of the last chapter it was indicated that if the resultant shear forces do not pass through the shear center of the beam cross sections, the forces will cause a twisting of the beam about some longitudinal axis. The couple causing a twisting about a longitudinal axis usually is called a *torque*. The torque acting on beams induces shear stresses on the cross sections in the plane of the torque. The simplest conditions of shear stresses caused by torque occur when only a pure torque is acting without transverse shear forces or beam bending moments and when the end sections of the torsion members are free to move in the axial direction. This latter condition occurs, for example, when no restraints, such as end plates or heavy fastenings to other structures, are present to prevent the end cross section of the torsion member from warping out of plane. This type of torsion will be discussed first.

12.2 Torsion of members with circular cross sections. Many members such as machine shafts, propeller shafts, and so on, have either solid

(a)   (b)   (c)
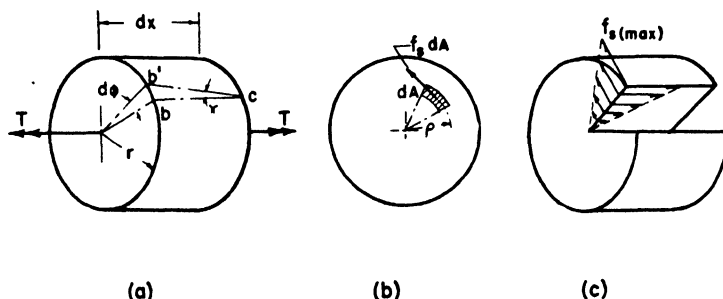
Fig. 12.1.   Torsion of Circular Section.

or hollow circular cross sections and are designed for transmitting torque. Our attention will be directed first to the analysis of uniform shafts of solid circular cross sections, and the following assumptions will be made:

(1) Sections remain circular after application of the torque
(2) Diameters remain straight
(3) Material is homogeneous, isotropic, and elastic.

In Figure 12.1 is shown a portion of a circular shaft of length dx with a torque T applied at one end and resisted at the other. Under the action of the torque, the left end will rotate counterclockwise relative to the right end. This rotation is denoted by $d\phi$. The point b will rotate up

to point b' so that the element of the cylinder bc will assume the position $b'c$ after the torque is applied. If γ is the angle between bc and $b'c$ on the surface of the cylinder, the corresponding angle a distance ρ from the center of the cylinder will be proportional to ρ or

$$\gamma = K\rho$$

However, γ is the change in the right angle or the shearing strain. The shear stress is

$$f_s = \gamma G = K\rho G$$

The force on a small element of area a distance ρ from the center as shown in Figure 12.1(b) is $f_s \, dA$, and the sum of the moments of all these forces must be equal to the torque or

$$T = \int_A f_s\rho \, dA = KG \int_A \rho^2 \, dA$$
$$= KGJ$$

where $\quad$ = polar moment of inertia of cross section (in⁴).

Therefore, $$K = \frac{T}{GJ}$$

and $$f_s = \frac{T\rho}{J} \tag{12.1}$$

$$f_{s_{(max)}} = \frac{Tr}{J} \tag{12.2}$$

where $\quad r$ = radius of shaft (in).

The shear stress distribution is shown in Figure 12.1(c). The shear stresses along the longitudinal elements of the cylinder are present since we know that the shear stresses must exist in equal and opposite pairs at a point.

The angle of twist of the shaft can be determined easily since

$$d\phi = \frac{\gamma \, dx}{\rho} = K \, dx = \frac{T}{GJ} \, dx$$

Therefore, $$\phi = \int_0^L \frac{T}{GJ} \, dx$$

and, if T, G, and J are constant,

$$\phi = \frac{TL}{GJ} \tag{12.3}$$

where $\quad \phi$ = angle of twist in shaft (rad)
$\quad L$ = length of shaft (in)
$\quad T$ = torque (lb in)
$\quad G$ = shear modulus of rigidity (psi)
$\quad J$ = polar moment of inertia of cross section (in⁴).

The angle of twist per unit length is

$$\theta = \frac{\phi}{L} = \frac{T}{GJ} \tag{12.4}$$

It should be emphasized that these formulas are correct only for torsion members with circular cross sections.

12.3 Torsion of members with non-circular cross sections. Unfortunately the formulas developed in the previous article cannot be applied to noncircular shafts. This lack of correspondence can be illustrated easily. According to the analysis of the circular shaft, the maximum shear stress is located at the fiber most distant from the axis of rotation

(a)   (b)

INCORRECT SHEAR   CORRECT SHEAR

(c)   (d)

CHANNEL SECTION   DEVELOPED LENGTH
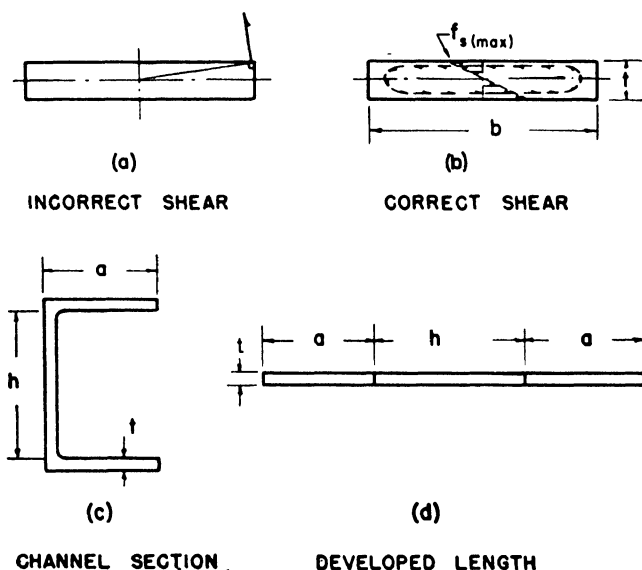
Fig. 12.2. Torsion of Rectangular Sections.

and is perpendicular to the radius vector connecting the center of twist and the stressed fiber. If these conditions are applied to a shaft of rectangular cross section, as shown in Figure 12.2(a), the most stressed fiber would be at one of the corners and the stress would be directed as shown. This stress then would have a component normal to surface with the corresponding shear stress along the surface, which is untrue. As a matter of fact, when a shaft of rectangular cross section is analyzed according to the methods of the theory of elasticity, it is found that the maximum shear stress occurs at the center of the long sides and the stresses at the corners are zero.

Only the results of the analysis of torque members with rectangular sections will be presented here since the rigorous analysis is complicated

and requires the use of the theory of elasticity. According to the Saint Venant theory for rectangular sections,

$$f_{s(max)} = \frac{T}{\alpha b t^2}$$

$$\phi = \frac{TL}{\beta b t^3 G} \qquad (12.5)$$

The value of the coefficients α and β are shown in Figure 12.3. It is
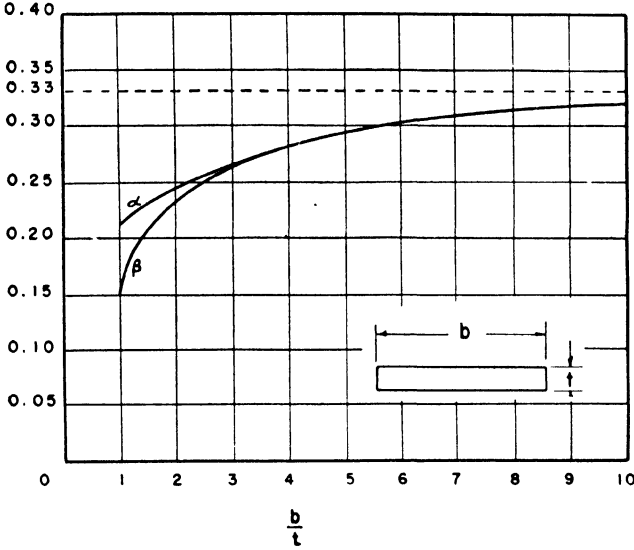
Fig. 12.3. Coefficients for Torsion of Bars with Rectangular Cross Section.

evident that for $b/t > 10$, α and β are approximately $\frac{1}{3}$ so that

$$\left. \begin{array}{l} f_{s(max)} = \dfrac{3T}{bt^2} \\[2mm] \phi = \dfrac{3TL}{bt^3 G} \end{array} \right\} \text{ for } \frac{b}{t} > 10 \qquad (12.6)$$

where $\qquad b = $ breadth of rectangle (in)

$\qquad t = $ thickness of rectangle (in).

It is interesting to note that these equations can be used for solving open sections made up of rectangles by replacing the breadth b by the developed length of the section determined by placing the rectangles end to end. Thus, if we refer to Figure 12.2, the maximum shear stress and angle of twist for the channel section are

$$f_{s(max)} = \frac{3T}{(2a + h)t^2}$$

$$\phi = \frac{3TL}{(2a + h)t^3 G} \qquad (12.7)$$

The reason for this will be apparent after studying the membrane analogy.

If the wall thicknesses are not the same for the rectangles composing the section, then it can be shown that the angle of twist per unit length is

$$\theta = \frac{3T}{(2at_1^3 + ht_2^3)G} \tag{12.8}$$

where t_1 = thickness of rectangle of length a (in)

                 t_2 = thickness of rectangle of length h (in).

The stress for this case is

$$f_s = G\theta t \tag{12.9}$$

The maximum stress occurs on the rectangle having the greatest thickness.

12.4 Membrane analogy. The shear-stress distribution for non-circular torsion members is complicated and difficult to determine analytically. It was pointed out by Prandtl, however, that the equation for the torsion of a bar and the equation for the deflection of a membrane subjected to a uniform pressure have the same form. It is therefore possible to determine the shear stress in a torsion member by performing an experiment and measuring certain quantities on a soap film or other thin membrane deflected by a uniform pressure. Careful techniques make it possible to determine the shear stresses accurately. However, the main advantage of the membrane analogy is that it provides a method of visualizing the stress conditions of a complicated torsion member.

Suppose the shear-stress distribution for a twisted bar of rectangular cross section is to be studied. Imagine a soap film stretched over a rectangular hole in a flat plate with the outline of the hole the same as the shape of the cross section of the twisted bar. If a slight pressure is applied on one side of the soap film, the film will bulge. The membrane analogy establishes the following relationships between the deflected membrane and the twisted bar:

(1) The slope of the membrane at any point is proportional to the magnitude of the shear stress at the corresponding point of the twisted bar.

(2) The tangent to a contour line at any point of the deflected membrane is the direction of the maximum shear stress at the corresponding point in the twisted bar.

(3) The volume included between the membrane and the plane of the flat plate is proportional to the applied torque on the bar required to produce a given angle of twist per unit length.

The contour lines for a soap film representing the conditions on a torsion member of rectangular cross section are shown in Figure 12.4(a). According to the membrane analogy, the shear stress across any section a-a is proportional to the slope α of the membrane. By referring to Figure 12.4(b) it is seen that the slope of the membrane is a maximum at

the edge and decreases to zero at the center line so that the shear stress is a maximum along the edge and zero at the center, as previously indicated. The direction and magnitude of the shear stresses along the horizontal and vertical center line of the rectangular cross section are indicated in Figure 12.4(c).

The effect of keyways, notches, and other stress concentrations can be determined qualitatively by imagining the effect on the slopes that these factors cause on the deflected membrane. The membrane analogy indi-

<div align="center">

(a)   (b)   (c)

CONTOUR LINES   SECTION a-a   SHEAR STRESS
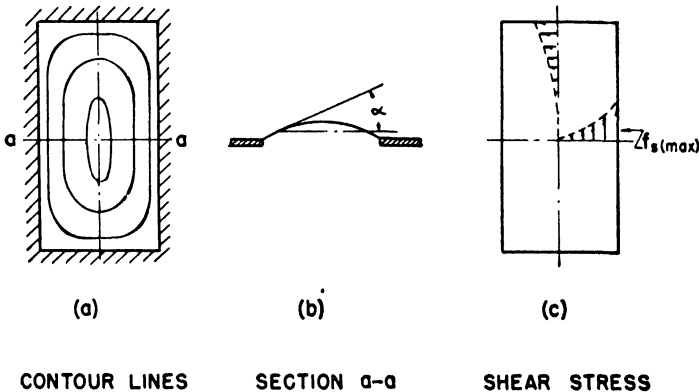
Fig. 12.4.   Membrane Analogy for Rectangular Section.

</div>

cates also why it is permissible to determine the shear stresses in sections such as channels and angles by assuming that the sections are made up of rectangles placed end to end. Comparing the shape of the membrane of the channel section with the membrane of a straight rectangle of the same width and the same overall length indicates that except for points of stress concentration, the maximum slope of the membrane and consequently the shear stress is about the same for the two cases.

12.5 Torsion of thin-walled cylinders. Equation 12.1 for the shear stress in solid circular sections is also applicable for hollow circular sections. Since the shear stress decreases linearly from the outside of the section to zero at the center, it would seem that weight can be conserved by moving some of the material in the region of the low stresses to the outside region of high stresses. This results in the hollow shaft which is often used for torque members. Of course, if this procedure is followed indefinitely, eventually the wall of the tube becomes so thin that it fails by buckling so that there is a minimum thickness to which the walls can be made and still increase the strength.

Figure 12.5(a) shows the effect of changing the wall thickness of the tube while the cross section area, and hence the weight, is kept constant. It will be noticed that as the wall thickness is decreased the difference

in the value of the stress on the outside and inside of the wall becomes smaller. For thin tubes the assumption usually is made that the stress is constant across the wall.

For a cylinder with any cross-sectional shape having thin walls it can be shown that the shear flow is constant everywhere on the periphery. Consider the cylinder of irregular cross section shown in Figure 12.5(b).

(a)

EFFECT OF DECREASING WALL THICKNESS

(b)
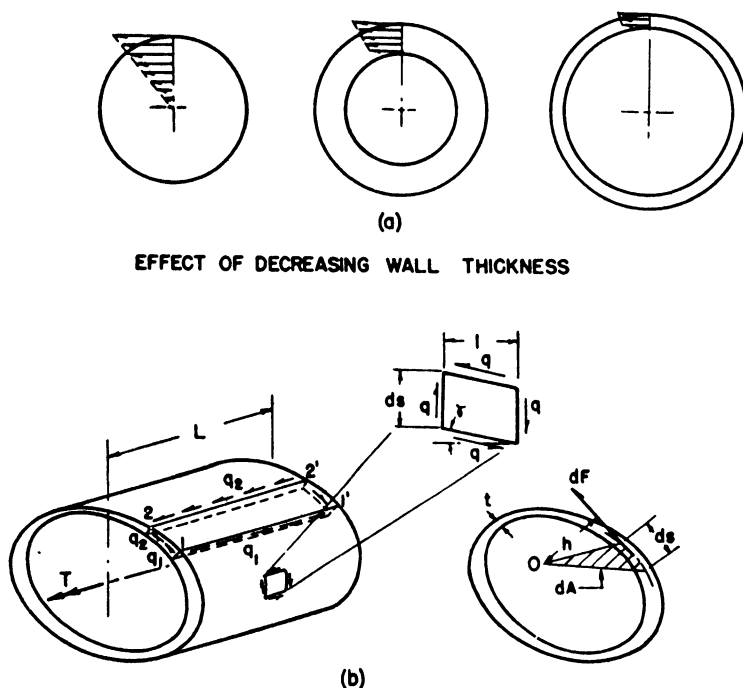
SHEAR FLOW

Fig. 12.5. Torsion of Noncircular Tube.

By assuming that the shear flow at point 1 is q_1 and that the shear flow at point 2 is q_2, then the shear flow along the cylindrical element 11' is q_1 and along 22' it is q_2. Since there are no axial forces acting on the cylinder, then for equilibrium in the axial direction we have

$$\Sigma F = 0 = q_1 L - q_2 L$$

or $$q_1 = q_2 \qquad (12.10)$$

By calling the shear flow along the periphery q, its value can be expressed in terms of the torque producing it. For an element of length ds of the periphery, the shear force is $q \, ds$. The torque about any point 0 due to this force is the force times the perpendicular distance h between the force and 0. But h times ds is twice the area dA of the shaded tri-

angle. Hence, the torque contribution dT of the shear flow along a length ds is

$$dT = qh\, ds = 2q\, dA$$

and the total torque is $\quad T = \int_A 2q\, dA$

Since q is constant, $\quad T = 2qA$

$$q = \frac{T}{2A} \qquad (12.11)$$

where A is the *enclosed* area of the mean periphery of the tube. The shear stress at any section is the shear flow divided by the thickness at that section or

$$f_s = \frac{T}{2At} \qquad (12.12)$$

The deformation of the thin-walled tube due to torque is determined most easily by use of Castigliano's theorem. Consider the element of unit length of the tube surface shown in Figure 12.5(b). The force on the left side of the element is $q\, ds$, and this force moves a distance $\gamma \times 1$ where γ is the change in the slopes of the horizontal elements of the tube. The elastic energy in this element is therefore

$$dU = \frac{q\, ds}{2}\, \gamma$$

But γ is the shear strain so that

$$\gamma = \frac{f_s}{G} = \frac{q}{Gt}$$

and $\quad q = \frac{T}{2A}$

Therefore, $\quad dU = \frac{T^2}{8A^2 Gt}\, ds$

$$U = \oint_c \frac{T^2}{8A^2 Gt}\, ds$$

The integral is the line integral around the closed periphery of length c. In accordance with Castigliano's theorem

$$\theta = \frac{\partial U}{\partial T} = \oint_c \frac{T}{4A^2 Gt}\, ds \qquad (12.13)$$

Since t is the only variable around the periphery, Equation 12.13 can be written in the following alternate forms

$$\theta = \frac{T}{4A^2 G} \oint_c \frac{ds}{t}$$

$$\theta = \frac{q}{2AG} \oint_c \frac{ds}{t} \qquad (12.14)$$

where $\qquad \theta =$ angle of twist per unit length (rad/in).

If necessary, the integral can be approximated by the sum of the quotients of the small elements of length Δs and the average thickness t for the intervals Δs. If the thickness is constant, the value of the integral is simply the length of the periphery divided by the thickness.

In each case for both open and closed sections the angle of twist per unit length can be expressed in terms of the torque, the geometric properties of the cross section, and the shear modulus of the material. It is convenient sometimes to combine the geometric properties of the cross section into one coefficient C. Thus,

$$\theta = \frac{T}{GC}$$

where $\qquad C = \dfrac{4A^2}{\oint \dfrac{ds}{t}}$ for thin-walled tubes

$$C = \frac{bt^3}{3} \text{ for thin rectangles, and so on.}$$

12.6 Comparison of open and closed sections in torsion. A comparison of the strength and rigidity characteristics of open-section and
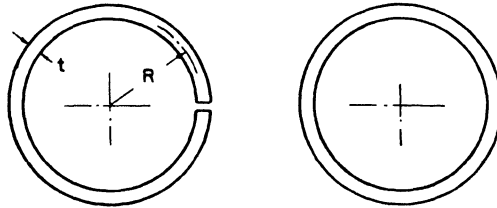
Fig. 12.6. Open and Closed Sections.

closed-section torsion members having the same cross-sectional area will indicate why, whenever possible, the open section is avoided for the transmission of torque.

A circular split tube and a closed tube of the same material, diameter, and wall thickness are shown in Figure 12.6. By assuming that the ends of each tube are free to warp, Equations 12.6, 12.12, and 12.14 previously developed can be used.

The stress in the open section is

$$f_{so} = \frac{3T}{bt^2} = \frac{3T}{2\pi Rt^2}$$

and for the closed section

$$f_{sc} = \frac{T}{2At} = \frac{T}{2\pi R^2 t}$$

Hence, $\qquad \dfrac{f_{so}}{f_{sc}} = \dfrac{3R}{t}$

If, for example, $R = 2$ inches and $t = 0.10$ inches, then $f_{so}/f_{sc} = 60$. In other words, the stress in the split tube is 60 times the stress in the closed tube for the same torque.

The angle of twist per unit length of the open section is

$$\theta_o = \frac{3T}{bt^3G} = \frac{3T}{2\pi Rt^3G}$$

and for the closed section

$$\theta_c = \frac{T}{4A^2G}\oint_c \frac{ds}{t} = \frac{T2\pi R}{4(\pi R^2)^2Gt}$$

Therefore,

$$\frac{\theta_o}{\theta_c} = \frac{3R^2}{t^2}$$

For the case $R = 2$ inches and $t = 0.10$ inches, $\theta_o/\theta_c = 1200$. The open tube is 1200 times more flexible than the closed tube.

Since open sections are weak in torsion, the effect of open-section stringers such as angles and channels on the torsional strength of closed boxes such as wings and fuselages is usually neglected.

12.7 Torsion of two-cell torque box. In many instances torque members used in aircraft construction are thin-walled tubes having two

(a)

(b)
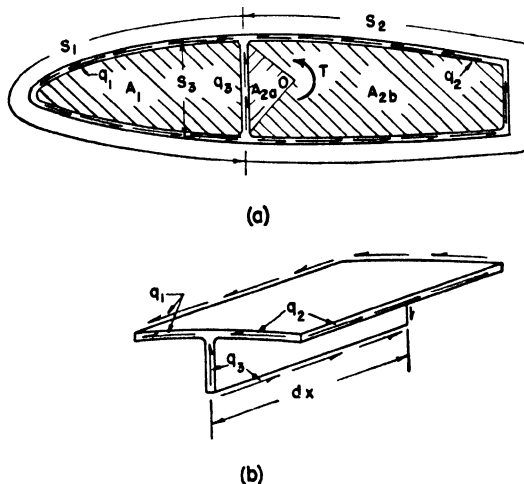
Fig. 12.7. Two-Cell Torque Box.

or more compartments or cells. An example is the wing section shown in Figure 12.7.

It is apparent that for equilibrium in the longitudinal direction the shear flow is constant in any wall, as indicated by Equation 12.10. The shear flow, however, may have a different value in each of the walls. By assuming shear flows in each of the three walls where they join and

isolating a length of the joint dx as indicated in Figure 12.7(b), then for equilibrium in the x direction we have

$$\Sigma F_x = 0 = q_1\, dx - q_2\, dx - q_3\, dx$$
$$q_1 = q_2 + q_3 \tag{12.15}$$

The shear flow out of the connection equals the shear flow in. The torque of the shear flows around any point 0 is equal to twice the swept area times the shear flow or

$$T = 2q_1(A_1 + A_{2a}) - 2q_3 A_{2a} + 2q_2 A_{2b}$$
But $\qquad q_3 = q_1 - q_2$
Therefore, $\quad T = 2q_1(A_1 + A_{2a}) - 2q_1 A_{2a} + 2q_2 A_{2a} + 2q_2 A_{2b}$
$$= 2q_1 A_1 + 2q_2 A_2 \tag{12.16}$$

where $\qquad\qquad\qquad A_2 = A_{2a} + A_{2b}$

This equation has two unknowns, q_1 and q_2, so that an additional condition is required for a solution. This condition is obtained from a consideration of the twist of the cells.

Since the cells are connected together, the twist of cell number one must equal the twist of cell number two. The two cells have the vertical wall in common. By considering the left cell as composed of the nose section and the vertical wall and using the second form of Equation 12.14, then

$$\theta_1 = \frac{1}{2A_1 G}\left[q_1 \int_0^{s_1} \frac{ds}{t} + q_3 \int_0^{s_3} \frac{ds}{t} \right]$$

and similarly $\qquad \theta_2 = \frac{1}{2A_2 G}\left[q_2 \int_0^{s_2} \frac{ds}{t} - q_3 \int_0^{s_3} \frac{ds}{t} \right]$

Let $\qquad\qquad\qquad a_1 = \int_0^{s_1} \frac{ds}{t}$

$$a_2 = \int_0^{s_2} \frac{ds}{t}$$

$$a_{12} = \int_0^{s_3} \frac{ds}{t}$$

where s is taken positive in the direction of the assumed shear flow. By substituting $q_3 = q_1 - q_2$ into the above equations, the condition $\theta_1 = \theta_2$ gives

$$\frac{1}{2A_1 G}[q_1 a_1 + (q_1 - q_2)a_{12}] = \frac{1}{2A_2 G}[q_2 a_2 - (q_1 - q_2)a_{12}] \tag{12.17}$$

The solution of the simultaneous Equations 12.16 and 12.17 for q_2 results in

$$q_2 = \frac{T}{2}\left[\frac{a_1 A_2 + a_{12} A}{a_1 A_2^2 + a_{12} A^2 + a_2 A_1^2} \right] \tag{12.18}$$

where $\qquad\qquad\qquad A = A_1 + A_2$

Knowing q_2, then q_1 and q_3 can then be determined by means of Equations 12.16 and 12.15.

EXAMPLE 12.1. A two-cell torque box similar to the one shown in Figure 12.7 carries a torque of 120,000 lb in. Determine the shear flow and shear stress in each wall, assuming that the wall thickness is constant for each cell.

Thickness of nose section $t_1 = 0.025$ in
Thickness of web $t_3 = 0.051$ in
Thickness of aft cell $t_2 = 0.032$ in
                       $A_1 = 170$ in^2
                       $A_2 = 390$ in^2
                       $s_1 = 36$ in
                       $s_2 = 70$ in
                       $s_3 = 15$ in

Solution. Since the wall thickness is constant for each cell

$$a_1 = \int_0^{s_1} \frac{ds}{t_1} = \frac{s_1}{t_1} = \frac{36}{0.025} = 1440.$$

$$a_2 = \int_0^{s_2} \frac{ds}{t_2} = \frac{s_2}{t_2} = \frac{70}{0.032} = 2188$$

$$a_{12} = \int_0^{s_3} \frac{ds}{t_3} = \frac{s_3}{t_3} = \frac{15}{0.051} = 294$$

From Equation 12.18

$$q_2 = \frac{T}{2}\left[\frac{a_1 A_2 + a_{12}A}{a_1 A_2^2 + a_{12}A^2 + a_2 A_1^2}\right]$$

$$= \frac{120,000}{2}\left[\frac{(1440 \times 390) + 294(170 + 390)}{1440(390)^2 + 294(170 + 390)^2 + 2188(170)^2}\right]$$

$$= 116 \text{ lb/in}$$

From Equation 12.16

$$q_1 = \frac{T - 2q_2 A_2}{2A_1} = \frac{120,000 - (2 \times 116 \times 390)}{2 \times 170} = 87 \text{ lb/in}$$

By using Equation 12.15

$$q_3 = q_1 - q_2 = 87 - 116 = -29 \text{ lb/in}$$

The minus sign on the value of q_3 indicates that the shear flow is opposite to the direction assumed. Therefore, the shear flow in the web is downward.

The values of the shear stresses are

$$f_{s1} = \frac{q_1}{t_1} = \frac{87}{0.025} = 3,480 \text{ psi}$$

$$f_{s2} = \frac{q_2}{t_2} = \frac{116}{0.032} = 3,625 \text{ psi}$$

$$f_{s3} = \frac{q_3}{t_3} = \frac{29}{0.051} = 570 \text{ psi}$$

12.8 Multi-cell torque box. In some cases there may be more than two cells in a torque box. The analysis of a multi-cell torque box is essentially the same as for the two-cell box. There will be one equation for the torque in terms of the n unknown shear flows and $n - 1$ equations relating the angles of twist of the adjacent cells. These equations then are solved simultaneously for the unknown shear flows.
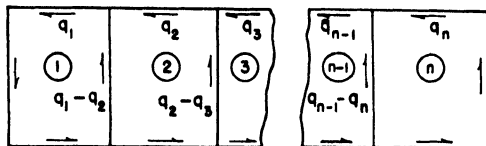
Fig. 12.8. Multi-Cell Torque Box

Figure 12.8 schematically indicates a torque box with n cells. The shear flow in each web can be expressed in terms of the shear flow in the skin of the adjacent cells by applying the rule that the shear flow going into a joint is equal to the shear flow going out. Thus, the shear flow on the web between 1 and 2 is $q_1 - q_2$. The torque is therefore

$$T' = 2q_1A_1 + 2q_2A_2 + \cdots 2q_nA_n \qquad (12.19)$$

and the angle of twist for cells one, two, three, and so on, is

$$2G\theta_1 = \frac{1}{A_1}[q_1a_1 + (q_1 - q_2)a_{12}]$$

$$2G\theta_2 = \frac{1}{A_2}[q_2a_2 - (q_1 - q_2)a_{12} + (q_2 - q_3)a_{23}] \qquad (12.20)$$

$$2G\theta_n = \frac{1}{A_n}[q_na_n - (q_{n-1} - q_n)a_{(n-1)n}]$$

There are $n - 1$ equations which result when the angles of twist are equated.

$$\theta_1 = \theta_2 \qquad (12.21)$$

$$\cdots \cdots \cdots$$

$$\theta_{n-1} = \theta_n$$

Equations 12.19 and 12.21 are then solved simultaneously for the unknown shear flows.

12.9 Nonuniform torsion. It has been shown that open-section members are very much more flexible and weaker than closed-section members subjected to torque. The suggestion has been made that open-section members are to be avoided wherever possible for torque-carrying structures. However, open-section members cannot always be avoided. For example, although a fuselage is mainly a closed member, there are always access openings, bomb-bays, and other openings whose covers cannot always be designed to carry the load across the opening in the same

manner as the load is carried in a completely closed section. Fortunately, there are other considerations which effectively stiffen the structure in these weak regions.

In all the torque analyses made thus far it has been assumed that the ends of the torque members are unrestrained so that the end cross sections can move in the longitudinal direction in any manner whatsoever. If a piece of paper is rolled up to form a tube and one end rotated with respect to the other, it will be noticed that the ends which are originally in a plane perpendicular to the longitudinal axis of the tube will not lie in a plane after the tube is twisted. In fact, the corners of the paper may move a considerable distance in the longitudinal direction. If the ends are restrained from warping by heavy end plates, then it will be found

(a)   (b)
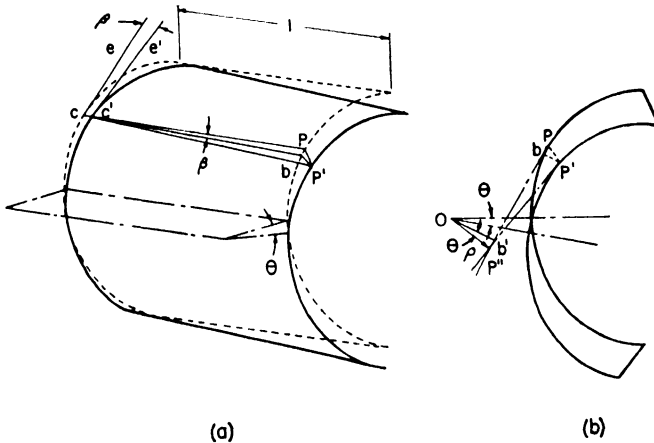
Fig. 12.9. Warping of C Section.

that the tube is stiffened considerably. We will call this *restrained torsion*.

An analysis of an open section with consideration of the warping will be made. This analysis is not rigorous, but it will show the nature of the problem. Consider the thin-walled *C*-section cylinder shown in Figure 12.9. The curved line representing the end section is the median line between the sides of the thin wall. If a torque is applied at each end so as to rotate the right end clockwise relative to the left, then since the shear stress is zero along the median line the net deformation due to shear strain will be zero. However, the right end will rotate as a rigid body about the center of twist 0, and the cylinder will distort, as shown in Figure 12.9(a).

A point p on the right end will rotate to its new position p'. The amount this point moves in a plane tangent to the shell surface and containing the line pc is pb. If a tangent pb' is drawn perpendicular to

the cylindrical element cp and a similar tangent at p' constructed, then the amount p moves in the tangential direction is $b'p''$. Now if ρ is the perpendicular distance from 0 to the tangent pb' then $b'p'' = \theta\rho$ and

$$pb = \theta\rho$$

The angle β between cp and $c'b$ is $\dfrac{pb}{1}$ or

$$\beta = \theta\rho$$

Since cc is a tangent at c on the left end before distortion and $c'e'$ is a tangent at the corresponding point c' after distortion, then ce is perpendicular to cp and $c'e'$ is perpendicular to $c'b$ which makes the angle between ce and $c'e'$ equal to β.
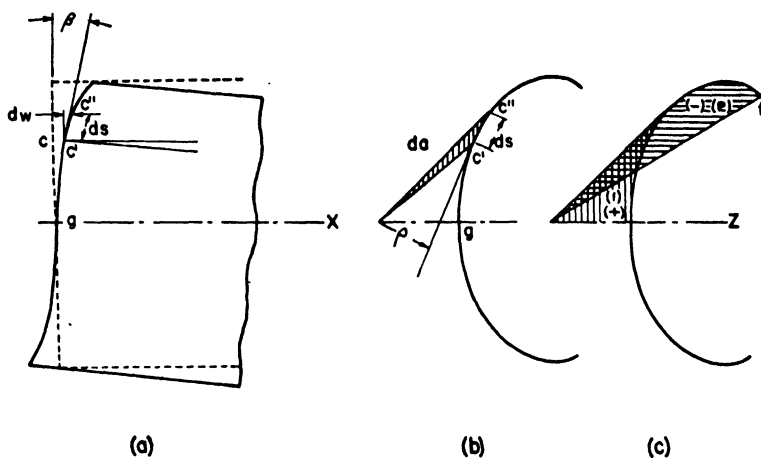
Fig. 12.10.   Swept Areas.

If we refer now to Figure 12.10, it is evident that the longitudinal distance c has moved is cc' and this is called the *warp at* c. The change in warp between point c' and a point on the periphery of the shell a distance ds from it will be called dw. If we assume that the angle β is a constant for the small distance ds, then

$$dw = \beta \, ds = \theta\rho \, ds \qquad (12.22)$$

But $\rho \, ds$ is twice the area of the shaded portion shown in Figure 12.10(b). If this small shaded area is called da, then

$$dw = 2\theta \, da \qquad (12.23)$$

In other words, the change in warping between two adjacent points a distance ds apart on the periphery is twice the area swept by the radius vector from the center of twist in moving a distance ds.

The warp at any point on the periphery is

$$w = 2\theta \int da$$
$$= 2\theta a + B$$

where $B =$ an arbitrary constant of integration.

If the swept area is measured from a point where the warp is zero, such as point g, then the warp is

$$w = 2\theta a \qquad (12.24)$$

where a is measured from the point of zero warp to the point where the warp w is to be determined. It should be pointed out that the swept area is positive for the radius vector moving counterclockwise and negative for the radius vector moving clockwise. Thus, the swept area to point f in Figure 12.10(c) is the algebraic sum of the positive area (1) and the negative area (2). The double-crosshatched area is positive when the radius vector is moving counterclockwise and negative when the radius vector is moving clockwise so that these areas cancel.

The ends of the cylinder are eventually to be restrained from warping. This does not mean that the warp of every cross section will be zero. Therefore, it is reasonable to assume that the warp at corresponding points of two different cross sections will be different. Let

$$w = \theta 2a = \theta w_1 \qquad (12.25)$$

where $w_1 =$ the warp at any point per unit angle of twist; w_1 is the same for similar points on different cross sections and is a geometric property of the sections. The rate of change of w along the longitudinal direction is

$$\frac{dw}{dx} = \frac{d\theta}{dx} w_1$$

But $\frac{dw}{dx}$ is the longitudinal strain in the x direction and if there are no lateral stresses, the stress in the x direction is

$$f = E \frac{dw}{dx} = E \frac{d\theta}{dx} w_1 \qquad (12.26)$$

If the stress is different at corresponding points on two different cross sections, then the force on an area dA of the right end of an element of the cylinder of length dx shown in Figure 12.11 is $(f + df)\, dA$ and the force on the left end for the same area is $f\, dA$. The shear flows on the two longitudinal sides of the element are q and $q + dq$. For equilibrium in the x direction

$$(f + df)\, dA + q\, dx - f\, dA - (q + dq)\, dx = 0$$
$$dq = \frac{df}{dx}\, dA$$

But
$$\frac{df}{dx} = E \frac{d^2\theta}{dx^2} w_1$$

Therefore,
$$dq = E \frac{d^2\theta}{dx^2} w_1 \, dA \tag{12.27}$$

The torque on any cross section of the cylinder is the sum of the shear flow times twice the area swept out by the radius vector from any convenient point such as the center of twist or

$$T_1 = \int_{A_1} q2 \, da = \int_{A_1} q \, dw_1 \tag{12.28}$$

where A_1 is the total swept area. Integrating this by parts, we have

$$T_1 = qw_1 \Big|_{A_1} - \int_{A_1} w_1 \, dq \tag{12.29}$$

For a section symmetrical about the z axis the value of the summation of qw_1 for the whole swept area A_1 is zero since there is as much area swept
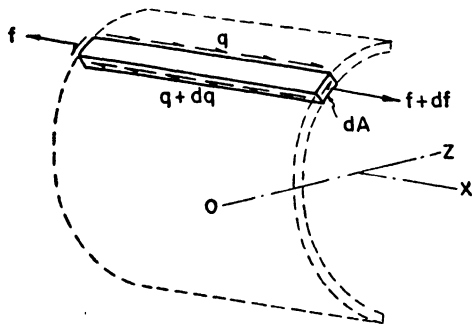
Fig. 12.11. Shear Flow on Element of Shell.

out in the positive direction as in the negative direction and q has the same sign at corresponding points above and below the z axis. Therefore, $qw_1\Big|_{A_1}$ of Equation 12.29 is zero. Hence, for symmetrical sections the torque due to the variation in warping between sections is

$$T_1 = - \int_{A_1} w_1 \, dq$$

But
$$dq = E \frac{d^2\theta}{dx^2} w_1 \, dA$$

Therefore,
$$T_1 = - E \frac{d^2\theta}{dx^2} \int_A w_1^2 \, dA$$

The integral of $w_1^2 \, dA$ is a geometric property of the cross section which we will call Γ. Thus,

$$T_1 = -E\Gamma \frac{d^2\theta}{dx^2} \tag{12.30}$$

The total torque on the cylinder will consist of the torque due to the variation of warping between sections and the Saint Venant torque due to the usual open-section shear-stress distribution. Since the Saint Venant torque is $T_2 = GC\theta$, the total torque is

$$T = GC\theta - E\Gamma \frac{d^2\theta}{dx^2} \tag{12.31}$$

where GC = torsional rigidity of the open section with ends free to warp

$$\Gamma = \int_A w_1^2 \, dA$$

From Equation 12.26 the axial stress at any point of the cross section is

$$f = E \frac{d\theta}{dx} w_1$$

where

$$w_1 = \int_a 2 \, da$$

If the applied torque is known, the angle of twist per unit length can be determined from Equation 12.31.

Equation 12.31 can be used for the case of a torsion member with restrained ends as well as for members for which the torque varies along the length. When T is variable, the solution of the equation is more difficult than the solution that follows for the case of constant torque. It can be shown in general that if the torque is not constant, axial tension and compression stresses of considerable magnitude are developed even though the ends of the member are not restrained from warping.

Equation 12.31 will be rewritten as

$$\theta - k^2 \frac{d^2\theta}{dx^2} = \frac{T}{GC}$$

where

$$k^2 = \frac{E\Gamma}{GC} \tag{12.32}$$

The solution of this equation for *constant* applied torque is

$$\theta = \frac{T}{GC}\left[1 + D_1 e^{\frac{x}{k}} + D_2 e^{-\frac{x}{k}}\right] \tag{12.33}$$

where D_1 and D_2 are arbitrary constants to be evaluated by the boundary conditions. Since $\sinh y = \frac{1}{2}(e^y - e^{-y})$ and $\cosh y = \frac{1}{2}(e^y + e^{-y})$, Equation 12.33 can be written also in a form that is sometimes more convenient.

$$\theta = \frac{T}{GC}\left[1 + B_1 \cosh \frac{x}{k} + B_2 \sinh \frac{x}{k}\right] \tag{12.34}$$

where again B_1 and B_2 are arbitrary constants.

It will be shown in the example that follows that considerable axial stresses can exist in open-section torque members if the ends are com-

pletely restrained from warping. In actual practice complete restraint of the ends is seldom realized since very rigid end plates are required. In the case of a fuselage, for example, the portion of the fuselage adjacent to the cutout comprising the open section is usually reinforced with a bulkhead, a stiffening around the opening, or by means of a stiffener ring. These stiffening members are not completely rigid so that an analysis assuming complete fixity of the ends of the cutout portion gives only an indication of the stresses. The actual stresses in members of this type are extremely complicated; and, although the methods given here are suitable for preliminary stress checks, tests should be made before the final design is completed.

Except for the uniform circular section that does not warp, the same type of stress condition exists in closed members subjected to torque where the ends are restrained from warping. Thus, we would expect axial stresses to develop where the wing joins the fuselage when the wing is subjected to torque. The axial stresses due to restrained warping for the closed section are usually of more of a local character than for the open section. This so called "root effect" should be investigated for critical conditions.

EXAMPLE 12.2. An aluminum I beam 3 feet long and with the cross section shown in Figure 12.12, has heavy end plates to prevent the ends from warping. If a torque T is applied at one end while the other end is held fixed, determine

(1) expression for angle of twist per unit length, θ
(2) maximum axial stress at fixed end
(3) shear stress in flange at fixed end.

The dimensions of the cross section are $h = 12$ in, $b = 5$ in, $t_2 = 0.544$ in, and $t_1 = 0.175$ in.

Solution. If we consider the cross section composed of three rectangles, the torsional constant C is

$$C = \frac{2bt_2^3 + h_1t_1^3}{3} = \frac{2 \times 5(0.544)^3 + 10.91(0.175)^3}{3} = 0.556 \text{ in}^4$$

The center of twist is at the midpoint of the web. The warp per unit angle of twist of any point on the median line of the flange is

$$w_1 = 2a = 2\left(\frac{sd}{4}\right) = 5.728s$$

and

$$\Gamma = \int_A w_1^2 \, dA = 4 \int_0^{2.5} (5.728s)^2 t_2 \, ds = 371.84 \text{ in}^6$$

$$k^2 = \frac{E\Gamma}{GC} = \frac{10.5 \times 10^6 \times 371.84}{3.8 \times 10^6 \times 0.556} = 1848$$

$$k = 42.98 \text{ in}$$

$$\frac{L}{2k} = \frac{36}{2 \times 42.98} = 0.419$$

By using the solution in the form of Equation 12.34, the part containing the sinh term can be omitted since θ is symmetrical about $x = 0$. That is for $x < 0$, $\theta > 0$, and for $x > 0$, $\theta > 0$; and the only
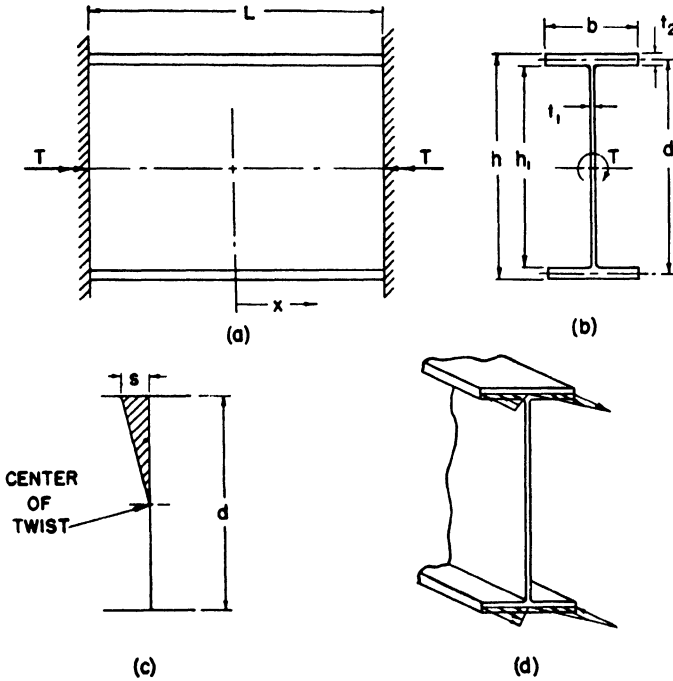
Fig. 12.12. Torsion of I-Beam with Ends Restrained from Warping.

functions satisfying these conditions are the constant term and the cosh term. Therefore,

$$\theta = \frac{T}{GC}\left[1 + B_1 \cosh \frac{x}{k}\right]$$

At the fixed end where $x = \frac{L}{2}$ the warp at every point is zero.

$$w = \theta w_1 = 0$$

Therefore,

$$\theta = 0 \text{ at } x = \frac{L}{2}$$

Then

$$0 = \frac{T}{GC}\left[1 + B_1 \cosh \frac{L}{2k}\right]$$

$$B_1 = -\frac{1}{\cosh \dfrac{L}{2k}}$$

and

$$\theta = \frac{T}{GC}\left[1 - \frac{\cosh \dfrac{x}{k}}{\cosh \dfrac{L}{2k}}\right]$$

Now $\qquad \cosh \dfrac{L}{2k} = 1.089$

so that $\qquad \theta = \dfrac{T}{GC}\left[1 - 0.918 \cosh \dfrac{x}{k}\right]$

The maximum angle of twist per unit length is at the midsection where $x = 0$. Therefore,

$$\theta_{\max} = \dfrac{T}{GC}\,[1 - 0.918] = 0.082\,\dfrac{T}{GC}$$

The angle of twist per unit length for the beam without end restraints would be T/GC. Therefore, restraining the ends reduces the maximum value of θ about 92%.

The axial stress is given by Equation 12.26:

$$f = E\dfrac{d\theta}{dx}\,w_1$$

But $\qquad \dfrac{d\theta}{dx} = \dfrac{d}{dx}\left[\dfrac{T}{GC}\left(1 - \dfrac{\cosh \dfrac{x}{k}}{\cosh \dfrac{L}{2k}}\right)\right]$

$$= -\dfrac{T}{GCk}\dfrac{\sinh \dfrac{x}{k}}{\cosh \dfrac{L}{2k}}$$

At the fixed end $x = \dfrac{L}{2}$

$$f = -\dfrac{TE}{GCk}\,w_1 \tanh \dfrac{L}{2k}$$

Substituting $w_1 = 5.728s$ for the left side of top flange gives

$$f = -\dfrac{T \times 10.5 \times 10^6 \times 5.728s \times 0.397}{3.8 \times 10^6 \times 0.556 \times 42.98} = -0.262Ts$$

Therefore, the stress varies uniformly across the flange, and the stress at the left corner of the upper flange where $s = 2.5$ in is

$$f = -0.655T \text{ (compression)}$$

The axial stress distribution is shown in Figure 12.12(d).
From Equation 12.27

$$dq = E\dfrac{d^2\theta}{dx^2}\,w_1\,dA$$

Therefore, $$q = E \frac{d^2\theta}{dx^2} \int w_1 \, dA$$

But $$\frac{d^2\theta}{dx^2} = -\frac{T}{GCk^2} \frac{\cosh \dfrac{x}{k}}{\cosh \dfrac{L}{2k}}$$

and at the fixed end where $x = \dfrac{L}{2}$

$$q = -\frac{ET}{GCk^2} \int w_1 \, dA$$

$$q = -\frac{ET}{GCk^2} \int_{2.5}^{s} (5.728s) t_2 \, ds$$

$$= -0.00419 Ts^2 \bigg|_{2.5}^{s} = -0.00419(s^2 - 6.25)T$$

12.10 Allowable stresses for torsion members. Unfortunately few data are available of a general nature concerning the ultimate allowable stresses for torsion members. The data that are available are in scattered references and usually are based on test results for specific types of members such as D sections, circular tubes or rods, boxes, and so forth. If the allowable load is based on an allowable stress that does not exceed the proportional limit of the material, then since the equations for the stresses in torsion members are based on the assumption that the material is elastic, the equations can be used directly unless buckling occurs. However, if the design load produces stresses that exceed the proportional limit of the material, then the allowable stress may be based on rupture, buckling, or a specified permanent set, and the elementary equations for predicting the stresses are not valid.

The data for the allowable stresses for the ultimate load of circular tubes are expressed usually in terms of a modulus of rupture in a manner similar to the allowable stresses for a beam in bending. The torsional modulus of rupture is the fictitious stress at which failure would occur if the stress distributions for the elastic material were valid up to the rupture point. Thus, for a circular rod or tube the torsional modulus of rupture is

$$TMR = \frac{T_{max} r}{J} \tag{12.35}$$

where T_{max} is the maximum torque the member can withstand without rupture or buckling failure. The maximum torque is determined by means of tests. Curves for the torsional modulus of rupture for circular tubes are given in the ANC-5.

Problems

12.1. A hollow steel propeller shaft is transmitting a torque of 3000 lb ft. If the shaft is 4 feet long and has an outer diameter of 3 inches and an inner diameter of $2\frac{1}{2}$ inches, determine

    (a) maximum shear stress
    (b) angle of twist.

12.2. A channel beam with cross section as shown in Figure 11.16 is loaded at the ends with forces of 100 pounds. If the line of action of the loads is along the center line of the web and the ends are not restrained from warping, determing

    (a) torque
    (b) maximum shear stress caused by torque. (Neglect stress concentrations.)

12.3. Determine the thickness of a 1-inch 4130 alloy-steel circular-control tube to carry a limit torque of 5,000 lb in if the allowable shear stress is 40,000 psi.

12.4. Determine the size of the lightest standard 4130 circular tube, 24 inches long, to carry an ultimate torque of 50,000 lb in. The ends of the tube are hinged.

12.5. Three shafts having the same weight and length and made of the same material are subjected to the same torque. The cross sections of the shafts are a solid circle, a square, and a rectangle for which the length is ten times the thickness. Determine

    (a) strongest shaft
    (b) most flexible shaft.

12.6. Determine the location of the maximum shear stress for a torsion member having an elliptical cross section and for one having an equilateral triangular cross section.
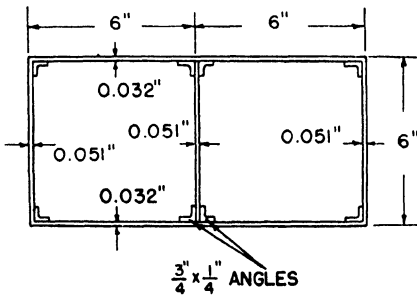
Fig. 12.13. Two-Cell Rectangular Torque Box.

12.7. Determine the shear flows in the walls and the angle of twist per unit length of the aluminum 2-cell rectangular torque box shown in Figure 12.13 if the applied torque is 9,000 lb in.

12.8. A 2-cell wing section similar to the one shown in Figure 12.7, except that it is symmetrical about a horizontal line, is to transmit a torque of 95,000 lb in. The length of the skin around the nose is 30 inches and has a thickness of 0.025 inches, whereas the distance measured along the top skin of the aft cell from the front web to the rear web is 30 inches and the skin thickness is 0.032 inches. The height of the front web is 16 inches and it is 0.051 inches thick. The height of the rear web is 10 inches and it is 0.032 inches thick. The enclosed area of the front and rear cells respectively are 150 in² and 381 in². Determine the shear flows and shear stresses in the walls.

12.9. If another web 0.051 inches thick is added to the wing section of problem 12.8 midway between the front and rear webs, determine the shear flows and shear stresses.

12.10. The I beam of Example 12.2 but of very long length is to be fixed at one end but free at the other. If a torque of 10,000 lb in is applied at the free

end, determine the maximum axial stress. (*Hint:* Use the exponential form of the solution and the fact that as the distance from the fixed end becomes large $\theta \rightarrow T/GC$.)

12.11. An aluminum beam with the cross section as show" in Figure 11.16 is 48 inches long and has ends restrained from warping. If the beam transmits a torque T, determine the maximum axial stress and the shear flow at the juncture of the web and flange at one end.

12.12. Half of a circular-arc fuselage-section model is shown in Figure 12.14. The stringers are spaced every 15° and have an area of 0.0382 square inches.
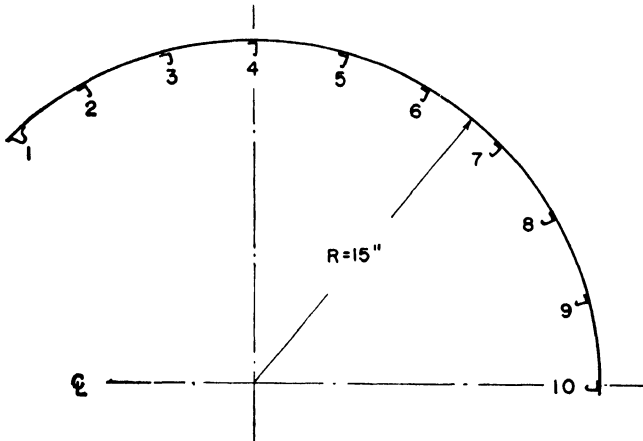
Fig. 12.14. Fuselage Section.

The area of the hat section is 0.360 square inches. The thickness of the skin is 0.016 inches. If the section is 40 inches long and the ends are restrained from warping, determine the axial stress in each stringer at the fixed end and the shear flow between each stringer for an applied torque T. Assume that the shear flow is constant between stringers.

References

Goodier, J. N. and M. V. Barton, "The Effects of Web Deformation on the Torsion of I-beams." *Journal of Applied Mechanics*, March 1944.

Hoff, N. J., "Stresses in Space-Curved Rings Reinforcing the Edges of Cutouts in Monocoque Fuselages." *Journal Royal Aeronautical Society*, September 1943.

Kuhn, Paul and E. M. Moggio, "Stresses Around Large Cutouts in Torsion Boxes." NACA, Tech. Note 1066, May 1946.

Payne, J. H., "Torsion in Box Beams." *Aircraft Engineering*, Vol. XIV, No. 155, January 1942.

Timoshenko, S., *Strength of Materials*, Parts I and II, 2nd Edition. McGraw-Hill, 1940.

Timoshenko, S., *Theory of Elasticity*. McGraw-Hill, 1934.

Von Kármán, Theodore and Wei-Zang Chien "Torsion with Variable Twist." *Journal of Aeronautical Sciences*, October 1946.

Von Kármán, Theodore and H. B. Christensen, "Methods of Analysis for Torsion with Variable Twist." *Journal of Aeronautical Sciences*, April 1944.

CHAPTER 13

Combined Torsion, Bending, and Shear

13.1 Introduction. It is not unusual for an aircraft structural member to transmit torsion, bending, and shear simultaneously. A wing is an example of such a member.

The stress distribution on a section of a member with this combined loading consists of the shear stresses, due to the torsion together with the shear stresses caused by the shear force, and the bending stresses. In the case of nonuniform torsion, the axial stresses caused by the restraint of the warping or varying torque will add algebraically to the bending stresses.

13.2 Bar with rectangular cross section. A bar with a rectangular cross section carrying an eccentric end load is shown in Figure 13.1.

(a)   (b)
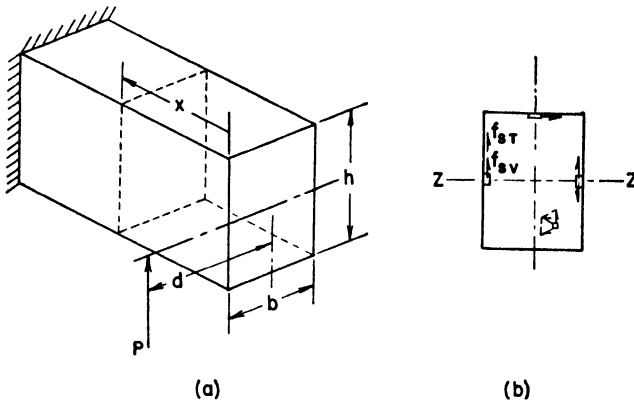
Fig. 13.1. Shear Stresses on Rectangular Bar.

If the load P is a distance d from the center of twist, then the torque at each section of the bar is Pd. The bending moment on any section a distance x from the end where the load is applied is Px, and the shear force on the section is P. The shear force and the torque cause shear stresses each of which may be determined by means of equations previously developed. Hence, the vertical shear stress along the horizontal line z-z due to the shear force is

$$f_{sv} = \frac{V}{bI} \int_{0}^{\frac{h}{2}} y \, dA = \frac{3}{2} \frac{P}{bh}$$

and the shear stress at the midpoint of the long sides due to the torque is

$$f_{sT} = \frac{T}{\alpha ht^2} = \frac{Pd}{\alpha ht^2}$$

Since these two stresses are in the same direction and act on the same area at the center of the long side nearest the load and each is a maximum at this point, the maximum shear stress on the cross section is

$$f_{s(\text{max})} = f_{sV} + f_{sT} = \frac{3}{2}\frac{P}{bh} + \frac{Pd}{\alpha ht^2} \tag{13.1}$$

The shear stresses at other points of the section can be determined separately and added vectorially, as indicated in Figure 13.1(b).

The bending stresses are not shown, but they are linearly distributed about the horizontal axis as in the case for pure bending. Axial stresses due to restraint of warping have not been considered in this case.

13.3 Closed section with flanges (approximate method using shear center). The most obvious manner of analyzing the stress conditions for a member transmitting shear, bending, and torque is to consider the effect of each of these actions separately and then to combine them for the final result, as indicated in the preceding article. In order to determine the applied torque caused by a shear loading, however, the position of the shear center must be known since the torque is the shear force times the perpendicular distance to the shear center. The position of the shear center for open sections having heavy flanges usually is determined easily, but in the case of closed sections the determination of the center of twist sometimes becomes difficult. Two methods will be developed for analyzing the shear stresses caused by the shear force: one involving the use of the shear center, the other using a reference axis other than the one through the shear center.

The first development involving the use of the shear center gives an approximate solution. Later, the exact solution will be indicated so that the significance of the approximation can be evaluated.

Consider the beam with a rectangular box section symmetrical about a horizontal axis and having heavy flanges as shown in Figure 13.2. Let a shear load V be applied a distance d from the left side of the box. By assuming that the shear center is located a distance e from the left side, then the shear force V can be considered as acting at the shear center along with a torque T which is equal to $V(e - d)$. The shear force at the shear center will cause only bending. and the torque will cause only twisting.

Consider now the effect of the shear force at the shear center. The shear flows on a section a distance x from the end are assumed in the directions indicated in Figure 13.2(b). The shear flow in the vertical web is

assumed constant as in previous analyses. The shear flow on any side is unknown, and we will assume that the shear flow is q_0 at the center of the top sheet. Since the shear flow varies linearly across the top and bottom side, the average shear flow is q_0. The shear flow on any other side consists of the shear flow q_0 plus, algebraically, any other shear flows required to satisfy the conditions of the problem. It is apparent that for equilibrium of the forces in the horizontal direction the average shear flow on the bottom side must equal q_0 in magnitude. It is apparent also

(a)   (c)

(b)   (d)

SHEAR FLOW FOR   **SHEAR FLOW FOR**
BENDING ONLY   **TORQUE AND BENDING**

Fig. 13.2.   Closed Section with Flanges.

that, since q_0 forms a closed circuit, it has no force resultant but it does provide a torque.

The values of the shear flows q_1 and q_2 which are present on the side webs along with q_0 can be determined from a consideration of the equilibrium of a flange element of length dx. Consider the upper right flange and half of the top sheet shown in Figure 13.2(c). The force on the flange and sheet changes by an amount dP in the distance dx because of the change in bending moment dM. As indicated before

$$dP = A \, df = \frac{dM}{I}\left(y_1 A_1 + \frac{b}{2}\, t_3 y_1\right)$$

Equilibrium of the forces in the x direction demand that

$$\Sigma F_x = 0 = P - (P + dP) + q_0\, dx - q_0\, dx + q_1\, dx$$

or $\qquad q_1 = \dfrac{dP}{dx} = \dfrac{dM}{dx\, I}\left(y_1 A_1 + \dfrac{b}{2} t_3 y_1\right) = \dfrac{V}{I}\left(y_1 A_1 + \dfrac{b}{2} t_3 y_1\right)$ (13.2)

Similarly for the left web

$$q_2 = \frac{V}{I}\left(y_2 A_2 + \frac{b}{2} t_3 y_2\right) \qquad\qquad (13.3)$$

where A_2 = flange area of flange No. 2 (in²)

$\quad b$ = length of top sheet (in)

$\quad t_3$ = thickness of top sheet (in)

$\quad y_2$ = distance of flange No. 2 and top sheet from neutral axis (in).

The shear flow in the left or front web is

$$q_f = q_2 + q_0 \qquad\qquad (13.4)$$

and for the rear web

$$q_r = q_1 - q_0$$

Although q_1 and q_2 can be evaluated since V, I, y, and A are known, q_0 is still unknown. The angle of twist per unit length for a closed section has been stated previously as

$$\theta = \frac{1}{2GA} \oint \frac{q}{t}\, ds \qquad\qquad (13.5)$$

where $\qquad\qquad A$ = enclosed area of section.

Since in this case the shear force is applied at the shear center, the beam will bend without twisting. Early investigators thus assumed that $\theta = 0$ and therefore

$$\oint \frac{q}{t}\, ds = 0 \qquad\qquad (13.6)$$

for the case of bending without twisting. By using this relation the value of q_0 then can be determined.

$$\oint \frac{q}{t}\, ds = 0 = q_0\left(\frac{h}{t_1} + \frac{h}{t_2} + \frac{2b}{t_3}\right) - q_1 \frac{h}{t_1} + q_2 \frac{h}{t_2}$$

$$q_0 = \frac{q_1 \dfrac{h}{t_1} - q_2 \dfrac{h}{t_2}}{\dfrac{h}{t_1} + \dfrac{h}{t_2} + \dfrac{2b}{t_3}} \qquad\qquad (13.7)$$

Equations 13.2, 13.3, 13.4, and 13.7 therefore make it possible to evaluate the shear flows.

If the shear flows are known, the location of the center of twist can be determined. The moment of the applied shear force V about any point

such as the lower left flange is equal to the moment of the shear flows on the section. Referring to Figure 13.2(b) we find that

$$Ve = -2\frac{A}{2}q_0 + 2\frac{A}{2}(q_1 - q_0) = -2Aq_0 + Aq_1$$

$$e = \frac{A(q_1 - 2q_0)}{V} \tag{13.8}$$

The torque on the box is $V(e - d)$. The shear flow caused by this torque is

$$q_T = \frac{V(e - d)}{2A} \tag{13.9}$$

Therefore, the shear flows on the front and rear webs of the box due to the original shear loading acting eccentric to the shear center are

$$q_f = q_0 + q_2 + q_T \atop q_r = q_1 - q_0 - q_T \tag{13.10}$$

and on the top and bottom sides the shear flows are

$$q_s = q_0 + q_T \tag{13.11}$$

13.4 Closed section with flanges· (accurate method using shear center). The determination of the unknown shear flow q_0 in the previous analysis depending on equating the angle of twist per unit length θ to zero for the case of bending without twisting. Thus,

$$\theta = 0 = \frac{1}{2GA} \oint \frac{q}{t}\,ds \tag{13.12}$$

Goodier has shown, however, (reference at end of chapter) that the average angle of twist per unit length for a beam carrying *both bending and torsion* is given by

$$2GA\theta = \oint \frac{q}{t}\,ds - \left(\frac{\mu}{1+\mu}\right)AV\frac{\bar{z}_c}{I} \tag{13.13}$$

where (see Figure 13.3) A = enclosed area of section (in²)

μ = Poisson's ratio

V = shear force in direction of vertical principal axis of section (lb)

$\bar{z}_c$ = z coordinate of centroid of A measured from the center of gravity of the section (in)

I = moment of inertia of section about horizontal principal axis z (in⁴).

The condition for zero twist in the case of bending without torsion therefore becomes

$$\oint \frac{q}{t}\,ds = \frac{\mu}{1+\mu}AV\frac{\bar{z}_c}{I} \tag{13.14}$$

instead of the relation 13.12 previously assumed.

The development of Goodier's theorem depends on a knowledge of the theory of elasticity which is beyond the scope of this text.   However, the use and significance of the theorem will be indicated.

The analysis of the last article is correct up to the determination of the shear flow q_0 in Equation 13.7.   By using Goodier's theorem this relation becomes

$$\oint \frac{q}{t}\,ds = \frac{\mu}{1+\mu}\,AV\frac{\bar{z}_c}{I} = q_0\left(\frac{h}{t_1} + \frac{h}{t_2} + \frac{2b}{t_3}\right) - q_1\frac{h}{t_1} + q_2\frac{h}{t_2}$$

Thus,
$$q_0 = \frac{\dfrac{\mu}{1+\mu}\,AV\dfrac{\bar{z}_c}{I} + q_1\dfrac{h}{t_1} - q_2\dfrac{h}{t_2}}{\dfrac{h}{t_1} + \dfrac{h}{t_2} + \dfrac{2b}{t_3}}$$
(13.15)

By using this corrected value of q_0, the analysis proceeds as before.   It is apparent that if the first term of the numerator is small compared with
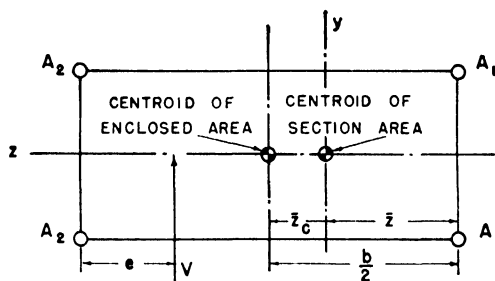
Fig. 13.3.   Coordinate System.

the other terms, the analysis of Article 13.3 can be used with little error. A comparison of these methods will be made in an example.

13.5 Closed section with flanges (approximate method without the use of the shear center).   Before comparing the methods developed in the last two articles for a specific case, a third method will be developed which gives the same results as the first approximate method in a simplified form.

In this method the shear force is not moved to the shear center so that the separate effects of bending and torsion can be evaluated and then combined, but both actions are considered simultaneously.   It is not necessary to know the location of the shear center.

Consider the section shown in Figure 13.4 similar to the section analyzed in the previous article.   A constant shear flow q_c on all the sides and additional shear flows q_2 and q_1 on the front and rear webs will be assumed as before.   The values of q_1 and q_2 are given by Equations 13.2 and 13.3.   Equating the torque of the shear flows on the section

about a reference point such as the lower left flange to the torque of the
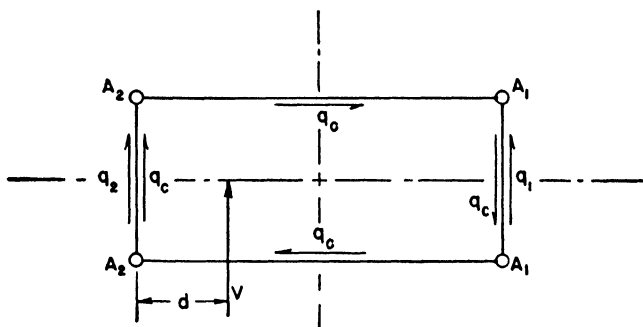
Fig. 13.4.   Shear Flows on Closed Section.

applied shear load about this point, we have

$$Vd = -2Aq_c + Aq_1$$

or
$$q_c = \frac{-Vd + Aq_1}{2A} \qquad (13.16)$$

Therefore, the total shear flow in the front web is

$$q_f = q_2 + q_c = q_2 + \frac{-Vd + Aq_1}{2A}$$

and in the rear web

$$q_r = q_1 - q_c = q_1 - \frac{-Vd + Aq_1}{2A} \qquad (13.17)$$

$$= \frac{q_1}{2} + \frac{Vd}{2A}$$

where
$$q_1 = \frac{V}{I}\left(y_1 A_1 + \frac{b}{2} t_3 y_1\right)$$

$$q_2 = \frac{V}{I}\left(y_2 A_2 + \frac{b}{2} t_3 y_2\right)$$

EXAMPLE 13.1.   Determine the shear flows on the sides of an aluminum rectangular box section similar to that shown in Figure 13.2 if the vertical shear load V is acting along the left web and

$A_1 = 2$ in²	$t_1 = 0.06$ in
$A_2 = 1$ in²	$t_2 = 0.04$ in
$h = 10$ in	$t_3 = 0.04$ in
$b = 30$ in	

The section is the same as that used by Hatcher (see reference at end of chapter).   Everything but the webs are assumed to carry the bending.

The solution will be made by the three methods given in Articles 13.3, 13.4, and 13.5.

Solution.

I. Approximate method using shear center.

$$I = 2\left(\frac{h}{2}\right)^2 (A_1 + A_2) + 2\left(\frac{h}{2}\right)^2 bt_3 + \frac{h^3}{12}(t_1 + t_2) = 2 \times 25(2 + 1)$$

$$+ (2 \times 25 \times 30 \times 0.04) + \frac{(10)^3}{12}(0.04 + 0.06) = 218 \text{ in}^4$$

$$A = bh = 30 \times 10 = 300 \text{ in}^2$$

$$y_1 = y_2 = \frac{h}{2} = 5 \text{ in}$$

$$\frac{h}{t_1} = \frac{10}{0.06} = 166.6$$

$$\frac{h}{t_2} = \frac{10}{0.04} = 250$$

$$\frac{b}{t_3} = \frac{30}{0.04} = 750$$

From Equations 13.2 and 13.3

$$q_1 = \frac{V}{I}\left(y_1 A_1 + \frac{b}{2} t_3 y_1\right) = \frac{V}{218}[(5 \times 2) + (15 \times 0.04 \times 5)] = 0.0596V$$

$$q_2 = \frac{V}{I}\left(y_2 A_2 + \frac{b}{2} t_3 y_2\right) = \frac{V}{218}[(5 \times 1) + (15 \times 0.04 \times 5)] = 0.0367V$$

Using Equation 13.7

$$q_0 = \frac{q_1\dfrac{h}{t_1} - q_2\dfrac{h}{t_2}}{\dfrac{h}{t_1} + \dfrac{h}{t_2} + \dfrac{2b}{t_3}} = \frac{0.0596V(166.6) - 0.0367V(250)}{166.6 + 250 + (2 \times 750)}$$

$$= 0.00040V$$

The location of the shear center is given by Equation 13.8

$$e = \frac{A(q_1 - 2q_0)}{V} = \frac{300(0.0596V - 2 \times 0.00040V)}{V}$$

$$= 17.65 \text{ in}$$

The shear flow due to the torque is obtained by means of Equation 13.9.

$$q_T = \frac{V(e - d)}{2A} = \frac{V(17.65 - 0)}{2 \times 300} = 0.0294V$$

Therefore, the final shear flow in the front web is

$$q_f = q_0 + q_2 + q_T = (0.00040 + 0.0367 + 0.0294)V$$
$$= 0.0665V$$

The shear flow on the rear web is

$$q_r = q_1 - q_0 - q_T = (0.0596 - 0.00040 - 0.0294)V$$
$$= 0.0298V$$

The shear flows on the top and bottom panels are

$$q_s = q_0 + q_T = (0.00040 + 0.0294)V = 0.0298V$$

II. Goodier method. By referring to Figure 13.3, the location of the centroid of the section will be found by taking the moments of the areas of the flange areas and skin about the right web.

$$\bar{z} = \frac{2A_2b + b^2t_3 + hbt_2}{2(A_2 + A_1) + 2bt_3 + h(t_1 + t_2)}$$

$$= \frac{(2 \times 30) + (\overline{30}^2 \times 0.04) + (10 \times 30 \times 0.04)}{2(1 + 2) + (2 \times 30 \times 0.04) + 10(0.04 + 0.06)}$$

$$= 11.49 \text{ in}$$

Therefore, $\bar{z}_c = \dfrac{b}{2} - \bar{z} = 15 - 11.49 = 3.51 \text{ in}$

The shear flows q_1 and q_2 are the same as before, but q_0 is now determined by means of Equation 13.15.

$$q_0 = \frac{\dfrac{\mu}{1 + \mu} AV\dfrac{\bar{z}_c}{I} + q_1\dfrac{h}{t_1} - q_2\dfrac{h}{t_2}}{\dfrac{h}{t_1} + \dfrac{h}{t_2} + \dfrac{2b}{t_3}}$$

$$= \frac{\dfrac{0.3}{1.3} \times \dfrac{300}{150}(3.51)V + 0.0596(166.6)V - 0.0367(250)V}{166.6 + 250 + (2 \times 750)}$$

$$= 0.00098V$$

The location of the shear center is therefore

$$e = \frac{A(q_1 - 2q_0)}{V} = \frac{300(0.0596 - 2 \times 0.00098)V}{V} = 17.30 \text{ in}$$

The shear flow caused by the torque is

$$q_T = \frac{V(e - d)}{2A} = \frac{V(17.30 - 0)}{2 \times 300} = 0.0288V$$

The final shear flows are

$$q_f = q_0 + q_2 + q_T = (0.00098 + 0.0367 + 0.0288)V$$
$$= 0.0665V$$
$$q_r = q_1 - q_0 - q_T = (0.0596 - 0.00098 - 0.0288)V$$
$$= 0.0298V$$
$$q_s = q_0 + q_T = (0.00098 + 0.0288)V = 0.0298V$$

In this particular case the shear flows determined by the Goodier method do not differ significantly from those obtained by the approximate

method. It should be pointed out, however, that the position of the shear center is somewhat different and that the shear flows considering bending only without the torque are different. It is apparent that the greater the distance between the centroid of the section and the centroid of the enclosed area, the greater the error in q_0 as determined by the approximate method.

III. Approximate method without use of shear center. By using Equation 13.16

$$q_c = \frac{-Vd + Aq_1}{2A} = \frac{-V(0) + 300(0.0596)V}{2 \times 300} = 0.0298V$$

Then
$$q_f = q_2 + q_c = 0.0367V + 0.0298V = 0.0665V$$
$$q_r = q_1 - q_c = 0.0596V - 0.0298V = 0.0298V$$

13.6 Single-cell box with stringers. The method developed in Article 13.5 will be used in all the analyses of combined bending, torsion,
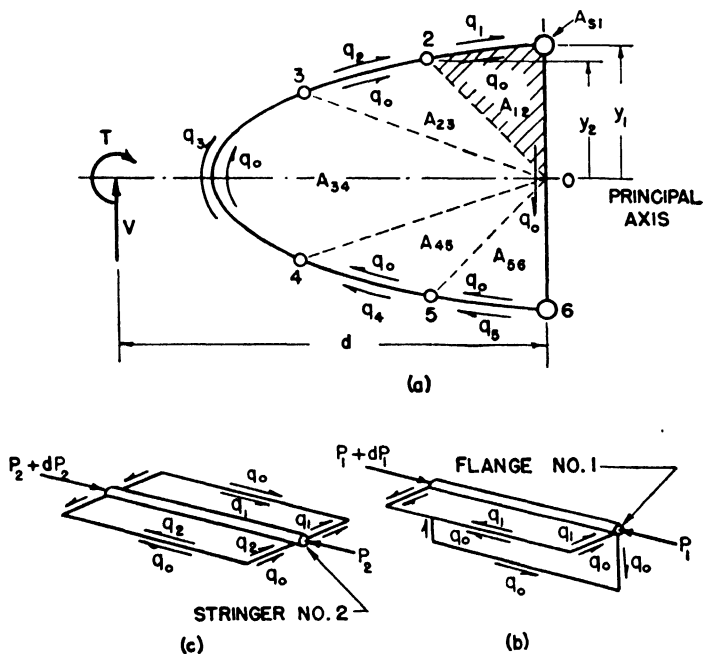
Fig. 13.5.   Single-Cell Box with Stringers.

and shear that follow. It should be emphasized that this method assumes that the correction involving Poisson's ratio indicated by Goodier is not considered. For a rigorous analysis this effect and the variation of shear flow in the webs should be taken into account.

Consider the single-cell section shown in Figure 13.5. A vertical shear force and a torque are applied at some point so as to produce bending of the section about the horizontal principal axis of the section

and a torsion about a longitudinal axis. Any convenient point on the horizontal principal axis such as 0 may be selected as a reference point. The shear flows are assumed composed of a flow q_0 that is constant on all the skin and a part q_v that is constant between stringers but may vary between one set of stringers and the next. The shear flow q_0 is taken as the shear flow in the web in this case. The varying shear flow q_1 between flange 1 and stringer 2 is determined from the equilibrium conditions at flange 1 and is found to be

$$q_1 = \frac{V}{I} y_1 A_{s1} = \frac{V}{I} Q_1 \tag{13.18}$$

where A_{s1} = area of stringer or flange No. 1 and effective skin area acting
with it (in^2)
y_1 = distance from principal axis to A_{s1} (in)
I = moment of inertia of whole section about principal axis (in^4).
This shear flow is assumed to act so that it has a component in the direction of the shear load producing it. A similar analysis of the equilibrium of stringer 2 (Figure 13.5(c)) indicates that

$$q_2 = q_1 + \frac{V}{I} y_2 A_{s2} = \frac{V}{I} (Q_1 + Q_2)$$

The varying shear flow between any stringers k and $k + 1$ is therefore

$$q_k = \frac{V}{I} \sum_{i=1}^{k} Q_i \tag{13.19}$$

where $Q_i = y_i A_{si}$ for any stringer i.
The total shear flow between any two stringers must include also the constant part q_0. Hence, the total shear flow between any two stringers is

$$q_r = q_0 + q_k \tag{13.20}$$

The torque of the applied loads about the reference point is equal to the torque of the shear flows about the same point. If the swept area between stringers 1 and 2 is A_1, and so on, and there are n stringers not including the bottom flange of the spar, then

$$Vd + T = 2q_0 \sum_{k=1}^{n} A_k + 2 \sum_{k=1}^{n} A_k q_k$$

But $\displaystyle\sum_{k=1}^{n} A_k = A$, total enclosed area so that

$$q_0 = \frac{Vd + T}{2A} - \frac{1}{A} \sum_{k=1}^{n} A_k q_k \tag{13.21}$$

where
$$q_k = \frac{V}{I} \sum_{i=1}^{k} Q_i$$

EXAMPLE 13.2. A symmetrical single-cell box beam with stringers similar to the one shown in Figure 13.5 carries a vertical shear load of 500 pounds 8 inches to the left of the vertical web, and a clockwise torque of 2,000 lb in. The thickness of the skin around the nose is 0.040 inches, and the web thickness is 0.064 inches. Other dimensions for the section are given in Table 13.1. Assuming that the bending is resisted only by the stringer areas, determine the shear flows.

Table 13.1

(1)	(2)	(3)	(4)	(5)	(6)	(7)	(8)	(9)	(10)
Stringer no.	A_i = area of str.	y_i	Q_i	$y_i^2 A_i$	ΣQ_i	q_k	A_k	$A_k q_k$	q (total)
See Fig. 13.5	given	meas-ured	(2) × (3)	(3) × (4)	Σ(4)	$\frac{V}{I}$ × (6)	meas-ured	(7) × (8)	q_0 + (7)
1	0.62	5.75	3.565	20.49					
					3.565	34.5	14.38	496	18.8
2	0.14	5.00	0.700	3.50					
					4.265	41.3	17.05	704	25.6
3	0.14	3.62	0.507	1.84					
					4.772	46.2	52.20	2412	30.5
4	0.14	−3.62	−0.507	1.84					
					4.265	41.3	17.05	704	25.6
5	0.14	−5.00	−0.700	3.50					
					3.565	34.5	14.38	496	18.8
6	0.62	−5.75	−3.565	20.49					
Totals				$I = 51.66$			115.1	4812	

Solution. The solution is indicated in the columns of Table 13.1. By using Equation 13.21

$$q_0 = \frac{Vd + T}{2A} - \frac{1}{A} \sum_{k=1}^{n} A_k q_k$$

$$= \frac{(500 \times 8) + 2000}{2 \times 115.1} - \frac{4812}{115.1} = -15.7 \text{ lb/in}$$

The minus sign indicates that the flow is upward on the web.

The shear flows are shown in Figure 13.6.

13.7 Two-cell box with stringers. The method of determining the shear distribution in a two-cell box is similar to the method used in the

previous article except that instead of one unknown shear flow there are now two unknown shear flows to be determined. Equating the angles of twist for each cell gives the additional condition required for solution.

A two-cell box with stringers is shown in Figure 13.7. The vertical shear loads are resolved into a vertical shear force, V, acting normal to the
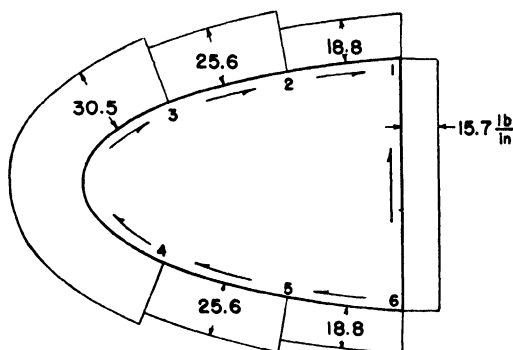
Fig. 13.6. Shear Flows on Single-Cell Box.

horizontal principal axis of the section and a torque, T, about the reference point, 0, which is at the intersection of the front web and the horizontal principal axis. Constant shear flows q_a in the nose and q_b in the aft cell are assumed to be acting as shown; q_a is the total shear flow in the skin just to the left of the top flange of the front spar, and q_b is the shear flow just to the right of the same point. The shear flow between
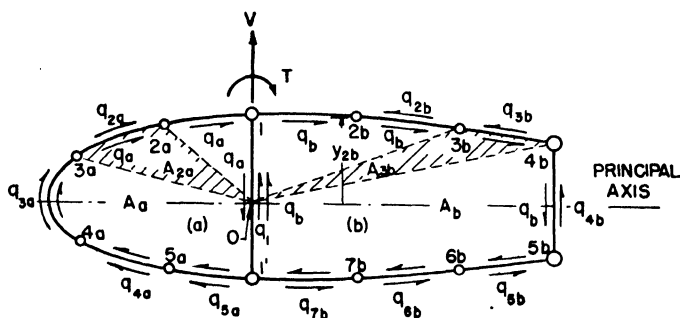
Fig. 13.7. Two-Cell Box with Stringers.

any two stringers in the nose or the aft cell other than the first panel is made up of two components, the constant part and a variable part which represents the change in shear flow due to the stringer load. By numbering the stringers on the aft cell clockwise from the top flange of the front spar which we will call 1, then the total shear flow between stringers 2 and 3 is

$$q_r = q_b - q_{2b} \tag{13.22}$$

but
$$q_{2b} = \frac{V}{I} Q_{2b}$$

$$Q_{2b} = y_{2b} A_{s2b}$$

where A_{s2b} = area of stringer No. 2 and effective skin acting with it on cell b (in^2)

y_{2b} = distance from horizontal principal axis to A_{s2b} (in).

Between any two stringers k and $k + 1$

$$q_{kb} = \frac{V}{I} \sum_{i=2}^{k} Q_{ib} \tag{13.23}$$

A similar expression is valid for the shear flow between the stringers of the nose cell

$$q_{ka} = \frac{V}{I} \sum_{i=2}^{k} Q_{ia} \tag{13.24}$$

A free body diagram of flange No. 1 indicates that the additional shear flow in the front web is

$$q_1 = \frac{V}{I} y_1 A_{s1} \tag{13.25}$$

Since the total torque about the reference point 0 is T, we have

$$T = 2q_a A_a + 2q_b A_b + 2 \sum_{k=2}^{m} q_{ka} A_{ka} - 2 \sum_{k=2}^{n} q_{kb} A_{kb} \tag{13.26}$$

where A_{ka} = area swept out by radius vector from 0 between any stringer k and stringer $k + 1$ (in^2)

A_a = total enclosed area of nose cell (in^2)

A_b = total enclosed area of aft cell (in^2)

m = number of stringers on cell (a), not including the bottom flange of front spar

n = number of stringers on cell (b), not including the bottom flange of front spar.

Equation 13.26 gives one relation with two unknowns, q_a and q_b. Another relationship can be determined by equating the angle of twist of the front and rear cells.

$$\theta_a = \frac{1}{2A_a G} \left\{ \left[\sum_{k=2}^{m} (q_a + q_{ka}) \frac{s_{ka}}{t_{ka}} \right] + q_a \frac{s_{1a}}{t_{1a}} + (q_a - q_b - q_1) \frac{h}{t_w} \right\}$$

$$\theta_b = \frac{1}{2A_b G} \left\{ \left[\sum_{k=2}^{n} (q_b - q_{kb}) \frac{s_{kb}}{t_{kb}} \right] + q_b \frac{s_{1b}}{t_{1b}} + (q_b + q_1 - q_a) \frac{h}{t_w} \right\} \tag{13.27}$$

where s_{ka} = distance measured along skin between any stringer k and $k + 1$ on cell (a) (in)

t_{ka} = thickness of skin between stringer k and $k + 1$ on cell (a) (in)·

h = height of front spar (in)

t_w = thickness of web of front spar (in).

Since $\theta_a = \theta_b$, we have another equation which can be solved simultaneously with Equation 13.26 to determine q_a and q_b. If we know q_a and q_b, the total shear flow between any two stringers can be determined by means of a relation of the type of Equation 13.22.

EXAMPLE 13.3. Determine the shear flows in the skin and the angle of twist per unit length of an aluminum section similar to the one shown in Figure 13.7 except that there are no stringers and all the bending is resisted by the flanges on the front and rear spars. The top flange of the front spar is number 1; the top flange of the rear spar is number 2; and the bottom flanges of the rear and front spars are numbered 3 and 4 respectively. Also

$A_a = 392$ in²	$A_{s1} = A_{s4} = 1.85$ in²
$A_b = 990$ in²	$A_{s2} = A_{s3} = 1.65$ in²
$A_{2b} = 440$ in²	$t_w = 0.051$ in
$h = 24$ in	$t_{1a} = 0.020$ in
$s_{1a} = 51$ in	$t_{1b} = 0.073$ in
$s_{1b} = 44$ in	$t_{2b} = 0.036$ in
$s_{2b} = 20$ in	$t_{3b} = 0.030$ in
$s_{3b} = 44$ in	$y_1 = -y_4 = 12$ in
$T = -230,000$ lb in (counterclockwise)	$y_2 = -y_3 = 10$ in
$V = 5,000$ lb	

Solution. The moment of inertia of the section is

$$I = 2y_1^2 A_{s1} + 2y_2^2 A_{s2} = 2(12)^2 1.85 + 2(10)^2 1.65 = 863 \text{ in}^4$$

From Equation 13.25

$$q_1 = \frac{V}{I} y_1 A_{s1} = \frac{5000}{863} \times 12 \times 1.85 = 128.6 \text{ lb/in}$$

and by means of Equation 13.24

$$q_{2b} = \frac{V}{I} \sum_{i=2}^{2} Q_i = \frac{V}{I} y_2 A_{s2} = \frac{5000}{863} \times 10 \times 1.65 = 95.6 \text{ lb/in}$$

$$q_{3b} = \frac{V}{I} \sum_{i=2}^{3} Q_i = \frac{V}{I} (y_2 A_{s2} + y_3 A_{s3}) = 0$$

Equation 13.26 becomes

$$T = 2q_a A_a + 2q_b A_b - 2 \sum_{k=2}^{3} q_{kb} A_{kb}$$

$$-230,000 = 2q_a(392) + 2q_b(990) - 2 \times 95.6 \times 440$$

or $q_a + 2.53q_b = -186$ (a)

By means of Equation 13.27

$$2G\theta_a = \frac{1}{A_a} \left\{ \left[\sum_{k=2}^{m} (q_a + q_{ka}) \frac{s_{ka}}{t_{ka}} \right] + q_a \frac{s_{1a}}{t_{1a}} + (q_a - q_b - q_1) \frac{h}{t_w} \right\}$$

$$= \frac{1}{392} \left[0 + q_a \frac{51}{0.020} + (q_a - q_b - 128.6) \frac{24}{0.051} \right]$$

$$= 7.71q_a - 1.20q_b - 154.3$$

and $2G\theta_b = \dfrac{1}{990} \left[q_b \dfrac{20}{0.036} + q_b \dfrac{44}{0.030} - 95.6 \times \dfrac{20}{0.036} + q_b \dfrac{44}{0.073} \right.$

$$\left. + (q_b + 128.6 - q_a) \frac{24}{0.051} \right]$$

$$= -0.48q_a + 3.13q_b + 7.48$$

Equating θ_a to θ_b, we have

$$8.19q_a - 4.33q_b = 161.9$$ (b)

Solving Equations (a) and (b) simultaneously gives

$$q_a = -15.8 \text{ lb/in}$$
$$q_b = -67.4 \text{ lb/in}$$

Therefore, shear flow in nose skin is

$$q_a = -15.8 \text{ lb/in}$$

Shear flow in front web is

$$q_f = q_1 + q_b - q_a = 128.6 - 67.4 + 15.8 = 77.0 \text{ lb/in (upward)}$$

Shear flow in rear web is

$$q_r = q_{2b} - q_b = 95.6 + 67.4 = 163.0 \text{ lb/in}$$

The shear flow in the top and bottom skin of the rear cell is

$$q_b = -67.4 \text{ lb/in}$$

The angle of twist per unit length is

$$\theta_b = \frac{1}{2G} (-0.48q_a + 3.13q_b + 7.48)$$

$$= \frac{1}{2 \times 3.8 \times 10^6} [-0.48(-15.8) + 3.13(-67.4) + 7.48]$$

$$= -25.8 \times 10^{-6} \text{ rad/in (counterclockwise)}$$

13.8 Single-cell box with shear force inclined to a principal axis. In the previous analyses it has been assumed that the applied shear loads could be resolved into a shear force acting normal to a principal axis of the section. In the general case this is not always possible since the resultant shear force may be inclined to the principal axes of the section. Such a shear load always can be divided into two components, each acting along a principal axis. The shear flows on the section thus will be composed of the shear flows due to the two shear forces at right angles to each other and the shear flow due to the torsion about a reference point.

A single-cell, three-flange section is shown in Figure 13.8. The resultant shear force V has been divided into two components in
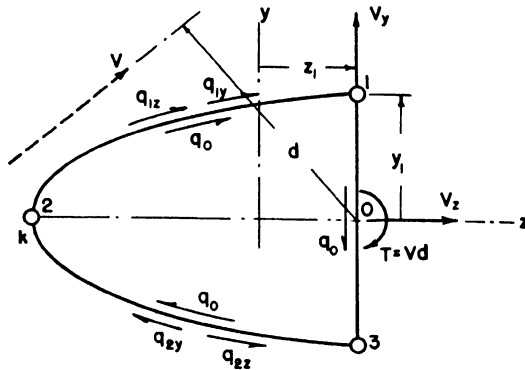
Fig. 13.8. Three-Flange Box.

the principal axis directions and a torque about the reference point 0. The shear flow between any two flanges is assumed to be composed of a constant shear flow q_0 and variable shear flows q_y and q_z, where q_y is the shear flow due to the shear load V_y and q_z is the shear flow caused by V_z. Considering the equilibrium of flange 1, it can be shown that the shear flow q_{1y} is

$$q_{1y} = \frac{V}{I_z} y_1 A_{s1} \tag{13.28}$$

where I_z = moment of inertia about principal axis z (in⁴)
  y_1 = distance to A_{s1} from z axis (in)
  A_{s1} = area of flange 1 and effective skin (in).

For stringer $k = 2$ $\qquad q_{2y} = \frac{V}{I} \sum_{i=1}^{k} Q_{zi}$

where Q_{si} = static moment of area of flange i about the z axis.

Similarly,
$$q_{1z} = \frac{V_z}{I_y} z_1 A_{s1} \tag{13.29}$$

and
$$q_{kz} = \frac{V_z}{I_y} \sum_{i=1}^{k} Q_{yi}$$

The total shear flow between flange 1 and 2 is therefore

$$q_r = q_{1y} + q_{1z} + q_0$$

The applied torque about 0 is equal to the torque of the shear flows or

$$T = 2q_0 A + 2 \sum_{k=1}^{n} A_k(q_{ky} + q_{kz}) \tag{13.30}$$

where A_k = swept area between flange k and flange $k + 1$ and reference point 0

A = total enclosed area of section

n = number of flanges not including the bottom flange of the spar.

For the three-flange beam shown in Figure 13.8, Equation 13.30 becomes

$$T = 2q_0 A + 2[A_1(q_{1y} + q_{1z}) + A_2(q_{2y} - q_{2z})] \tag{13.31}$$

Therefore,
$$q_0 = \frac{T - 2[A_1(q_{1y} + q_{1z}) + A_2(q_{2y} - q_{2z})]}{2A} \tag{13.32}$$

The shear flow at any point can then be determined by the algebraic addition of the component parts q_0, q_y, and q_z.

In this particular case of the three-flange cell, the shear flows could have been determined more easily by assuming unknown shear flows q_1, q_2, and q_3 between each of the flanges and applying the conditions of equilibrium $\Sigma F_z = 0$, $\Sigma F_y = 0$ and $\Sigma T = 0$. However, when there are more than three flanges, the method developed in this article will be found useful. This method can be extended also to the multicell box by adding the shear flows caused by the additional shear load in the z direction to the shear flows considered in Article 13.7.

13.9 Additional comments. The determination of the bending stresses and shear stresses in non-tapering box sections and thin-web beams with heavy flanges has been based usually on the assumptions that the flange or stringer areas together with their effective skin area carry all the bending moment and the skin carries all the shear force. Because of these assumptions the shear flow between stringers is constant and the moments of inertia of the cross section is the sum of the moments of inertia of the stringer and flange areas with the effective skin about the principal axes of the section. Actually, of course, the skin does con-

tribute to the bending resistance of the section and the flanges do resist some of the shear load. Since the skin on the compression side usually buckles at low loads, the length of effective skin acting with the stringers is usually taken between 10 and 30 times the skin thickness or the effective width formulas are used. This skin is then assumed to act with the stringer at the center of gravity of the combination of the two. All the skin on the tension side is assumed effective. Sometimes it is assumed also that up to one sixth the area of the web of beams acting with the flange area is effective in resisting bending.

Including skin and web areas in determining shear flows means that the assumption of constant shear flow between stringers or flanges is not valid. We have seen, for example, that the shear flow distribution is parabolic for a beam for which all the web is effective. It can be shown that shear flow in the skin parallel to the neutral axis of a box beam varies linearly. These variations of shear flow are often neglected in the design of beams.

Problems

13.1. A hollow, steel propeller shaft is transmitting a torque of 3200 lb ft. The shaft is subjected also to a shear force of 500 pounds acting perpendicular to the axis of the propeller shaft and passing through the center of the shaft. If the outer diameter of the shaft is 3 inches and the inner diameter is $2\frac{1}{2}$ inches, determine

(a) maximum shear stress
(b) angle of twist of shaft per unit length.

13.2. For the channel section of Problem 11.3 assume that the vertical shear force is acting along the web, and determine

(a) applied torque
(b) maximum shear stress neglecting stress concentrations at corners.

13.3. An aluminum four-flange rectangular box section similar to the one shown in Figure 13.2 carries a vertical shear load of 2500 pounds 10 inches to the left of the left web. Assuming that the shear flow is constant between flanges, determine

Fig. 13.9. Four-Flange D Section.

(a) shear center by Goodier method
(b) shear flows in skin by Goodier method
(c) shear flows by approximate method,

when $A_2 = 2.5$ in^2 $h = 12$ in $t_1 = t_2 = 0.040$ in
$A_1 = 1$ in^2 $b = 10$ in $t_3 = 0.064$ in

13.4. A non-tapering, four-flange D section is loaded as shown in Figure 13.9. If the thickness of the nose skin is 0.025 inches and the thickness of the web is 0.052 inches, whereas $b = 3$ inches, $R = 5$ inches, $A_1 = A_4 = 2$ square inches, and $A_2 = A_3 = 0.5$ square inches, determine

(a) shear stresses in skin

(b) axial stresses in flanges and stringers at a section 24 inches along the beam from which the loads are applied.

13.5. A circular fuselage section has 16 equispaced stringers around the periphery, each having an area of 0.10 square inches. The skin is 0.025 inches thick, and the radius of the shell is 15 inches. The secti n carries a bending moment of 200,000 lb in about the horizontal axis and a vertical shear load of 2500 pounds 4 inches to the left of the center line of the fuselage. Assuming that only the stringers resist bending determine

(a) shear flows

(b) stringer stresses.

Also determine these same quantities, assuming that all the skin on the tension side is effective in resisting bending and that the length of effective skin with each stringer is $30t$ on the compressive side.

13.6. A symmetrical non-tapering wing section is shown in Figure 13.10. The vertical load acting perpendicular to the horizontal principal axis of the
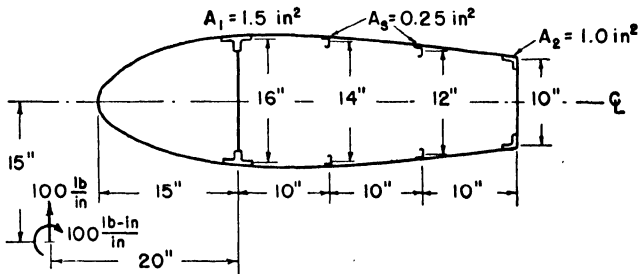
Fig. 13.10. Wing Section.

section is 100 pounds per inch of span distributed along the load axis which is parallel to the leading edge of the wing. The distributed moment along the load axis is 100 pound inches per inch of span. Determine the shear flows and shear stresses in the skin and the axial flange and stringer stresses at a section of the wing 40 inches inboard of the station where the distributed load begins.

All external skin thickness	= 0.032 in
Front and rear web thickness	= 0.051 in
Length of nose skin	= 50 in
Enclosed area of nose	= 150 in

Assume that skin line is straight between stringers of rear cell.

References

Ebner, H., "The Strength of Shell and Tubular Spar Wings." NACA Tech. Memo. No. 933, 1940.

Goodier, J. N., "A Theorem on the Shearing Stress in Beams with Applications to Multicellular Sections." *Journal of Aeronautical Sciences*, Vol. 11, No. 3, July 1944.

Hatcher, Robert S., "Rational Shear Analysis of Box Girders." *Journal of Aeronautical Sciences*, Vol. 4, No. 6, April 1937.

Kuhn, Paul, "Some Elementary Principles of Shell Stress Analysis with Notes on the Use of the Shear Center." NACA Tech. Note No. 691, March 1939.

CHAPTER 14

Combined Stresses and Allowable Stresses

....

14.1 Introduction. The various types of loading such as tension, compression, bending, torsion, and shear have been considered separately and in certain combinations in the preceding chapters. In each case, a normal stress acting perpendicular to an area and a shear stress acting along a surface have been determined on a somewhat arbitrarily oriented plane, such as the cross section of a beam or column. There is no reason to suppose that stresses on such sections are necessarily the maximum stresses induced by the loads at a given point. In fact, it is usually possible to determine a stress in some direction which is greater in magnitude than the stress determined in the arbitrarily chosen direction. It becomes necessary therefore to investigate the stresses in various directions at a point in the material. Stresses that arise from combinations of simple normal and shearing stresses are called *combined stresses*.

After determining the combined stresses, the value of the limiting stresses to prevent structural failure should be considered. Of course, this depends to some extent on the criteria chosen for engineering failure of the structure. Engineering failure may be based on any number of factors such as yielding, rupture, buckling, or fatigue. In each case the stresses that can be permitted are called the *allowable stresses*, and the determination of the allowable stresses for complicated, induced-stress conditions is usually difficult.

There are a number of theories of failure of material that have been proposed in an effort to correlate the properties of a material, such as can be determined from a simple tension test, with the failure of the same material subject to more complicated loading. Two of the many theories are the *maximum normal-stress theory* and the *maximum shear-stress theory*. The maximum normal-stress theory is based on the assumption that failure by rupture occurs when the maximum combined normal stress in a member is equal to the maximum normal stress in a tensile specimen at rupture. This theory is used sometimes for predicting fracture of brittle material. In the maximum shear-stress theory it is assumed that when the maximum shear stress reaches a limiting value as determined by a tensile or shear test, the member fails. This theory is used sometimes for ductile materials.

Another method widely used in the aircraft industry for specifying the allowable stresses is that of *interaction curves*. The interaction curve is a means of indicating how much of each of two or more loadings, such as tension and torque, the member can withstand before it fails.

14.2 Combined shear stress and normal stress. Many times in the preceding chapters, the stress conditions have been determined at various points on the cross section of a structural member, and these stresses have been composed of a shear stress and a normal tension or compression stress acting on the same surface. The stress condition in the web on the cross section of a beam is an example. Another example

(a)

(b)   (c)

(d)   (e)

NORMAL STRESS   SHEAR STRESS
DISTRIBUTION   DISTRIBUTION
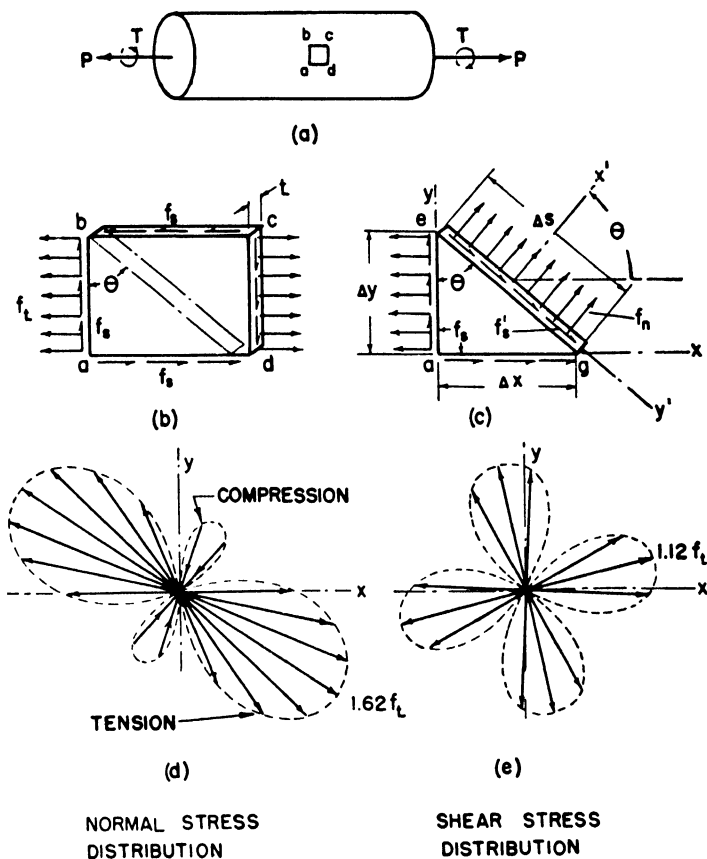
Fig. 14.1. Combined Stresses.

is shown in Figure 14.1 of a propeller shaft carrying a torque load and a tensile load.

The stresses induced by the tensile load and torque on the sides of an elemental block *abcd* of the propeller surface are shown in Figure 14.1(b). The thickness of the block, *t*, is assumed small enough so that the stress distribution can be considered uniform across the depth. The problem is to determine the stresses on some plane inclined at an angle to the plane of the applied stresses. The stresses on the inclined plane are composed of a normal component f_n and a shear component f'_s. These stresses will

be determined by a consideration of equilibrium of the triangular element
aeg. Since in dealing with stresses the area is involved, the stresses
cannot be added together vectorially. Stresses can be added only
directly when the stresses act along the same axis so that the area on
which they act is the same for each. For this reason the stresses are
expressed in terms of the forces on the sides of an element before they are
added. If we refer to Figure 14.1(c) and remember that the force on the
side of the block is the stress times the area on which it acts, then for
equilibrium of the forces in the direction x' normal to inclined plane, we
have

$$\Sigma F_{x'} = 0 = f_n t\, \Delta s + f_s t\, \Delta y \sin \theta + f_s t\, \Delta x \cos \theta - f_t t\, \Delta y \cos \theta$$

But $$\Delta y = \Delta s \cos \theta;\ \Delta x = \Delta s \sin \theta$$

Therefore, $$f_n + 2f_s \cos \theta \sin \theta - f_t \cos^2 \theta = 0$$

Since $$2 \cos \theta \sin \theta = \sin 2\theta$$

and $$\cos^2 \theta = \frac{1 + \cos 2\theta}{2}$$

then $$f_n = \frac{f_t}{2}(1 + \cos 2\theta) - f_s \sin 2\theta \qquad (14.1)$$

From a similar consideration of the forces in the y' direction along the
inclined plane we obtain

$$f_s' = \frac{f_t}{2} \sin 2\theta + f_s \cos 2\theta \qquad (14.2)$$

For the special case where $f_t = f_s$, the distribution of the normal and shear
stresses for various directions of the inclined plane are shown in Figure
14.1(d) and (e).

It is evident that the normal stress attains a greater value than the
applied stress f_t. The orientation of the inclined plane on which f_n
becomes a maximum can be determined by the usual methods. Thus,

$$\frac{df_n}{d\theta} = 0 = -f_t \sin 2\theta - 2f_s \cos 2\theta$$

$$\tan 2\theta = -\frac{2f_s}{f_t} \qquad (14.3)$$

Substituting the value for θ given by Equation 14.3 into Equation 14.1
gives

$$f_{n(max)} = \frac{f_t}{2} + \sqrt{\left(\frac{f_t}{2}\right)^2 + f_s^2} \qquad (14.4)$$

It is interesting to note that if the value of θ for maximum normal stress is
substituted into the Equation 14.2 for the shear stress on that plane, the
value of the shear stress is zero. The maximum normal stress always
occurs on a plane where the shear stress is zero. The maximum normal
stress and the normal stress at right angles to it are called *principal
stresses.*

The orientation of the inclined plane for maximum shear stress can be determined by differentiating the expression for the shear stress,

$$\frac{df'_s}{d\theta} = 0 = f_t \cos 2\theta - 2f_s \sin 2\theta$$

$$\tan 2\theta = \frac{f_t}{2f_s} \tag{14.5}$$

The expression for the maximum shear stress is therefore

$$f'_{s(\text{max})} = \sqrt{\left(\frac{f_t}{2}\right)^2 + f_s^2} \tag{14.6}$$

14.3 Mohr's circle. The stress conditions in any direction for the case of stresses in a plane easily can be represented graphically by a diagram known as *Mohr's circle*. The diagram makes it possible to determine the principal stresses and the maximum shear stress at a point. The main value of the diagram, however, is the means it provides for visualizing the combined stress conditions in various directions in the material.

The method of constructing Mohr's circle for the case of applied tension and shear stress considered in the preceding article will be indicated first. Proof that the diagram is a graphical representation of the stress relations given in Equations 14.1 and 14.2 will then be made.

The construction of Mohr's circle shown in Figure 14.2(a) which represents the stress system of combined shear and tension is as follows:

(1) Construct as coordinate axes, a horizontal normal-stress axis and a vertical shear-stress axis.

(2) Lay off to scale along the normal-stress axis a line OE representing the value of the applied stress f_t.

(3) From E parallel to the shear-stress axis construct the line ED representing the applied shear stress f_s on plane cd of Figure 14.1(b).

(4) From the origin construct a line OF opposite in direction to ED and equal in length. This line represents the shear stress on plane cb of Figure 14.1(b).

(5) Connect points F and D. This line intersects the normal-stress axis at B.

(6) With B as a center, describe a circle through F and D.

The location of points on the circle indicates the values of the stresses on various planes of the material. Thus, for example, point D' represents the values of the combined stresses on a plane making an angle θ with the plane on which the stress f_t acts. The horizontal distance from the vertical axis to D' is the value of the normal stress, and the vertical distance is the shear stress. The angle β is the angle between the plane on which f_t acts and the plane of the maximum principal stress, since OC represents the value of the maximum normal stress for the system.
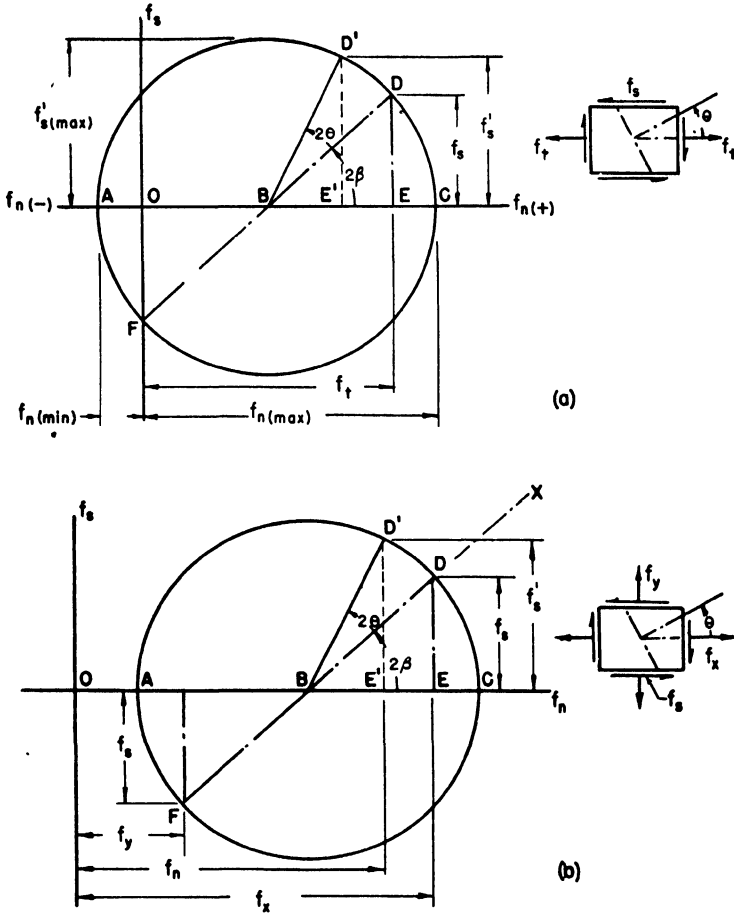
Fig. 14.2. Mohr's Circle Diagram.

The correspondence between the circle and the equations for the stresses can now be shown.

$$f_n = (OB) + (BE') = \frac{f_t}{2} + R \cos(2\theta + 2\beta)$$

where R = the radius of the circle = $\sqrt{\left(\frac{f_t}{2}\right)^2 + f_s^2}$

But $\cos(2\theta + 2\beta) = \cos 2\theta \cos 2\beta - \sin 2\theta \sin 2\beta$

and $\cos 2\beta = \dfrac{(BE)}{R} = \dfrac{f_t}{2R}$

$$\sin 2\beta = \frac{(DE)}{R} = \frac{f_s}{R}$$

Therefore, $$f_n = \frac{f_t}{2} + \frac{f_t}{2} \cos 2\theta - f_s \sin 2\theta \qquad (14.7)$$

which corresponds to Equation 14.1. A similar process shows that Mohr's circle gives the value for the shear stress f'_s corresponding to Equation 14.2.

Maximum combined shear stress is represented by the radius of the circle which is

$$f'_{s\,(max)} \qquad \sqrt{\left(\frac{f_t}{2}\right)^2 + f_s^2}$$

and the maximum combined normal stress, which is the principal stress, is determined by the intersection of the circle with the normal-stress axis or

$$f_{n\,(max)} = \frac{f_t}{2} + \sqrt{\left(\frac{f_t}{2}\right)^2 + f_s^2}$$

Mohr's circle for the case of biaxial stress consisting of two applied normal stresses and shear stresses on planes at right angles to each other is shown in Figure 14.2(b). The construction is the same in principle as for the uniaxial stress case previously discussed. The stress condition on the plane on which f_x acts is indicated by point D on the circle, and the stress condition on the plane where f_y acts is indicated by point F. The stress conditions on other planes making an angle θ with the plane on which f_x acts can be determined by the position of the points on the circle an angle 2θ from D. By means of the circle the normal stress on any plane can be shown to be

$$f_n = \frac{f_x + f_y}{2} + \frac{f_x - f_y}{2} \cos 2\theta - f_s \sin 2\theta \qquad (14.8)$$

and the shear stress to be

$$f'_s = \frac{f_x - f_y}{2} \sin 2\theta + f_s \cos 2\theta \qquad (14.9)$$

The maximum normal stress and shear stress are

$$f_{n\,(max)} = \frac{f_x + f_y}{2} + \sqrt{\left(\frac{f_x - f_y}{2}\right)^2 + f_s^2} \qquad (14.10)$$

and $$f'_{s\,(max)} = \sqrt{\left(\frac{f_x - f_y}{2}\right)^2 + f_s^2} \qquad (14.11)$$

The angle between the stress in the x direction and the maximum principal stress is given by

$$\tan 2\beta = -\frac{2f_s}{f_x - f_y} \qquad (14.12)$$

In constructing Mohr's circle the applied tension stresses which are considered positive are laid on the positive normal-stress axis. Compression stresses are laid off in the negative normal-stress axis direction.

Combined stresses for other applied stress conditions are special cases of the biaxial system shown in Figure 14.2(b). Thus, for the case of applied pure shear stress, $f_x = f_y = 0$, and Mohr's circle becomes a circle with center at the origin and with radius f_s. Mohr's circle for the case of applied pure tension for which $f_y = f_s = 0$ is a circle tangent to the f_s axis and of radius $f_t/2$.

EXAMPLE 14.1. On the cross section of a beam the stresses at a point on the web are found to be 46,800 psi tension and 27,600 psi shear. If the allowable tensile stress for the material is 60,000 psi and the allowable shear stress is 37,500 psi, determine the margin of safety in tension and shear.

Solution. The maximum normal stress at the point in accordance with Equation 14.4 is

$$f_{n(max)} = \frac{f_t}{2} + \sqrt{\left(\frac{f_t}{2}\right)^2 + f_s^2}$$

$$= \frac{46,800}{2} + \sqrt{\left(\frac{46,800}{2}\right)^2 + (27,600)^2} = 59,600 \text{ psi}$$

Then $\qquad MS = \dfrac{F_t}{f_{n(max)}} - 1 = \dfrac{60,000}{59,600} - 1 = 0.01$

From Equation 14.6

$$f'_{s(max)} = \sqrt{\left(\frac{f_t}{2}\right)^2 + f_s^2} = \sqrt{\left(\frac{46,800}{2}\right)^2 + (27,600)^2} = 36,200 \text{ psi}$$

Therefore, $\qquad MS = \dfrac{F_s}{f'_{s(max)}} - 1 = \dfrac{37,500}{36,200} - 1 = 0.03$

14.4 Interaction curves. Many theories have been proposed to explain the failure of material under combined stresses. No single theory seems to be adequate to explain the failure of all types of material under all possible combined stress conditions. Such theories will not be discussed here, but a method of presenting data pertaining to the failure of material under various types of combined loading and combined stresses will be considered. These data are given in the form of *interaction curves* for which the parameters are *stress ratios*.

A stress ratio is defined as

$$R = \frac{f}{F} \tag{14.13}$$

where $\qquad\qquad f$ = applied stress
$\qquad\qquad F$ = allowable stress.

For example, if a member is subjected to bending for which the applied bending stress is f_b and the allowable bending stress is the modulus of rupture F_b, then the stress ratio is

$$R_b = \frac{f_b}{F_b}$$

and the margin of safety is

$$MS = \frac{1}{R_b} - 1$$

It is reasonable to suppose that the strength of a member under one type of loading is influenced by the addition of another type of loading. For example, if a tube is subjected to bending so that it is carrying one half of its allowable bending load, the addition of a sufficient torque load will
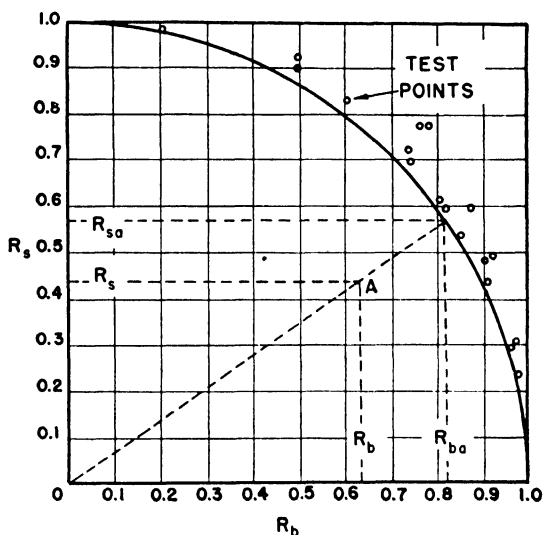
Fig. 14.3.   Interaction Curve for Combined Bending and Torsion of Tubing.

cause the members to fail although neither of the loadings acting alone are sufficient to cause failure.   The relative proportion of each type of loading required to cause failure is indicated by the interaction curve. The interaction curve is usually determined by test.   Figure 14.3 shows an interaction curve for tubing under combined bending and torsion. This curve is determined in the following manner.   A bending load less than that required to produce failure is applied and then a torque load is applied until the tube fails.   This determines a point on the curve.   This process is repeated until a set of points is obtained which spans the region of failure from pure bending moment, represented by the stress ratio $R_b = 1$ on the horizontal axis, to failure by a pure torque loading, represented by $R_s = 1$ on the vertical axis.   A curve is then

fitted through these test points. For the case considered, it is found that an arc of a circle closely fits the test points. Analytically, therefore, the curve can be expressed as

$$R_b^2 + R_s^2 = 1 \tag{14.14}$$

where
$$R_b = \frac{\text{applied bending stress}}{\text{allowable bending stress}}$$

$$R_s = \frac{\text{applied torsional shear stress}}{\text{allowable torsional shear stress}}$$

It is evident that if the member is carrying a bending and torque load so that the sum of the squares of the stress ratios is less than unity, the member does not fail. The region between the coordinate axes and the interaction curve therefore represents combinations of stress ratios that are safe.

The margin of safety for given values of stress ratios can be determined. Suppose the stress ratios are such as to determine point A in Figure 14.3. If both the bending load and torque load are increased simultaneously by proportional amounts, point A will move out along a radial line until it lies on the interaction curve, indicating failure of the member. If we denote R_{ba} and R_{sa} the stress ratios at failure, then the margin of safety is

$$MS = \frac{R_{ba}}{R_b} - 1 \text{ or } \frac{R_{sa}}{R_s} - 1$$

whichever is most convenient. From similar triangles

$$\frac{R_{ba}}{R_b} = \frac{\sqrt{R_{ba}^2 + R_{sa}^2}}{\sqrt{R_b^2 + R_s^2}}$$

But R_{ba} and R_{sa} determine a point on the curve so that $R_{ba}^2 + R_{sa}^2 = 1$. Therefore,

$$MS = \frac{1}{\sqrt{R_b^2 + R_s^2}} - 1 \tag{14.15}$$

14.5 Interaction curves for other combined loading conditions. The interaction curve for two combined loadings can be expressed mathematically as

$$R_1^a + R_2^b = 1$$

where R_1, R_2 = stress ratios for simple loading
a, b = coefficients that determine the shape of the curve.

Typical interaction curves are shown in Figure 14.4 together with the equations for the curves. The different values of the coefficients a and b determine various types of curves. For example, if $a = b = 1$, the curve is a straight line, and if $a = b = 2$ the curve is the arc of a circle. As the values of a and b become greater, the curve bulges more and more toward

the axes $R_1 = 1$ and $R_2 = 1$. If the curve actually fits the axes $R_1 = R_2$ = 1, it means that the strength of the member with the loading R_1 is not influenced by adding R_2. In other words, there is little interaction between the loading when a and b are large. Conversely, when a and b are small, there is considerable interaction between the loadings. This is the case of combined bending and compression for which a bending
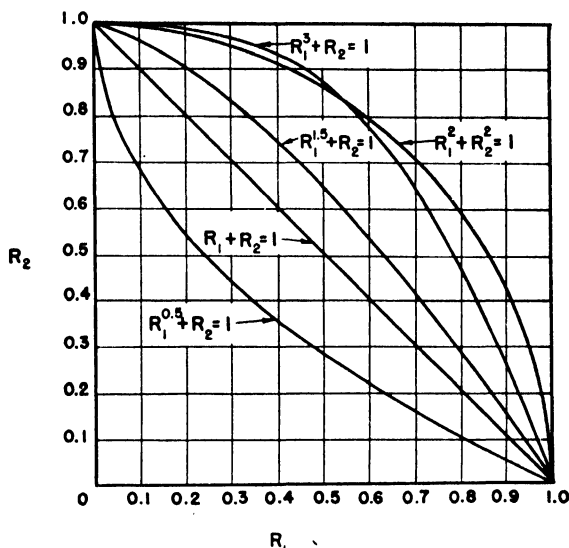
Fig. 14.4. Typical Interaction Curves.

deflection increases the effect of the axial loading, which thus increases the bending deflection, and so on, as in beam columns.

Some equations of interaction curves for specific cases of combined loading taken from the ANC-5 are cited below.

Conditions for buckling of flat panels.

Combined compression and bending: $R_b^{1.75} + R_c = 1$
Combined compression and shear: $R_s^{1.5} + R_c = 1$
Bending and shear: $R_b^2 + R_s^2 = 1$

Thin-walled cylinders.

Combined transverse shear and bending: $R_b^2 + R_s^2 = 1$
Combined bending and compression: $R_c + R_b = 1$
Combined bending and torsion: $R_b^2 + R_s^2 = 1$

Interaction curves were developed first for determining the failure of members by buckling. The method is being extended now for other types of failure, such as the rupture of bolts under combined tension and shear. Until more is understood about the failure of material under combined loading so that failure can be predicted analytically, the

interaction curve presents a useful means of presenting experimental data.

An extension of the method showing the interaction between two loadings can be made for the case of three loadings.   Thus,

$$R_1^a + R_2^b + R_3^c = 1$$

defines an interaction surface.

Problems

14.1. Draw Mohr's circle diagram for the data given in Example 14.1, and then plot the polar diagram for the normal-stress distribution at a point.

✓ **14.2.** A 1-0.049 4130 tube 5 inches long is fixed at one end and carries a 500 pound shear load and a 3000 pound inch torque at the other.   Determine the maximum combined normal stress and shear stress in the tube.

14.3. Prove that the sum of the maximum and minimum principal stresses is equal to the sum of the applied normal stresses acting on two planes at right angles to each other.

14.4. A tension member with a cross-sectional area of 6 square inches carries a tensile load P.   The normal stresses on two planes at right angles to each other are 6,000 psi and 12,000 psi.   Determine

(a) load P
(b) shear stress on planes on which the given normal stresses act
(c) angle between axis of bar and direction of 12,000 psi stress.

14.5. The beam section shown in Figure 11.3 carries a vertical shear load of 35,000 pounds, and a bending moment about the horizontal axis of 130,000 lb in. Assuming that the web carries all the shear but that the web takes its part of the bending stress, determine the direction and values of the maximum combined compression and tension stresses at the neutral axis and at the point where the web joins the flange.

14.6. In a forming operation a sheet is subjected to a 10,000 psi compressive stress in one direction and a 25,000 psi tensile stress at right angles to it.   Determine the maximum shear stress.   Draw Mohr's circle.

14.7. A test is performed on a thin-walled cylinder, and it is found that the allowable stress is 10,000 psi in compression and 20,000 psi in torsion.   If failure of the cylinder under combined loading occurs at the following values, plot the interaction curve and select a typical interaction curve from Figure 14.4 that most nearly fits the data.

Stress in torsion is		stress in compression is
18,400 psi	when	2,000 psi
16,600		4,000
14,000		6,200
12,000		7,800
8,000		9,200
4,000		9,800

14.8. The failure for a member is given by $R_1 + R_2 = 1$.   Determine the expression for the margin of safety.

14.9. A $2\frac{1}{4}$-0.065 4130 tube has a modulus of rupture in torsion of 38,600 psi and a modulus of rupture in bending of 98,000 psi.   If the tube carries a bending

moment of 9,400 lb in and a torque of 10,900 lb in, determine the margin of safety.

References

Bruhn, E. F., "Tests on Thin-Walled Celluloid Cylinders to Determine the Interaction Curves Under Combined Bending, Torsion and Compression or Tension Loads." NACA Tech. Note 951, January 1945.

Marin, Joseph, *Mechanical Properties of Materials and Design.* McGraw-Hill, 1942.

Shanley, F. R. and E. I. Ryder, "Stress Ratios." *Aviation Magazine*, June 1937.

CHAPTER 15

Connections

....

15.1 Introduction. From a structural standpoint it would be desirable to make the airplane from one continuous material similar to a casting or an extrusion. If this were possible, whole wings could be produced as a unit. However desirable this might be structurally, production procedure, accessibility for repair, and maintenance require that the aircraft be made up of a composite structure in which the various parts are assembled into subassemblies and the subassemblies fitted and joined together for the complete structure.

The three main methods of joining structural units are those depending on mechanical, fused, or cemented connections. Among mechanical fastenings are riveted or bolted joints and fittings, tie rods, and so on. Fused connections depend on the joining of the parts by fusion such as welding, brazing, and so on. Cemented connections depend on the adhesive action of such materials as glue or plastic for joining the units. All three types are commonly used in the aircraft structure, although the mechanical connection is most common especially for detachable fastenings such as may be used for joining together large units, for example, the wing and fuselage. A mechanical fastening designed for joining together two or more units is sometimes called a *fitting*.

15.2 Riveted and bolted connections. Four types of failure of simple riveted or bolted connections are shown in Figure 15.1. Of these four types of failure, the shear tearout, Figure 15.1(b), can be prevented by selecting a proper minimum edge distance *e*. This edge distance for riveted connections is usually at least twice the rivet diameter. Tearing of the sheet between rivets, Figure 15.1(d), is prevented by limiting the minimum distance between rivets (rivet spacing) to three times the rivet diameter. This leaves only failure due to rivet shear and the crushing of sheet or rivet to consider in the design of a riveted connection. For maximum efficiency it is desirable to have the strength of the connection in shear and crushing about the same since the connection fails at the weaker of the two, and it is undesirable to have excess strength which implies excess weight.

Regardless of the type of failure the allowable load per rivet or bolt is

$$P_a = AF \tag{15.1}$$

where F = allowable stress (psi)

A = critical area on which stress acts (in²).

270
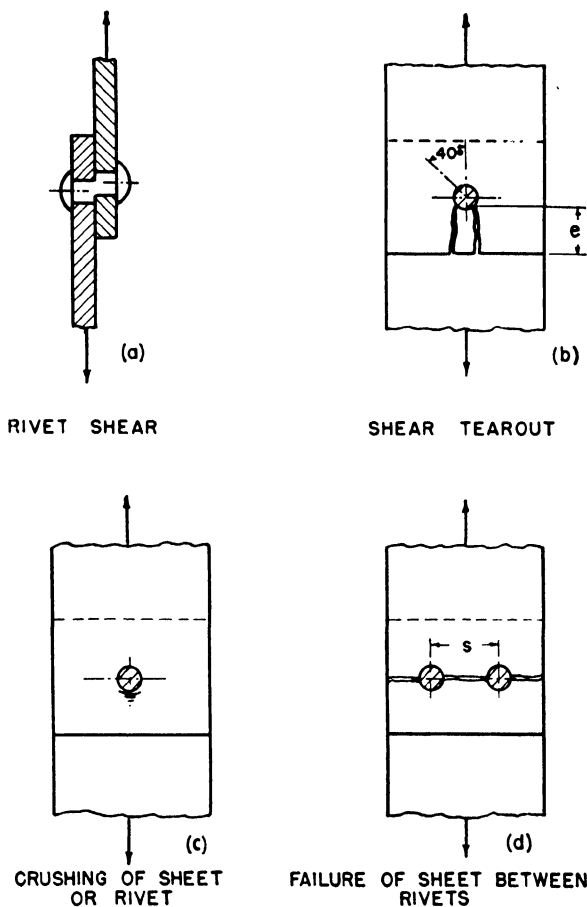
Fig. 15.1. Types of Failure of Riveted Joints.

Thus, for failure of the sheet between rivets

$$A = \text{net area between rivets.}$$

For shear tearout

$$A = 2et$$

where
$$e = \text{edge distance (in)}$$
$$t = \text{sheet thickness (in)}.$$

For bearing of sheet or rivet

$$A = \text{projected area of rivet} = td$$

where
$$d = \text{diameter of rivet (in)}.$$

For rivet shear

$$A = \text{total shear area}$$
$$= K \frac{\pi d^2}{4}$$

where K = number of surfaces in shear.

Very often data are given for the allowable load on a standard rivet in shear or the allowable load for a rivet and sheet in crushing. A table for shear and bearing strengths of aluminum alloy rivets and sheet will be found in section 5 of the ANC-5. When these values are available, they are easier to use than the equivalent expression of the allowable stress times the area.

If the load per linear inch to be transmitted by a single lap joint is P, then the number of rivets required per inch is

$$n = \frac{P}{P_a}$$

The spacing between rivets is therefore

$$s = \frac{1}{n} = \frac{P_a}{P} \tag{15.2}$$

EXAMPLE 15.1.   Determine the rivet size and spacing for a simple lap joint between two 0.032 24ST aluminum-alloy sheets if the load is 500 pounds per inch and 17ST rivets are to be used.

Solution.   This problem will be solved by using the data in section 5 of the ANC-5 (Revised 1946).

Consulting pages 5–26 and 5–26a of ANC-5, we find that for $\frac{1}{8}''$ rivets

allowable load in single shear = $494 \times 0.964 = 476$ lb
allowable crushing load = $411 \times 1.29 = 530$ lb

and for $\frac{3}{32}''$ rivets

allowable load in single shear = $275 \times 1 = 275$ lb
allowable bearing load = $307 \times 1.29 = 396$ lb

Since the allowable loads are more nearly equal for the two types of failure for the $\frac{1}{8}''$ rivets, this size will be used. The design will be based on the allowable shear value since this is the smaller of the two allowables. Thus,

$$s = \frac{P_a}{P} = \frac{476}{500} = 0.952 \text{ in} \qquad \text{use } \frac{15}{16} \text{ in}$$

Since this spacing is greater than $3d$, the sheet between the rivets will not fail first. The edge distance should be at least $2d$.

EXAMPLE 15.2.   Determine the rivet size and spacing for the butt joint shown in Figure 15.2 if the applied load is 1200 pounds per inch. The design requires the use of 17ST rivets in 24ST sheet.

Solution. In this example the rivets are in *double* shear, and the bearing is considered on the combined thicknesses of the splice plates or the main plate, whichever is smaller.
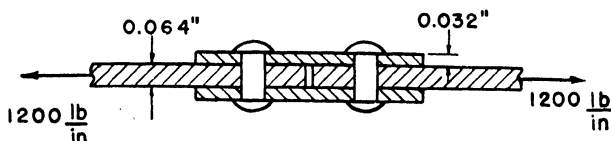
Fig. 15.2 Butt Joint.

From the ANC-5 for $\frac{1}{8}''$ rivets

$$\text{allowable shear} = 2 \times 494 \times 0.935 = 924 \text{ lb}$$
$$\text{allowable bearing} = 822 \times 1.29 = 1060 \text{ lb}$$

Then $\qquad s = \dfrac{P_a}{P} = \dfrac{924}{1200} = 0.77 \text{ in} \qquad \text{use } \dfrac{11}{16} \text{ in}$

15.3 Eccentrically loaded connection. An eccentrically loaded connection is shown in Figure 15.3. Since the load is applied at some distance from the rivet group, it is apparent that the load tends to rotate the member on which it acts. The point about which the arm rotates is called the *rivet group center.*

If the load is resolved into a force and a couple at the group center, then the rivets must resist the effects of the direct load and the couple. The total force on a rivet is the sum of the forces due to the direct load and the couple, as indicated in Figure 15.3(c).

The amount of load carried by each rivet depends upon its resistance to deformation, which may in turn be based on its cross-sectional area or its minimum strength in shear or bearing. For example, in considering only the effect of the couple, if there are two rivets located at distances r_1 and r_2 from the group center respectively, then for a given rotation of the arm the deformation of the rivets are proportional to their distance from the group center. For the case of elastic deformation, the stress in a rivet is proportional to its deformation and the modulus of elasticity. The load carried by the rivet is the stress times its cross-section area. Therefore, for rivets having the same deformation and modulus of elasticity, the loads are proportional to the cross-section areas. A viewpoint more commonly accepted in designing aircraft joints is based on the assumption that the resistance to deformation is proportional to the allowable loads. Thus, for two rivets having the same deformation, the one with the higher allowable load is assumed to carry the greater load in proportion to the ratio of the allowable loads for each. If the areas and material of the rivets in a group are the same, both of these assumptions produce the same results. Neither of these assumptions is strictly

true, but the latter one seems to give the best results as compared with tests.

Consider the forces on the rivets or bolts due to the couple M. If rotation is assumed about point 0 of Figure 15.3(d), then the force on

(a)

ECCENTRIC
CONNECTION

(b)

FORCES AT GROUP
CENTER

(c)

FORCES ON RIVETS

(d)

COMPONENTS OF FORCE
ON RIVET NO.3 DUE TO
COUPLE
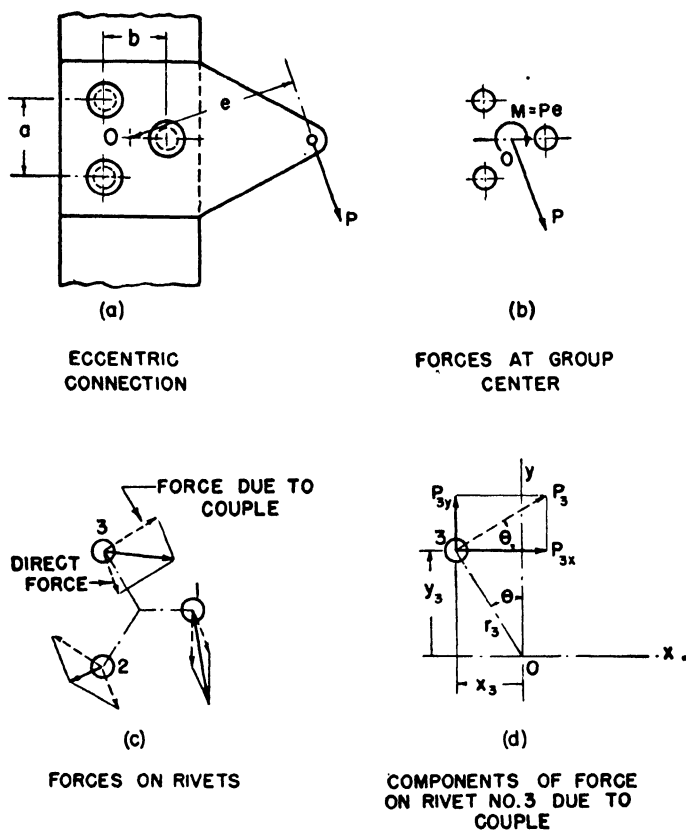
Fig. 15.3. Eccentrically Loaded Connection.

each rivet is perpendicular to the line between the rivet center and the group center. In accordance with the assumption that the force on the rivet is proportional to its distance from the group center and its allowable load, then the load on rivet number 3 is

$$P_3 = Kr_3 P_{a3}$$

where K = constant of proportionality
        r_3 = distance from group center to rivet No. 3 (in)
      P_{a3} = allowable load for rivet No. 3 (lb).

Selecting point 0 as an origin for the x and y coordinates makes the forces on rivet number three in the x and y directions become

$$P_{3x} = P_3 \cos \theta = P_3 \frac{y_3}{r_3}$$

$$P_{3y} = P_3 \sin \theta = -P_3 \frac{x_3}{r_3}$$

and

$$P_{3x} = Kr_3 P_{a3} \frac{y_3}{r_3} = KP_{a3}y_3$$

$$P_{3y} = -KP_{a3}x_3$$

Similar forces on the other rivets can be determined in a like manner. Since these forces produce a couple, the summations of the forces in the x and y directions are zero.

$$P_{1x} + P_{2x} + P_{3x} = 0$$
$$KP_{a1}y_1 + KP_{a2}y_2 + KP_{a3}y_3 = 0$$

or

$$\Sigma yP_a = 0$$

similarly,

$$\Sigma xP_a = 0 \tag{15.3}$$

These conditions are satisfied if the origin is located at the centroid of the allowable rivet loads.

Equating the moment of the rivet loads to the applied moment, we have

$$M = P_1 r_1 + P_2 r_2 + P_3 r_3$$
$$= Kr_1^2 P_{a1} + Kr_2^2 P_{a2} + Kr_3^2 P_{a3}$$

Therefore,

$$K = \frac{M}{\Sigma r^2 P_a}$$

and

$$P_3 = \frac{Mr_3 P_{a3}}{\Sigma r^2 P_a} \text{ and so forth}$$

In terms of the distances x and y, the x and y components of force on any rivet n are

$$P_{nx} = \frac{MP_{an}y_n}{\Sigma(x^2 + y^2)P_a}$$

$$P_{ny} = -\frac{MP_{an}x_n}{\Sigma(x^2 + y^2)P_a} \tag{15.4}$$

The direct loads on the rivets will be distributed also in proportion to their allowable loads or

$$P'_{nx} = \frac{P_x P_{na}}{\Sigma P_a} \tag{15.5}$$

$$P'_{ny} = \frac{P_y P_{na}}{\Sigma P_a}$$

where P'_{nx} = force on rivet in x direction due to direct load P_x in x direction.

The total load on any rivet determined by force resolution is

$$P_n = \sqrt{(P_{nx} + P'_{nx})^2 + (P_{ny} + P'_{ny})^2} \qquad (15.6)$$

The equations are considerably simplified if the allowable loads for all the rivets are the same. In this case

$$P_{nx} = \frac{My_n}{\Sigma(x^2 + y^2)} \qquad (15.7)$$

$$P'_{nx} = \frac{P_x}{\text{number of rivets}}$$

EXAMPLE 15.3. A riveted connection similar to the one shown in Figure 15.3 is held together by $3\text{-}\frac{3}{16}''$ 17ST rivets in 0.064" 24ST clad sheet. A vertical load of 500 pounds acting downward is supported on an arm $3''$ to the right of the right rivet. In the figure, $a = 2''$ and $b = 1''$. Determine the margin of safety for the rivet group.

Solution. Since all the rivets are the same, Equation 15.7 is used for the solution.

The centroid of the rivet group lies on a horizontal axis through the right rivet because of symmetry. The position of the centroid from the left rivet is

$$\bar{x} = \frac{\Sigma x P_a}{\Sigma P_a} = \frac{1(P_a)}{3P_a} = 0.33 \text{ in}$$

The moment on the rivet group is therefore

$$M = 500 \times 3.67 = 1835 \text{ lb in (clockwise)}$$

From the conditions of the problem, the applied loads are

$$P_x = 0 \qquad P_y = -500 \text{ lb}$$

It is convenient sometimes to set up a table to determine the required values. If we remember that $P_{nx} = \dfrac{My_n}{\Sigma(x^2 + y^2)}$ and $P'_{nx} = \dfrac{P_x}{\text{no. rivets}}$, and so on, then

Rivet No.	x	y	x^2	y^2	P_{nx}	P_{ny}	P'_{nx}	P'_{ny}	P_n
1..........	0.67	0	0.45	0	0	−460	0	−167	627
2..........	−0.33	−1.0	0.11	1.0	−686	226	0	−167	688
3..........	−0.33	+1.0	0.11	1.0	686	226	0	−167	688

$$\Sigma x^2 = 0.67 \quad \Sigma y^2 = 2.00$$

Rivet numbers 2 and 3 carry the highest loads. From the ANC-5 the allowable loads are found to be

$$\text{allowable shear} = 1090 \times 1 = 1090 \text{ lb}$$
$$\text{allowable bearing} = 1220 \times 1.25 = 1525 \text{ lb}$$

Therefore, the margin of safety is

$$MS = \frac{P_a}{P} - 1 = \frac{1090}{688} - 1 = 0.58 \text{ or } 58\%$$

15.4 Fused joints. Welding by electric arc or gas is the most common method of joining structural units by fusion.

The allowable load on the weld metal in welded seams according to the ANC-5 is

$$
\begin{aligned}
P &= 32,000 \, Lt \qquad \text{for low carbon steel} \\
P &= 0.48 \, Lts \qquad \text{for chrome-molybdenum steel} \qquad (15.8)
\end{aligned}
$$

where L = length of welded seam (in)

t = thickness of thinnest material joined by the weld in the case of lap welds between two steel plates or between plates and tubes (in)

t = average thickness of the weld metal in the case of tube assemblies. This cannot exceed 1.25 times the thickness of the welded stock (in)

s = 90,000 psi for material not heat-treated after welding.

Whenever possible the weld should be placed so that it is in compression or shear.

15.5 Fitting design conditions. A fitting is usually designed and a minimum margin of safety specified for two loading conditions, limit load and ultimate load. The limit load is the load that the aircraft components may be subjected to during the normal operation of the airplane. The ultimate load, usually a certain factor (1.5) times the limit load, is the maximum load the aircraft components are expected to withstand without failure. On application of the limit load the parts of the aircraft structure should not experience excessive permanent set. Likewise, the structural components must be able to carry the ultimate load without rupture or collapse.

Because of the importance of fittings and the difficulty of analysis, a generous margin of safety is usually allowed in their design. A minimum margin of safety of 15% for military aircraft and 20% for commercial planes is required, although it is not unusual to have a margin of safety of 50% on major fittings. A fitting such as a wing attachment is called a *major fitting* because its failure would cause destruction of the airplane structure. A *minor fitting* is one whose purpose is to support equipment or to join less vital parts of the structure. Another reason for using a high margin of safety for fittings is because of the uncertainty of the load conditions and their effect on the material of the fitting. For example, there may be shock, vibration, or impact conditions which would modify the assumed applied loads an unknown amount.

15.6 Efficiency and economy. A fitting used in joining two structural members must transmit the forces from one member to the other. Since the fittings usually overlap the structural members to provide adequate attachment, there is some duplication of material. This duplication, as well as the necessary parts for attachment such as rivets or bolts, makes the fitting assembly involve considerable weight. For economy of weight and cost it is essential that the number and size of fittings be held to a minimum. At the same time efficiency of the fitting in transmitting forces should be high.

There are some general rules in fitting design that may be formulated in order to increase the fitting strength and decrease the weight required. They are:

(1) Whenever possible, a fitting should be located where the forces to be transmitted are relatively small.

(2) Avoid application of eccentric loads through the fitting. An eccentric load introduces a bending moment that will cause additional stresses in the fitting and the member to which it is attached.

(3) Use generous fillets and gradually tapered sections to avoid stress concentrations.

(4) Avoid changes in direction of the load carrying member. A fitting joining such members at a "kink" must be very strong to provide proper restraint.

15.7 Fitting stress analysis. After the loads to be transmitted by a fitting are known, it may be the designer's problem either to strength check an existing fitting design or to determine the size and shape of material for a new design. The principles of analysis are the same for either case. For simplicity, only the strength check procedure will be discussed.

Very few general rules for stress analysis can be formulated because of the complexity and variety of fittings. The designer's experience is usually relied upon to determine the critical (weak) points of a fitting. While considering the distribution of load in the fitting it is helpful to remember that the total load being transmitted by the fitting is equal to the applied load.

The following are a few considerations to be made when strength checking a fitting:

(1) tension on net sections

(2) shear on net sections, bolts, and rivets

(3) crushing or bearing of net sections

(4) bending of net sections

(5) torsion of net sections

(6) effect of a combination of two or more of the above acting simultaneously

(7) effect of variation in loading, stress concentration, and fatigue.

EXAMPLE 15.4.   A fitting attachment for a streamline strut is shown in Figure 15.4.   The fitting is made of 24ST bar stock and is attached to the streamline tubing by 8-$\frac{5}{16}''$ 24ST rivets.   The ultimate load in tension is 27,000 pounds.   If the load is applied without shock but the fitting has small relative motion about the connecting ¹olt, stress check the fitting.
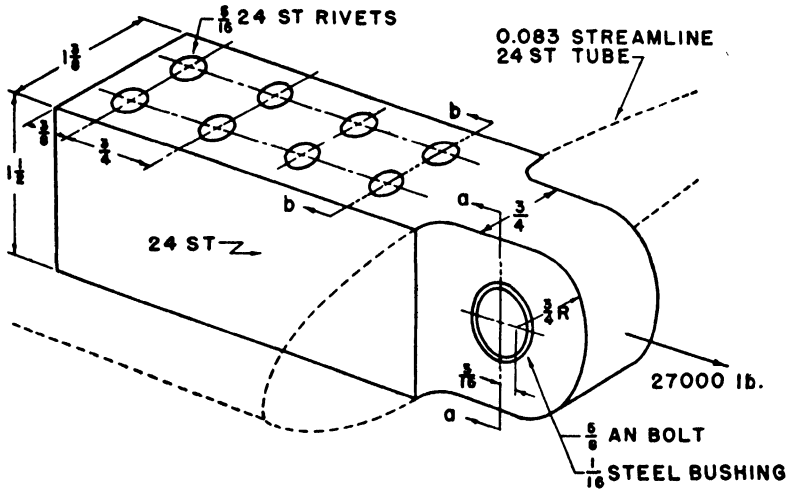
Fig. 15.4.   Fitting.

The margin of safety for the fitting is to be at least 20%.

Solution.   The stress check will begin at the load application point and include all possible modes of failure.

The following data taken from the ANC-5 pertain to the fitting material and load conditions.

24ST Bar.
$$\left.\begin{array}{l} F_{tu} = 64{,}000 \text{ psi} \\ F_{su} = 38{,}000 \text{ psi} \\ F_{br} = 122{,}000 \text{ psi} \end{array}\right\} \text{(page 5-8 ANC-5)}$$

Steel Bushing.   Use steel bushing heat treated to $F_{tu} = 100{,}000$ psi.

Then $\qquad F_{br} = 140{,}000$ psi $\qquad$ (page 4-13)

For infrequent relative rotation the bearing factor is

$$B = 2.0 \qquad \text{(page 4-5)}$$

Rivets.   Allowable loads for $\frac{5}{16}''$ 24ST rivets in 0.083 24ST sheet are

$$\text{double shear} = 3360 \times 2 \times 0.688 = 4630 \text{ lb} \qquad \text{(page 5-26)}$$
$$\text{double bearing} = 2 \times 2620 \times 1.29 = 6760 \text{ lb} \qquad \text{(page 5-26a)}$$

Bolt. Strength of $\frac{5}{8}''$ AN bolt heat treated to $F_{tu} = 125,000$ psi

single shear $= 23,000$ lb   (page 4-43)
bearing, $F_{br} = 175,000$ psi   (page 4-13)

1. *Strength of bolt in shear.* Since the bolt is in double shear,

$$P_a = 2 \times 23,000 = 46,000 \text{ lb}$$
$$MS = \frac{P_a}{P} - 1 = \frac{46,000}{27,000} - 1 = 0.70$$

2. *Strength of bolt in bearing.*

$$P_a = \frac{\text{projected area} \times \text{stress}}{\text{bearing factor}} = \frac{tdF_{br}}{B}$$
$$= \frac{\frac{3}{4} \times \frac{5}{8} \times 175,000}{2} = 41,000 \text{ lb}$$
$$MS = \frac{41,000}{27,000} - 1 = 0.52$$

3. *Bearing of bolt on bushing.*

$$P_a = \frac{tdF_{br}}{B} = \frac{\frac{3}{4} \times \frac{5}{8} \times 140,000}{2} = 32,800 \text{ lb}$$
$$MS = \frac{32,800}{27,000} - 1 = 0.21$$

4. *Bearing of bushing on fitting lug.* Since there is no motion between the bushing and the lug, the bearing factor is one. Then

$$P_a = tdF_{br} = \tfrac{3}{4}(\tfrac{5}{8} + \tfrac{1}{8})122,000 = 68,600 \text{ lb}$$
$$MS = \frac{68,600}{27,000} - 1 = 1.54$$

5. *Shear tearout of bolt end.*

Edge distance $e = (\tfrac{3}{4} + \tfrac{3}{16}) - (\tfrac{5}{16} + \tfrac{1}{16}) \cos 40°$
$$- [\tfrac{3}{4} - \sqrt{(\tfrac{3}{4})^2 - (\tfrac{5}{16} + \tfrac{1}{16})^2 \sin^2 40°}]$$
$$= 0.611 \text{ in}$$

Net area in single shear $= 0.611 \times \tfrac{3}{4} = 0.458 \text{ in}^2$
$$P_a = 2AF_{su} = 2 \times 0.458 \times 38,000 = 34,800 \text{ lb}$$
$$MS = \frac{34,800}{27,000} - 1 = 0.29$$

6. *Tension at net section at bolt hole.* Section *a-a*

Area of net section $= (1\tfrac{1}{2} - \tfrac{5}{8} - 2 \times \tfrac{1}{16})\tfrac{3}{4} = 0.562 \text{ in}^2$
$$P_a = F_{tu}A = 64,000 \times 0.562 = 36,000 \text{ lb}$$
$$MS = \frac{36,000}{27,000} - 1 = 0.33$$

7. *Strength of rivets.* Since the rivets are critical in shear, the failure in shear only will be considered. There are eight rivets.

$$P_a = 8 \times 4630 = 37,040 \text{ lb}$$
$$MS = \frac{37,040}{27,000} - 1 = 0.37$$

8. *Failure of bar at net section of first rivets.* Section *b-b*

$$A = (1\tfrac{3}{8} - 2 \times \tfrac{5}{16})1\tfrac{1}{2} = 1.12 \text{ in}^2$$
$$P_a = 1.12 \times 64,000 = 71,600 \text{ lb}$$
$$MS = \frac{71,600}{27,000} - 1 = 1.65$$

9. *Failure of first six rivets in shear and end of bar in shear tearout.* Load carried by six rivets in shear

$$P_1 = 6 \times 4630 = 27,780 \text{ lb}$$
$$\text{Edge distance on last rivets} = \frac{3}{8} - \frac{\tfrac{5}{16}}{2}\cos 40° = 0.255 \text{ in}$$
$$\text{Area in tearout} = 2 \times 2 \times 0.255 \times 1\tfrac{1}{2} = 1.53 \text{ in}^2$$
$$P_2 = 1.53 \times 38,000 = 58,000 \text{ lb}$$
$$P_a = P_1 + P_2 = 27,780 + 58,000 = 85,780 \text{ lb}$$

This type of failure obviously will not occur.

Since the margin of safety is least for the bushing in bearing, the margin of safety for the fitting is 0.21.

Problems

15.1. A 0.072-inch 24ST aluminum-alloy sheet is fastened to the spar cap of a beam with a single row of 17ST rivets. If the horizontal shear load on the sheet is 1550 pounds per inch, determine the size and spacing of the rivets.

15.2. A double strap butt joint similar to the one shown in Figure 15.2 is carrying a tension load of 1250 pounds per inch. If the main sheet is 0.091-inch 24ST clad and the splice plates are 0.040-inch 24ST clad, determine the size and spacing of the rivets.

15.3. The fitting shown in Figure 15.5 is attached to a 0.064-inch 24ST clad bulkhead by four 17ST rivets. If the fitting is 0.125-inch 24ST aluminum alloy
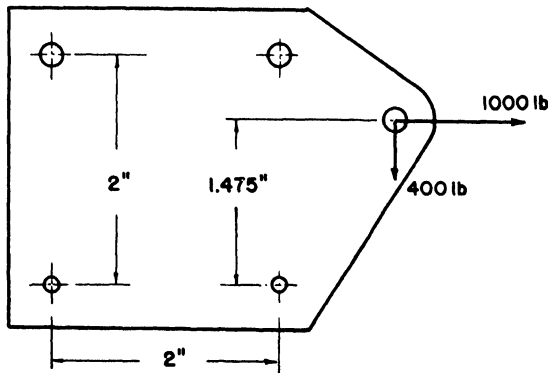
Fig. 15.5. Bulkhead Fitting.
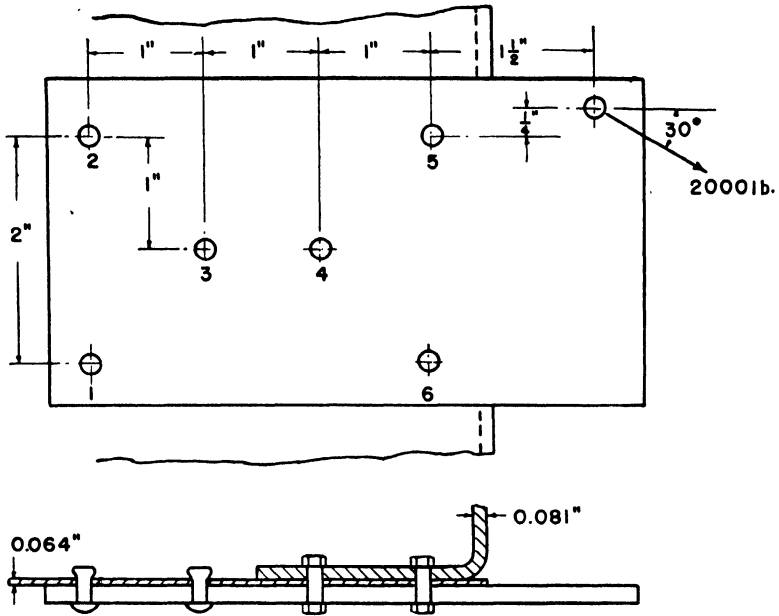
Fig. 15.6. Eccentrically Loaded Connection.
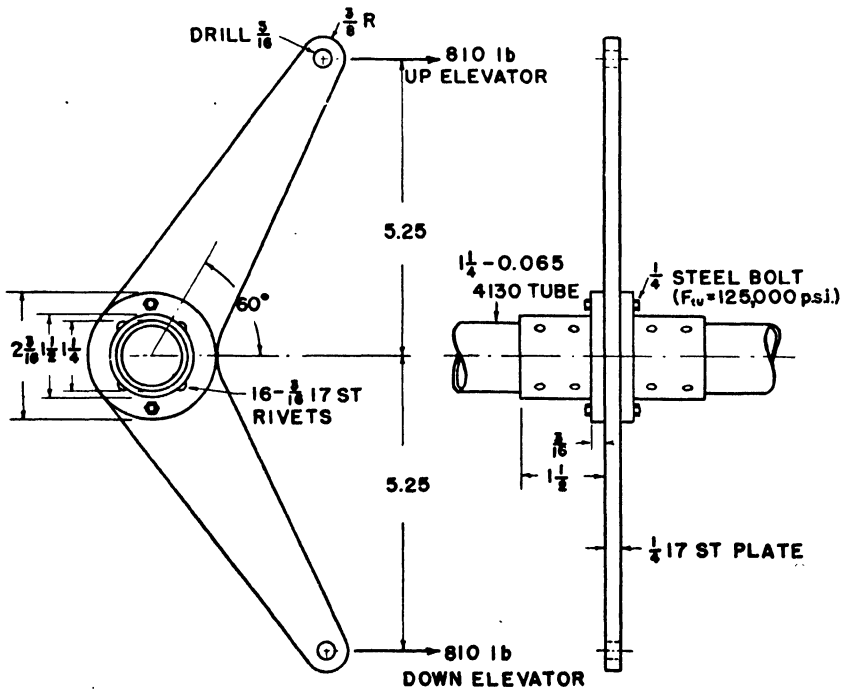
Fig. 15.7. Elevator Horn.

and the two top rivets are $\frac{3}{16}$ inch in diameter and the two bottom rivets are $\frac{1}{8}$ inch in diameter, determine the loads on the rivets.

15.4. Fastenings 1, 2, and 3 of Figure 15.6 are $\frac{3}{16}$-inch A-17ST rivets bearing in 0 064-inch 24ST clad; whereas 4, 5, and 6 are $\frac{1}{4}$-inch bolts bearing in 0.081 plus 0.064 24ST clad. Determine the margin of safety for each rivet and bolt.

15.5. Strength check the elevator control horn shown in Figure 15.7. The limit load transmitted by the control wire is 810 pounds for either moving the elevator up or down. The fitting is required to have a minimum margin of safety of 20% based on the ultimate load for all parts except the main horn lever. Since this latter part should be very rigid, it is required to have a margin of safety on yielding of at least 20% based on the limit load.

The control wire ends of the horn are fitted with steel bushing.

CHAPTER 16

General Design Considerations

16.1 Introduction. After the fundamentals of analysis of aircraft structures have been mastered, there is still much to learn before an efficient structural design can be made or stress checked. Most of this latter knowledge is obtained through experience in the industry and through a continuing day by day study of the problems and latest developments. Many of the attributes of a good designer, such as the ability to estimate the size and shape of a structure because it "looks right," the ability to devise ingenious devices for performing complicated functions, the ability to simplify complex structures, and a comprehension of the interrelation of the functions of design, production processes, and so forth, can be achieved only after considerable experience in the industry. The judgment required to separate the significant and the negligible factors in an analysis also develops with experience.

Some of the important considerations the designer should bear in mind are discussed in the following articles.

16.2 Stress concentration. One of the most important factors a designer must continually bear in mind pertains to the problem of stress concentration.

In local regions of some structural members, the stresses are not distributed as indicated by the elementary theory. Localized variations in stress distribution called stress concentrations are caused by sharp discontinuities in the shape of the member, by nonhomogeneity of structure of the material, or by strain incident to processing.

The localized stresses are frequently of comparatively large magnitude and, under the action of the loads, may cause a crack at the region of the localized stresses. Such a crack usually leads to failure of the member by rupture.

Some of the causes of stress concentration are:

(1) *Variation in properties of materials from point to point in a member.* Some examples are (a) internal cracks and flaws, (b) cavities in welds, (c) air holes in steel, and (d) nonmetallic inclusions.

(2) *Internal strains due to processing.* Some examples of this type of stress concentration are (a) shrinkage in casting, (b) cold working, (c) overstraining, and (d) improper heat treatment.

(3) *Pressures at points or areas at which loads on a member are applied.* Some examples of this type of stress concentration are (a) contact between a pulley and rope, (b) contact between the balls and races of a ball bearing, (c) contact between a beam and its supports, and (d) contact between gear teeth.

(4) *Abrupt changes of section.* There are two classes of this type of stress concentration. One involves surface condition, such as scratches due to machining errors or roughness in handling, and scratches incident to machining operations. In machining, the dimensions of the scratches or irregularities vary from very large in roughing operations, to microscopic in fine finishing. The other stress concentration may be caused by abrupt changes in form of a member. Stress concentration of this kind may be extremely serious, and its prevention lies solely within the designer's responsibility.

16.3 Stress concentration due to holes and notches. (a) *Tension member with a transverse hole.* In a prismatic bar as shown in Figure 16.1(a) subjected to a tensile load, the stress is uniformly distributed over a cross section *A-A* of the bar.
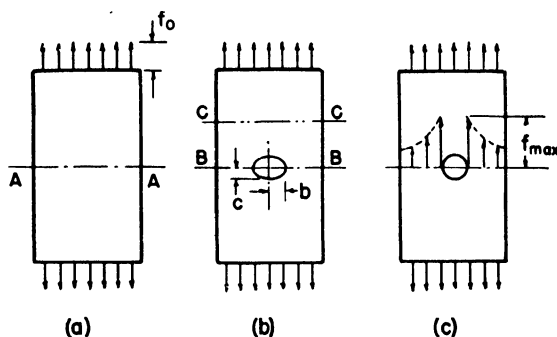
Fig. 16.1. Effect of Hole on Stress Distribution in Tension Member.

If the same bar has an elliptical hole as shown in Figure 16.1(b), the stress at a section *C-C* remote from the hole will be uniformly distributed over the section. However, the stress over the cross section *B-B* through the hole will not be uniformly distributed over the net section carrying the load. The maximum stress will be induced at the edge of the hole, and it may have a value several times that of the stress at the section *C-C*. The value of the maximum stress in terms of the stress at the section *C-C* is given by the expression

$$f_{\max} = f_0 \left(1 + 2\frac{b}{c} \right) \qquad (16.1)$$

in which f_0 is the stress at the section *C-C* and b and c are the semiaxes of the ellipse perpendicular and parallel respectively to the line of the load as shown in the figure.

It may be seen from Equation 16.1 that for large values of b/c, which represent an ellipse approaching the form of a transverse slit, $f_{\max}$ reaches a very high value.

For small values of b/c, which represent an ellipse approaching a longitudinal slit, f_{max} is not markedly increased over f_0.

For the case of a circular hole, $b = c$, $f_{max} = 3f_0$. The stress distribution for this case is shown in Figure 16.1(c).

(b) *Tension member with notches.* The stress concentration in the notched tension member in Figure 16.2 is influenced by the depth b of the notch and the radius r at the bottom of the notch. The maximum stress may be calculated by the following equation, which applies to members having notches which are small in comparison with the width of the bar.
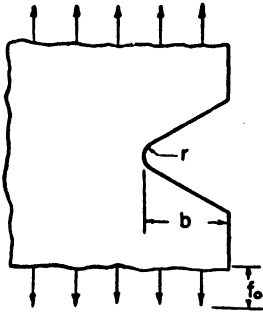
Fig. 16.2. Notch in Edge of Tension Member.

$$f_{max} = f_0 \left(1 + 2\frac{b}{r}\right) \qquad (16.2)$$

in which f_0 is the uniformly distributed stress at a section remote from the notch.

16.4 Seriousness and mitigation of stress concentration. Stress concentration should not be overlooked by the designer. It is evident from the preceding discussion that very high concentration of stresses may exist in certain regions in machine and structural members. Since a crack which may form at a region of stress concentration usually leads to failure of the member, it is important that the designer reduce the concentration to the practicable minimum. The designer can reduce stress concentration effectively in most cases by simple expedients, such as the use of gradual transition curves and generous fillets.

The seriousness of stress concentration depends on the properties of the material and on the type of loading, namely whether the load is static or repetitive.

(a) *Static loading.* It was noted in Article 16.3 that the stress at the edge of a small transverse circular hole in a tension member has a value three times that in the sections remote from the hole. The distribution of stresses across the section including the hole is indicated in Figure 16.1.

If the material of which the member is made has a stress-strain diagram which is a straight line up to rupture, the *shape* of the stress-distribution diagram in Figure 16.1(c) will not be altered as the load on the member is increased. This is true because the stresses increase proportionally until the maximum stress in the member reaches the breaking stress of the material. At this stage a crack forms at the edge of the hole. The crack has the effect of introducing additional stress concentration and of decreasing the section carrying the load. Both of these effects cause very rapid failure of the member.

Brittle materials like cast iron undergo relatively little yielding; therefore a member made of brittle material with stress concentration will

fail as described above since the concentration of stress as indicated by Figure 16.1(c) remains in the member until failure occurs.

In considering the failure of a member made of a *ductile material* having a stress concentration, it is necessary to note that the stress-strain diagram for the material includes a region which involves considerable plastic flow. The plastic flow occurs beyond the yield point and allows considerable strain to take place before failure occurs. The stress-distribution diagram in Figure 16.1(c) is valid if the stresses are below
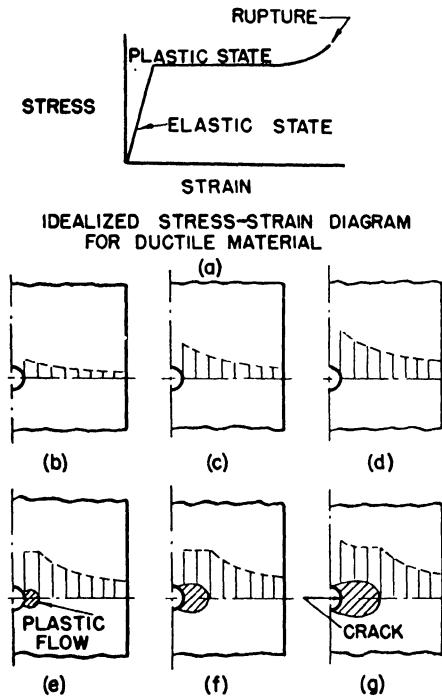
Fig. 16.3. Redistribution of Stress in Ductile Material.

the proportional limit; however, beyond the yield point, plastic flow at the region of stress concentration will cause the stresses to be redistributed. The redistribution of stresses tends to produce a uniform distribution. To illustrate this change in distribution, one half of the section in Figure 16.1(c) is drawn as shown in Figure 16.3. Figure 16.3(a) shows an idealized stress-strain diagram for a ductile material, and (b) represents a portion of the bar adjacent to the hole and the stress-distribution diagram for low stresses in the member. Figure 16.3(c) represents the diagram for increased stresses, and (d) the stage when the maximum or peak stress is just equal to the yield point. Figure 16.3(e) shows the diagram for an increased load on the member, and the corresponding cross-sectioned area indicates the region which has undergone plastic

flow, leading to the next state (f), and finally (g) indicates the condition at the time the peak stress reaches the breaking stress of the material, when a crack forms and the member fails.

From the above sequence of diagrams, it is apparent that plastic flow in ductile materials will lessen the seriousness of stress concentration. Frequently this plastic flow takes place in machine and structural members when the working loads are applied. As examples of this kind of reduction of stress concentration may be mentioned structural members with rivet holes, keyways in shafting, and riveting or welding.

In conclusion, it may be stated that stress concentration in *static loading* is very serious in brittle materials, and is less serious in ductile materials due to the relieving of stress concentration by plastic flow. However, the designer should reduce stress concentration wherever possible without regard to the class of material of which the member is made.

(b) *Repeated loading and fatigue failure.* In the preceding discussion it was noted that in static loading, stress concentration is especially serious in members made of brittle materials and somewhat less serious in members made of ductile materials. In the latter case it has been found that the seriousness of stress concentration is lessened by the local plastic flow which results in a more favorable distribution of stresses.

In many instances in the aircraft structure a structural member is not subjected to a single application of load, but to a continual variation of load. Every time an airplane hits a gust or changes its flight attitude the loads vary. This repetition of load sometimes will cause a member to fail at a lower load than would be required to produce failure for a single application of the load, much as a paper clip will break eventually if it is bent back and forth enough. The lowest stress a member can withstand without failure under repeated loading is called the *endurance limit.* Stress concentration is always serious in members subjected to repeated loading since the ductility of the material is not effective in relieving the concentration of stress caused by cracks, flaws, surface roughness, or any sharp discontinuity in the geometrical form of the member or in the metallurgical structure of the material. If the stress at *any* point in a member is above the endurance limit of the material, a crack will develop under the action of the repeated load and the crack will, in all probability, lead to failure of the member. It is important to realize that even though the region subjected to the peak stress is of extremely small size, the crack is likely to form, and once formed will lead quickly to failure of the member.

The last statement is emphasized by a report that approximately 90% or more of the load cycles necessary to produce failure of a member are undergone before the crack may be detected by laboratory means. It is evident then that the opportunity for an inspector to detect a crack under service conditions in time to prevent failure is relatively slight.

Figure 16.4 shows the effect of surface condition on the endurance

limit of test specimens. The figure illustrates the marked reduction in endurance limit due to small scratches and grooves inherent in finishing operations. The figure indicates also that the higher strength alloy steels are more sensitive to stress concentration. The lower ductility of the high strength alloy steels is probably partly responsible for the increased sensitivity; however, it is not generally true that high ductility is the best insurance against stress concentration in fatigue failure.
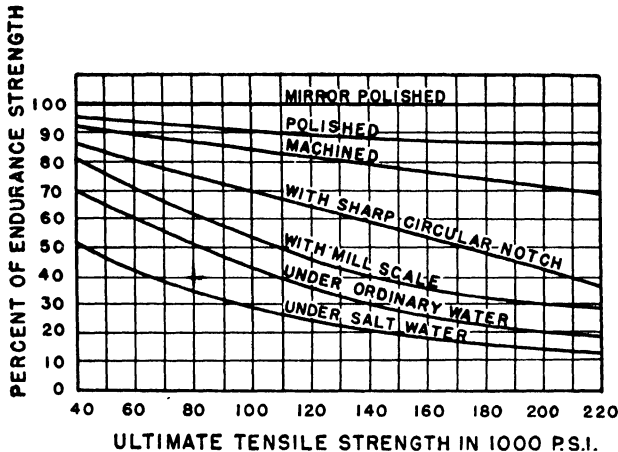
Fig. 16.4. Effect of Surface Conditions on Endurance Strength.

The gain in endurance limit because of polishing is one of the reasons for the practice of polishing aircraft engine connecting rods and link rods. The overall polish is a very expensive operation, although justified by the resulting increase in safety.

16.5 Stress concentration factors. The stress concentration factor is defined as

$$k = \frac{\text{actual maximum stress}}{\text{stress calculated by elementary theory}}$$

The stress concentration factor is always greater than one and may sometimes be as high as twenty.

Analytical methods have been used for determining the stress concentration factor in many cases, but it is necessary generally to resort to experimental methods. Stress concentration factors for flat plates in tension are given in Figure 16.5. Notice that the stress concentration factor, and therefore the maximum stress, becomes high as the fillet radius is decreased. We should always remember to use *generous fillets* and *smooth transition sections* in any design.

16.6 Standard parts. Whenever possible, in order to save time and expense, standard parts should be used. Dimensions should usually be "rounded out" from calculated values to a standard size. Standard parts are carried in stock by the suppliers of aircraft materials, and there-

fore no time is lost in making up a special order.   Many standard sizes of tubing, extruded sections, angles, tees, Z sections, bolts, and rivets are found in the many handbooks published by various manufacturers.
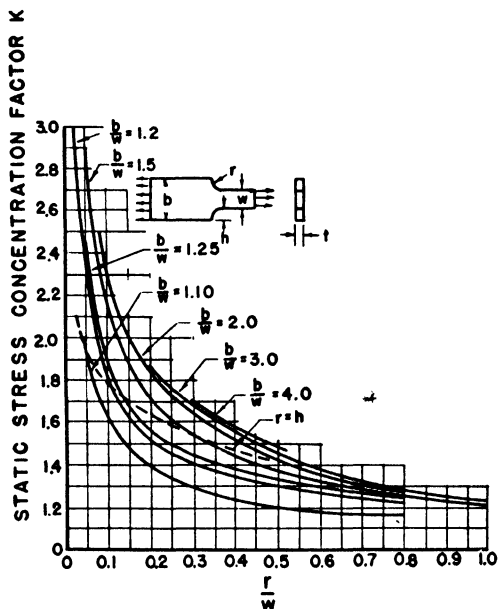
Fig. 16.5.   Static Stress Concentration Factors for Flat Plates in Tension or Compression.

Remember also that the airplane probably will be serviced a long way from the factory and that it is easier to obtain a standard part than a special one.

16.7 Weight reduction.   The importance of weight reduction in aircraft cannot be overemphasized.   The designer constantly must consider means for saving weight consistent with sufficient strength.

It has been estimated that one pound of weight saved in a commercial two-engined airplane would save in manufacturing, investment, and operating costs, and in increased revenue, about $230, based on an airplane life of six years.   Suppose an airline is using 100 of these airplanes and 100 pounds of excess weight is eliminated on each.   The saving for a six-year period would be $2,300,000, a tidy sum.

References

Ayers, John, "The Value of a Pound Saved by Weight Control." *Aero Digest*, November 1942.

Black, P. H. and M. V. Barton, *Notes on Machine Design*.   Edwards Brothers, 1942.

Prevention of the Failure of Metals Under Repeated Stress.   Battelle Memorial Institute.   John Wiley & Sons, 1941.

Index

DATE OF ISSUE

This book must be returned
within 3, 7, 14 days of its issue A
fine of **ONE ANNA** per day will
be charged if the book is overdue.